New ways to test beta cell functionality in health and diabetes

Korsgaard, Thomas Vagn

Publication date:
2011

Document Version
Publisher's PDF, also known as Version of record

New ways to test beta cell functionality in health and diabetes

PhD Thesis

Thomas Vagn Korsgaard

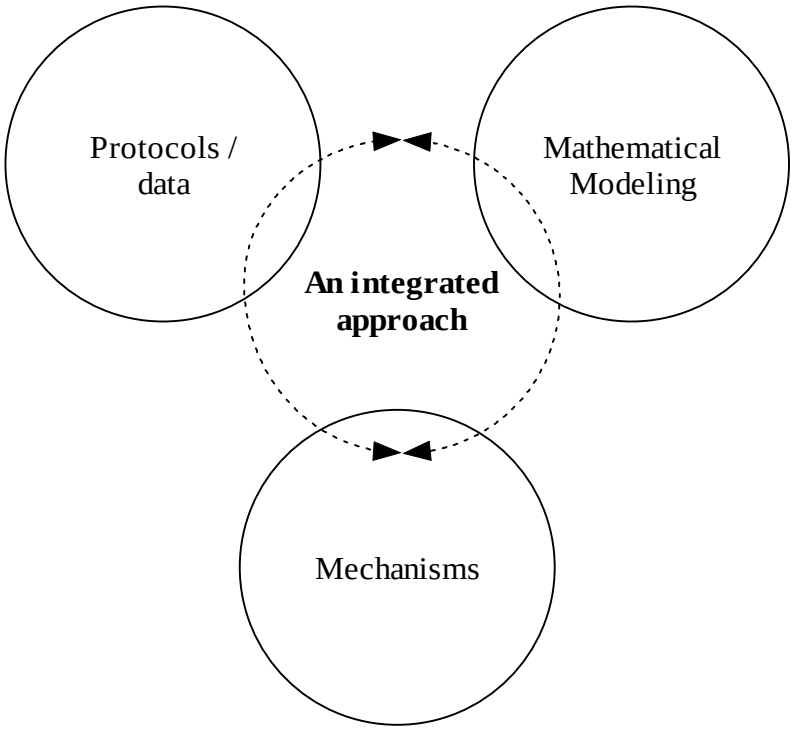

Clinical Pharmacology – Biosimulation, Novo Nordisk A/S

Department of Physics, Technical University of Denmark

Copenhagen 2011

Preface

This PhD thesis presents the work I have performed through the last three years while employed as an Industrial PhD at Novo Nordisk A/S. The project was performed in collaboration with Novo Nordisk A/S and DTU, the Technical University of Denmark and was co-funded by the Danish Ministry of Science, Technology and Innovation, Corporate Research Affairs, Novo Nordisk A/S and the European Union Network of Excellence, BioSim.

I would like to express my gratitude to my two supervisors Prof. Erik Mosekilde, Department of Physics (DTU) and Prof. Morten Colding-Jørgensen, Clinical Pharmacology – Biosimulation (Novo Nordisk A/S). Together with René Norman Hansen (Novo Nordisk A/S) these experienced researchers have provided invaluable guidance and inspiration throughout my project. I would also like to thank Christine Erikstrup Hallgreen for moral support, and the rest of the guys at Biosimulation, Novo Nordisk A/S and people I have collaborated with within Device Research and Development in Hillerød, Novo Nordisk A/S. I am thankful to them for contributing with a great and supportive atmosphere. Words cannot express how deeply grateful I am with the encouragement and understanding my family has shown me, thank you.

Thomas Vagn Korsgaard

Copenhagen, February 2011

Abstract

Beta cell functionality is often characterised by indices describing different phases of insulin secretion. The typical biphasic insulin secretion pattern observed with a square wave glucose stimulation has laid the foundation for most modelling work regarding quantification of beta cell function. Within the context of control theory, the beta cell functionality is usually modelled as versions of a classic Proportional-Integral-Differential (PID) controller, and the different phases of insulin secretion are described in relation to the different control component, with the first phase of insulin secretion being related to the differential control component, and the second (late) phase to the integral control component. This is, of course, a phenomenological description.

We propose a model of the glucose sensing mechanisms in the beta cell describing the time-dependent physiological processes underlying the different insulin secretion phases. The model results show that glucokinase is the key regulatory step in the glucose sensing mechanisms. We argue that it is not glucose per se, but some signal(s) downstream of the glycolytic pathway that controls the activity of glucokinase, and hence the final insulin secretion pattern. We show that the first phase of insulin secretion is related to the rate of change of glucose in a non-linear saturable fashion, and that the second phase is due to translocation of glucokinase from an inactive to an active state. Hence, the glucose sensing mechanisms in the beta cell can, in some sense, be regarded as working as a classic PID controller, with intrinsic non-linearities in the sensing machinery.

A meal tolerance test (MTT) is the best test for assessing beta cell indices as well as indices for insulin action in a physioloigcal relevant setting. In that context we have analysed MTT data from a large population of healthy subjects and from subjects with type 2 diabetes displaying a wide range of fasting plasma glucose (FPG) concentrations. Due to the heterogeneity in the FPG values of the subjects with diabetes, we stratified them according to their FPG and divided the subjects into five groups. Interestingly, when correcting for the FPG, the mean plasma glucose concentration profiles from each of the five groups are strikingly similar, despite quite large differences in the corresponding mean plasma insulin profiles. From the graphs of the means of the differentiated individual glucose profiles within the respective groups of subjects with diabetes, this similarity of the glucose profiles is even more evident. Same results are obtained when analysing the data from the database, where the subjects with type 2 diabetes have been followed throughout years, and where different standard treatments are also present.

The graph of the mean healthy glucose profile shows a clear distinction from the corresponding graphs from subjects with type 2 diabetes. Of special interest is the observation that for the healthy persons the plasma insulin is still high even though plasma glucose has returned to fasting values, hence secretion of insulin continues despite glucose has returned to fasting values, and the increased insulin does not lead to hypoglycaemia. Hence in healthy subjects it appears that the glucose uptake is controlled in such a way as to follow the rate of glucose appearance from the meal. Similar conclusions cannot be drawn from the meal profiles of the subjects with type 2 diabetes. The glucose profiles for the subjects with type 2 diabetes seem similar despite different insulin profiles, and it appears that insulin merely follows the glucose profile without controlling it. However glucose undershoot is observed, probably due to elevated insulin concentration at the end of the meal test.

The analysis of the MTT data provides a new tool to distinguish the healthy after-meal responses from responses of people with diabetes. Furthermore our analysis indicates that a mechanism that works more or less independent of insulin is activated in healthy persons after a meal and that this mechanism apparently is damaged and/or diminished in persons with type 2 diabetes.

We argue, by referring to literature, that this mechanism is a result of the brain participating in the overall control of glucose concentration and fluxes of glucose equivalents. Hence, neural effects seem to be an important component that needs to be added to models that are set up to describe beta cell functionality as well as glucose uptake in a physiological relevant setting.

Dansk resumé (Danish summary)

De insulin producerende betacellers funktion karakteriseres ofte ved hjælp af indices, som beskriver forskellige faser af insulinsekretionen. Det typiske bifasiske insulinsekretions mønster, der kan observeres efter en firkant glukose-stimulering, har dannet grundlaget for det meste af modelarbejdet som netop omhandler kvantificering af betacelle funktionaliteten. Med udgangspunkt i teknisk kontrolteori bliver betacellen ofte modelleret som versioner af en Proportionel-Integral-Differentiel (PID) kontrolenhed, og de forskellige sekretionsfaser bliver beskrevet i forhold til de forskellige kontrolkomponenter, hvor den første sekretionsfase er relateret til den differentielle kontrolkomponent, og den anden (sene) fase til den integrale kontrolkomponent.

Vi foreslår en model af glukose-registreringen i betacellen som beskriver de tidsafhængige fysiologiske mekanismer som ligger til grund for de forskellige sekretionsfaser. Modelresultaterne viser at glukokinase er den vigtigste regulatoriske faktor i glukose-registrerings mekanismerne. Vi argumenterer for, at det ikke er glukose, men nogle signal(er) i den glykolytiske proces som kontrollerer aktiviteten af glukokinase, og dermed det endelige insulin sekretionsmønster. Vi viser at den første fase af insulinsekretion er relateret til den tidsafledede af glukose på en mætbar ikke-lineær måde, samt at den anden fase skyldes translokation af glukokinase fra en inaktiv til en aktiv tilstand. Glukose-registerings mekanismerne kan følgeligt i en vis forstand opfattes som en klassisk PID kontrol-enhed, med iboende u-lineariteter i registreringsapparatet.

En måltids tolerance test (MTT) er den bedste test til at vurdere såvel indices for betacelle funktionaliteten som indices for insulin virkning i fysiologisk relevante omgivelser. Derfor har vi analyseret MTT data fra en stor population af raske samt fra personer med type 2 diabetes med et stort interval af forskellige faste plasma glukose (FPG) værdier. På grund af den store forskel i FPG værdierne for personerne med type 2 diabetes, stratificerede vi i forhold til deres FPG værdier og inddelte dem i fem grupper. Middel plasma glukose koncentrationsprofilerne for de fem grupper korrigeret for deres FPG værdier, er bemærkelsesværdig ens, på trods af ganske store forskelle i de tilsvarende middel plasma insulinprofiler. Denne lighed af glukoseprofilerne ses endnu mere tydeligt af kurverne for middelværdierne af de individuelle differentierede glukoseprofiler. Samme resultater opnås ved analysen af data fra databasen hvor personer med type 2 diabetes er blevet fulgt gennem flere år, og hvor forskellig standard behandlinger også er inkluderet.

Kurven for den raske middel glukoseprofil er markant forskellig fra de tilsvarende kurver fra personer med type 2 diabetes. Særlig interessant for de raske data er, at plasma insulin er stadig høj.

Det betyder at secerneringen af insulin fortsætter selvom plasma glukose er vendt tilbage til fasteværdien, samt at den forøgede insulin ikke forårsager hypoglykemi. I raske personer ser det derfor ud til, at glukoseoptaget er reguleret på en sådan måde, så optaget følger glukose absorptionshastigheden. Tilsvarende konklusioner kan ikke drages af profilerne fra personerne med type 2 diabetes. Glukoseprofilerne for personerne med type 2 diabetes er tilsyneladende ens på trods af forskellige insulinprofiler, og det ser ud til at insulin blot følger glukoseprofilen uden at kontrollere den. Dog ses glukose værdier under fasteværdien (”undershoot”), der formentligt skyldes forøget insulinproduktion i slutningen af måltids testen.

Analysen af MTT resultaterne giver et nyt værktøj til at skelne mellem det raske og type 2 diabetes måltids svar. Endvidere indikerer analysen at nogle mekanismer, som fungerer mere eller mindre uafhængigt af insulin, aktiveres hos raske efter et måltid, samt at disse mekanismer tilsyneladende er ødelagt og/eller formindsket hos personer med type 2 diabetes.

På grundlag af oplysninger i litteraturen argumenterer vi for, at disse mekanismer skyldes, at hjernen deltager i den overordnede kontrol af glukose-koncentration og bevægelser. Følgelig ser det ud til, at neural indvirkning er en vigtig komponent, som mangler i de modeller, der beskriver betacelle funktionaliteten og glukoseoptaget i relevante fysiologiske omgivelser.

Symbols and abbreviations

AIR	Acute insulin release
AUC	Area under curve
CC	Signal from controller to effector
CI	Desired value (or trace) of controlled variable, see CO
CV	Coefficient of variation
CO	Controlled variable
DI	Disposition index
DNL	De novo lipogenesis
ECF	Extracellular fluid
EE	Energy expenditure
EGC	Euglycemic glucose clamp
FA	Fatty acids
FPG	Fasting plasma glucose
FPI	Fasting plasma insulin. Used interchangeably with I_b
FSIGT	Frequently sampled intravenous glucose tolerance test
G_b	Basal glucose. Used interchangeably with FPG
G6P	Glucose-6-phosphate
GEZI	Glucose effectiveness at zero Insulin
GIP	Glucose-dependent insulinotropic polypeptide
GIR	Glucose infusion rate
GK	Glucokinase
GLP-1	Glucagon-like peptide-1
GNG	Gluconeogenesis
GGIT	Graded glucose infusion test
HbA1c	Glycosylated haemoglobin
HGC	Hyperglycemic glucose clamp
HGO	Hepatic glucose output (including any renal contribution)
I_b	Basal insulin. Used interchangeably with FPI
IDVG	Initial distribution volume of glucose

IDVS	Initial distribution volume of sucrose
IV	Intravenous
IVGTT	Intravenous glucose tolerance test
HOMA	Homeostatic model assessment
MPC	Model predictive control
MTT	Meal tolerance test
OMM	Oral minimal model
OGTT	Oral glucose tolerance test
PID	Proportional, integral, derivative
R_a	Rate of appearance
R_d	Rate of disappearance
RRP	Readily-releasable pool
S_G	Glucose effectiveness at steady state basal insulin
S_I	Insulin sensitivity at steady state
SR	Secretion rate
T2DM	Type 2 Diabetes Mellitus
TG	Triacyl glycerol
WRES	Weighted residuals

Table of Contents

Chapter 1

Introduction

Insulin is an essential hormone with many vital functions, especially for uptake and utilisation of glucose by the different insulin sensitive cells, primarily muscle and adipose tissue cells, throughout the body. The beta cells situated in the pancreas normally secrete insulin upon stimulation by glucose providing a negative feedback regulation to ensure well-controlled glucose levels. Glucose is the most prominent signalling nutrient for insulin release, and the relation between changes in glucose concentration and the resulting changes in insulin release is denoted beta cell function or functionality. Investigation of the beta cell functionality has been ongoing for decades. Still today, research continues, in order to understand the physiology and the pathophysiology of beta cell functionality in especially type 2 diabetes. During the years a tremendous amount of data has been gathered in-vitro as well as in-vivo in many different species and under many different circumstances. The task at hand is thus to convey the information in the data into an understanding of the biological processes governing the pathogenic state.

Mathematical modelling with focus on the right description of the biological mechanisms offers a way to understand the impact of treatments and can be used to pinpoint potential new targets for treatment. The main challenge is to balance the description of the involved mechanisms in the right way. The human body is an extraordinary complex system to describe, and the complexity may become even more expressed in multifactorial pathogenic states such as diabetes. Hence to include all involved mechanisms is an impossible task. Even more important in connection with drug development is that the models need to be validated, a task that may become difficult with large models. On the other hand, the models must capture the important features of the system under investigation. Hence biological modelling, or biosimulation, becomes a delicate matter of neither including too little or too much to describe the system under investigation.

1.1 Biosimulation as an integral part in systems biology

Biosimulation has grown out of the need for a combination of skills within different different fields of natural sciences, in order to understand the many facets of complex diseases, through in-silico experiments. As such biosimulation is a vital part of systems biology, which is a reasonable new field. Systems biology integrates classic fields like physics, chemistry, biology and mathematics in

the quest for understanding the complexity of biological function (Alberghina and Westerhoff 2005). The many "-omics" like genomics, proteomics, metabolomics, etc. used in biology today have provided a wealth of biological information, where perhaps the most prominent result from genomics being the unravelling of the human genome. Even though extremely valuable for collecting biological information for data analysis, these omics do not provide approaches for a quantitave and predictive assessment of the biology, which is important for a full understanding of biological processes.

One examples of the valuable use of systems biology, or biosimulation in drug development of multifactorial diseases include virtual heart simulations to discover potential drug targets in order to avoid cardiac arrythmia (Noble 2008). Such simulations require extensive modelling effort, and biological understanding of all the diffrerent currents of ions partaking in the development of the action potential and potential depolarisation/repolarisation problems associated with the arrythmic state. Other examples includes detailed kinetic models known as silicon cell models, especially of the glycolysis in yeast (Bruggeman *et al.* 2008), or the modelling of chronotherapy for the optimisation of the temporal delivery of anticancer drugs (Altinok *et al.* 2008).

1.2 Thesis objective and outline

The aim of this thesis is to develop a new way to test beta cell function in people with diabetes as well as healthy. The new way will consist of combination of results from the traditional methods with biosimulation models. This task is highly inter-disciplinary and thus well-suited for systems biology and biosimulation. Only very little chemistry is used throughout the thesis, thus the results generated and presented will largely be reflected by the combination of physics and mathematics applied to biology. By this approach the hope is to provide insight into new mechanisms and potential new treatment targets. To achieve the goal of combining the traditional methods with the biosimulation models a clear understanding of both approaches it needed. With this in mind the thesis has been divided in the following chapters.

Chapter 2 Current tests of beta cell functionality

The most common current tests for assessment of beta cell functionality and insulin action are discussed and compared with one another. Pitfalls are highlighted, that may occur when one tries to evaluate the results of a test in a context where the test is not applicable, e.g. when results from un-physiological clamp tests are extrapolated to explain physiological mechanisms. It is stressed that

each test must be evaluated in its own context and that the oral tests, especially the meal tolerance tests, are most suitable for evaluating beta cell functionality and insulin action. State of the art mathematical models of beta cell function during meals are discussed.

Chapter 3 Minimal model analysis of Owens MTT data

An analysis of MTT data with the oral glucose and C-peptide minimal models with the largest number of subjects with type 2 diabetes presently reported in literature is presented.
The estimates for each of the indices of insulin action and beta cell functionality all displayed a large interval both within the group of subjects with diabetes, and within a healthy group. Despite this, a clear distinction between the two groups was evident from the disposition indices plot.
MTT data from a small subset of subjects with type 2 diabetes that were followed at year 0, 1, and 5, to record disease progression and treatment effect, was also analysed with the minimal models. Values for indices of insulin action and beta cell functionality all increased from year 0 to year 1, demonstrating treatment effect. From year 1 to year 5, the value of the indices decreased, demonstrating decline in treatment effect and/or progression of disease. However no clear pattern and no clear difference between the years were found from the disposition indices plot.

Chapter 4 The phase plot

The plot between the plasma glucose and insulin concentration after a meal, i.e. the phase plot is introduced as a simple way to characterise beta cell function. Clear differences in the characteristic measures are found both between healthy and subjects with type 2 diabetes and within the group of subjects with diabetes with different fasting plasma glucose values. These differences are analysed with a simple model introduces to describe the insulin responses.

The oral glucose minimal model is applied to analyse the effect of variability of the model parameters on the characteristics of the phase plot. The model parameters are found to elicit both common and different effects on the characteristics of the phase plot, with a possible complex outcome as a result.

Chapter 5 The meal response

The meal-related responses, i.e. the responses corrected for fasting values, of glucose and insulin after a meal tolerance test for a large dataset of healthy subjects and subjects with type 2 diabetes are analysed.

For the healthy subjects, the analysis shows that the disappearance rate of glucose seems to be regulated in such a way as to follow the appearance rate. The analysis also shows that the meal-responses from the subjects with type 2 diabetes are quite similar regardless of insulin levels, treatment and/or disease progression, but differ fundamentally from the healthy responses. On the other hand fasting plasma glucose, FPG may be affected by treatment, and the variability and regulation of FPG are analysed and discussed.

Chapter 6 Glucose sensing and control

The common view of regarding the glucose-insulin control system as an isolated system to control plasma glucose concentration is shown to be incomplete in several ways. Firstly, the glucose sensing mechanisms in the beta cell is shown to possess important intrinsic non-linear properties and the beta cell works in a complex network with other glucose sensors. Secondly, the handling of metabolites inside and between the different organs is shown to be critical for glucose control. Both insulin and signals from the brain are important components in the control system.

Chapter 2

Current tests of beta cell functionality

The most common current tests for assessment of beta cell functionality and insulin action are discussed and compared with one another. Pitfalls are highlighted, that may occur, when one tries to evaluate the results of a test in a context where the test is not applicable, e.g. when results from un-physiological clamp tests are extrapolated to explain physiological mechanisms. It is stressed that each test must be evaluated in its own context and that the oral tests, especially the meal tolerance tests, are most suitable for evaluating beta cell functionality and insulin action. State of the art mathematical models of beta cell function during meals are discussed.

2.1 Methods for assessing insulin sensitivity and beta cell function

Different methods exist for the assessment of insulin sensitivity and/or beta cell function. Table 2.1 provides an overview of the most commonly used experimental tests (protocols), and their usefulness. A common feature of nearly all the tests summarised in Table 2.1 is that one can obtain a multitude of empirically derived indices describing either insulin sensitivity or beta cell function from them (Cobelli *et al.* 2007; Mari *et al.* 2002a; Muniyappa *et al.* 2008). However one should be cautious about directly relating the results obtained from the different methods with one another. In fact, as will be discussed, the different methods should be viewed each in their own context.

Protocol	Is It Physiological?	Is It Simple?	Can It Assess β-Cell Function?	Can It Assess Insulin Sensitivity?	Can It Assess Hepatic Insulin Extraction?
Basal state	Yes	Yes	Yes, but limited	Yes, but limited	No
Intravenous perturbation					
Hyperglycemic clamp	No	No	Yes, but limited without a model	Yes, but requires a model	Yes, but requires a model
Euglycemic clamp	No	No	No	Yes	No
IVGTT	No	No	Yes, but limited without a model	Yes, but limited without a model	Yes, but requires a model
Graded infusion	No	No	Yes, but limited without a model	Yes, but requires a model	Yes, but requires a model
Oral perturbation					
OGTT	Yes, but no nutrients	Yes	Yes, but limited without a model	Yes, but requires a model	Yes, but requires a model
Meal	Yes	Yes	Yes, but limited without a model	Yes, but requires a model	Yes, but requires a model

Table 2.1: The different experimental tests (protocols) and their characteristics. IVGTT, intravenous glucose tolerance test; OGTT, oral glucose tolerance test. Adapted from Cobelli *et al.* 2007.

2.1.1 Homeostatic model assessment, HOMA

The homeostatic model assessment, HOMA is a method used to assess beta cell function and insulin sensitivity, based on fasting plasma concentration values of glucose, insulin and/or C-peptide (Matthews *et al.* 1985; Wallace *et al.* 2004). The method consists of non-linear equations evaluated at basal state to give indices of beta cell function and insulin sensitivity and hinges on the premise of a negative feedback between hepatic glucose output and beta cell insulin secretion (Matthews *et al.* 1985; Turner *et al.* 1979).

The solutions of the model based version (Levy *et al.* 1998) are shown in Fig. 2.1(a). Fig. 2.1(b) shows the graph between fasting plasma glucose, FPG and fasting plasma insulin, FPI in 84 healthy and 356 newly-diagnosed subjects with type 2 diabetes from the large database provided by Dr. David Owens, cf. chapter 3. There seems to be no (simple) correlation between FPG and FPI, as the data more or less cover the whole HOMA diagram in Fig. 2.1(a). Hence, either the subjects do elicit all the different combinations of insulin sensitivity and beta cell function predicted by the HOMA model, or there exists some other mechanisms regulating FPG and/or FPI not handled by the model.

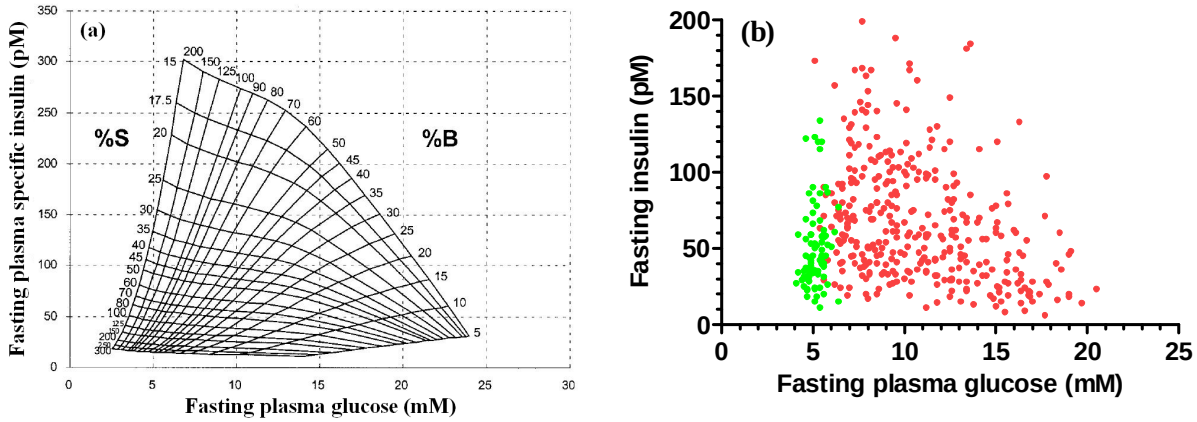

Fig. 2.1: (a) The HOMA diagram, showing the solutions to the HOMA model. %S and %B describe insulin sensitivity and beta cell function, respectively, relative to healthy subjects. Adapted from Wallace *et al.* 2004. (b) The relation between fasting plasma glucose and fasting plasma insulin in 84 healthy (green dots) and 356 newly-diagnosed subjects with type 2 diabetes (red dots). Data from Dr. David Owens.

2.1.2 Glucose clamps

The idea behind a glucose clamp test is to keep glucose at a constant level by IV infusion of glucose with a glucose infusion rate, GIR. In practise this is a cumbersome and complex task. A typical test period extends over two hours, where a considerable number of blood samples are taken (DeFronzo *et al.* 1979; Elahi 1996; Hansen 2004). If the course of the hepatic glucose output, HGO under the clamp is wanted, tracers need to be added to separate the exogenous and endogenous glucose fluxes, thus increasing the complexity of the method.

Hyperglycemic glucose clamp, HGC

With the hyperglycemic glucose clamp method, basal glucose concentration is acutely raised by a priming infusion of glucose to a hyperglycemic level. The steady-state glucose level is then maintained by GIR. The test gives a typical biphasic pattern in the insulin response, with an early or first phase occurring within the first 5-10 min, and a consecutive linearly rising late or second phase (Elahi 1996). Typically the average incremental insulin concentration obtained in the first 5-10 min after the glucose infusion, is used as a model-independent index, AIR (Acute Insulin Release) for the first phase insulin secretion. Different model-independent measures for the second phase can also be calculated.

Hyperinsulinemic-euglycemic clamp

In this test, insulin is acutely raised above basal value and maintained there throughout the test period. Glucose is maintained at constant levels by GIR. This test is denoted the gold standard for measuring insulin sensitivity, where the ratio between GIR and the steady state insulin level is taken as a measure of the insulin sensitivity (DeFronzo *et al.* 1979; Elahi 1996).

Fluxes during a glucose clamp

Assuming that a steady state glucose level is obtained, which as noted above is not an easy task, the glucose infusion rate, GIR is described by (Hallgreen *et al.* 2008)

$$GIR = J_{upt} - HGO \tag{2.1}$$

where J_{upt} is the sum of the saturable peripheral tissue (muscle and adipose tissue) uptake, J_{PT} (ignoring a possible efflux of interstitial glucose) and the (usually constant) uptake by the brain, $J_{brain} = 1.14$ mg kg^{-1} min^{-1}, and HGO is the hepatic glucose output (including renal contribution) (Hallgreen *et al.* 2008).

The glucose uptake by the peripheral tissues, J_{PT} is saturable and can be described by the Michëlis-Menten relation (Hallgreen *et al.* 2008)

$$J_{PT} = V_{GLUT} \frac{G}{K_M + G} \tag{2.2}$$

where V_{GLUT} is the maximal transport capacity of both the insulin-independent glucose transporter GLUT1 and the insulin-dependent glucose transporter GLUT4, G is glucose concentration, and K_M is a Michaëlis-Menten constant assumed equal for both GLUT1 and GLUT4 with K_M = 5 mM (Hallgreen *et al.* 2008).

Assuming V_{GLUT1} to be constant, V_{GLUT1} = 0.78 mg $kg^{-1}min^{-1}$ (Hallgreen *et al.* 2008), the effect of insulin, I on glucose uptake can be described by

$$V_{GLUT4} = \frac{V_{max} I^2}{K_I^2 + I^2} \tag{2.3}$$

with V_{max} = 20 mg kg^{-1} min^{-1} and K_I = 180 pM (Hallgreen *et al.* 2008)

The effect of insulin on HGO is assumed hyperbolic (Groop *et al.* 1989; Hallgreen *et al.* 2008; Hansen 2004) and described by

$$HGO = \frac{HGO_{max} K_{HGO}}{K_{HGO} + I} \tag{2.4}$$

with HGO_{max} = 4.7 mg $kg^{-1}min^{-1}$ being the HGO at zero insulin, and K_{HGO} = 30 pM (Hallgreen *et al.* 2008; Hansen 2004).

Fig. 2.2 shows the relation between the fluxes determining GIR, as given by Eqs. (2.1)-(2.4) and different values of insulin, assuming the basal state G = 5 mM and I = 40 pM (Hallgreen *et al.* 2008). In the beginning, with small to moderate insulin, GIR and insulin increases almost linearly, whereas the relation saturates for large insulin. As the insulin sensitivity is determined by the ratio between GIR and the prevailing insulin, it is seen that different values are obtained for different insulin levels. The contribution from HGO vanishes for large insulin. However in subjects with type 2 diabetes the inhibiting effect of insulin on HGO is impaired (Groop *et al.* 1989). Hence HGO will probably not be entirely inhibited in those subjects, and the HGO contribution will complicate the interpretation of the results even more.

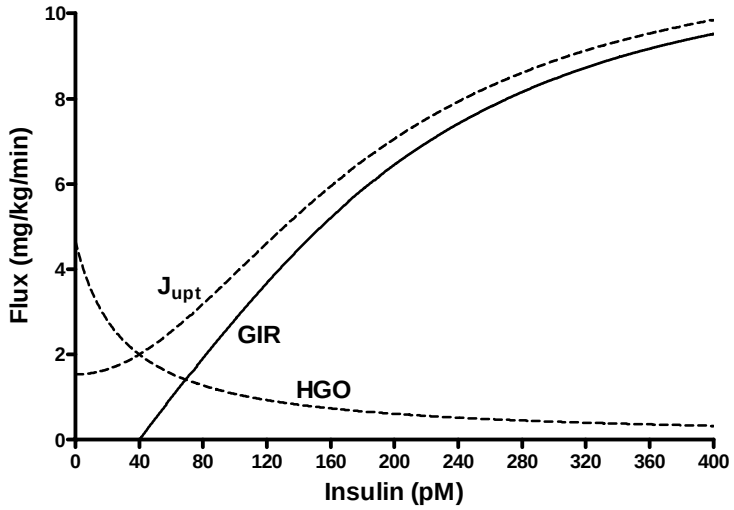

Fig. 2.2: Relation between the total glucose uptake J_{upt}, HGO and GIR as described by Eq. (2.1), for different values of insulin. Adapted from (Hallgreen *et al.* 2008).

2.1.3 Graded Glucose Infusion Test, GGIT

A typical setup for the GGIT is consecutive 40 min glucose infusions steps of increasing size, such that the glucose level rises gradually. Glucose and C-peptide concentrations are measured, and insulin secretion rate is calculated by deconvolution of the C-peptide data (Polonsky *et al.* 1986). The mean glucose and mean insulin secretion rate at each end are plotted against one another to obtain a dose-response relation between glucose and insulin secretion by the beta cells (Byrne *et al.* 1995). An up&down GGIT has been analysed with the C-peptide minimal model (Toffolo *et al.* 2001). The GGIT yields a more physiological glucose stimulation profile than the other IV tests. However, its level of complexity makes it less attractive as a routine test.

2.1.4 Intravenous glucose tolerance test, IVGTT

IVGTT is the most common test for assessment of first phase insulin secretion.
The typical procedure is that after an overnight fast (8-12 h) a bolus of glucose is injected intravenously over 1 min, with a standard dose around 0.3 mg/kg body weight. Sampling is done frequently in the beginning (regular-FSIGT) of glucose, insulin and often also C-peptide concentrations. The regular-FSIGT also comes in an insulin-modified version (Insulin-modified-FSIGT), were at time t = 20 min a non-primed infusion of insulin begins and lasts for 5 min, infused in the same vein as glucose was injected. Infusion for 5 min is used instead of a bolus, because a bolus will give very high levels of the hormone, resulting in saturation of the insulin receptors.

Modelling analysis could therefore underestimate the insulin effect. Furthermore, the slower infusion compared to a bolus gives a better distribution of the hormone.
The IVGTT elicit a brisk stimulation on the beta cells for measuring intrinsic beta cell response to a fast increase in glucose concentration. However, an IVGTT can often only be used to asses one phase of insulin secretion and cannot stand alone as a single test of beta cell function. Furthermore the stimulation pattern is un-physiological and, hence, does not resemble normal physiological stimulation of the beta cells.

IVGTT and glucose kinetics

IVGTT is also used to assess glucose kinetics and effects of insulin upon the kinetics. The most widely used method for assessing glucose kinetics is the description of the IVGTT interpreted with the glucose minimal model (Bergman *et al.* 1979). One major problem with the IVGTT is its transient nature (Hallgreen *et al.* 2008). The mean transit time for the systemic blood circulation is around 1 min, but blood returning from e.g. the legs has a mean transit time in the order of 10-15 min. The spread in mean transit times result in an initial distribution phase corresponding to an apparent glucose dependent initial glucose uptake. Hence the initial glucose uptake may be overestimated.

Another problem with the IVGTT is the desire to describe the glucose kinetics by exponential decline, i.e. using linear modelling of glucose uptake. The glucose dynamics after an IVGTT can in a simplified manner (Hallgreen *et al.* 2008) be described by

$$V_G \frac{dG}{dt} = V_{GLUT}\left(\frac{G_b}{K_M + G_b} - \frac{G}{K_M + G}\right) \qquad (2.5)$$

where V_G is the glucose distribution volume and G_b is the basal (pre-test) glucose concentration.

Fig. 2.3 shows the dynamics of glucose after a typical IVGTT described by Eq. (2.5). The glucose decline is more linear than exponential, especially at the beginning, hence describing the decline as exponential is wrong and may lead to wrong estimates of glucose uptake (Hallgreen *et al.* 2008)

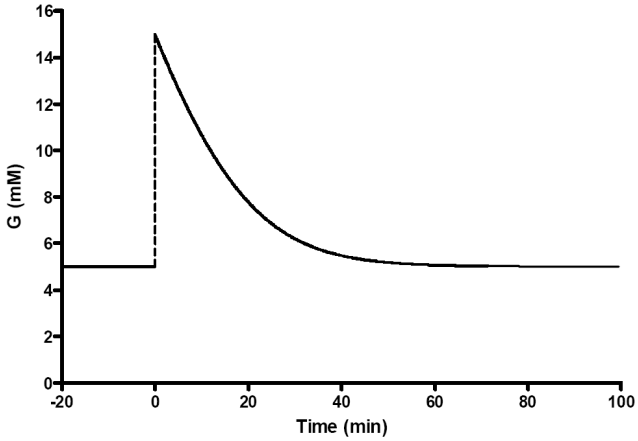

Fig. 2.3: The dynamics of glucose after a typical IVGTT with peak glucose at 15 mM. Adapted from (Hallgreen *et al.* 2008)

The attempt to describe the glucose decline after an IVGTT by exponentials leads to another major problem. In the paper by Ferrannini *et al.* (Ferrannini *et al.* 1985), the authors proposed a three compartment model describing the glucose kinetics, based on the observation that three exponentials could describe (fit) the data well. They were able to show that a two-compartment description would suffice, described by a fast and slow pool. However, a closer look at the initial distribution volume of glucose, IDVG reveals some problematic issues concerning the compartmentalization according to rate constants. IDVG is calculated by giving an intravenous, IV bolus infusion of 5 g glucose and measure the arterial blood glucose for 3 to 10 min after (Hahn 2005; Hirota *et al.* 1999), as illustrated in Fig. 2.4(a).

Sucrose is used to measure extracellular fluid, ECF volume, as it is poorly metabolised (Ishihara and Giesecke 2007). The initial distribution volume of sucrose, IDVS is the same as for glucose as seen in Fig. 2.4(b), hence IDVG is a measure of ECF volume, and correlates with the cardiac output as seen in Fig 2.4(c). Thus IDVG is dependent on the blood flow. A high perfusion will resemble a large IDVG and a low perfusion will resemble a small IDVG. The result is that the fast kinetics of glucose is highly dependent on the blood flow, hence large discrepancies are to be expected under different experimental conditions.

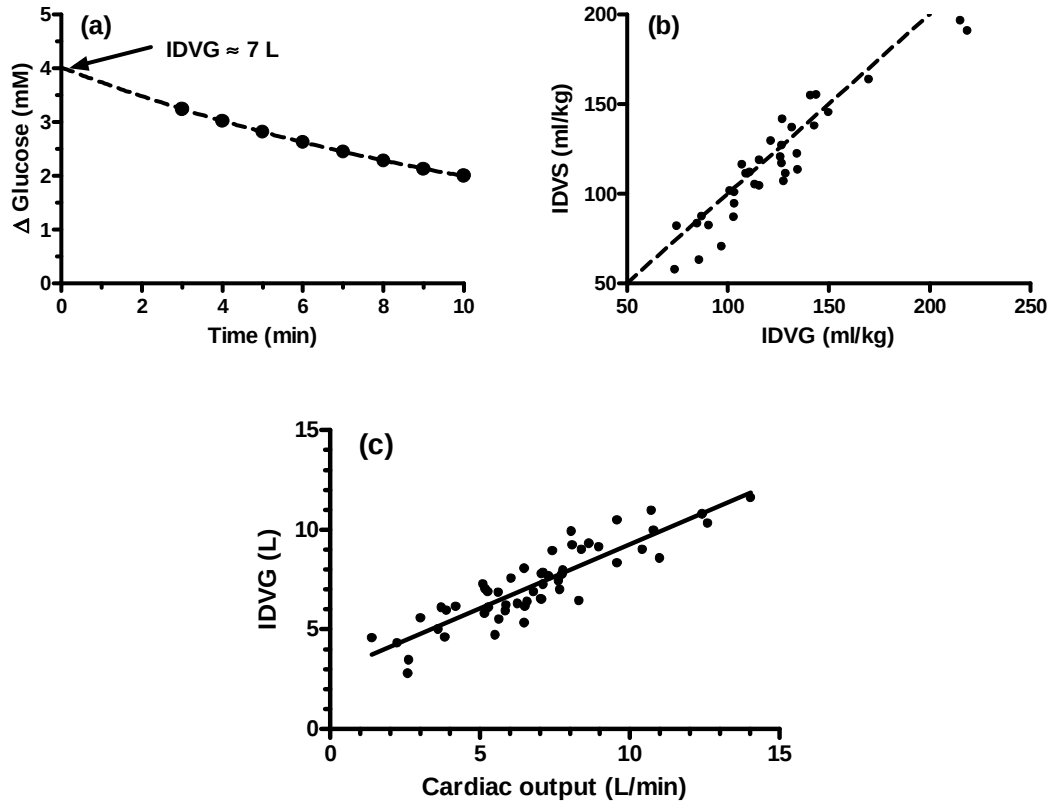

Fig. 2.4: (a) Illustration of the calculation of the initial distribution volume of glucose, IDVG after a 5 g IV bolus infusion of glucose. (b) The initial distribution volume of sucrose, IDVS correlates strongly with IDVG. (c) IDVG correlates with the cardiac output. Adapted from (Ishihara and Giesecke 2007).

2.1.5 Oral glucose tolerance test, OGTT and meal tolerance test, MTT

In a standard oral test the subjects receive glucose orally (≈75g) after an overnight fast either as pure glucose, OGTT or within a meal, MTT. (Ahren and Pacini 2004; Ferrannini and Mari 2004; Mari *et al.* 2002a). Measurement of plasma glucose, insulin and possibly C-peptide is then typically recorded for 2-3 hours in OGTT and 4-5 hours in MTT, after the glucose administration. Different empirically derived indices can be obtained, typically ratios between insulin and glucose levels or area under the curve, AUC ratios. Probably the most widely used empirically derived measure is the insulinogenic index that gives the ratio between the increments at 15 or 30 min for insulin and glucose. The empirically derived indices are simple to calculate, but it is difficult to relate them to specific measures of beta cell function.

The appearance of glucose in the intestine elicit a complex interplay between hormonal and neural effects, with the most prominent case being the incretin effect (Holst *et al.* 2008), i.e. the enhancement in insulin response due to oral glucose administration as compared with IV glucose insulin response, cf. Fig. 2.5. As different amount of glucose ingested lead to similar glucose excursions, another way to describe the incretin effect is that it keeps glucose excursions at certain low levels regardless of the ingested amount of glucose (Holst *et al.* 2008).

The most important incretin hormones are glucagon-like peptide-1, GLP-1 and glucose-dependent insulinotropic polypeptide, GIP. As illustrated in Fig. 2.6, these hormones can exert a multiplicity of actions on different organs. Besides the described incretin effect on the insulin secretion, GLP-1 has been shown to strongly decrease glucagon secretion, inhibit gastric emptying, appetite and food intake. All these actions are designed to lower the glucose excursions. On the contrary, besides the incretin effect, GIP has been shown to increase glucagon release. Hence even though the enhancement of insulin release seems to be the most important role of the incretin hormones, they both trigger other complex mechanisms that differ in their actions. Furthermore some of their actions (primarily GLP-1) may be mediated by the nervous system (Holst *et al.* 2008).

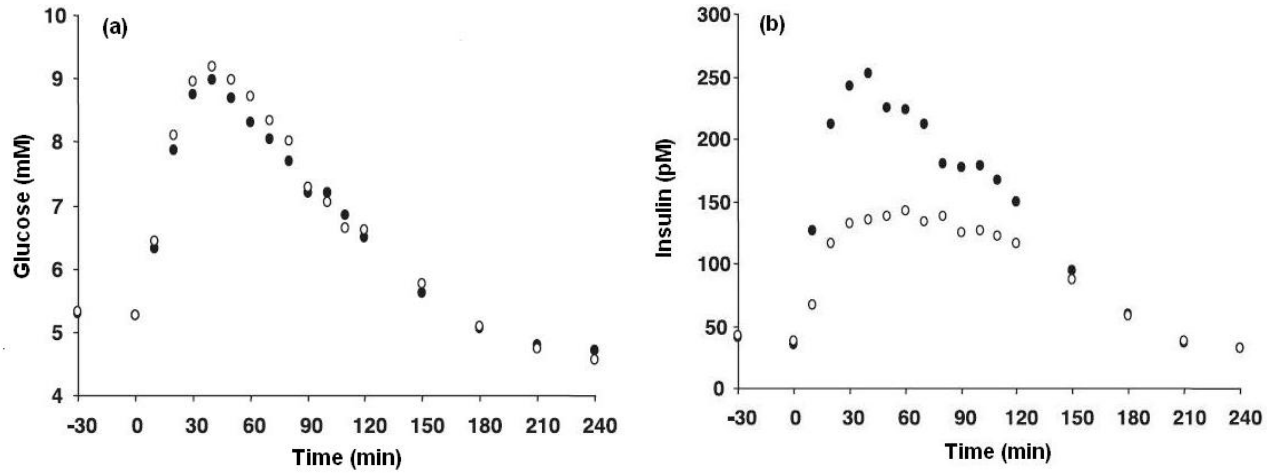

Fig. 2.5: Illustration of the incretin effect. (a) Plasma glucose and (b) plasma insulin concentrations in healthy subjects receiving an oral glucose test (filled dots) and IV glucose infusion to mimic oral glucose excursion (circles). The incretin effect is the difference between the two insulin responses Adapted from (Campioni *et al.* 2007).

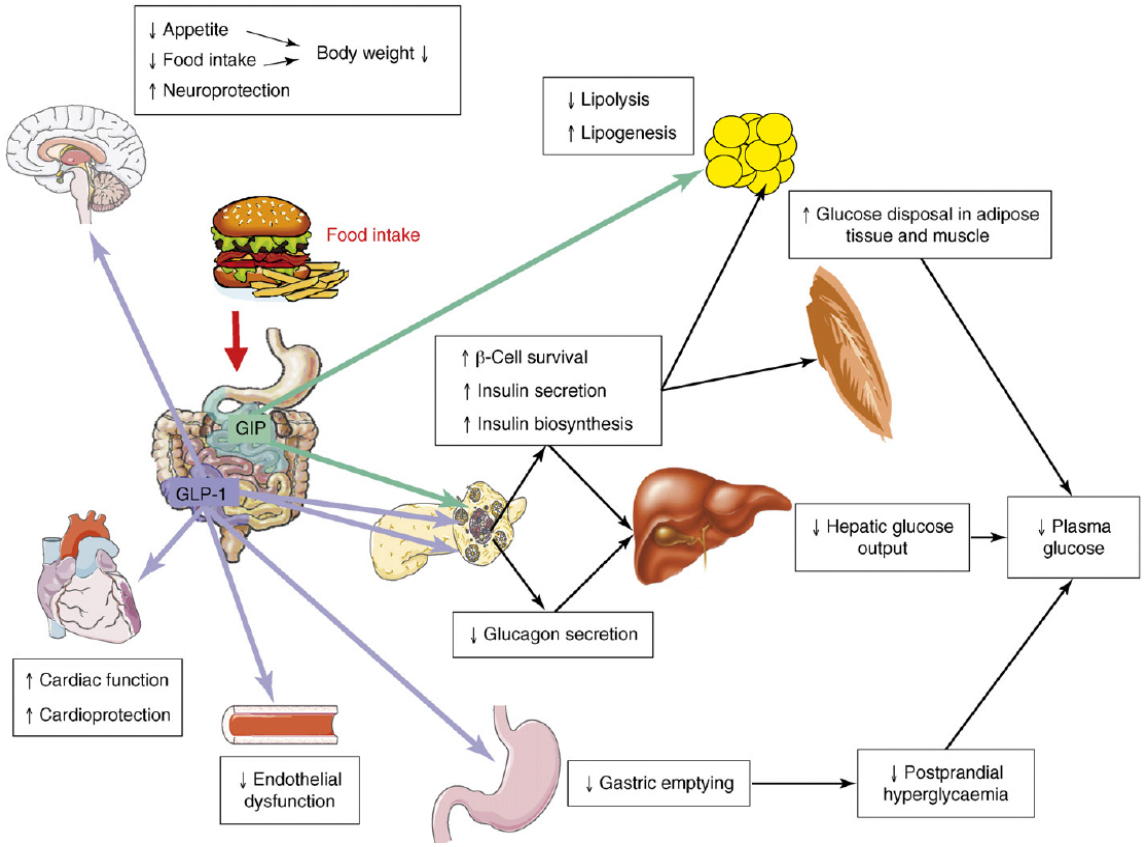

Fig. 2.6: Illustration of the multiplicity of actions exerted on different organs by the incretin hormones, GLP-1 and GIP. Details can be found in Holst *et al.* 2008.

2.1.6 Comparison of the tests

The intravenous glucose tolerance tests, i.e. the IVGTT, HGC, and GGIT are all non-physiological and cumbersome to perform. All three tests can with the application of mathematical models be used to assess both insulin action and beta cell functionality, cf. Table 2.1. However as pointed out above, the outcomes of an IVGTT and HGC must be interpreted with caution. Furthermore, even though the GGIT elicit a more physiological glucose stimulation pattern than the other IV tests, it still does not evaluate the physiological responses triggered by oral administration of glucose. The oral tests, i.e. the OGTT and MTT, triggers the complex pathways of the entero-insular axis, and hence results in a true physiological response, however the OGTT lacks the actions of amino acids and fatty acids, as compared with the MTT with all nutrients included. Compared with the IV tests, the oral tests are much easier to perform, however the complexity of the actions of the different hormonal and neural pathways triggered by the oral routes makes modelling work a vital, though difficult, component for the interpretation of the outcome of these tests. The basal state is the easiest

test for assessing measures of insulin action and beta cell functionality. However the basal state is only one single point in the highly dynamical glucose-insulin system, and cannot stand alone as a measure of insulin action and/or beta cell functionality.

2.2 Mathematical tests

From the different methods described in the previous sections used to stimulate the beta cell with different pattern of glucose levels, several different empirically-derived indices representing beta cell functionality can be calculated, where perhaps the most widely used are the AIR index of first phase insulin release derived mostly from the IVGTT and the HGC, and the insulinogenic index derived from the oral tests. Although these indices are easy to calculate their use is limited and the obtained values must be interpreted cautiously. Much more specific and clear information about the functionality of the beta cell can be gained when the protocols are interpreted with the help of a mathematical model that relates the glucose change to indices that can describe the pattern in insulin secretion, i.e. beta cell function.

2.2.1 Insulin secretion vs. beta cell function

Although the terms insulin secretion and beta cell function often is used interchangeably, insulin secretion will here refer to absolute insulin secretion, whereas beta cell function refers to the ability of the beta cells to respond to stimuli. The assessment of insulin secretion (absolute) is most often performed by the use of the “raw” insulin or C-peptide concentration values (Hovorka and Jones 1994; Mari 2006). Use of insulin concentration to assess true insulin secretion is limited by the fact that insulin undergoes a high (>50%) and concentration dependent hepatic extraction (Caumo *et al.* 2007; Hovorka and Jones 1994; Meier *et al.* 2005; Toffolo *et al.* 2006). However under dynamic situations, the insulin concentration may be a reasonable estimate of the secretion rate, due to the fast elimination (half-time 5-10 min) of insulin in plasma (Luzi *et al.* 2007). In spite of this, insulin concentration reflects post-hepatic insulin appearance, and is therefore not a true measure of insulin secretion. C-peptide is secreted in equimolar amounts as insulin, and in contrast with insulin, not cleared by the liver to any significant extend (Hovorka and Jones 1994; Luzi *et al.* 2007). Thus C-peptide offers a way to assess pre-hepatic, and thus actual, insulin secretion. However the elimination of C-peptide in plasma is slow (half-time around 30 min), thus fast changes in secretion pattern is more pronounced in the insulin data, than in the C-peptide data. Furthermore in order to

determine insulin secretion from C-peptide data a model of the C-peptide kinetics is needed, and a two-compartment model has been found to be appropriate (Eaton *et al.* 1980). The deconvolution method proposed by (Eaton *et al.* 1980) to assess the insulin secretion rate where later validated by (Polonsky *et al.* 1986), and has become the gold standard method for the assessment of the insulin secretion rate (Kjems *et al.* 2000). To avoid the need of a bolus injection of C-peptide for each subject, in order to calculate the kinetics parameters, the population based approach proposed by (Van-Cauter *et al.* 1992) can be used, as the error it introduces is no larger than the intra-individual variation of the kinetic parameters. A recent study has however shown that large insulin concentration values induced by exogenous insulin administration increases the clearance of C-peptide (Bouche *et al.* 2010). Thus it may be that methods based on C-peptide data to assess the insulin secretion give rise to (modest) underestimation of the secretion rate during dynamic assessments.

2.2.2 Mathematical modelling of the beta cell function

Some of the earliest work done on mathematical modelling of beta cell function dates back to the work of Grodsky (Grodsky 1972) and the work of Cerasi *et al.* (Cerasi *et al.* 1974). Both groups formulated models based on the biphasic nature of the beta cell, i.e. that the beta cells respond to an abruptly and elevated glucose by a fast initial release (first phase), lasting 5-10 min followed by a slowly rising second phase.

The group of Grodsky originally formulated a two-pool model, and postulated that the first phase release was due to emptying of insulin granules from a labile pool, whereas the second phase slowly rise was due to a glucose sensitive refill (provision) of insulin from an insulin precursor pool to the labile pool. In order to explain the increasing first phase secretion when glucose was applied as staircase stimulation, Grodsky hypothesised that the insulin in the labile pool was contained in different granules eliciting different glucose threshold values, hence when glucose is progressively increased more insulin containing granules will become active and release insulin. This threshold hypothesis or package-storage hypothesis was found able to explain the glucose rate dependency of the first phase insulin release (Licko 1973).

The work of Cerasi *et al.* is based on entirely different assumptions. They noted that consecutive glucose stimulation with a short time interval in between could inhibit the secretion pattern. Hence Cerasi *et al.* proposed that glucose elicit three time-dependent effects upon the beta cells; An immediate effect characterising the first phase; an inhibiting effect responsible for the

decline in secretion pattern upon consecutive stimulation with short time interval in between, and a potentiating effect responsible for the development of the second phase (Nesher and Cerasi 2002). Whereas the model by Grodsky *et al.* is based on the assumptions of insulin being confined within different compartments, the model by Cerasi *et al.* is based on the assumptions that glucose generates different time-dependent signals in the beta cells modulating the secretion pattern. Both theories are despite, or because of, their entirely different grounds, the cornerstones of the current mathematical modelling of beta cell function. The threshold hypothesis by Grodsky is widely applied in the concept of the minimal modelling of the beta cell function, now referred to as the C-peptide minimal model, and this model has been applied to both IV glucose tests (Toffolo *et al.* 1995; Toffolo *et al.* 1999; Toffolo *et al.* 2001) as well as oral tests (Breda *et al.* 2001; Breda *et al.* 2002; Steil *et al.* 2004). Recently a model has been proposed that combines the present knowledge regarding the subcellular events occurring in the beta cells upon glucose stimulation with the threshold hypothesis applied to the single beta cells (Pedersen *et al.* 2008). The ideas of Cerasi *et al.* have been applied in the work of Mari *et al*. (2002a, 2002b) where they especially have found the concept of the potentiation effect relevant with the description of beta cell function throughout 24 h living.

Fig. 2.7(a) shows the structure of the C-peptide minimal model and Fig. 2.7(b) shows the structure of the model proposed by Mari *et al*. The most important difference between these two strategies lies in the description of the dose-response relation between glucose and insulin release. The C-peptide minimal model introduces a delay between glucose and resulting release, whereas the dose-response relation between glucose and release is modulated by a time-varying potentiation factor, generated by various signals. In relation with meals, these potentiation factor signals have been proposed to be related with the actions of incretin hormones.

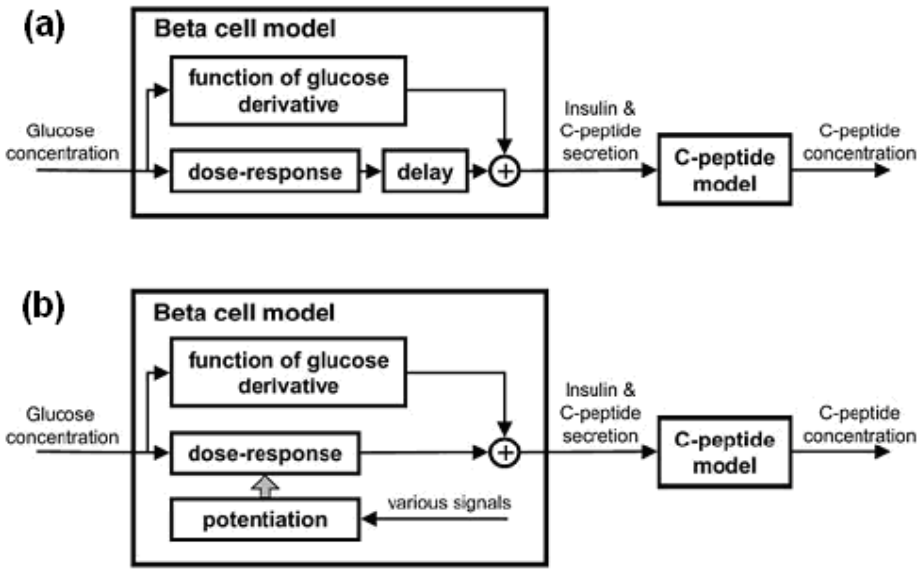

Fig. 2.7: (a) Structure of the C-peptide minimal model. (b) Structure of the model proposed by Mari *et al*. 2002. Adapted from Ferrannini and Mari (2004).

Other models to describe beta cell functionality during a meal have been proposed. They differ essentially only in the way the different components given in Fig. 2.7(a) are combined. The model by Hovorka et al. (1998) to assess beta cell function after a MTT is the simplest representation of the structure given in Fig. 2.7(a). The model includes a dose-response relation between C-peptide secretion and glucose, presented as a linear function of glucose. The model assumes no delay between glucose stimulation and secretion, and no glucose derivate component either. The model by Cretti et al. (Cretti *et al.* 2001) to describe beta cell function after OGTT using C-peptide data employs a delay between glucose stimulation and a linear function of glucose, with no glucose derivative component.

Hence current mathematical models to assess beta cell functionality are largely based on either the C-peptide minimal model concept, or the concept of potentiation as applied by Mari *et al*.

2.2.3 Intracellular mechanisms behind biphasic insulin secretion

Current knowledge of the intracellular mechanisms responsible for the biphasic nature of insulin secretion seen when a hyperglycemic stimulus is applied to the pancreatic islets are in favour of two non-exclusive views. One being that the insulin granules are contained within functionally distinct pools, where the first phase is explained by the emptying of granules from a readily releaseble pool, RRP, and where the second phase is explained by a glucose dependent mobilization of granules from a reserve pool, with consecutive events of docking to cell membrane, priming and release

(Rorsman and Renstrøm 2003). These ideas dates back to the ones put forward by (Grodsky 1972), however with more detailed knowledge of the individual molecules partaking in the exocytotic events. The other view concentrates on the intracellular pathways of signal generation for insulin secretion, cf. Fig. 2.8 (Henquin 2009). Two pathways are considered to be activated upon glucose stimuation. The well-studied and well-recognised triggering pathway, involving accelerated glucose metabolism, ATP generation (with a resulting decrease in ADP), closure of ATP-sensitive K^+ channels, depolarisation, opening of voltage-sensitive Ca^{2+} channels, with a resulting increase in cytosolic Ca^{2+} concentration, $[Ca^{2+}]_c$.

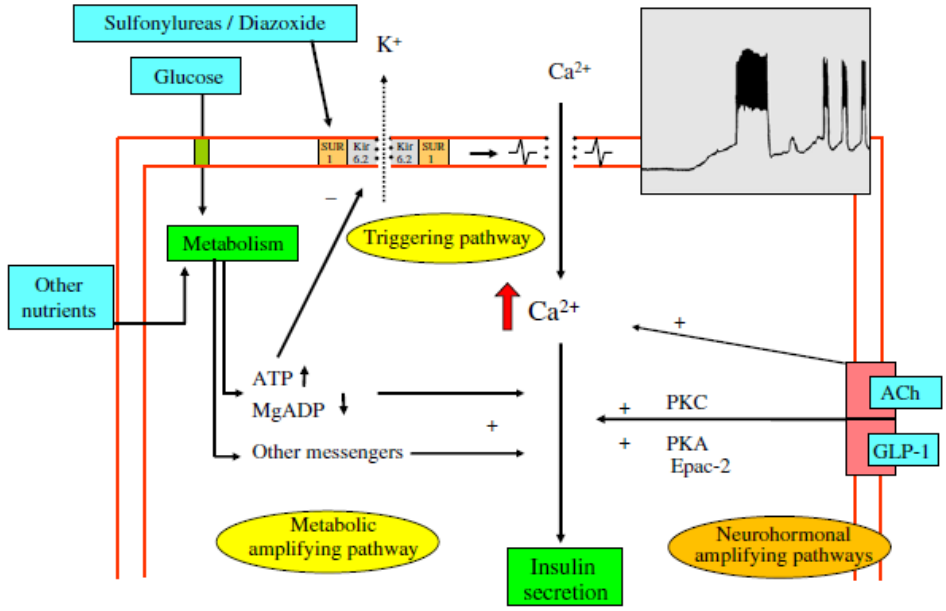

Fig. 2.8: Schematic representation of the triggering and metabolic amplifying pathways that triggers insulin secretion upon stimulation with glucose. Also illustrated is the neurohormonal amplifying pathways. Dotted line indicates a decreased flow. +, stimulation; -, inhibition. Adapted from (Henquin 2009).

The other pathway, the metabolic amplifying pathway is far less understood. For this pathway to be active, glucose needs to be metabolised, and cytosolic Ca^{2+} concentration needs to be increased. Hence normally this leaves a hierarchical regulation where the triggering pathway preceeds the amplifying pathway. The messenger(s) responsible for the metabolic amplifying effect of glucose have not been discovered, but ATP could possibly also serve as a messenger for this pathway (Henquin 2009). The triggering pathway is important for both phases of insulin secretion, and the amplifying pathway takes part in the second phase of insulin secretion. Interestingly the author

proposed that the amplifying pathway also influences the first phase, and estimated the contribution to be around 50%. That the amplifying pathway is rapid and augments both the first and second phase was given further support in two recent studies (Mourad *et al.* 2010). In these studies the authors also put forward the hypothesis that the amplifying pathway corresponds to acceleration of the priming process, giving release competence to the granules.

An explanation to the non-sense to glucose and especially the loss of first phase insulin secretion in subjects with type 2 diabetes from the view of the triggering and amplifying pathways is not straightforward. However as glucose metabolism in the beta cell is diminshed in type 2 diabetets, as seen by reduced glucose transporter capacity as well as glucokinase activity (Del *et al.* 2005), the signals generated by the triggering and amplifying pathways are dimished. In combination with a decrease in RRP (Rorsman and Renstrøm 2003), this would result in diminshed first phase and a blunted second phase.

Non-glucose stimuli such as arginine are able to elicit a first phase response, even though glucose-stimulated insulin secretion is absent or severly impaired, but the effect is potentiated by glucose (Ishiyama *et al.* 2006). Arginine is very slowly metabolished by the beta cell, and its products do not elicit insulin secretion (Ishiyama *et al.* 2006). However Arginine is a cation, i.e. it is positive charged, hence when it enters the beta cell it depolarises the cell. Thus it depolarises the membrane, and enhances insulin secretion in-dependent of ATP generation. Increasing glucose concentration will trigger the amplifying pathway, and eventually maybe also the triggering pathway. Hence the glucose potentiation may thus provides two compotents for enhancement of the arginine-induced insulin secretion, the potentiation of the secretion due to the generation of amplifying signals, and the potentiation due to the increase of cytosolic Ca^{2+} via the triggering pathway.

In this chapter the most commonly used protocols and tests for the assessment of beta cell function and insulin action have been described and some problematic issues concerning these have been highlighted. More specifically it has been shown that:

- ***The basal state cannot be used to evaluate a connection between beta cell function and insulin action. The basal state only reflects one single point in the highly dynamical glucose-insulin interaction pathway, it may however give a rough impression of the state***
- ***The IV glucose tests can be standardised, however they are cumbersome and un-physiological. The hyperinsulinemic-euglycemic glucose clamp is the gold standard for assessing insulin action. However due to the inhibition of the hepatic glucose production by insulin and due to the saturability of glucose uptake, no well-defined measure of insulin action can be obtained, not even for the gold standard method.***
- ***The fast kinetics during an IVGTT results in overestimation of the initial glucose uptake due to the spread in mean transit time for blood return and/or due to the (wrong) assumption of linear kinetics of glucose uptake. Furthermore the fast kinetics is highly dependent on the blood flow which makes the assessment of the initial glucose uptake even more problematic and highly variable from time to time.***
- ***The physiological OGTT and MTT trigger a complex interwoven network of hormones and neural pathways that elicit effects on both the beta cell functionality and the insulin action. This makes mathematical modelling vital for the interpretation of these tests.***
- ***State-of-the-art mathematical models to quantify beta cell functionality during oral tests have their roots in the description of the biphasic insulin release pattern during square-wave glucose stimulation by classic control theory***
- ***The models can essentially be split up in two directions: The "storage-limited" or the "signal-limited" approaches.***
- ***The models differ primarily on the description of the dose-response relation between glucose changes and corresponding changes in insulin release taking into account that the relation between glucose and insulin release is not static.***

Chapter 3

Minimal models analysis of Owens MTT data

An analysis of MTT data with the oral glucose and C-peptide minimal models with the largest number of subjects with type 2 diabetes presently reported in literature is presented.
The estimates for each of the indices of insulin action and beta cell functionality all constituted a large interval both within the group of subjects with type 2 diabetes, and within a healthy group. Despite this a clear distinction between the two groups was evident from the disposition indices plot.

MTT data from a small subset of subjects with type 2 diabetes that were followed at year 0, 1, and 5, to record disease progression and treatment effect, was also analysed with the minimal models. Values for indices of insulin action and beta cell functionality all increased from year 0 to year 1, demonstrating treatment effect. From year 1 to year 5, the value of the indices decreased, demonstrating decline in treatment effect and/or progression of disease. However no clear pattern and no clear difference between the years were found from the disposition indices plot.

3.1 Presentation of Owens MTT data

The Owens MTT data refers to a large database of data from subjects with type 2 diabetes who were subjected to a standard meal tolerance test, MTT. The database was constructed by Dr. David Owens and colleagues, in collaboration with Novo Nordisk A/S. Around 400 subjects were followed from diagnosis start (year 0), and a subset of those through visits at year 1, 2, 5, 10, 15 and 20. At each visit, MTT data, like plasma glucose, insulin and C-peptide concentrations, and data like sex, age, weight, height, HbA1C were collected and recorded in the database. Standard treatments according to need were given after diagnosis at the first visit (year 0), hence subjects at year 0 were all without treatment. Unfortunately, no record of the specific treatment is present in the database. MTT data from around 80 healthy volunteers were also recorded.

3.2 Subset of data analysed

In collaboration with C. Cobelli and C. Dalla Man I have analysed subjects with type 2 diabetes subjects at first visit (year 0), and healthy subjects from the Owens database. Insulin sensitivity was assessed by the recently proposed oral glucose minimal model (Dalla Man *et al.* 2002). To assess measures of beta cell function the same subjects were analysed with the oral C-peptide minimal model (Breda *et al.* 2001; Breda *et al.* 2002; Toffolo *et al.* 2001).

Only subjects that had measurements at all sampling times, i.e. at 0, 10, 20, 30, 40, 50, 60, 75, 90, 120, 150, 180, 210, and 240 min were included in this analysis.

This restriction was used to ease the estimation process while at the same time obtaining a reliable estimate of the parameter describing the dynamic secretion phase in the C-peptide minimal model. According to Breda *et al.* (2001) and Dalla Man *et al.* (2005a) reliable estimates require samples at 10 and 20 min.

The number of subjects left then was 206 for the subjects with type 2 diabetes. Of these subjects, 18 subjects had very small or odd insulin and/or C-peptide plasma concentrations and therefore were disregarded. In 19 subjects the estimation procedure gave extremely bad fit and/or estimation of parameters, primarily with the C-peptide minimal model (not shown). These were also disregarded in the following analysis. Hence 169 subjects with type 2 diabetes were left.

For the healthy subjects, 41 subjects were left when only including those with measurements at all sampling times, and excluding extreme outliers. Most of the subjects that were disregarded were due to extremely bad fit to the C-peptide concentration as assessed by the C-peptide minimal model (not shown).

Fig. 3.1 shows the plasma concentration of glucose, insulin, and C-peptide of the 169 subjects with type 2 diabetes and Fig. 3.2 shows the corresponding plasma concentrations for the 41 healthy subjects. A small subset of subjects with type 2 diabetes who underwent MTT's at the years 0, 1, and 5 were also analysed.

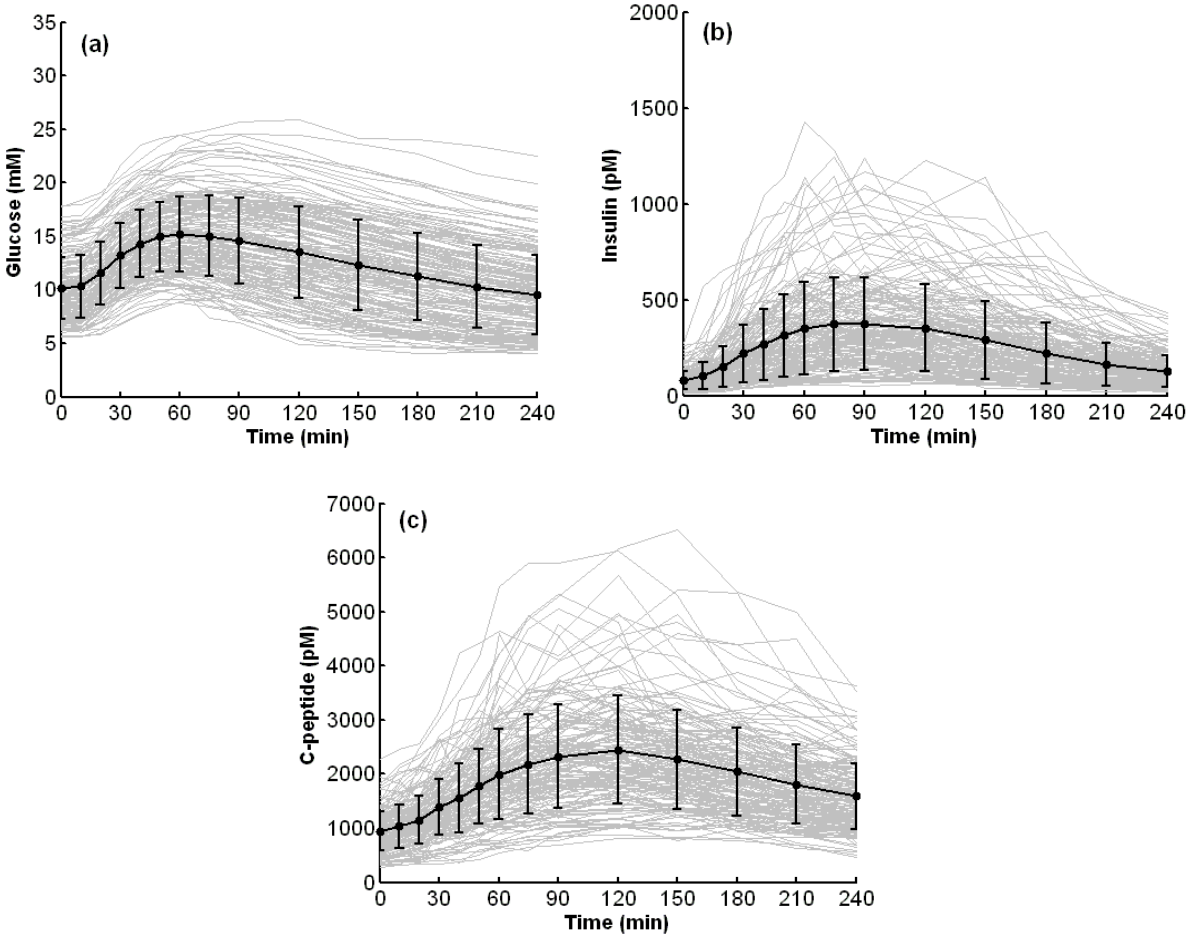

Fig. 3.1: Plasma concentrations of (a) Glucose, (b) Insulin, and (c) C-peptide after MTT of 169 subjects with type 2 diabetes. Mean ± SD (full black line). Individual concentrations are drawn with grey lines.

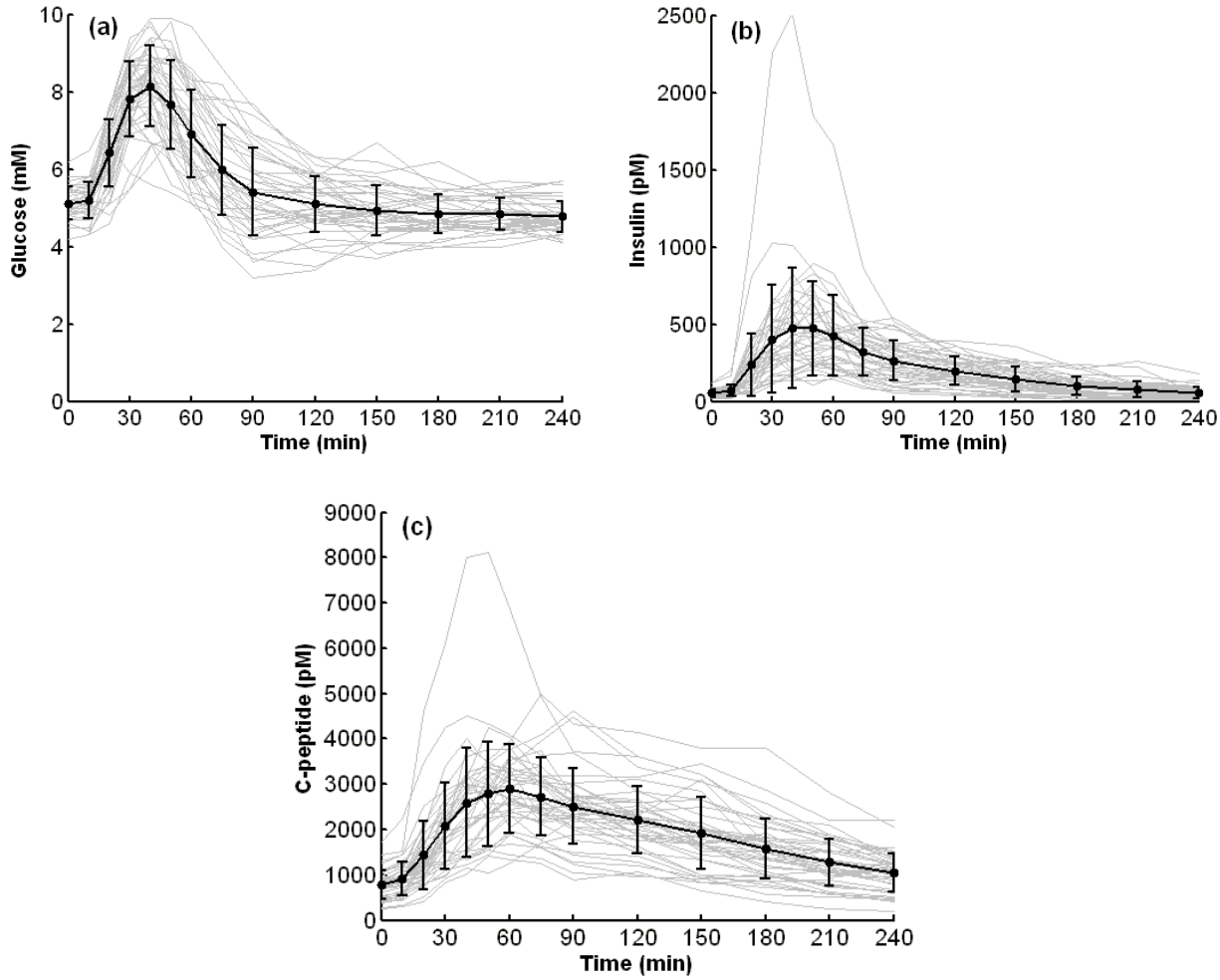

Fig. 3.2: Plasma concentrations of (a) Glucose, (b) Insulin, and (c) C-peptide after MTT of 41 healthy subjects. Mean ± SD (full black line). Individual concentrations are drawn with grey lines.

3.3 The oral glucose minimal model

The oral glucose minimal model was developed by C. Dalla Man *et al* in 2002 (Dalla Man *et al.* 2002) in order to obtain measures of the insulin sensitivity from oral routes of glucose administration. The structure of the oral model is similar to the original glucose minimal model (Bergman *et al.* 1979) that was developed to describe the glucose kinetics after an intravenous glucose tolerance test, IVGTT in dogs and later applied to humans (Bergman *et al.* 1981). This model was selected amongst six other models as being the best representation of the glucose kinetics data, according to statistical criteria and the principle of parsimony (Occam´s Razor), i.e. the model should unambiguously explain the observed behaviour in the data with the simplest structure (Bergman 2005; Bergman *et al.* 1979).

Fig. 3.3 shows the structure of the glucose minimal model where the oral version includes a description of the absorption of glucose from the gastrointestinal tract. The intravenous glucose input is represented with a dashed arrow. Plasma insulin above the basal value $I-I_b$ is the input to the model and plasma glucose is the output. The variation over time of plasma glucose is determined by the balance between the glucose administration rate, the net hepatic glucose output, J_{HGO} and the peripheral tissue glucose uptake, J_{PT}, where

$$J_{HGO} = HGO_0 - (k_5 + k_6 I')G \tag{3.1}$$

$$J_{PT} = (k_1 + k_4 I')G \tag{3.2}$$

where HGO_0 is the net hepatic glucose output at zero glucose, k_1 and k_5 are rate constants describing glucose effect on J_{HGO} and J_{PT}, respectively. k_4 and k_6 are rate constants describing the effects of insulin on J_{HGO} and J_{PT}, respectively. The effect of insulin on glucose is in both cases assumed to occur from a remote compartment, I'.

Hence in the original formulation, the minimal model equations to describe the glucose kinetics after an oral administration can be written

$$\begin{aligned}\frac{dG}{dt} &= \frac{R_a}{V} + J_{HGO} - J_{PT} = HGO_0 - (k_5 + k_6 I')G - (k_1 + k_4 I')G \\ &= \frac{R_a}{V} + HGO_0 - [(k_1 + k_5) + (k_4 + k_6)I']G\end{aligned} \tag{3.3}$$

$$\frac{dI'}{dt} = k_2(I - I_b) - k_3 I' \tag{3.4}$$

where R_a is the glucose rate of appearance from the gastrointestinal tract, V is the glucose distribution volume, k_2 is the rate constant for transfer of plasma insulin into the remote compartment and k_3 the rate constant determining the half-life of insulin in the remote compartment.

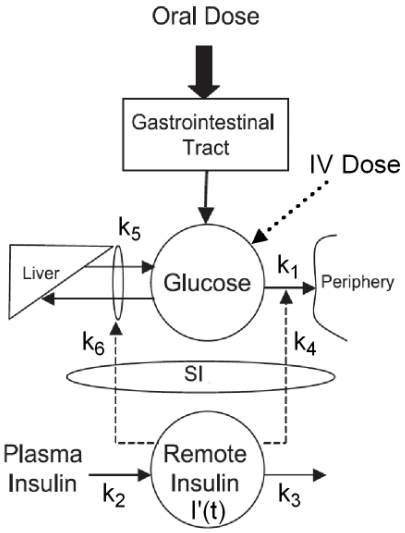

Fig. 3.3: The structure of the oral model is identical to the original model (IV) except that the oral model includes a description of the rate of appearance of glucose, R_a from the gastrointestinal tract. Plasma glucose is represented by one compartment, where the liver adds glucose determined by the net hepatic glucose balance, that is regulated by glucose and by a delayed action of insulin, represented by the remote insulin, I'(t). Adapted from Cobelli *et al.* 2007.

Assuming the steady state values G_b and I_b, Eqs (3.3) and (3.4) can with some re-parameterisation be written

$$\frac{dG}{dt} = \frac{R_a}{V} + S_G(G_b - G) - S_I XG; \qquad G(0) = G_b \tag{3.5}$$

$$\frac{dX}{dt} = p_2((I - I_b) - X); \qquad X(0) = 0 \tag{3.6}$$

where S_G is the glucose effectiveness at steady state basal insulin, S_I is the steady state insulin sensitivity, and p_2 is the rate constant determining remote insulin action. suffix "b" denotes basal (time t = 0 min) values.

Rate of appearance of glucose, R_a

To estimate the insulin sensitivity, S_I from a meal tolerance test, it is necessary to know the glucose rate of appearance. However, measuring R_a is a complex task involving the need for glucose tracers. This has previously been an obstacle for using oral glucose tests to measure insulin sensitivity. The oral glucose minimal model was developed to overcome the difficulty of measuring the absorption rate of glucose (Dalla Man *et al.* 2002). In the paper the idea was to implement a parametric representation of R_a and then reconstruct R_a from the estimated parameters. Three different models

(or parametric presentation) were tested; a piecewise-linear, a spline, and a dynamic representation. The piecewise-linear was found to be the most optimal.

In this analysis of the Owens MTT data I specified R_a as a piecewise-linear function with 7 break points (k_0, k_1 ... k_6) at 0, 20, 30, 60, 90, 180, and 240 min, i.e.

$$R_a(t) = \begin{cases} k_{i-1} + \dfrac{k_i - k_{i-1}}{t_i - t_{i-1}}(t - t_{i-1}), & t_{i-1} \le t \le t_i \quad i = 1...6 \\ 0, & \text{otherwise} \end{cases} \tag{3.7}$$

with $R_a(0) = k_0 = 0$.
Hence six parameters need to be estimated to reconstruct the R_a.

I choose the piecewise-linear representation of R_a in order to follow the estimation strategies put forward by Dalla Man *et al* (Dalla Man *et al.* 2002; Dalla Man *et al.* 2004), and also because the time course of the estimated R_a seems to be reasonable as compared with the time course reconstructed by a tracer method (Dalla Man *et al.* 2004). On the other hand, a two-exponential description of R_a could be a better choice, as only three parameters would needed to be estimated, i.e. two rate constants and an amplitude (Hansen 2004).

3.3.1 Model identification and parameter estimation procedure

With the chosen specification of R_a the total number of parameters to be estimated is 10 and these are; k_1, k_2 … k_6, V, S_G, S_I, and p_2. To achieve a robust model identification, a strategy similar to the one used in (Dalla Man *et al.* 2002; Dalla Man *et al.* 2004) was applied. This strategy involves several steps.

Firstly, to make the model a priori identifiable, the value of the parameter V was fixed and set equal to the median value of a population of subjects (Dalla Man *et al.* 2004).
In (Dalla Man *et al.* 2004) S_G was fixed to the median value of the population. However with this approach it turned out that the estimation of the insulin sensitivity index S_I and the parameter describing insulin action, p_2 was unreliable for the subjects with type 2 diabetes (C. Dalla Man, personal communication). On the other hand S_G is usually well estimated (C. Dalla Man, personal communication). Based on these experiences, in order to improve model identification, the following relation linking S_I to S_G was applied

$$S_G = \frac{GEZI}{V} + S_I \cdot I_b \tag{3.8}$$

where GEZI is the glucose effectiveness evaluated in steady state at zero insulin (Kahn *et al.* 1990). Eq. (3.8) can be realised by applying the definition of glucose effectiveness (Bergman *et al.* 1979) to the model given by Eqs. (3.5) and (3.6) at zero insulin evaluated at steady state. The GEZI parameter was fixed at 0.025 dl/kg/min.

As the rate parameter p_2 governing the remote insulin action is often difficult to estimate with precision, prior knowledge was added (maximum a posteriori Bayesian estimation) as in (Dalla Man *et al.* 2002) to increase the estimation robustness. More specifically, as the distribution of p_2 was found not to be normal-distributed, whereas the square root of p_2 was, it was assumed that $\sqrt{p_2}$ was normal distributed with mean 0.1 $min^{-½}$ and coefficient of variation, CV = 10% (Dalla Man *et al.* 2004).

Finally, to increase the estimation accuracy (numerical identifiable), the following relation was applied

$$\int_0^{240} Ra \cdot dt = \frac{f \cdot D}{BW} \tag{3.9}$$

where f (assumed known) is the fraction of glucose actually absorbed (bioavailability), D is the ingested glucose dose, and BW is the body weight.
Eq. (3.9) assumes that all glucose is absorbed by the end of the 4-hour meal test period and the relation reduces the number of parameters to be estimated by one.

Applying the above described assumptions the parameters to be estimated is p_2, S_I and five of the break points specifying R_a, hence the number of parameters to be estimated is reduced by four. The model parameters that need to be fixed are given in Table 3.1.

Parameter	Value	Meaning	Ref
V (dl/kg)	1.45	Glucose distribution volume	Dalla Man et al 287 (2004)
GEZI (dl/kg/min)	0.025	Glucose effectiveness at zero insulin	Dalla Man (Personal communication)
f (Unit less)	0.9	Bioavailability of ingested glucose	Dalla Man et al 287 (2004)
D (mg)	75000	Amount of glucose in meal	

Table 3.1: Fixed model parameters used for both the subjects with type 2 diabetes and the healthy subjects in glucose OMM.

The steps taken in order to achieve a robust model identification serve some comments.
Firstly the linkage between the glucose effectiveness, S_G and the insulin sensitivity, S_I via the glucose effectiveness at zero insulin, GEZI as given in Eq. (3.8) needs some attention.
The glucose minimal model has been found inappropriate to describe the glucose dynamics during an IVGTT with an overestimation of the glucose effectiveness, S_G and an corresponding imprecise and inaccurate underestimation of the insulin sensitivity, S_I in subjects with diabetes (Quon *et al.* 1994; Saad *et al.* 1994). This has been ascribed to the necessity of a two-compartment glucose kinetic model to describe the IVGTT (Caumo *et al.* 1996). However as described in the previous chapter, the fast kinetics during an IVGTT is dependent on the blood flow, which makes the assessment of the effect of glucose and insulin on the glucose disappearance during an IVGTT even more problematic.

Even though a one-compartment model may be appropriate to describe the slow glucose dynamics after a meal, the difficulties of estimating S_I with precision in the subjects with type 2 diabetes resemble the problems encountered with the IVGTT. The glucose effect on the glucose disappearance is described by the sum of the glucose effectiveness at basal insulin, S_G and the effect of the dynamic insulin, i.e. the product of the insulin sensitivity, S_I and the insulin action, X (Bergman *et al.* 1979). Linking S_G and S_I by the relation given in Eq. (3.8) with the GEZI parameter fixed means that S_G and S_I is not estimated independently; an overestimation of S_G will result in an overestimation in S_I and correspondingly with an underestimation. Also, insulin-independent effects are not estimated, as these are described by the GEZI parameter that has been fixed.
Furthermore as mentioned in the previous chapter and as will be discussed in chapter 5, the glucose uptake is a saturable process. Hence the glucose uptake and thereby the glucose effectiveness depends on the insulin concentration as well as on the glucose concentration.
Thus the description of constant measures of the effect of glucose, S_G and insulin, S_I on the glucose disappearance as given in the glucose minimal model is only valid in a limited range of glucose and insulin concentration values, as the glucose dependent part of the glucose uptake saturates relatively fast for increasing glucose concentration, cf. chapter 5. Therefore, the difficulties of estimating S_I in subjects with type 2 diabetes properly, seems partly to be due to a wrong description and hence overestimation of the glucose effectiveness.

The difficulty of estimating p_2 with precision is also linked with the problem of the overestimation of the glucose effectiveness and the compensatory bias between S_G and $S_I \cdot X$ when fitting the glucose concentration curve. As mentioned above, the glucose effectiveness of the

glucose disappearance is given by the sum of these two factors and hence fitting the glucose curve is primarily a task of estimating the values of these two factors. If S_G is overestimated it means that $S_I \cdot X$ must be underestimated. With no further restriction on either of the factors S_I and X it means that any value of S_I and X can be obtained, as long as the product gives a reasonable value that compensates for the estimation of S_G, e.g. one can obtain an extremely high estimate of S_I due to a compensatory reduction in the effect of X through an extremely low estimated value of p_2. In fact, the relation given by Eq. (3.8) means that an overestimation of S_G gives an overestimation of S_I, with the result of a compensating small effect of X and hence a small estimated value of p_2. In subjects with type 2 diabetes with a small insulin effect, this would result in a very low value of p_2 and hence an imprecise estimation.

The problem of estimating p_2 with precision is handled by assuming a known (prior) distribution of the values with a known mean and standard deviation. In the present estimation procedure only normal distributions can be handled. The distribution of p_2 has been found to be skewed (non-normal), whereas the square root of p_2 has been found to be (approximately) normal distributed (Dalla Man *et al.* 2004), hence the distribution of the square root of p_2 was used as the a priori information. However it must be stressed that the square root of p_2 is only approximately normal distributed, as the square root of a skewed distribution will never give a normal distribution.

The relation given by Eq. (3.9) to reduce the number of parameters to be estimated, from the rate of glucose appearance, by one, assumes that all glucose is absorbed by the end of the 4-hour test period. However as can be seen from Fig. 3.4 this is seemingly not the case, as the estimated R_a is different from zero at the end of the test period. On the other hand, integrating R_a to infinity by specifying R_a as a monoexponential decay from time 240 and onwards as in (Dalla Man *et al.* 2002), does not alter the values of the estimated parameters significantly (not shown), hence the relation given by Eq. (3.9) seems to be a reasonable approximation.

With these considerations in mind the following results of the model have to be interpreted with caution. Even though the model may give a reasonable fit to the glucose concentration data, the estimated parameter values may be misleading, in part due to doubtful assumptions, e.g. fixation of parameters, in part due to wrong description of the glucose dependency of the glucose uptake, and in part due to the compensating bias in the estimated parameters.

The parameter estimation procedure was done by applying non-linear least squares method.

Measurement error on the glucose data was assumed normal distributed with zero mean and known standard deviation, SD (CV = 10 %) (Dalla Man *et al.* 2004). The insulin data was assumed to be known without errors.

3.3.2 Results from the analysis with the oral glucose minimal model

Rate of appearance, R_a

The estimated rate of glucose appearance, R_a for the subjects with type 2 diabetes and healthy subjects are shown in Fig. 3.4(a) and Fig. 3.4(b), respectively.

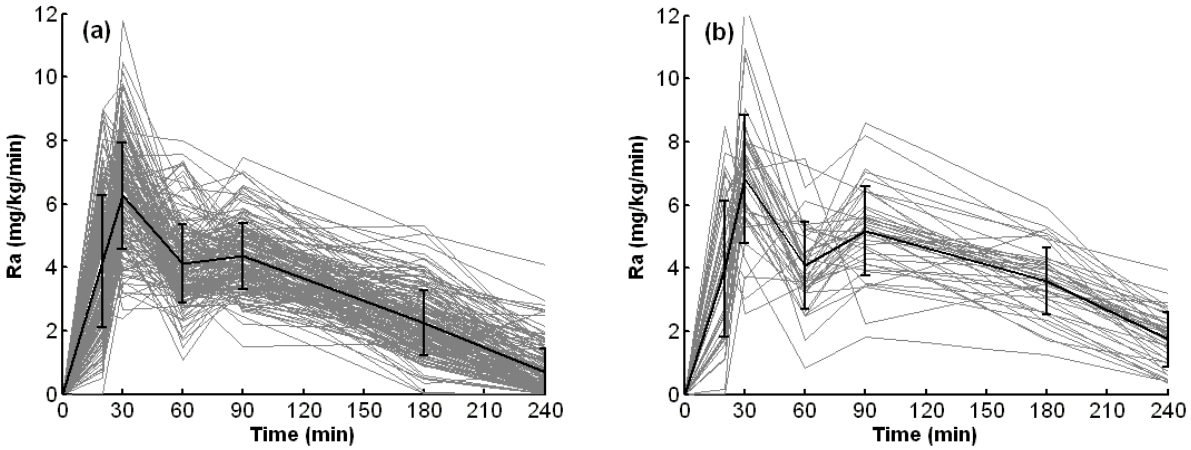

Fig. 3.4: Estimated glucose rate of appearance, R_a for (a) subjects with type 2 diabetes (N = 169), and (b) healthy subjects (N = 41). Mean ± SD (full black line). Individual estimates are drawn with grey lines.

The mean profile of the estimated R_a for both the subjects with type 2 diabetes and the healthy subjects elicit a bump that has also been found previously with this parameterisation of R_a in both MTT (Dalla Man *et al.* 2002; Dalla Man *et al.* 2004) and OGTT (Dalla Man *et al.* 2005a). No physiological explanation to this has been achieved (Dalla Man *et al.* 2002; Dalla Man *et al.* 2004), however the estimated profile of R_a by the model has previously been validated against the gold standard (tracer method), to determine R_a, and the prediction was found to be reliable both with MTT (Dalla Man *et al.* 2004) and OGTT (Dalla Man *et al.* 2005a).

Goodness of fit

The model provided a good fit of the glucose data for both the subjects with type 2 diabetes as well as the healthy subjects. The average weighted residuals did not show any systematic deviation from

zero and was at all instances of time within the range [-1, +1] for the subjects with type 2 diabetes, and only slightly escaped the range [-1, +1] at times below 30 min, for the healthy subjects, cf. Fig. 3.5.

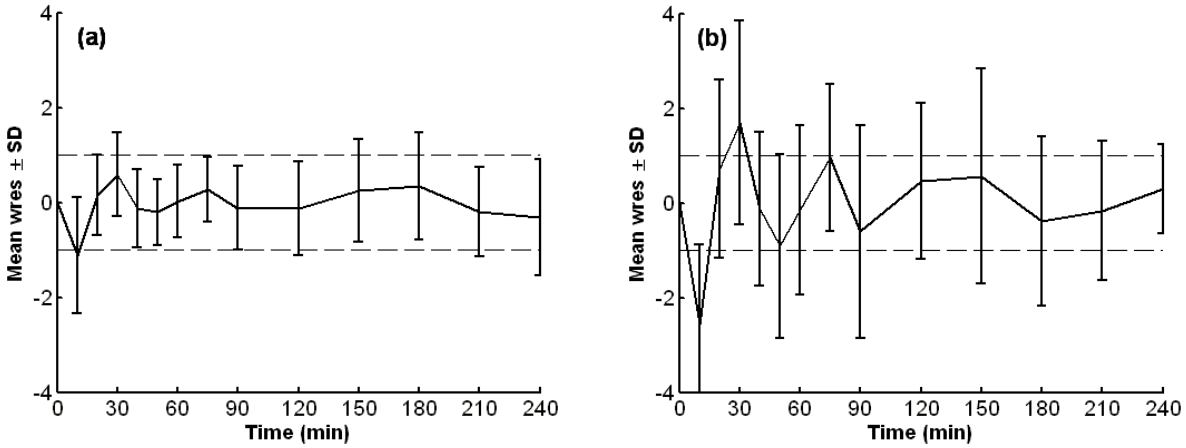

Fig. 3.5: Mean ± SD weighted residuals, wres for (a) subjects with type 2 diabetes (N = 169), and (b) healthy subjects (N = 41). Fit obtained with glucose OMM.

Insulin sensitivity

The distribution of the insulin sensitivity index, S_I is shown in Fig. 3.6. From this figure it seems that S_I is not normal distributed.

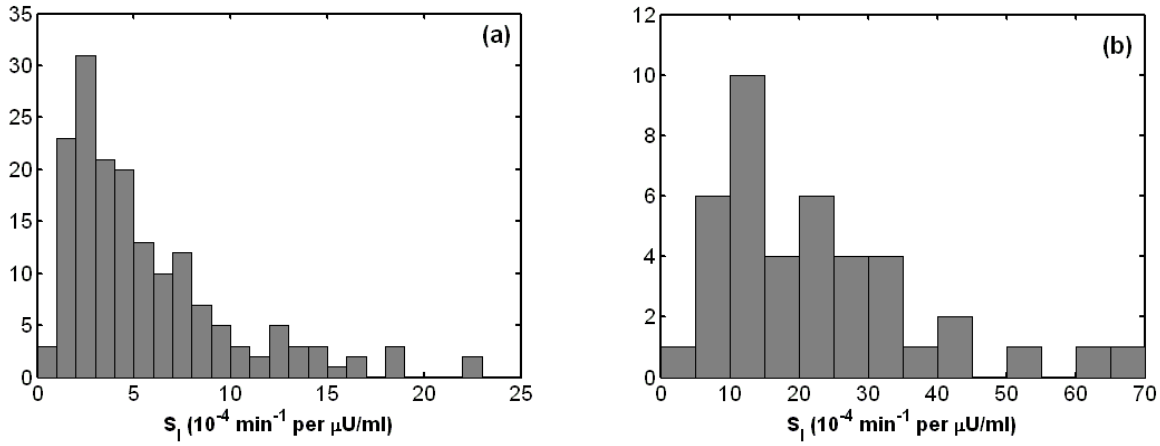

Fig. 3.6: Distribution of S_I for (a) subjects with type 2 diabetes (N = 169), and (b) healthy subjects (N = 41), estimated from glucose OMM.

For the subjects with type 2 diabetes, S_I was estimated (Mean ± SE) at $S_I = 5.7 \pm 0.3 \cdot 10^{-4}$ per µU/ml, with precision expressed as coefficient of variation of the estimate, CV = 10.6 ± 0.6 %, cf. Table 3.2. Reported literature values of S_I estimated by the glucose OMM in subjects with type 2 diabetes receiving MTT, range from $2\text{-}6 \cdot 10^{-4}$ dl/kg per µU/ml (Bock *et al.* 2006; Bock *et al.* 2007). In comparison the mean estimated S_I in the same units ($S_I \cdot V$) yields $8.3 \cdot 10^{-4}$ dl/kg per µU/ml with V = 1.45 dl/kg (cf. Table 3.1 and 3.2). As S_I is not normal distributed, it may be more reasonable to compare with the median estimate. The median estimate of S_I for the subjects with type 2 diabetes in the same units as reported in the literature yields $S_{I,median} = 6.4 \cdot 10^{-4}$ dl/kg per µU/ml. Hence the value of the median of the estimated S_I for the subjects with type 2 diabetes is reasonable compared with reported literature values.

For the healthy subjects, S_I was estimated (Mean ± SE) at $S_I = 22.5 \pm 2.3 \cdot 10^{-4}$ per µU/ml, with precision expressed as coefficient of variation of the estimate, CV = 5.3 ± 0.6 %, cf. Table 3.2. Reported literature values of S_I estimated by the glucose OMM in healthy receiving MTT, range from $11\text{-}17 \cdot 10^{-4}$ dl/kg per µU/ml (Basu *et al.* 2003; Bock *et al.* 2006; Bock *et al.* 2007; Caumo *et al.* 2000; Dalla Man *et al.* 2002; Dalla Man *et al.* 2005a; Dalla Man *et al.* 2004). In comparison the mean estimated S_I in the same units ($S_I \cdot V$) yields $32.6 \cdot 10^{-4}$ dl/kg per µU/ml with V = 1.45 dl/kg (cf. Table 3.1 and 3.2).

Hence the mean of the estimated S_I is a factor 2-3 larger than reported values in the literature. The median estimate of S_I for the healthy subjects in the same units as reported in the literature yields $S_{I,median} = 26.1 \cdot 10^{-4}$ dl/kg per µU/ml. Hence even when the literature values are compared with the median of the estimated S_I, the estimate of the healthy S_I exceed the literature values with a factor 1.5 – 2.4. At present no good explanation to this discrepancy has been found.

S_I (10^4 min^{-1} per μU/ml)	Mean ± SE (Median)	Range	CV (%) Mean ± SE	CV (%) Range
Type 2 diabetes	5.72 ± 0.34 (4.4)	0.93 - 22.93	10.62 ± 0.59	1.59 - 105.34
Healthy	22.46 ± 2.33 (18)	1.91 - 68.07	5.27 ± 0.62	0.00 - 16.02

Table 3.2: Insulin sensitivity index S_I estimates and precisions in subjects with type 2 diabetes and healthy, obtained from glucose OMM.

Remote insulin action

As previously described, a priori knowledge was added to increase the "robustness" of the estimate of p_2. As p_2 was found not to be normal distributed, but $\sqrt{p_2}$ was, $\sqrt{p_2}$ was restricted to have a known mean with known standard deviation. The estimate and precision of $\sqrt{p_2}$ is given in Table 3.3. The mean p_2 for the subjects with type 2 diabetes was estimated at $p_2 = 0.0098$ min^{-1}, and for the healthy subjects $p_2 = 0.01$ min^{-1}.

$\sqrt{p_2}$ ($min^{-½}$)	Mean ± SE	Range	CV (%) Mean ± SE	CV (%) Range
Type 2 diabetes	0.099 ± 0.001	0.036 - 0.166	9.70 ± 0.17	0.34 - 16.21
Healthy	0.101 ± 0.003	0.057 - 0.129	5.99 ± 0.57	0.041 - 12.02

Table 3.3: Estimates and precisions of √p2 in subjects with type 2 diabetes and healthy, obtained from glucose OMM.

3.4 The oral C-peptide minimal model

The oral C-peptide minimal model, C-peptide OMM proposed in (Breda *et al.* 2001; Breda *et al.* 2002; Toffolo *et al.* 2001) was used to estimate beta cell function indices. The model is based on the kinetics of C-peptide, where the two-compartment model proposed in (Eaton *et al.* 1980) is used to

represent C-peptide kinetics. Hence the beta cell function indices estimated from this model represents pre-hepatic insulin secretion pattern.

The model proposed to describe the C-peptide kinetics is described shortly below.

C-peptide kinetics

C-peptide kinetics is described by the two-compartment model, proposed by Eaton *et al.* (Eaton *et al.* 1980) with the following equations:

$$\dot{C}_1(t) = SR(t) + k_{12}C_2(t) - (k_{01} + k_{21})C_1(t); \quad C_1(0) = C_{1b} \tag{3.10}$$

$$\dot{C}_2(t) = k_{21}C_1(t) - k_{12}C_2(t); \qquad C_2(0) = k_{21}/k_{12}\cdot C_{1b} \tag{3.11}$$

where C_1 and C_2 are the C-peptide concentrations in compartment 1 (accessible) and 2 (peripheral), respectively, k_{01}, k_{12}, k_{21} are C-peptide kinetics rate constants, and SR is the C-peptide secretion rate, cf. Fig. 3.7. Suffix "b" denotes basal (time t = 0 min) values.

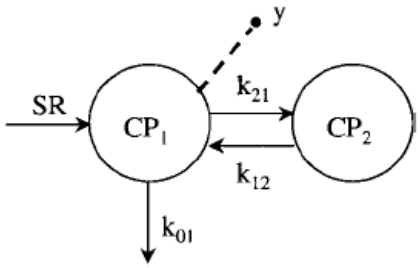

Fig. 3.7: The two-compartment model of C-peptide kinetics proposed by (Eaton *et al.* 1980). C_1 and C_2 are the concentration of C-peptide in compartment 1 (accessible) and compartment 2 (peripheral), respectively. k_{01}, k_{21}, k_{12} are rate parameters. SR is the C-peptide secretion rate normalised to the C-peptide distribution volume of compartment 1. Adapted from (Toffolo *et al.* 2001).

Secretion

The secretion model is based on the idea of the "package storage hypothesis" (Grodsky 1972; Licko 1973).

SR is assumed to be composed of the sum of two components, i.e.

$$SR = SR_D + SR_S \tag{3.12}$$

where SR_S, denoted static component, describes the effect of glucose, G to enhance secretion, and SR_D, denoted dynamic component, describes the effect of the rate of change of glucose, dG/dt to enhance secretion.

Static secretion

The static component SR_S is assumed equal to the provision of new insulin in the beta cell, Y, i.e

$$SR_S(t) = Y(t) \quad (3.13)$$

where Y is assumed to depend on glucose, G according to:

$$\frac{dY}{dt} = \alpha(Y_\infty - Y) \quad (3.14)$$

α describes the rate constant by which Y tends towards the steady state provision Y_∞ assumed linearly related to G through the parameter β according to

$$Y_\infty = \beta(G-h) + SR_B \quad (3.15)$$

h is the threshold value by which, if G is above this value, new insulin is provisioned. SR_B denotes basal secretion.

Hence, SR_S is not linearly related to glucose concentration, but tends, with the rate constant α, towards the steady state provision Y_∞, that is linearly related to G by Eq. (3.15). In the estimation procedure, Y_∞ is restricted to non-negative values, i.e. if $Y_\infty < 0$, Y_∞ is set equal to zero.

The static beta cell function index, or sensitivity, Φ_S describes the ratio between the static secretion, above basal, and the glucose, above the threshold h, at steady state, i.e.

$$\Phi_S = \beta \quad (3.16)$$

The static sensitivity Φ_S provides a measure of the effect of glucose on secretion.

Dynamic secretion

The dynamic secretion component SR_D is assumed proportional to the rate of increase of glucose according to

$$SR_D(t) = K_D \cdot dG/dt \quad (3.17)$$

where K_D is a proportionality parameter.

The dynamic secretion is assumed only to contribute to the secretion, if the rate of change of glucose is positive, hence if $dG/dt < 0$ then $SR_D(t) = 0$. SR_D is interpreted as describing secretion of insulin that is already stored in a readily-releasable pool (RRP) in the beta cell.

The dynamic beta cell function index, or sensitivity, Φ_D describes the ratio between the dynamic secretion and the rate of glucose increase, i.e. according to Eq. (3.17)

$$\Phi_D = K_D \tag{3.18}$$

Φ_D is a measure of the effect of an increasing rate of glucose on secretion.

Basal secretion

The basal secretion component, SR_B is found from the combination of Eqs. (3.10) and (3.11) evaluated in the basal steady state, i.e.

$$SR_B = k_{01}C_{1b} \tag{3.19}$$

The basal beta cell function index, or sensitivity, Φ_B describes the ratio between the basal secretion and basal glucose G_b, i.e.

$$\Phi_B = k_{01}C_{1b}/G_b \tag{3.20}$$

Φ_B is not estimated from the model, but calculated based on the data and the C-peptide kinetic parameter.

Total beta cell function

Also a total, or global, beta cell function index, or sensitivity, Φ_{Total} can be defined. Φ_{Total} is defined as the ratio between average increase of secretion above basal and average glucose above basal, i.e.

$$\Phi_{Total} = \frac{\int_0^\infty (SR(t) - SR_B)dt}{\int_0^\infty (G(t) - h)dt} \tag{3.21}$$

Assuming that the system returns to the basal steady state for t -> ∞, Φ_{Total} can be calculated as

$$\Phi_{Total} = \Phi_S + \frac{\Phi_D (G_{max} - G_b)}{\int_0^\infty (G(t) - h)dt} \tag{3.22}$$

where G_{max} is the maximal value of G obtained throughout the test period.

By using Eqs. (3.10) and (3.11), a model independent expression of Φ_{Total} can be obtained (Breda *et al.* 2001),

$$\Phi_{Total} = \frac{k_{01}\int_{0}^{\infty} C_1(t)dt}{\int_{0}^{\infty}(G(t)-h)dt} \quad (3.23)$$

Hence Φ_{Total} gives a measure of the ratio between the *area under the curve*, AUC of the C-peptide concentration in the accessible compartment and the AUC of glucose concentration above the threshold value.

3.4.1 Model identification and parameter estimation

The C-peptide kinetics rate constant was calculated based on the population based approach proposed by Van Cauter *et al.* (Van-Cauter *et al.* 1992). This approach determines the C-peptide kinetics rate constants based on population standard parameters, and seems not to introduce major errors, as the difference between the estimates of secretion rate based on standard parameters and that based on individually determined kinetic parameters, is similar to the difference of replicate studies in the same subject (Van-Cauter *et al.* 1992). However the approach is not to be used in subjects with kidney failure, as the kidney is the major site for C-peptide clearance (Van-Cauter *et al.* 1992).

Previous experience shows that the threshold value h is always estimated at values close to the basal glucose value G_b (Breda *et al.* 2001), hence in the estimation procedure, h is set equal to G_b as in (Dalla Man *et al.* 2005a). The other model parameters (α, Φ_S, Φ_D) were estimated by a non-linear least squares method, similar to the method described in (Breda *et al.* 2001; Breda *et al.* 2002; Toffolo *et al.* 2001) and implemented in MATLAB.

To increase the precision of estimate of α, maximum a posteriori Bayesian estimation was used, where α was assumed normal distributed with known mean and CV (Breda *et al.* 2001). The glucose data was linearly interpolated, and the time derivative assumed known without error. Errors in C-peptide data were assumed normal distributed with zero mean and known CV as in (Toffolo *et al.* 2006).

3.4.2 Results from the analysis with the oral C-peptide minimal model

In the C-peptide OMM glucose is used as the input, and the C-peptide data are the ones to be fitted. The data used for the subjects with type 2 diabetes and healthy subjects are presented in Fig. 3.1 and Fig. 3.2, respectively.

For the subjects with type 2 diabetes, the model provided a reasonable fit as evident from the weighted residuals shown in Fig. 3.8(a). No systematic deviation from zero was present for the mean weighted residuals, and only occasionally escaped the range [-1; 1].
The fit for the healthy subjects were less good, as evident from Fig. 3.8(b). However the mean weighted residuals varied in an acceptable range, with no systematic deviation from zero.

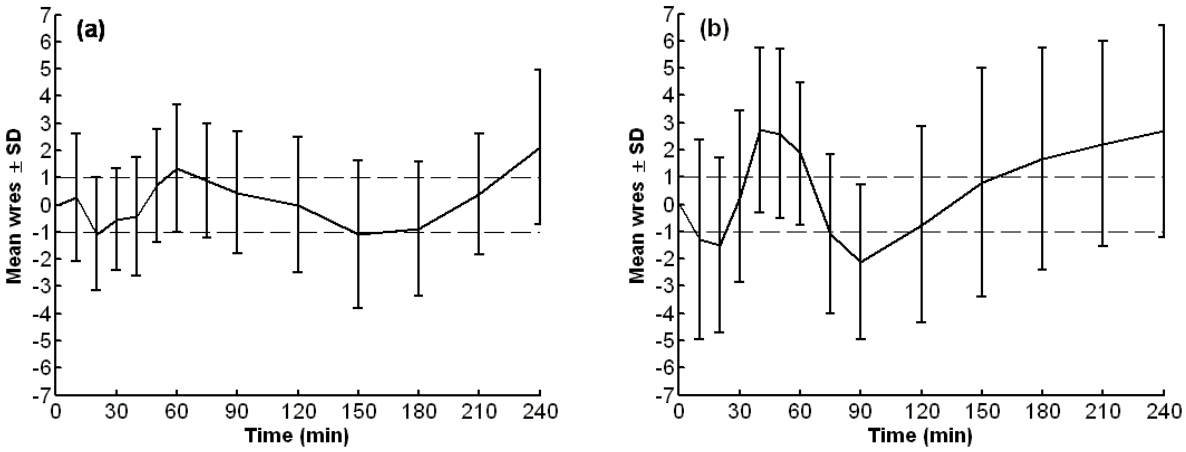

Fig. 3.8: Mean ± SD weighted residual, wres for (a) subjects with type 2 diabetes (N = 169), and (b) healthy subjects (N = 41). Fit obtained with C-peptide OMM.

Parameter estimates

For the subjects with type 2 diabetes the α parameter was assumed to be normally distributed with mean 0.09 min^{-1} and CV = 50%.

For the healthy subjects it was found that changing the restriction on the α parameter to have the mean 0.04 min^{-1} and CV = 112.5 % gave a better fit.

Fig 3.9(a) shows the distribution of α for the subjects with type 2 diabetes, and Fig. 3.9(b) shows the corresponding distribution for the healthy subjects. It is seen for both populations that the distribution of α is not a normal distribution. The mean estimated parameter value for the median values of α for the subjects with type 2 diabetes and healthy subjects were 0.030 min^{-1} and 0.027 min^{-1}, respectively (cf. Table 3.4 and 3.5). The value found for the subjects with type 2 diabetes is larger than the corresponding value for healthy subjects, in contrast with literature findings (Breda *et al.* 2002).

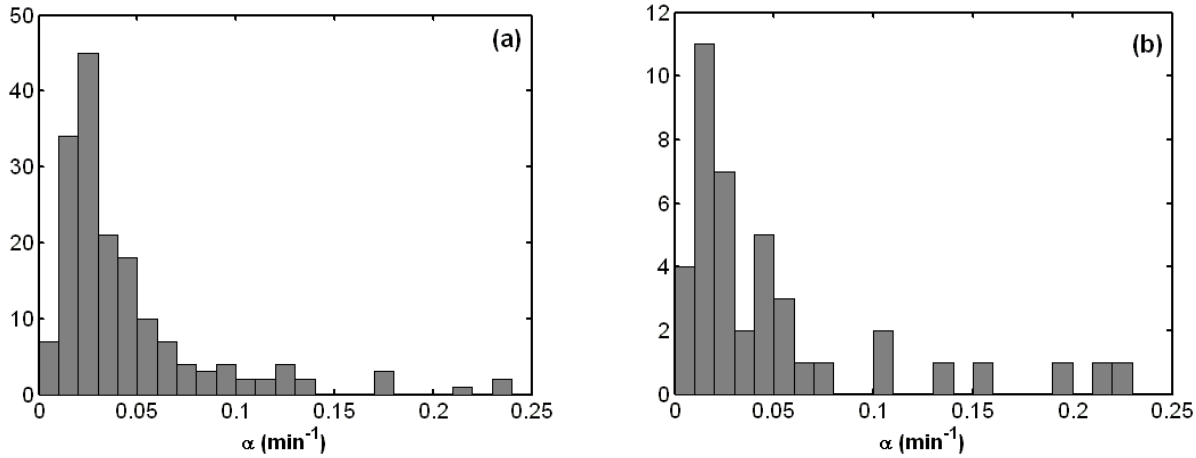

Fig. 3.9: Distribution of α for (a) subjects with type 2 diabetes (N = 169), and (b) healthy subjects (N = 41), estimated from the C-peptide OMM.

The estimated model parameter values and precisions for the subjects with type 2 diabetes are shown in Table 3.3 and the corresponding parameters for the healthy are given in Table 3.4. Large range of variability of the estimated parameters was found for both the subjects with type 2 diabetes and healthy subjects, where the largest range of variability of the parameter estimates was found for the subjects with type 2 diabetes for all three parameters estimated. The highest precision of the parameter estimates, as evaluated by the mean and range of CV, was found for the healthy subjects, except for the estimate of α, cf. Table 3.3 and 3.4.

	Mean ± SE (Median)	Range	CV (%) Mean ± SE	CV (%) Range
K_D (pM per mg/dl)	16.9 ± 0.8	1.39 - 56.97	11 ± 1	0.11 - 96.5
α (min^{-1})	0.045 ± 0.003 (0.03)	0.0027 - 0.24	10.6 ± 0.7	0.001 - 73.5
β (pM min^{-1} per mg/dl)	1.8 ± 0.1	0.30 - 7.15	4.2 ± 0.4	0.29 - 59.9

Table 3.3: Estimated parameters and precisions for the C-peptide OMM in subjects with type 2 diabetes.

	Mean ± SE	Range	CV (%) Mean ± SE	CV (%) Range
K_D (pM per mg/dl)	44 ± 4	10 - 141	6.1 ± 1.3	0.0002 - 35.5
α (min^{-1})	0.050 ± 0.007 (0.027)	0.01 - 0.24	17 ± 6	0.0100 - 173
β (pM min^{-1} per mg/dl)	5.4 ± 0.4	1.8 - 12.5	2.6 ± 0.1	0.7 - 4.6

Table 3.4: Estimated parameters and precisions for the C-peptide OMM in healthy subjects.

Fig. 3.10 shows the distribution of the three beta cell indices for the subjects with type 2 diabetes and healthy subjects. The basal beta cell function index seems to be normal distributed for both groups, whereas the dynamic and static indices have a skewed distribution for the subjects with type 2 diabetes. The dynamic beta cell index for the healthy seems to be normal distributed, whereas the static, as with the group of subjects with diabetes seems to have a skewed distribution. However no strict investigation of the distribution pattern has been performed, hence no safe conclusions can be drawn. Furthermore, the 41 healthy subjects may be a too low value, to represent the “true” distribution.

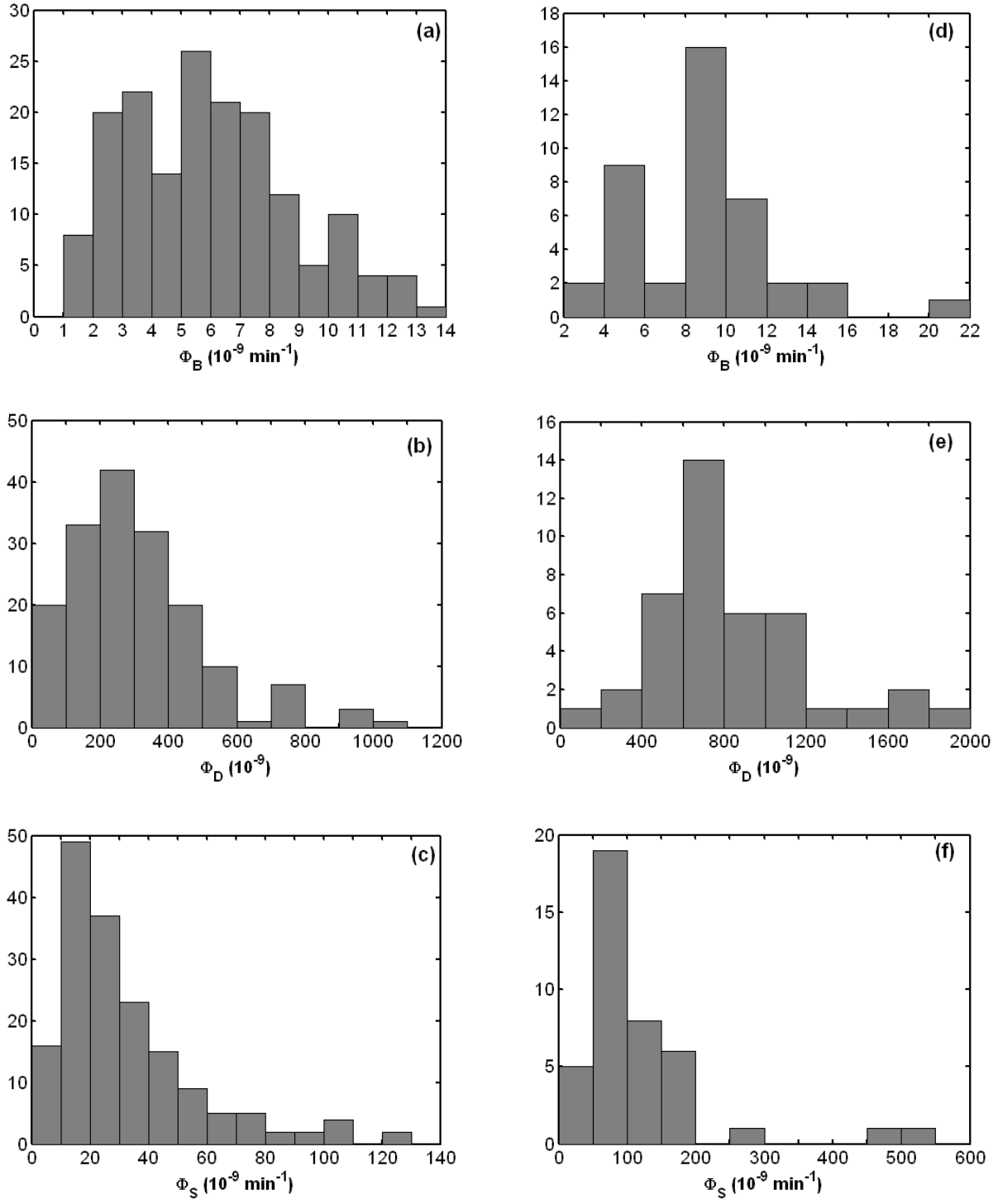

Fig. 3.10: Distribution of the three independent beta cell function indices for the subjects with type 2 diabetes (left column, (a)-(c)) (N = 169), and the healthy subjects (right column, (d)-(f)), estimated from the C-peptide OMM.

The one study found in literature reporting beta cell measures for the dynamic and static secretion after a similar MTT for 8 subjects with diabetes (Bock *et al.* 2006) yields mean estimates, $\Phi_D \approx 417 \cdot 10^{-9}$ and $\Phi_S \approx 30 \cdot 10^{-9}$ min^{-1} (values read off from a graph).

Compared with the values given in Table 3.5, the estimated $\Phi_D = 304 \cdot 10^{-9}$ is somewhat lower than reported in the literature. However, as the estimated values for Φ_D cover a wide range of values, it is difficult to compare the values, as the number of subjects analysed here is much larger than the number of subjects in the literature study (169 vs. 8). Secondly as the distributions of Φ_D and Φ_S seemingly are skewed, more appropriately would be to compare median estimates. These are however not given in the literature study.

Despite the above mentioned, the estimated mean value of $\Phi_S = 32 \pm 1.9$ is in agreement with the value from literature. However the median value of Φ_S is somewhat lower, cf. Table 3.5.

Studies report of beta cell function indices estimates for healthy subjects undergoing standard MTT (Basu *et al.* 2003; Bock *et al.* 2006; Dalla Man *et al.* 2005b) yields ranges $\Phi_D = 400\text{-}580 \cdot 10^{-9}$ and $\Phi_S = 35\text{-}40 \cdot 10^{-9}$ min^{-1}. The mean estimate $\Phi_D = 828 \cdot 10^{-9}$ given in Table 3.5 is much larger than the values reported in literature. The mean estimated $\Phi_S = 121 \cdot 10^{-9} min^{-1}$ is also much larger than the reported values. Even the median values are outside the range of reported parameter values. Presently no good explanation to the discrepancy between the estimated parameter values and the values found in the literature exists.

	Type 2		Healthy	
	Mean ± SE (Median)	Range	Mean ± SE (Median)	Range
Φ_B (10^9 min^{-1})	6.1 ± 0.2 (5.8)	1.3 - 14.7	8.8 ± 0.5 (9.0)	2.8 - 20.2
Φ_D (10^9)	304 ± 15 (261)	25 - 1026	828 ± 59 (752)	171 - 1802
Φ_S (10^9 min^{-1})	32 ± 1.9 (24)	5 - 129	121 ± 16 (92)	31 - 528
Φ_{Total} (10^9 min^{-1})	39 ± 3	6 - 311	123 ± 16	-88 - 445

Table 3.5: Calculated beta cell indices of the C-peptide OMM in subjects with type 2 diabetes and healthy subjects.

3.5 Disposition index

The observation that the beta cell seem to be able to regulate its insulin secretion in relation to a corresponding change in insulin action, has lead to the concept of the disposition index, DI.
DI measures the ability of the beta cell to respond to a change in insulin action, and can in this context be regarded as a measure of beta cell function.
In obesity with resulting insulin resistance, a compensating rise in insulin secretion has been observed hence in obese people, even in the presence of insulin resistance, glucose tolerance is kept normal or near-normal, due to the compensating rise in insulin.
The original idea of a disposition index comes from IVGTT, where the first-phase beta cell index, Φ_1 and the second-phase beta cell index, Φ_2 were plotted against the insulin sensitivity index, S_I. The resulting plot elicited a hyperbolic relation between the measures of beta cell function and the insulin sensitivity, ie.

$$DI_{beta} = S_I \cdot \Phi_{beta} \tag{3.24}$$

where the beta suffix denotes different measures of beta cell function.

Fig. 3.11 shows the three different disposition index plots corresponding to the dynamic, static, and total index. It can be seen that on average, for each disposition index measure, the healthy subjects beta cell compensate better for a change in insulin action, than the subjects with type 2 diabetes.

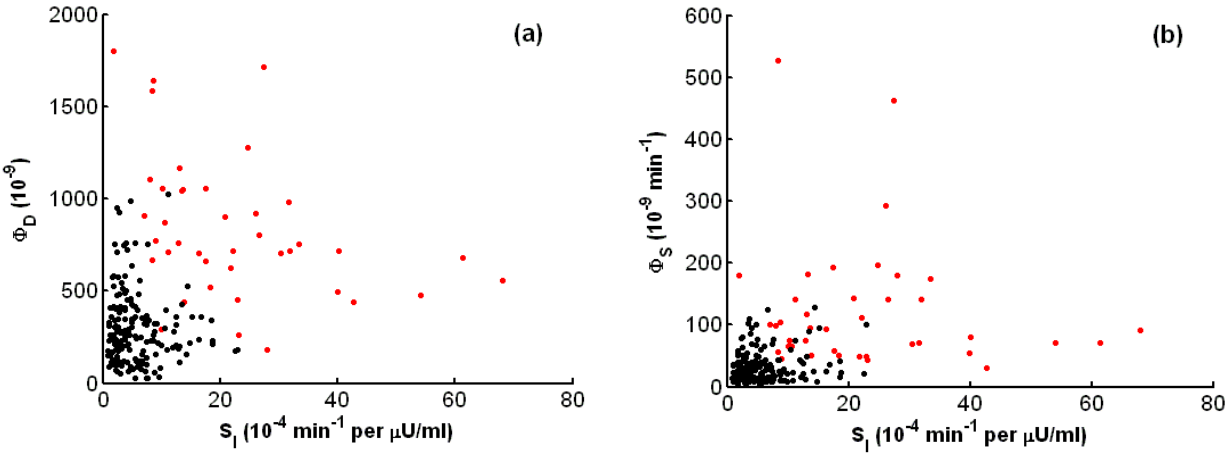

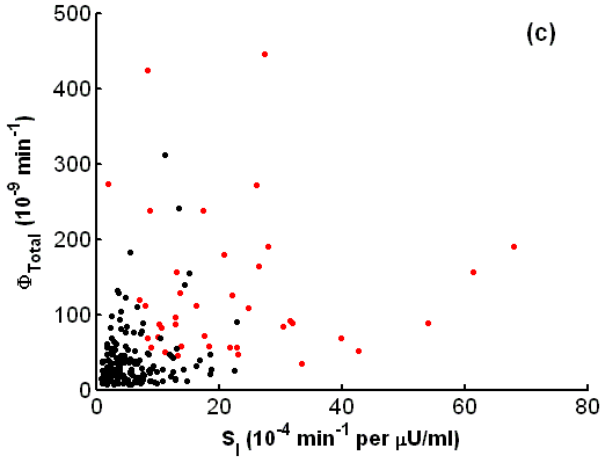

Fig. 3.11: Disposition index plot of healthy (red) and subjects with type 2 diabetes (black) for (a) dynamic, (b) static, and (c) total disposition index.

3.6 Analysis of disease progression

Data from 17 subjects with type 2 diabetes from the Owens database, that were followed at the years 0, 1, and 5 were also analysed with the glucose and C-peptide minimal models, i.e. the subjects are a subset of the 169 subjects already analysed. Fig 3.12 shows the plasma glucose, insulin, and C-peptide responses after a standard MTT of these 17 subjects.

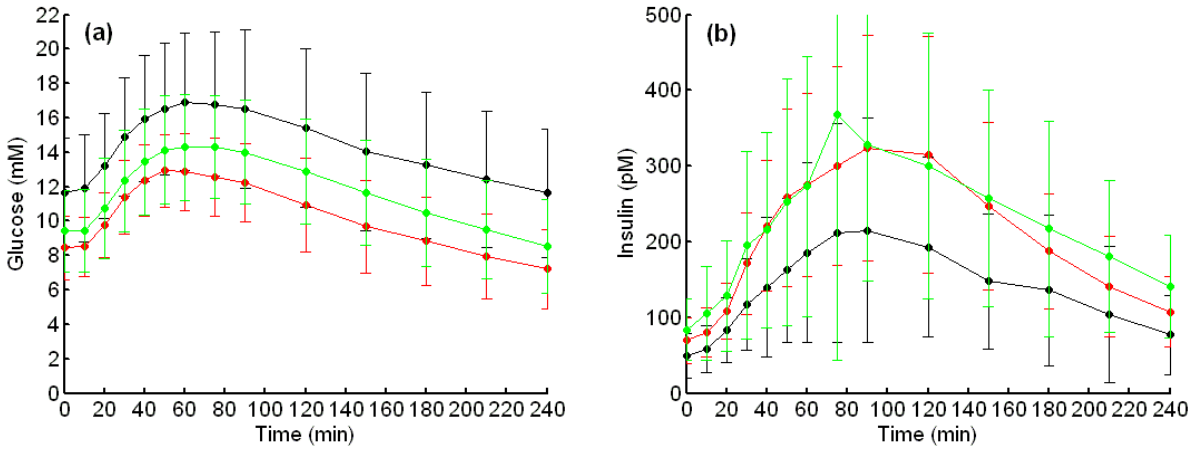

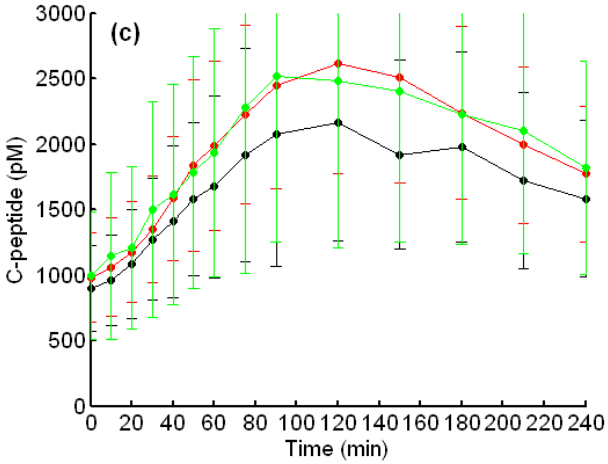

Fig. 3.12: Plasma concentrations of (a) Glucose, (b) Insulin, and (c) C-peptide after MTT of 17 subjects with type 2 diabetes followed at year 0 (black), year 1(red), and year 5 (green). Mean ± SD.

The procedure for estimation of the parameters of both the glucose as well as the C-peptide OMM was done exactly as described in the previous sections. Hence only the final parameter estimates are reported.

Table 3.6, 3.7, and 3.8 shows the most important estimated parameter values, for the year 0, 1, and 5 subjects analysed with the glucose and C-peptide OMM.

As previously described most of the parameters seem to be non-normal distributed, and hence the median estimate may be a better measure to use. Furthermore, estimated values from potential outliers are suppressed in the median measure. Hence the between year comparison of the parameter estimates will primarily be inspection by use of the median values.

Evaluated by the median, all the beta cell function indices increases from year 0 to year 1, and then decreases from year 1 to year 5, cf. Table 3.8.

From Table 3.6 is seen that p_2 more or less obtain the same value at all years. α decreases by 25 % from year 0 to year 1, and then increases by 19 % from year 1 to year 5, as evaluated by the median measures. As α is a measure of the response time (delay) for the beta cell to react on decreasing glucose values (Breda *et al.* 2002), it means that from year 0 to year 1, an increase in the response time is obtained, whereas from year 1 to year 5, the response time is decreased. Hence from year 0 to year 1, an improvement in the beta cell functionality, as measured by the response time, has been obtained. However this improvement is lessened from year 1 to year 5.

	p_2 (min^{-1}) Mean (Median)	α (min^{-1}) Mean (Median)
Year 0	0.0099 (0.01)	0.049 (0.028)
Year 1	0.012 (0.0099)	0.026 (0.021)
Year 5	0.010 (0.0099)	0.031 (0.023)

Table 3.6: Mean parameter estimates from the 17 subjects with type 2 diabetes followed at year 0, year 1, and year 5, of p_2, obtained from glucose OMM, and of α, obtained from C-peptide OMM.

The insulin sensitivity is decreased by 3 % from year 0 to year 1, and decreases by 31 % from year 1 to year 5, as evaluated by the median. Evaluated by the mean values it is seen that the insulin sensitivity increases slightly (5 %) from year 0 to year 1, and then decreases from year 1 to year 5. Hence, the insulin sensitivity is unaffected, or slightly increased, from year 0 to year 1, and then it decreases from year 1 to year 5, cf. Table 3.7.

As mentioned in section 3.1, the specific treatment is not recorded. Hence it cannot be assess whether the changes in the beta cell function indices and/or insulin sensitivity indices between the different years are reflections of disease progression, treatment effect, or combinations. Future studies need to clarify this.

S_I (10^4 min^{-1} per μU/ml)	Parameter Mean ± SE (Median)	Parameter Range	CV (%) Mean ± SE	CV (%) Range
Year 0	7.4 ± 0.9 (6.4)	2.2 - 15.3	15 ± 6	7 - 105
Year 1	7.8 ± 1.2 (6.2)	1.9 - 19.7	8.8 ± 0.6	3.1 - 11.8
Year 5	6.2 ± 1.1 (4.3)	1.3 - 16.3	10.2 ± 1.3	4.3 - 31.0

Table 3.7: Insulin sensitivity index S_I estimates and precisions in 17 subjects with type 2 diabetes followed at year 0, year 1, and year 5, obtained from glucose OMM.

Φ_B (10^9 min^{-1})	Mean ± SE (Median)	Range
Year 0	5.0 ± 0.7 (5.0)	1.8 - 12.2
Year 1	7.0 ± 0.7 (6.8)	2.0 - 14.7
Year 5	6.5 ± 0.9 (4.8)	2.8 - 15.5

Φ_D (10^9)	Mean ± SE (Median)	Range
Year 0	230 ± 44 (179)	25 - 723
Year 1	320 ± 29 (327)	155 - 628
Year 5	375 ± 81 (231)	119 - 1260

Φ_S (10^9 min^{-1})	Mean ± SE (Median)	Range
Year 0	28 ± 6 (20)	6 - 96
Year 1	42 ± 5 (37)	8 - 80
Year 5	32 ± 7 (20)	12 - 123

Φ_{Total} (10^9 min^{-1})	Mean ± SE (Median)	Range
Year 0	34 ± 9 (20)	7 - 155
Year 1	47 ± 6 (41)	10 - 100
Year 5	36 ± 8 (23)	14 - 145

Table 3.8: Calculated beta cell indices of the C-peptide OMM in 17 type 2 followed at year 0, 1 and 5.

Disposition index plot of disease progression and treatment effect

Fig 3.13 shows the disposition index plot for the three beta cell function indices; dynamic, static and total. Disregarding outliers, no clear pattern seems to be present in any of the three graphs, i.e. no clear hyperbolic relation between the specific beta cell function index and insulin sensitivity is seen. However as only 17 subjects are present for each year, the number of subjects may be to inferior to obtain a clear relation.

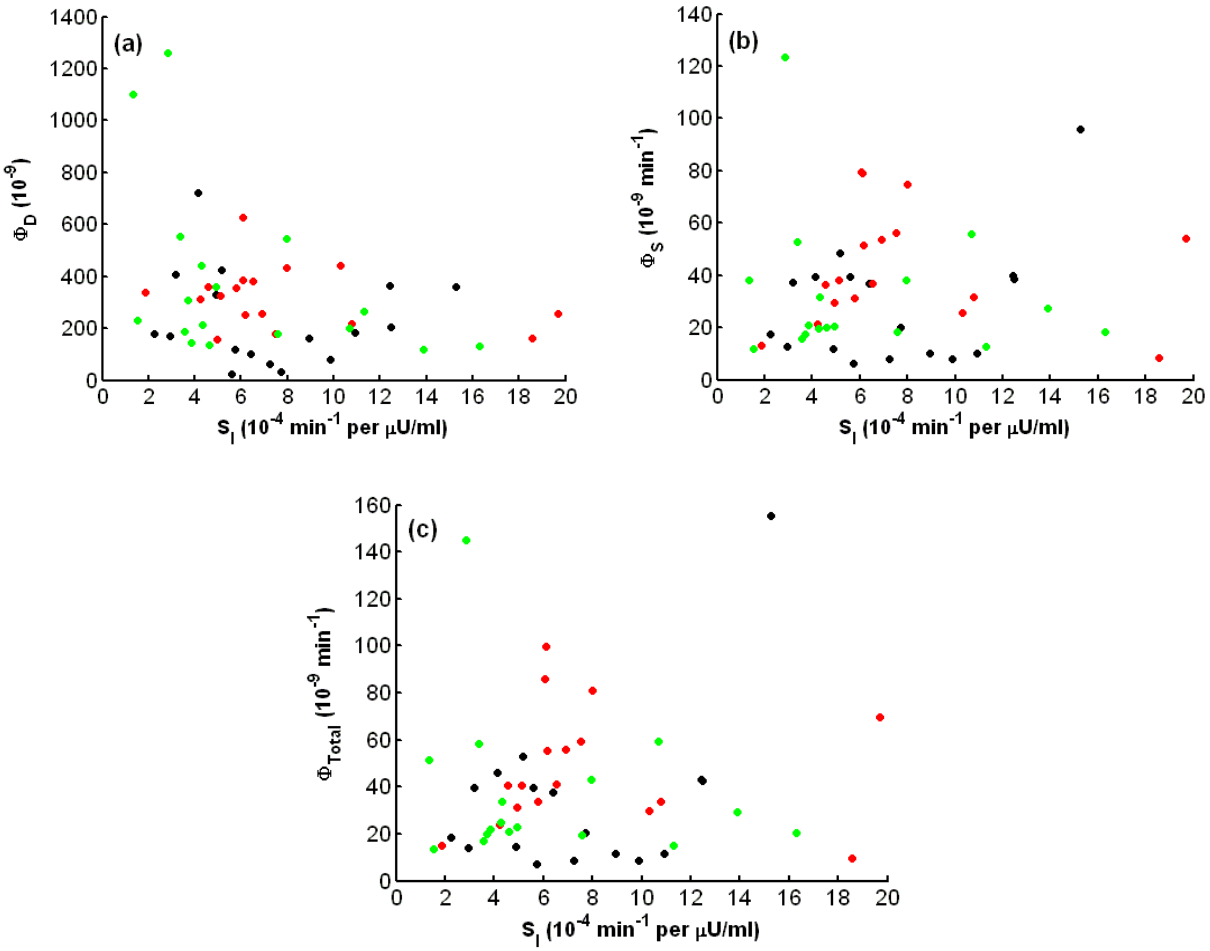

Fig. 3.13: Disposition index plot of 17 subjects with type 2 diabetes for (a) dynamic, (b) static, and (c) total disposition index followed at year 0 (black), year 1 (red), and year 5 (green).

Is the calculation of the disposition indices reliable?

To evaluate the reliability of the disposition index with the present indices for the beta cell function and insulin sensitivity requires comparison against a gold standard for determining the disposition indices during meals. To my knowledge such methods do not exist. However the euglycemic-hyperinsulinemic clamp is considered the gold standard for determining insulin sensitivity, even

though this method is problematic (see e.g. section 2.1.2). Despite this, the oral minimal model-derived index for insulin sensitivity has been found to correlate well with the insulin sensitivity measure from an euglycemic-hyperinsulinemic clamp (Dalla Man *et al.* 2005b; Steil *et al.* 2004), even though the values obtained differs.

To my knowledge there exist no gold standards for determining the different beta cell function indices during meals. Perhaps the most common used (model-independent) index for assessing the first phase insulin secretion (during an IVGTT or clamp), AIR reflects the insulin released during the first 5-10 min. However being based on the insulin concentration, the index also incorporates the hepatic insulin extraction, and therefore does not represent an independent measure of beta cell function (Cobelli *et al.* 2007). Furthermore it is difficult to extrapolate the information gained from the intravenous glucose tests, about the beta cell function, to the indices obtained with the oral minimal model describing C-peptide, as they elicit entirely different stimulation profiles on the beta cell. Thus at present time it is very difficult to say if the disposition indices calculated are reliable, as no gold standard exists, especially for the determination of beta cell function during oral tests.

Presently what can be done, in order to evaluate the reliability of the calculated disposition indices for the subjects presented in the thesis is to compare with the values obtained in literature, where the same models have been applied, as the one used in the thesis. Table 3.6 show the mean and standard deviation of the calculated disposition indices for the healthy as well as the subjects with type 2 diabetes. For both the healthy as well as the subjects with type 2 diabetes, there is a large dispersion in all three measures of disposition. As both the insulin sensitivity indices as well as the beta cell function indices demonstrated large dispersion for both the healthy as well as the subjects with type 2, the large dispersion in the disposition indices where expected. In Bock *et al* (Bock *et al.* 2006), the dynamic disposition index $DI_{dynamic}$ were calculated at ~ 12,000 and ~ 1667 (10^{-14} dl/kg·min^{-1} per pM) for healthy and subjects with impaired fasting glucose/diabetes, respectively. The static disposition index DI_{static} were calculated at ~ 625 and ~ 125 (10^{-14} dl/kg·min^{-2} per pM) for healthy and subjects with impaired fasting glucose/diabetes, respectively. The total disposition index DI_{total} were calculated at ~ 800 and ~ 150 (10^{-14} dl/kg·min^{-2} per pM) for healthy and subjects with impaired fasting glucose/diabetes, respectively. As evident from Table 3.6 there are markedly differences between the calculated indices in this thesis as compared with the values found in Bock et al 2006.

The large discrepancies found between the disposition indices from the thesis and Bock *et al* (Bock *et al.* 2006)are due to the discrepancies in both the estimated insulin sensitivity index as well as the beta cell function indices. The numbers of subjects analysed in the thesis compared with Bock *et al* (Bock *et al.* 2006), differ considerably for the subjects with type 2 diabetes (169 vs. 8). One explanation to the large discrepancies between the indices could then be because of the non-normal distribution found for most of the indices. However as the number of healthy subjects (41 in thesis vs. 32 in Bock *et al*) differ only slightly, this explanation is hardly valid, for the healthy subjects at least. Thus presently it may be speculated that some bug has occurred in the estimation procedure. With that said, a clear distinction between the healthy and the subjects with type 2 diabetes is demonstrated.

Table 3.7 shows the development of the disposition indices along the years. Even though a large dispersion persists, a trend towards a larger value for all the disposition indices at year 1 is present. Thus effect of treatment may be visible at year 1. At year 5, the presumed effect of treatment is completely abolished. However a slight increase in the dynamic disposition index is seen, as compared with year 0. This increase is solely due to a higher dynamic beta cell index at year 5 as compared with year 0.

	Healthy (Mean ± SD)	Type 2 (Mean ± SD)
Dynamic disposition index (10^{14} dl/kg·min^{-1} per pM)	39936 ± 25466	3989 ± 3879
Static disposition index (10^{14} dl/kg·min^{-2} per pM)	6194 ± 5926	483 ± 711
Total disposition index (10^{14} dl/kg·min^{-2} per pM)	6352 ± 7501	620 ± 1133

Table 3.6: Dynamic, static, and total disposition indices for the healthy subjects and the subjects with type 2 diabetes. Values are presented as mean ± standard deviation, SD.

	Dynamic disposition index (10^{14} dl/kg·min^{-1} per pM)	Static disposition index (10^{14} dl/kg·min^{-2} per pM)	Total disposition index (10^{14} dl/kg·min^{-2} per pM)
Year 0	3959 ± 3684	581 ± 833	741 ± 1336
Year 1	5663 ± 3054	786 ± 593	898 ± 749
Year 5	4195 ± 2640	438 ± 373	485 ± 405

Table 3.7: Dynamic, static, and total disposition indices for the subjects with type 2 diabetes at year 0, 1, and 5. Values are presented as mean ± standard deviation, SD.

Summary on the analysis of the Owens MTT data with the minimal models

169 newly diagnosed subjects with type 2 diabetes and 41 healthy subjects were analysed with the oral glucose and C-peptide minimal models to obtain measures of insulin sensitivity as well as beta cell functionality. The number of subjects with type 2 diabetes is presently the largest number of subjects ever analysed with the minimal models.

The main findings from the oral glucose minimal model, glucose OMM, analysis are:

- Good fit to data was found for both the group of subjects with diabetes as well as the healthy group
- S_I (10^{-4} min^{-1} per μU/ml) was found to be non-normal distributed with a large range of variability for both groups; 1-20 (subjects with diabetes) and 2-45 (healthy), excluding outliers
- Median estimate of S_I for the group of subjects with diabetes was found reasonable compared with literature findings
- Median estimate of S_I for the healthy group was found to be a factor 1.5-2.4 larger than reported literature values

The main findings from the oral C-peptide minimal model, C-peptide OMM, analysis are:

- Good fit to data was found for the group of subjects with diabetes and acceptable fit for the healthy group
- The dynamic beta cell function index was lower than values reported in the one study found for the group of subjects with diabetes, whereas the static index obtained values that was comparable to the literature study

- The dynamic index of the healthy group was estimated at a factor 1.4-2 larger than the range reported in the literature, and the static was estimated at a factor 3-3.5 larger than the range of reported values

A large range of variability were found for all parameter estimates of both groups, however a clear distinction between the healthy and group of subjects with diabetes was evident from the disposition index plot, implying that the healthy beta cell compensates better for a change in insulin action, than the beta cell in subjects with type 2 diabetes.

Disease progression and effect of treatment

17 subjects that underwent MTT at year 0, 1, and 5, to follow disease progression and treatment efficacy, was also analysed with the minimal models. Main findings are:

- Indices of insulin action and beta cell functionality all showed improvements at year 1 compared with year 0
- Decline in the effect of treatment and/or the result of disease progression from year 1 to year 5 was evident in all indices of insulin action and beta cell functionality

In the first part of this chapter an analysis of MTT data from a large database of newly-diagnosed subjects with type 2 diabetes and healthy subjects was performed with the widely used state-of-the-art mathematical models to describe glucose kinetics and beta cell functionality known as the glucose and C-peptide oral minimal model, respectively. The analysis showed that:

- ***The oral glucose and C-peptide minimal models provided good fit to data for both the healthy and the subjects with diabetes***
- ***Large spreads of values for the estimated parameters of the models were found for both the healthy and the subjects with diabetes***
- ***A clear distinction between the healthy group and the group of subjects with type 2 diabetes was however evident from the disposition index plot, implying that the healthy beta cell compensates better for a change in insulin action, than the beta cell of subjects with type 2 diabetes***

The second part of the chapter included an analysis of subjects with type 2 diabetes that were followed at the years 0, 1, and 5. The results showed that:

- ***Treatment between year 0 and year 1 was evident in all the estimated parameters***
- ***Treatment decline and/or disease progression was demonstrated in parameter values from year 1 to year 5***

The values of the estimated parameters and especially the parameters estimated from the glucose minimal model may however be questionable. The assumptions that were needed to achieve robust parameter estimation can be explained by an oversimplified description of the glucose uptake by the assumption of linear kinetics that lead to wrong estimates of both the glucose effectiveness and the effect and sensitivity of insulin.

Chapter 4

The phase plot

The plot of plasma glucose versus insulin concentration after a meal, i.e. the phase plot is introduced as a simple way to characterise beta cell function. Clear differences in the characteristic measures are found both between healthy and subjects with type 2 diabetes and within the groups of subjects with diabetes with different fasting plasma glucose values. These differences are analysed with a simple model introduces to describe the insulin responses. The oral glucose minimal model is applied to analyse the effect of variability of the model parameters on the characteristics of the phase plot. The model parameters are found to elicit both common and different effects on the characteristics of the phase plot, with a possible complex outcome as a result.

To examine the differences in the insulin responses of newly-diagnosed subjects with type 2 diabetes subjects and healthy subjects after a meal we analysed MTT glucose and insulin response data from the Owens database. Fig. 4.1 shows the MTT responses from 417 newly-diagnosed subjects with type 2 diabetes and 85 healthy subjects, and includes (but extends) the data analysed in chapter 3.

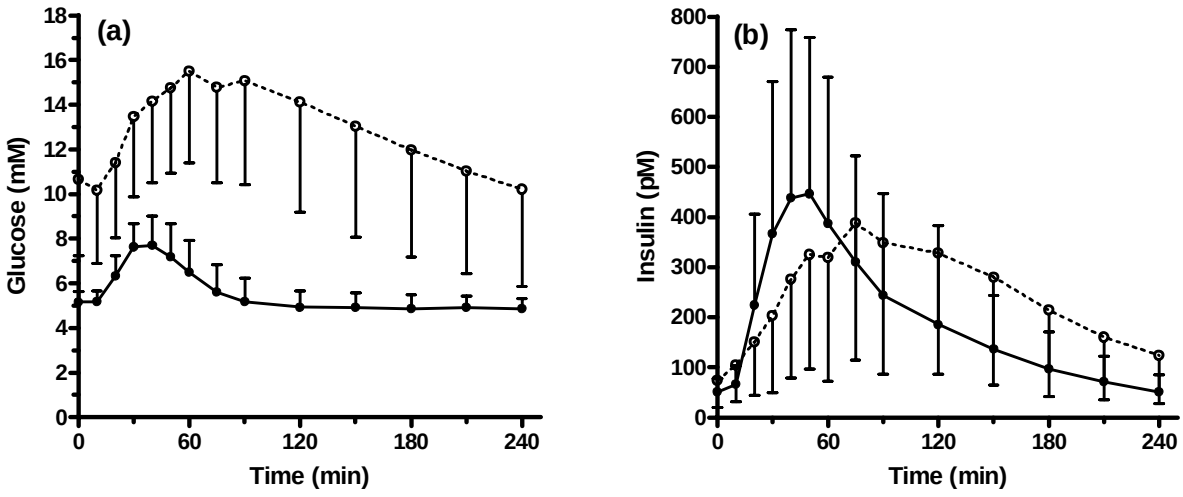

Fig. 4.1: (a) Mean plasma glucose and (b) mean plasma insulin after a MTT in 417 newly-diagnosed subjects with type 2 diabetes (open circle) and in 85 healthy subjects (full circle). Error bars represents standard deviation, SD.

Clear differences between the subjects with type 2 diabetes and the healthy subjects in both the glucose and insulin data are visible. Maximal mean glucose values are reached faster in the healthy subjects (t_{max}=40 min) compared with the subjects with type 2 diabetes (t_{max}=60 min). In the healthy subjects mean glucose returns to the basal (t=0 min) value, within 90 min, where it stays throughout the 4-hour test period. In contrast the mean glucose in the subjects with type 2 diabetes subjects declines slowly and almost linearly throughout the rest of the test period. Maximal insulin value in the healthy subjects is reached at t_{max}=50 min in contrast with the corresponding value for the subjects with type 2 diabetes, t_{max}=75 min. The healthy insulin profile returns back to its basal value by the end of the test period.

In contrast, the insulin profile from the subjects with diabetes is still above its basal value by the end of the test period. There is a large spread of the glucose responses in the subjects with type 2 diabetes compared with the healthy subjects, as seen by a large standard deviation, SD of the subjects with type 2 diabetes compared with the healthy subjects, cf. Fig. 4.1(a). In contrast, a large variation in the insulin responses is visible in both the subjects with type 2 diabetes and in the healthy subjects, cf. Fig. 4.1(b).

As shown in chapter 2 (cf. Fig. 2.1), and for easy reference, shown again in Fig. 4.2, there is a large spread in the fasting plasma glucose values, FPG for the subjects with type 2 diabetes, ranging from 5-21 mM, whereas the healthy FPG is kept within 4-7 mM.

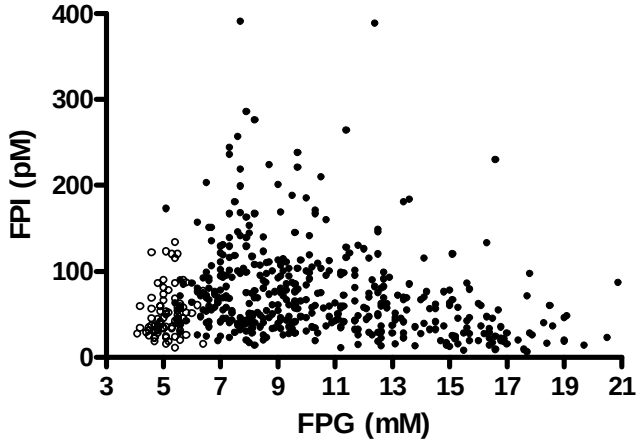

Fig. 4.2: Fasting plasma insulin, FPI against fasting plasma glucose, FPG for 85 healthy subjects (open circle) and 417 newly-diagnosed subjects with type 2 diabetes (full circle).

To examine the effect of different FPG values on the insulin meal responses, we stratified the subjects with type 2 diabetes in five groups (Grp.1-5) according to their FPG values, as given in Table 4.1.

Subjects stratification	FPG (mM)	Number
Grp. 0 (healthy)	< 7	85
Grp. 1	< 7	45
Grp. 2	[7,9[	118
Grp. 3	[9,11[	84
Grp. 4	[11,13[	68
Grp. 5	≥ 13	102

Table 4.1: Stratification of the 417 newly-diagnosed subjects with type 2 diabetes according to their fasting plasma glucose values.

4.1 Phase plot characteristics

The mean phase plots, i.e. the plots between the mean plasma glucose and the mean plasma insulin for the five groupings of T2D (Grp. 1-5) and the healthy group (Grp. 0) as given in Table 4.1 are shown in Fig. 4.3. Clear differences between the phase plots can be seen. We have previously found that the phase plot can be characterised by at least three parameters; slope, offset and delay (Korsgaard and Jönsson 2005).

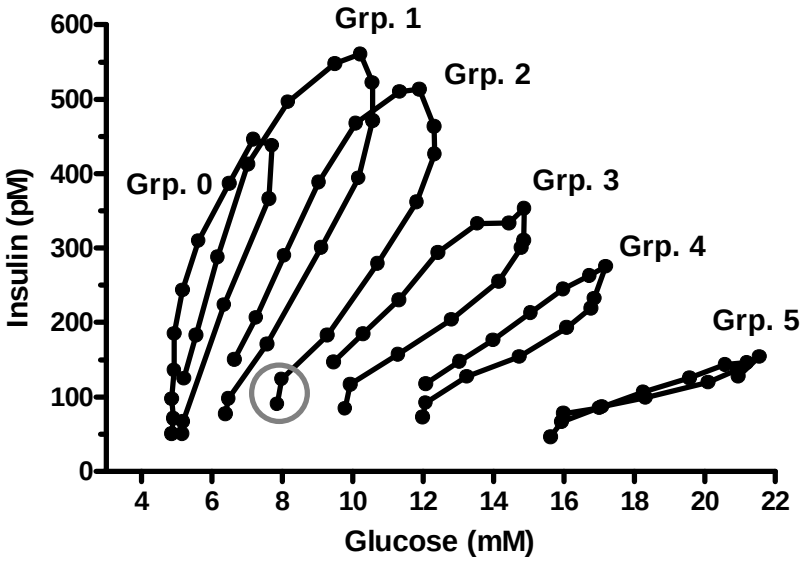

Fig. 4.3: Phase plot between the mean plasma glucose and mean plasma insulin for healthy (Grp. 0) and five groupings (Grp. 1-5), according to FPG, of subjects with type 2 diabetes as given in Table 4.1. Three parameters that characterise the phase plot can be defined; Slope, offset, and delay. The slope decreases for increasing FPG. The offset correlates with FPG. The delay decreases for increasing FPG values. The grey circle shows the cephalic insulin release.

Slope

The slope represents the beta cell glucose sensitivity, i.e. the change in insulin release for a given change in glucose. The phase plots in Fig. 4.3 clearly show that the relation between glucose and insulin responses for increasing glucose concentration is not the same as the relation when glucose decreases, for the healthy group (Grp. 0) as well as for the groups of subjects with type 2 diabetes (Grp. 1-4). The phase plots elicit a (hysteresis) loop. Hence, as the relation between glucose and the resulting insulin release is highly dynamical, no single well-defined measure for the slope can be given. The slope is a qualitative measure that characterises the relation between glucose and insulin. Fig. 4.3 shows a clear decline in the slope for the mean phase plot with increasing fasting plasma values, where the loop more or less collapses for large FPG values.

Offset

The offset is defined as the glucose value at which insulin starts to increase, i.e. it is a measure of the starting point for glucose sensitivity in the beta cell. Fig. 4.3 shows that the offset is correlated with the FPG.

Delay

As described above, the phase plot between glucose and insulin elicit an open curve. The delay, or lag, is a measure of the "openness" of the phase plot. Fig. 4.3 shows that the phase plots close for increasing FPG to collapse for large FPG values.

Cephalic insulin release

The phase plots in Fig. 4.3 show that, particularly for healthy subjects, insulin starts to increase before any noticeable increase in glucose. This may be explained by the cephalic insulin, i.e. the neurally mediated secretion of insulin occurring before nutrient absorption. Ahrén and Holst (Ahrén and Holst 2001) found evidence to show that the cephalic insulin release, lasting around 10 min (in accordance with the data in Fig. 4.3), is largely mediated by autonomic activation, and that incretins (GLP-1, GIP) are not involved. Furthermore they found that the cephalic phase is required for a normal glucose tolerance.

4.2 Analysis of the phase plot with the insulin model

To analyse the phase plots and their characteristics as shown in Fig. 4.3, in greater details, we applied a modified version of the model which we previously had developed for a mathematical analysis of the phase plot (Korsgaard and Jönsson 2005). The idea behind the model development was to extract as much possible information out from the phase plots in a simplified, yet informative, manner to characterise the beta cell function.

In the model the glucose concentration, G is the input and the insulin concentration, I the output of the model. The relation between glucose and insulin is described as

$$I(t) = \alpha \cdot X(t) + \beta \cdot Y(t) + I_b \qquad (4.1)$$

where X(t) and Y(t) are assumed to depend on glucose. α and β (pM/mM) describes the effect of X and Y on the insulin, respectively, and I_b describes basal insulin.

A detailed description and analysis of the relation between X, Y and glucose can be found in (Korsgaard and Jönsson 2005).

Briefly, X describes an immediate effect of glucose, G on insulin given by

$$X(t) = \begin{cases} G(t) - G_b, & \text{for } G(t) > G_b \\ 0, & \text{otherwise} \end{cases} \qquad (4.2)$$

where G_b is the basal glucose concentration value (t=0 min). It is assumed that the immediate effect of glucose only is present for glucose concentration values above the basal value.

Y is assumed to depend on glucose according to

$$\frac{dY(t)}{dt} = \frac{1}{\tau} \cdot \left(X(t) - Y(t)\right) \tag{4.3}$$

where X(t) is given by Eq. (4.2).

In this formulation, X(t) can be described as the steady state relation, by which Y(t) tends towards with the time constant τ.

The parameters α and β represents the immediate and the delayed effects of glucose on insulin, respectively. These parameters are to be interpreted as representing indices for the secretion of insulin by the beta cells, hence characterising beta cell function. Some remarks are here in order:

Firstly, Eq. (4.1) describes the relation between the glucose level and the resulting insulin level. Hence it is not the secretion rate of insulin as in (Korsgaard and Jönsson 2005) that is assessed by the model. However, the elimination of insulin in the body is fast, with half-life for elimination in the order of 5-10 min (Luzi *et al.* 2007). Assuming one-compartment first-order insulin elimination, which appear to be a reasonable assumption for normal physiological insulin values (Hansen 2004; Nucci and Cobelli 2000) we have

$$\frac{dI}{dt} = SR - kI \tag{4.4}$$

where SR is the insulin secretion rate and k is the insulin elimination rate.

Due to the small elimination half-life (large k), it is seen from Eq. (4.4) that the insulin level and the secretion rate differ only by the proportionality constant k. Hence it seems reasonable to assess insulin secretion rate by the insulin levels. The argument hinges on the fast elimination of insulin.

Secondly, because insulin undergoes first-pass hepatic extraction, the indices found by this method are a measure of the post-hepatic insulin appearance, and not a true measure of the insulin secretion rate. Methods based on C-peptide kinetics more correctly measures beta cell functions, as C-peptide is not extracted by the liver to any significant extend. However, as discussed in chapter 2, these methods have other drawbacks.

4.2.1 Model selection

In the development of the insulin model described by Eqs. (4.1) - (4.3) different combinations of the X and Y components described by Eqs. (4.2) and (4.3), together with a component describing the positive rate of change of glucose, were tested. Details of the model selection can be found in Appendix A. Briefly, when considering only one component at a time it was found that the delayed effect component was a much better description of the data, than the immediate component alone. Evaluating all other combinations, it was found that the combination of the immediate and delayed component was the best choice. Including all three components gave only a slightly better description.

A first order insulin kinetics elimination model as in Eq. (4.4) was also tested, assuming a fixed insulin half-life. It was found that the data was best described by the "direct" relation given in Eq. (4.1).

4.2.2 Effect of fasting plasma glucose, FPG on beta cell function indices

In order to find the most important variables that could explain the variability of the model parameters between the subjects, we carried out a covariate analysis as detailed in Appendix A. Briefly, it was found that FPG was the best variable to explain both the variability of α and β, with the correlation shown in Fig. 4.4.

We found that the immediate effect index α decreased by 16% and the delayed effect index β decreased with 25% when FPG increased by 1 mM, hence the mechanism responsible for the delayed effect seems to be more affected by changes in FPG than the immediate. This seems to be in contrast with the finding that the decrease of the first phase of insulin release is one of the earliest marker for the development of diabetes. However caution should be made to relate the immediate effect of insulin with the first phase of insulin release as assessed by IVGTT.

Furthermore we found that waist circumference was the most important variable to explain variation in the basal insulin, I_b.

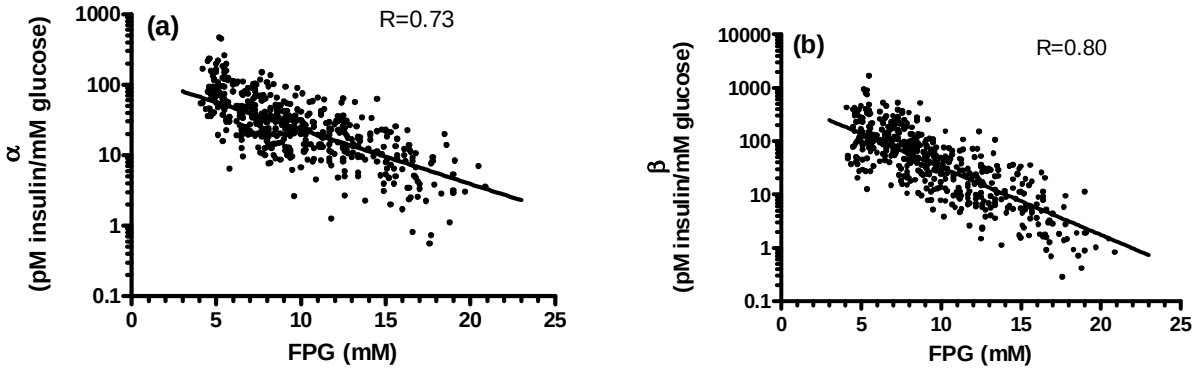

Fig. 4.4: (a) Correlation between the fasting plasma glucose, FPG and the estimates of α for all subjects. (b) Correlation between FPG and β for all subjects.

4.3 Analysis of the phase plot with the oral glucose minimal model

As earlier described, the glucose minimal model is one of the most widely used models to describe the plasma glucose dynamics after a perturbation. The model was applied in chapter 3 to analyse the differences within and between the meal response data for healthy and subjects with type 2 diabetes from the Owens database.

In this section the scope is to apply the oral glucose minimal model, glucose OMM to analyse the phase plot by investigating the effect of variation of the model parameters on the characteristics of the phase plot.

For this purpose, data and parameter estimates are taken from already published results (Dalla Man *et al.* 2004). Briefly, the data consists of 88 healthy subjects that had undergone a MTT. The mean curves of the measured plasma glucose and insulin concentrations are redrawn in Fig. 4.5, together with the glucose rate of appearance, and the phase plot between glucose and insulin.

Comparing the Dalla Man data in Fig. 4.5 with the Owens healthy data, cf. Fig. 4.1, glucose is seen to reach maximum value at similar time point, t=40 min. The maximum value of glucose is however larger in Dalla Man than in the Owens data (8.9 vs. 7.7 mM). Glucose reaches basal value within 180 min in the Dalla Man data, as compared with 90 min in the Owens data. Maximum insulin value is reached faster in the Dalla Man data as compared with Owens data (30 vs. 50 min), but similar maximum values are obtained (440 vs. 446 pM). Insulin returns to basal value at t=420 min in the Dalla Man data, as compared with t=240 min in Owens data.

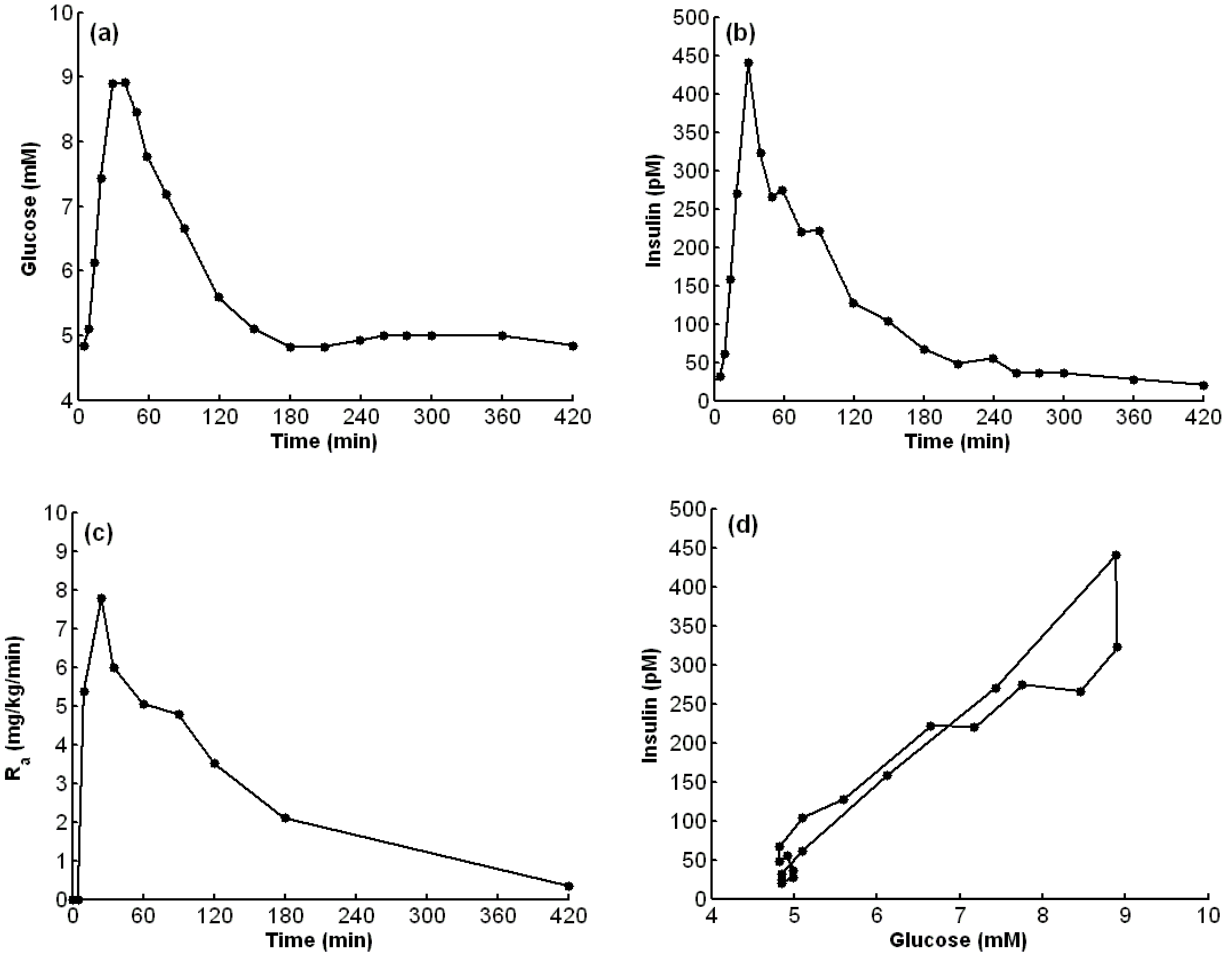

Fig. 4.5: Measured plasma concentration profiles of (a) glucose, (b) insulin, (c) glucose rate of appearance, (d) The phase plot between glucose and insulin during a MTT in healthy subjects (Mean, n=88). Redrawn from (Dalla Man *et al.* 2004).

The difference in the glucose and insulin responses between these two data sets seems unlikely to be explained by the amount of glucose given (77 vs. 75 g. in Dalla Man and Owens, respectively) an the subjects had similar body weights.

The difference may be attributed to the meal compositions. In Dalla Man the energy content of the meal was distributed as 45% carbohydrates, 40% fat, and 15% proteins. Whereas in the Owens data, the meal energy content was distributed as 58% carbohydrates, 22% fat and 20% proteins, cf. Appendix A. The largest difference in the meal energy content distributions is in the fat energy contribution, with an almost doubling in the energy contribution from fat in the Dalla Man data as compared with the Owens data. However one would expect that the larger fat contribution in the Dalla Man meal would lower the plasma glucose and insulin concentration excursions as

compared with the Owens data, as fat is known to lower the meal absorption rate (Hansen 2004). However, we do see slower dynamics in the glucose and insulin responses, after maxima are reached, as would be expected from a meal with larger fat content (Hansen 2004).

On the other hand, the glucose rate of appearance, R_a as given in Fig. 4.5(c) seems to elicit faster dynamics than would be expected with high fat content (Hansen 2004).

Fig.4.5(d) shows that the fast drop in the insulin concentration while glucose is still elevated, results, in the beginning, in a clock-wise direction of the glucose-insulin path in the phase plot, where after, however, the glucose decreases at still elevated insulin, as in the phase plot of the healthy Owens data.

As also noted in the Owens data, there is a fast increase in the insulin level, before any noticeable increase in glucose, which is most probably due to cephalic insulin secretion, as discussed earlier.

The equations of the oral glucose minimal model were given in Eqs. (3.5)-(3.6), and are for clarity given again below:

$$\dot{G} = \frac{R_a}{V} + S_G(G_b - G) - S_I X G, \quad G(0) = G_b \tag{4.5}$$

$$\dot{X} = p_2((I - I_b) - X), \qquad X(0) = 0 \tag{4.6}$$

with the same notation as before.

As previously mentioned, the glucose OMM estimates the parameters S_I, p_2 and the parameters describing the rate of appearance, α_i (i=1...8). The fixed and estimated model parameters from (Dalla Man *et al.* 2004) are given in Table 3.5.
All parameters were estimated with precision (Dalla Man *et al.* 2004). From table 3.5 it is seen, however, that all parameters elicit large spread in the between subjects estimates, as evaluated by the standard deviation.

Parameter	Mean value	Standard error (SE)	Standard deviation (SD)
f (unitless), fixed	0.9		
V (dl/kg), fixed	1.45	-	-
S_G (min^{-1}), fixed	0.025	-	-
p_2 (min^{-1}), restricted	0.011	0.0005	0.005
S_I ($10^4 dl \cdot kg^{-1} \cdot min^{-1} \cdot \mu U^{-1} \cdot ml$)	11.68	0.73	6.8
α_1 ($mg \cdot kg^{-1} \cdot min^{-1}$)	5.36	0.33	3.1
α_2 ($mg \cdot kg^{-1} \cdot min^{-1}$)	7.78	0.24	2.3
α_3 ($mg \cdot kg^{-1} \cdot min^{-1}$)	6.00	0.28	2.6
α_4 ($mg \cdot kg^{-1} \cdot min^{-1}$)	5.05	0.22	2.1
α_5 ($mg \cdot kg^{-1} \cdot min^{-1}$)	4.77	0.28	2.6
α_6 ($mg \cdot kg^{-1} \cdot min^{-1}$)	3.52	0.19	1.78
α_7 ($mg \cdot kg^{-1} \cdot min^{-1}$)	2.09	0.09	0.84
α_8 ($mg \cdot kg^{-1} \cdot min^{-1}$)	0.34	0.05	0.47

Table 3.5: Fixed and estimated model parameter values (mean and SE) from the glucose OMM in healthy (N=88) subjects. SD is calculated as SD = SE·√n. Adapted from Dalla Man *et al.* (2004)**.**

4.3.1 Simulation results

Fig. 4.6 shows the result of a simulation of the glucose OMM model with the parameters given in Table 3.5. The simulated glucose differs from the measured because only mean estimates of the parameters are available and, as evident from Table 3.5, the estimated parameters have a large spread. Dalla Man *et al.* (2004) investigated the deviation on the estimate of S_I introduced as a consequence of fixing the parameters f, V and S_G, and restricting the estimate of p_2,.

The authors found that f, S_G and p_2 contribute to explaining the deviation of S_I estimate compared with reference S_I estimate. The fixing of V did not contribute to the deviation. On average the authors found the estimate of R_a to be in good agreement with the reference tracer estimate of R_a.

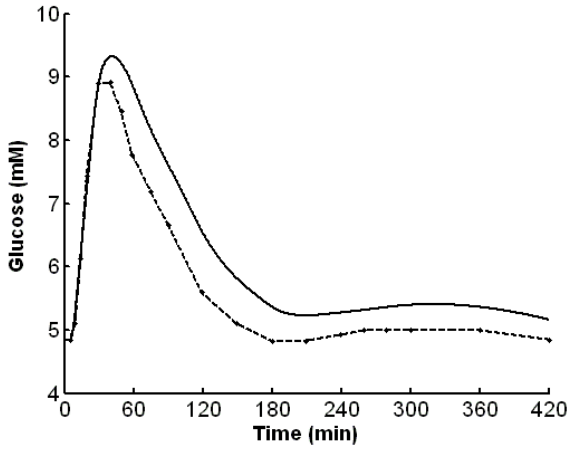

Fig. 4.6: Simulated (full line) and measured (dashed line) plasma glucose concentration.

As mentioned, the scope of this section is to investigate the effects of variation of the different model parameters on the characteristics of the phase plot. This will be achieved by changing the different parameters one by one, and analyse the resulting effects on the simulated curves.

In the following, unless otherwise stated, all parameters will be set to the values given in Table 3.5, except of course the parameters that are varied.

Effect of p_2 on the phase plot

Fig. 4.7 shows the effect of three different values of p_2, taken as the mean estimated values of p_2 and the values of $p_2 \pm 2 \cdot SD$. The step $2 \cdot SD$ has been taken the majority of estimated values lie in the interval with endpoints $2 \cdot SD$ away from the mean estimated value. For decreasing values of p_2 the phase plot turns down, i.e. the upstroke slope decreases, and the phase plot opens up. This is due to the increasing delay between changes in insulin and insulin action, X. It is also evident that for decreasing values of p_2 glucose at the end declines faster, which is caused by the longer lasting effect of X.

Fig. 4.8 shows the effect of p_2 in the extreme cases where $p_2 = 0$ min^{-1}, i.e. X = 0 pM, and $p_2 >> 1$, i.e. $X = I\text{-}I_b$. For the case $p_2 = 0$ min^{-1}, insulin has no effect on the glucose concentration, and the phase plot elicit a large open loop. The decreasing glucose is only due to the glucose effectiveness S_G. In a situation with a vanishing glucose absorption rate, glucose would decrease exponentially fast, with a time constant given by S_G, towards its basal value. In the situation where $p_2 >> 1$ min^{-1}, i.e. $X = I\text{-}I_b$, the effect of insulin on the glucose uptake is immediate, hence glucose is quickly lowered in the beginning when insulin is still high. When insulin starts to decrease, glucose

begins to increase due the absorption of glucose that still takes place. For large time glucose approximates the glucose profile obtained when $p_2 = 0$ min^{-1}, as insulin approximates its basal value, i.e. X approximates 0 pM. For the situation with $X = I - I_b$, the glucose minimal model simplifies to a previous thoroughly analysed model (Korsgaard and Jönsson 2005).

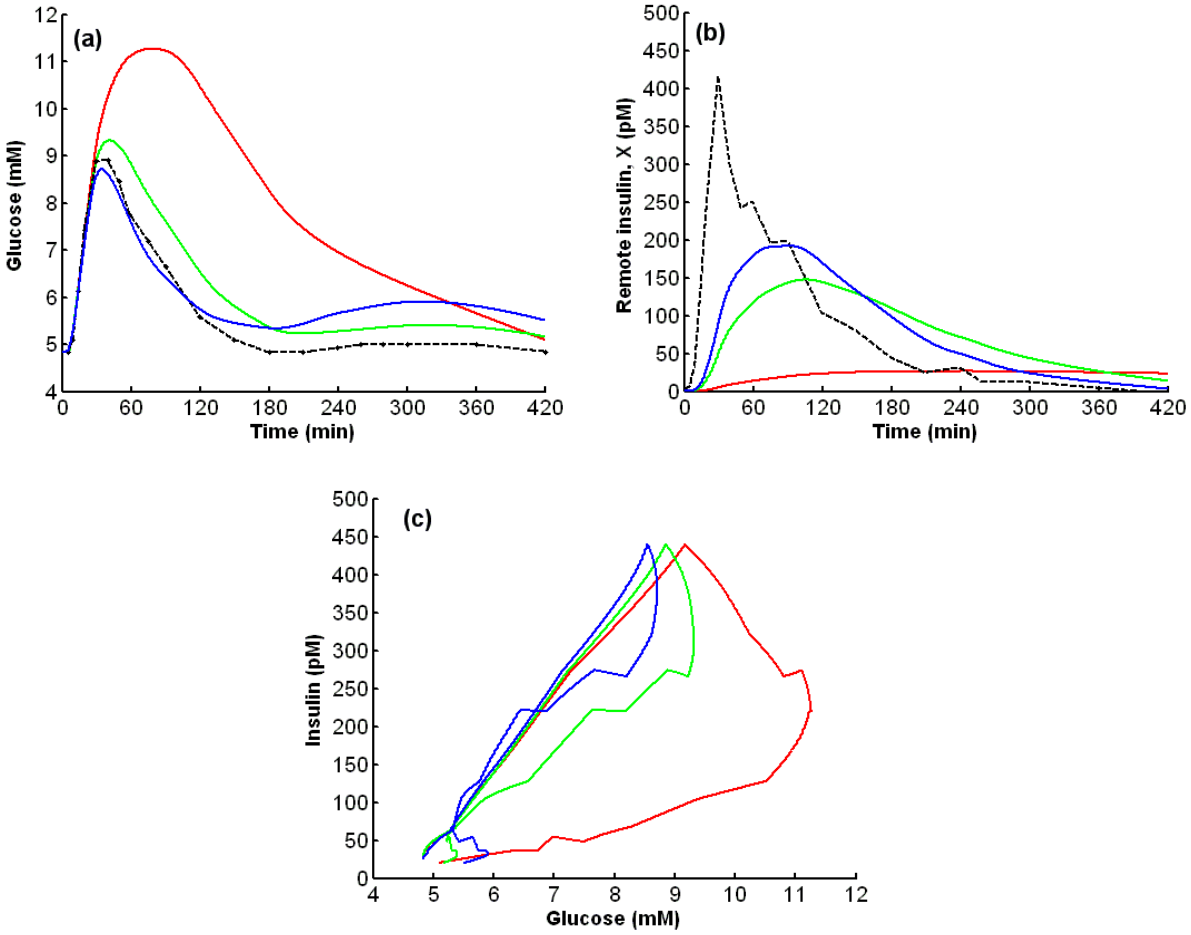

Fig. 4.7: Effect of variation of p_2 on (a) plasma glucose, (b) remote insulin, X, and on (c) the phase plot. The variation of p_2 (min^{-1}) is taken as mean ± 2SD, i.e. p_2 has value 0.011 – 2SD (red), 0.011 (green), 0.011 + 2SD (blue). Dashed line show measured plasma glucose and plasma insulin, respectively, where the plasma insulin is given as the difference from the fasting value.

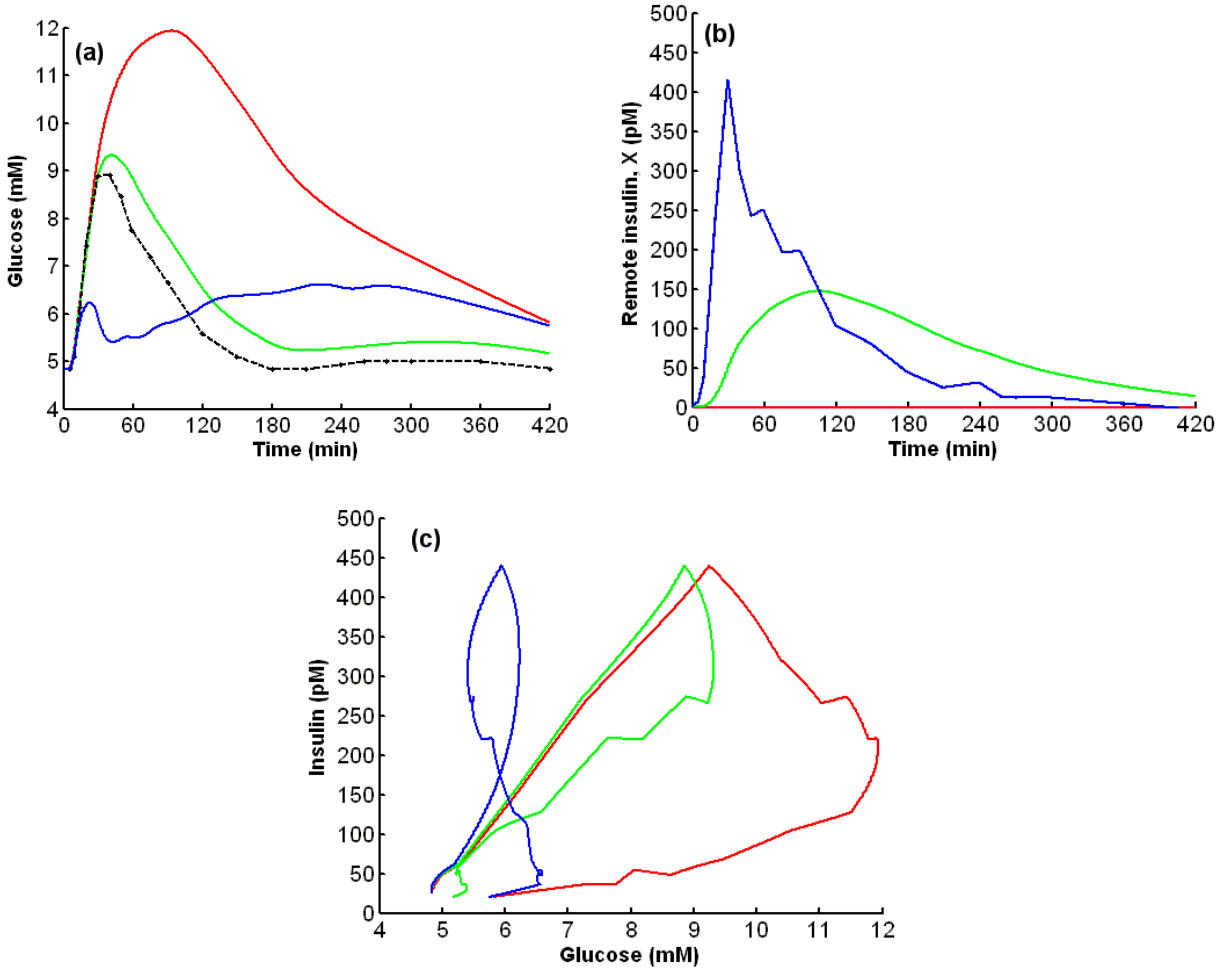

Fig. 4.8: Effect of variation of p_2 on (a) plasma glucose, (b) remote insulin, X, and on (c) the phase plot, in the extreme cases $p_2 = 0$ min^{-1}, i.e. X=0 pM (red) and $p_2 >> 1$ min^{-1}, i.e. $X = I - I_b$ (blue), and in the mean case $p_2 = 0.011$ min^{-1} (green).

Summary on the effect of p_2 on the phase plot

- Decreasing p_2 values decreases the upstroke slope and increases the loop size
- Increasing p_2 decreases the time for insulin effect, resulting in decreasing glucose value followed by increasing glucose value, before glucose decreases again, i.e. the phase plot elicit a s-shape at the end

Effect of S_I on the phase plot

Fig. 4.9 shows the effect of different values of S_I. As previously noted, S_I has a large spread in the estimated values, cf. Table 3.5.

For large values of S_I the upstroke slope increases, but a large undershoot in the glucose profile develops. For decreasing S_I the upstroke slope decreases. For smaller values than the mean estimated (blue), the loop starts to open up. For large S_I values, the glucose-insulin path followed in the phase plot turns from clockwise to counter clockwise, due to the faster drop in glucose than insulin.

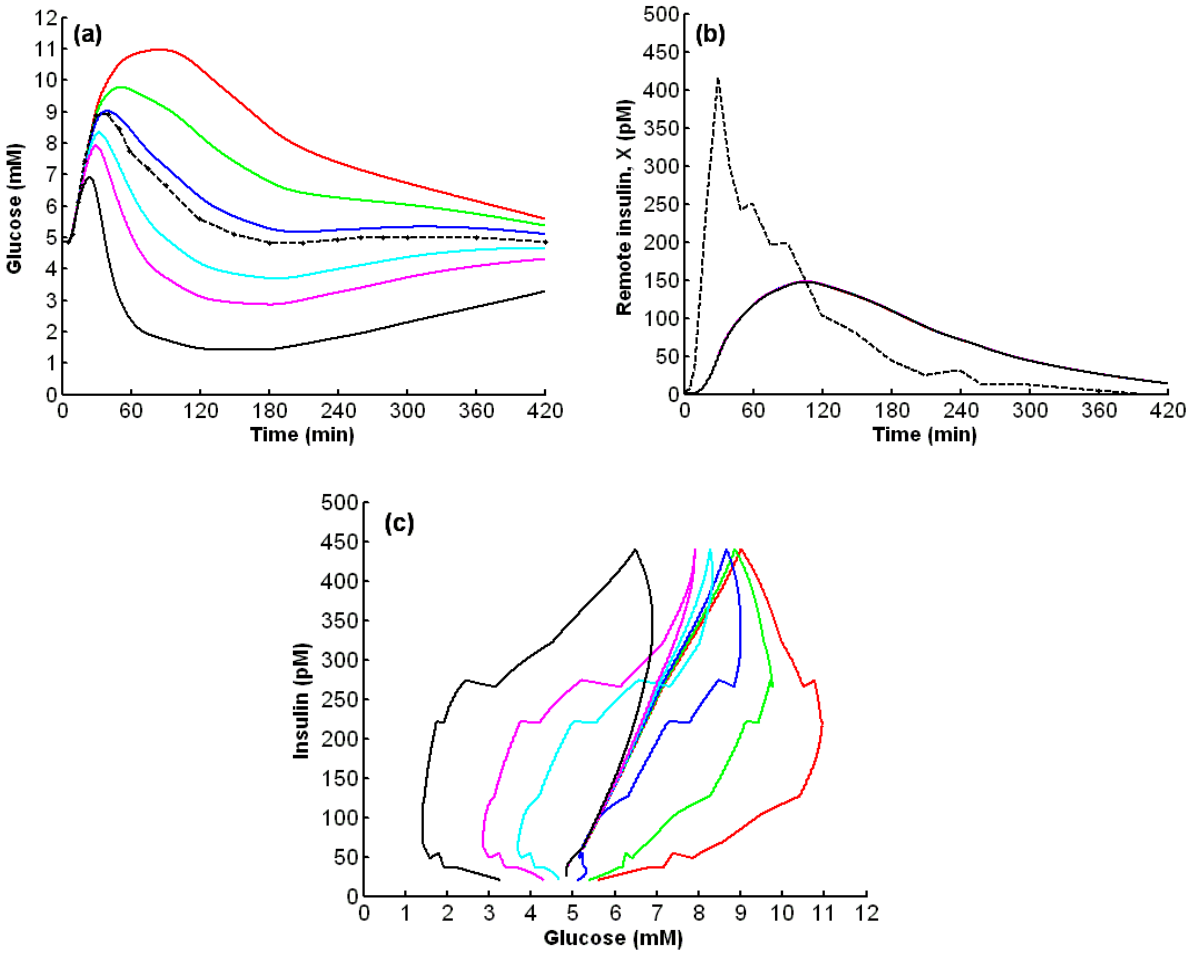

Fig. 4.9: Effect of different values of S_I (10^{-4}dl·kg^{-1}·min^{-1}·μU^{-1}·ml) on (a) plasma glucose and (c) the phase plot. S_I = 0 (red), S_I = 11.68 - 1·SD (green), S_I = 11.68 (blue), S_I = 11.68 + 2·SD (cyan), S_I = 11.68 + 4·SD (magenta), S_I = 100 (black). Dashed line shows (a) measured plasma glucose and (b) measured plasma insulin.

Summary on the effect of S_I on the phase plot

- Increasing values of S_I increases the upstroke slope
- For large S_I, a large undershoot in glucose is evident
- The path followed in the phase plot turns its rotation for increasing S_I

Effect of S_G on the phase plot

Fig. 4.10 shows the effect of different values of S_G. For increasing S_G the upstroke slope increases, and the loop collapses. For the case $S_G = 0$ min^{-1}, glucose increases at the end due to the absorption that is still present and due to the small effect of insulin. The extreme case where $S_G = 1$ min^{-1} is shown to illustrate the important fact that increasing S_G will never result in glucose undershoot, in contrast with increasing S_I.

The model is constructed in such a way that glucose, when absorption and effect of insulin is vanishing, will approach the basal value exponentially fast with a time constant given by S_G, hence the larger S_G the faster will glucose approach its basal value. Increasing S_G will lower an undershoot in glucose, as seen in Fig. 4.11, where a undershoot of glucose is simulated with a large value of S_I, cf. Fig. 4.9 (cyan curve).

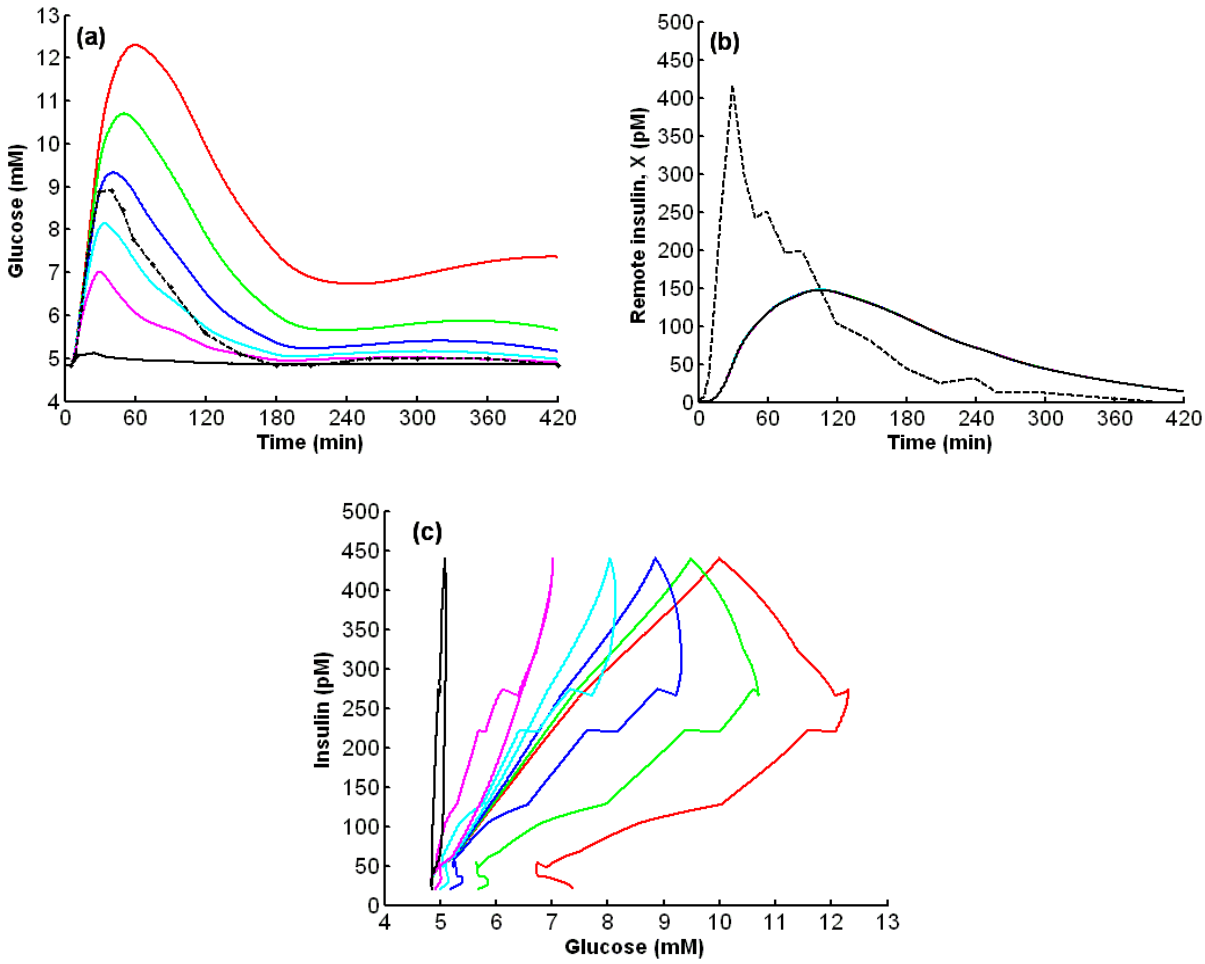

Fig. 4.10: Effect of different values of S_G (min^{-1}) on (a) plasma glucose and (c) the phase plot. S_G = 0 (red), S_G = 0.01 (green), S_G = 0.025 (blue), S_G = 0.05 (cyan), S_G = 0.1 (magenta), S_G = 1 (black). Dashed line shows (a) measured plasma glucose and (b) measured plasma insulin.

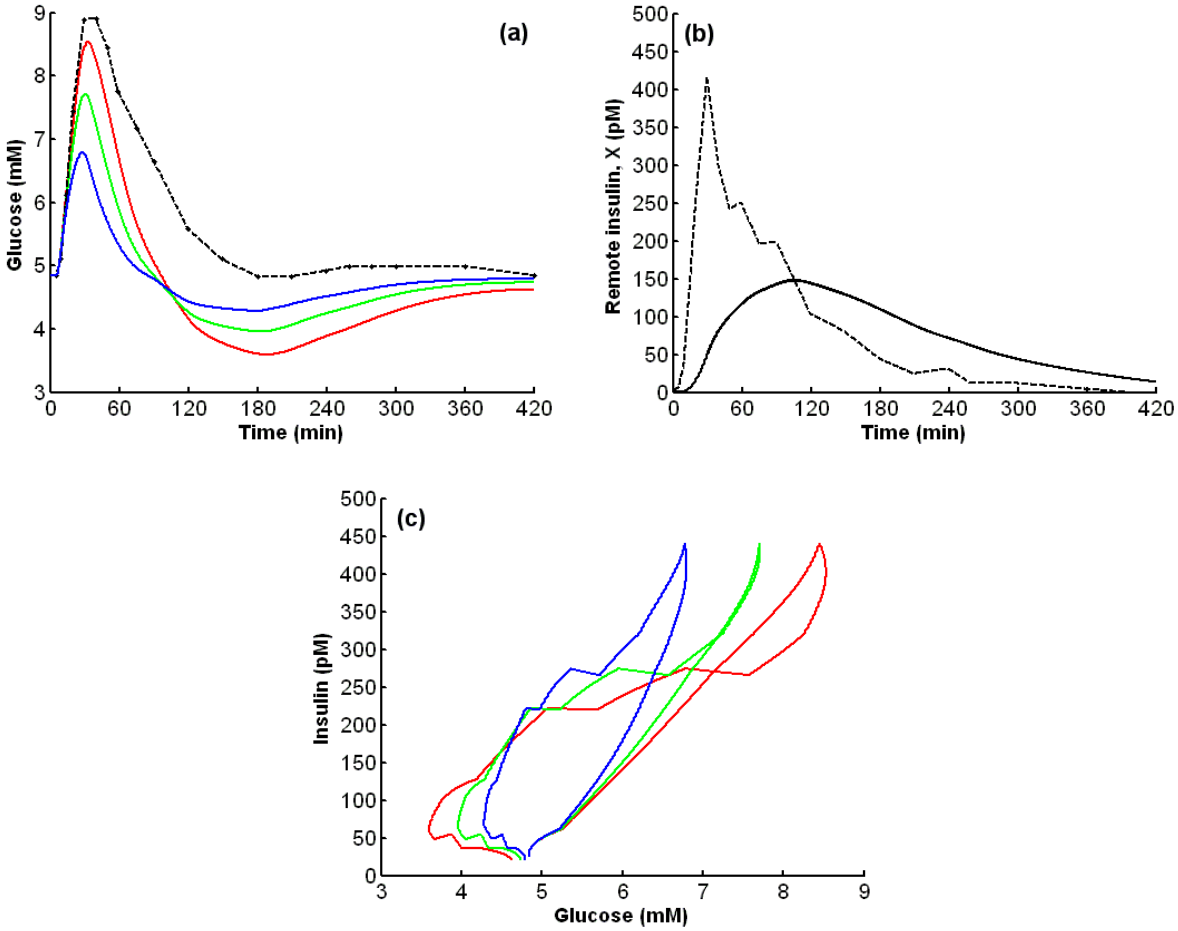

Fig. 4.11: S_G (min^{-1}) reduces a glucose undershoot, simulated with $S_I = 11.68 + 2 \cdot SD$ ($10^{-4} dl \cdot kg^{-1} \cdot min^{-1} \cdot \mu U^{-1} \cdot ml$). $S_G = 0.025$ (red), $S_G = 0.05$ (green), $S_G = 0.1$ (blue). (a) Plasma glucose, (b) Remote insulin, X, and (c) phase plot.

Summary on the effect of S_G on the phase plot

- Increasing values of S_G increases the upstroke slope and narrows the loop
- Increasing values of S_G lowers a glucose undershoot
- The path followed in the phase plot turns its rotation for increasing S_I

Effect of absorption rate

The absorption process is an extremely complex process, where the gastric emptying rate depends on many things (Hansen 2004). Even though the mean estimated absorption rate was found to be in good agreement with the rate obtained by the tracer method (Dalla Man *et al.* 2004), it is evident from Table 3.5 that the parameters determining the rate of appearance $\{\alpha_i\}$ obtain large dispersion.

To simulate the effect of different glucose appearance rate, the apperance rate R_a is modelled by a two-exponential function (Hansen 2004; Korsgaard and Jönsson 2005)

$$R_a = m_0 \frac{k_1(k_1 + k_2)}{k_2} e^{-k_1 t}(1 - e^{-k_2 t}) \qquad (4.7)$$

where it has been assumed that the absorption starts at t = 0 min. m_0 (mg/kg) is the amount of glucose entering plasma, k_1 can be interpreted as the transfer rate from stomach to intestine, and k_2 the transfer rate from intestine to plasma (Korsgaard and Jönsson 2005). As the meal contains 1 g glucose / kg body weight and the bioavailability, f is fixed at f= 0.9 (Dalla Man *et al.* 2004), m_0 is calculated to be m_0 = 900 mg/kg.

This representation of the mechanisms behind glucose absorption is extremely simplified, but it is used to demonstrate the impact on the glucose concentrations for different absorption profiles. To simplify even further k_1 is set equal to k_2.

Fig. 4.12 shows that fast absorption rates gives large glucose excursion and large glucose undershoot as also previously shown in (Korsgaard and Jönsson 2005). Decreasing absorption rates increases the upstroke slope in the phase plot, while glucose tends to overshoot due to the slow absorption process.

Summary on the effect of glucose rate of appearance on the phase plot

- Increasing glucose absorption rates results in large glucose excursions, both hyperglycemic and hypoglycemic values
- Decreasing glucose absorption rates results in increasing upstroke slopes in the phase plot, and a tendency for glucose overshoot is observed for very small absorption rates

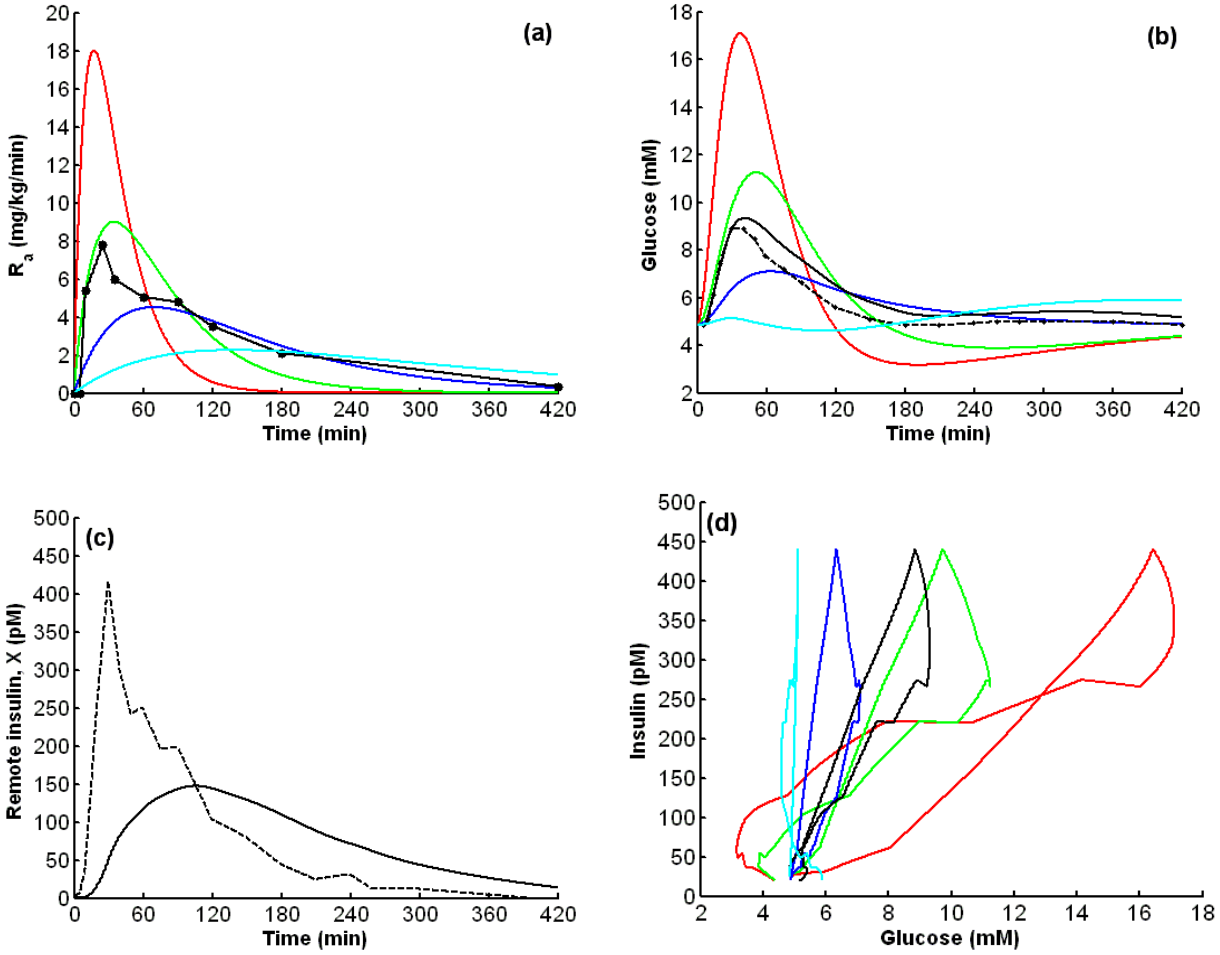

Fig. 4.12: (a) Effect of different absorption profiles modelled by Eq. (4.7) on (b) plasma glucose and (d) the phase plot. The rate constants k_1 and k_2 is set equal to one another, with k_1= 0.04 min^{-1} (red), k_1 = 0.02 min^{-1} (green), k_1 = 0.01 min^{-1} (blue), k_1 = 0.005min^{-1} (cyan). Full black line denotes (a) the estimated R_a, (b) simulated glucose with estimated R_a, (c) remote insulin , X, and (d) the simulated phase plot with the estimated R_a. Dashed black line denotes (b) measured plasma glucose concentration and (c) measured plasma insulin concentration.

In the first part of this chapter the phase plot was used as a simple method to gain information about the beta cell functionality in healthy and in subjects with type 2 diabetes after a MTT. We used a model that we had previously developed that took glucose concentration as input and insulin concentration as output in order to describe the phase plot. The model was based on the assumptions of an immediate and a delayed effect of glucose on the insulin response. From this model we found that:

- ***Fasting plasma glucose was the variable that best explained the variations of both the parameter describing the immediate as well as the delayed effect of glucose on insulin, i.e. fasting plasma glucose explained the variations in the slope of the phase plots***
- ***The parameter describing the delayed effect of glucose on insulin response was more decreased than the immediate, indicating that mechanism(s) responsible for the delayed effect are more sensible to changes in fasting plasma glucose than the mechanism(s) responsible for the immediate effect***
- ***Waist circumference was found to be the variable that best explained variations in the basal insulin level, adding more to the evidence of no (simple) relation between the fasting plasma glucose and fasting plasma insulin***

The second part of the chapter investigated the variability of the phase plot described by the glucose oral minimal model, where insulin was used as input and glucose as output. The phase plot was investigated by changing model parameters one by one and analysing the outcome of the simulation. The simulations showed that:

- ***Early deterioration of glucose meal response when insulin response is normal or near normal may be prevented by increasing insulin action (p_2) and/or sensitivity. An isolated increase in insulin action may however lead to (transiently) elevated glucose levels as the time for effect of insulin is correspondingly lowered. An isolated increase in insulin sensitivity may on the other hand lead to undesirable glucose undershoot.***
- ***A better strategy could be to increase the effect of glucose, as this would decrease a glucose overshoot, but would not lead to glucose undershoot. Another choice could be to lower the glucose absorption rate. However a too low absorption rate would (transiently) lead to elevated glucose. A combination of an increasing effect of glucose and a decreasing glucose absorption rate could be a good choice***

Chapter 5

The meal response

The meal-related responses, i.e. the responses corrected for fasting values, of glucose and insulin after a meal tolerance test for a large dataset of healthy subjects and subjects with type 2 diabetes are analysed.
The analysis show that for the healthy subjects the disappearance rate of glucose seems to be regulated in such a way as to follow the appearance rate. The analysis also show that the meal-responses from the subjects with type 2 diabetes are quite similar regardless of insulin levels, treatment and/or disease progression, but differ fundamentally from the healthy responses. On the other hand fasting plasma glucose, FPG may be affected by treatment, and the variability and regulation of FPG are analysed and discussed.

5.1 Owens MTT data

Fig. 5.1 shows the mean plasma glucose and plasma insulin profiles after a standard meal tolerance test, MTT of 356 newly diagnosed subjects with type 2 diabetes and 85 healthy subjects from the Owens database, cf. Chapter 3. The subjects with type 2 diabetes are divided in five groups according to their fasting plasma glucose, FPG values, where the stratification according to FPG is similar to the one performed in Chapter 4, cf. Table 4.1.

For all the subjects with type 2 diabetes it can be seen that both the plasma glucose profiles and the insulin profiles peak later than the healthy profile. The subjects with type 2 diabetes have a later return to their FPG values than the healthy subjects.

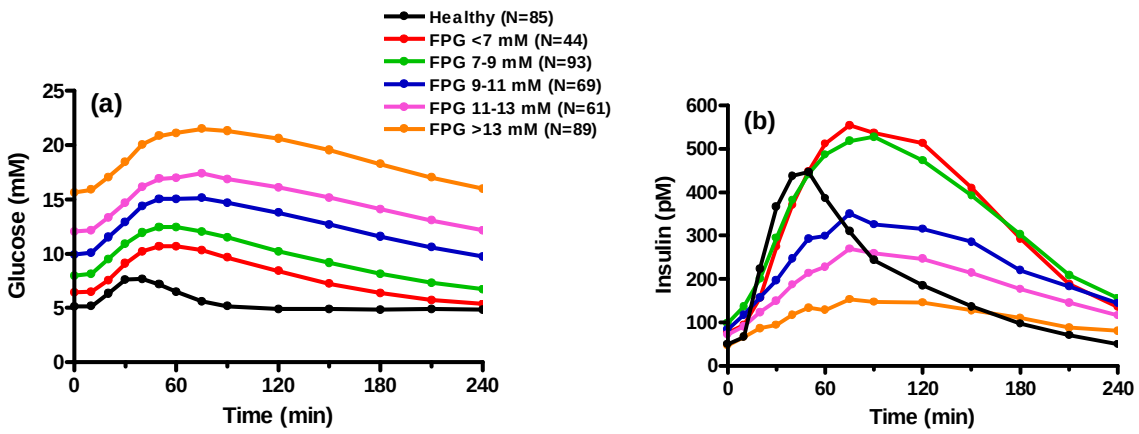

Fig. 5.1: (a) Plasma glucose responses in 85 healthy and 356 newly-diagnosed subjects with type 2 diabetes grouped according to their fasting plasma glucose, FPG after a MTT. (b) The corresponding insulin responses. The legends in (a) show the colour coding used for the groups, and the number of subjects in each group. The stratification according to FPG as shown in Table 4.1 is used, however the number of subjects in each group differ.

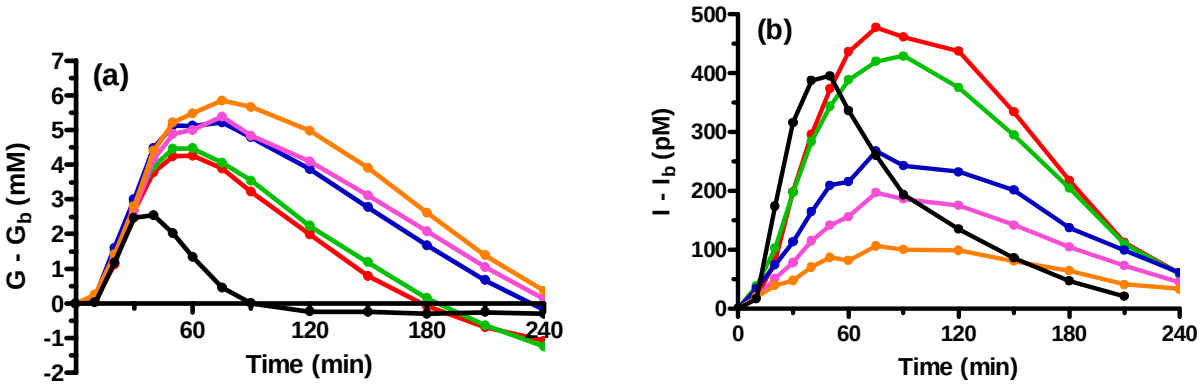

Fig. 5.2: (a) The plasma glucose responses from Fig. 5.1 subtracted by the basal (fasting) glucose at t=0 min. (b) The corresponding insulin responses subtracted with the respective basal value.

Fig. 5.2 shows the same profiles and groupings as in Fig. 5.1, but now the profiles have been corrected for their respective fasting values. The profiles for increasing glucose are similar for the first approximately 30 min for all the subjects, healthy as well as the subjects with type 2 diabetes. As described in Chapter 3 the mean maximal glucose value for the healthy is reached faster (t_{max} = 40 min) than the subjects with type 2 diabetes (t_{max}=50-75 min), and the basal state is reached within 90 min. Strikingly, the glucose downstrokes for the subjects with type 2 diabetes are almost parallel. The large differences present in the subjects insulin profiles are not much apparent in the

glucose profiles where the overall glucose response shape seems to be similar for the subjects with type 2 diabetes. The major effect of insulin on the glucose profile seems to be on the glucose peak value and peak time, with smaller glucose peak values and peak times for larger insulin levels. The large insulin levels at t=180 min for the T2DM groups with FPG < 9 mM leads to glucose undershoot. The healthy subject glucose profile is fundamentally different from the profile in the subjects with type 2 diabetes with a fast return to pre-meal glucose values.

5.1.1 Subjects followed through years

Figs. (5.3)-(5.6) show data of subjects with type 2 diabetes from the Owens database that have been followed through the years 1, 2, 5, and 10. Even with different subjects and numbers and with different treatments included, the overall conclusion is the same as with the data from the newly-diagnosed subjects, cf. Fig. 5.2. The effect of insulin is primarily on the time to reach the maximum glucose concentration and on the respective maximum value. The glucose downstrokes are almost parallel and decline in a slowly linear fashion. For some subjects, a large glucose undershoot is present. Furthermore, for all years a clear difference between the subjects with type 2 diabetes and the healthy is evident.

Year 1

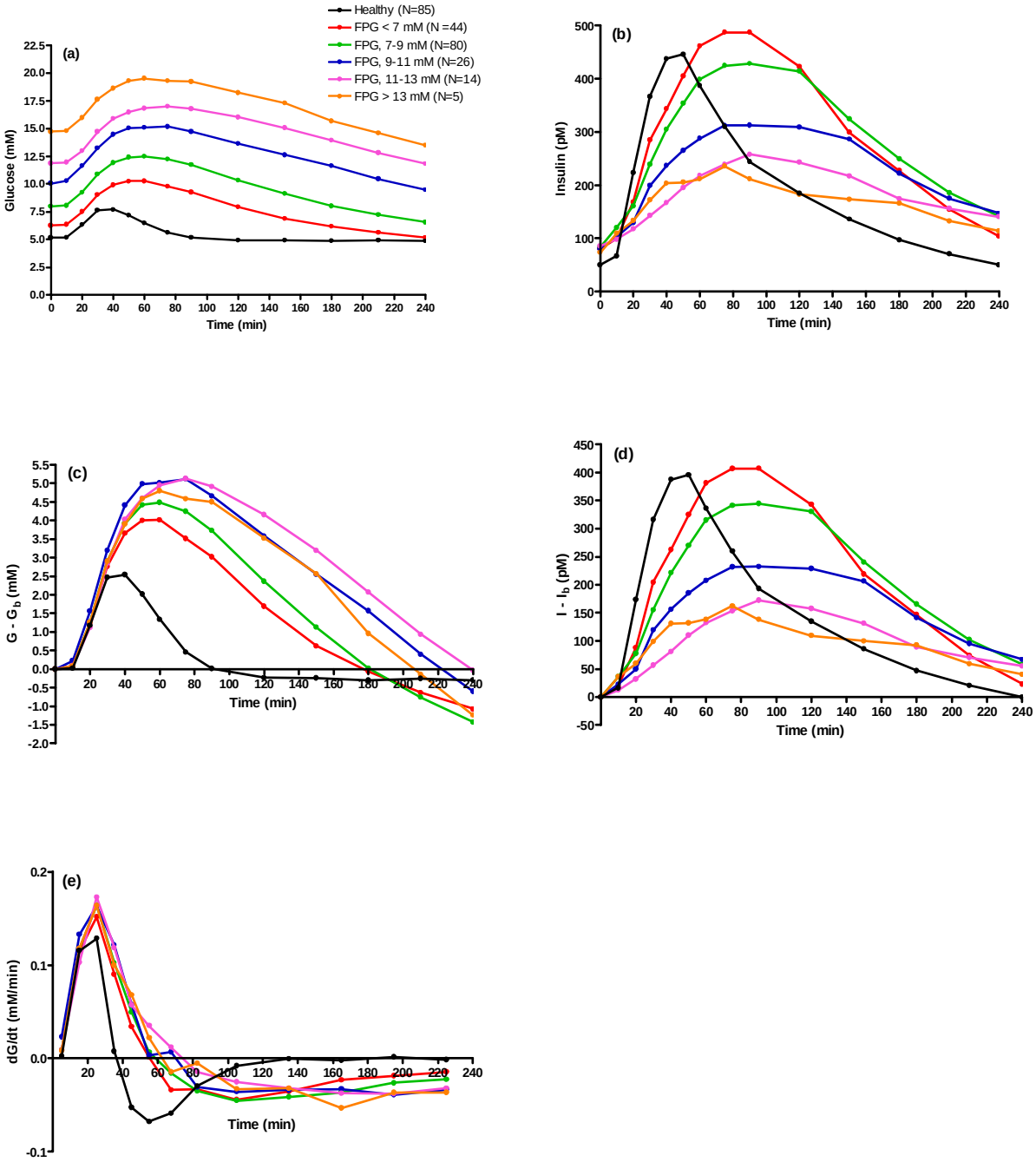

Fig. 5.3: (a) Plasma glucose and (b) plasma insulin for the subjects with type 2 diabetes at year 1 visit. The corresponding plasma profiles of (c) glucose and (d) insulin where the fasting values (t=0 min) have been subtracted. (e) The differentiated glucose profiles.

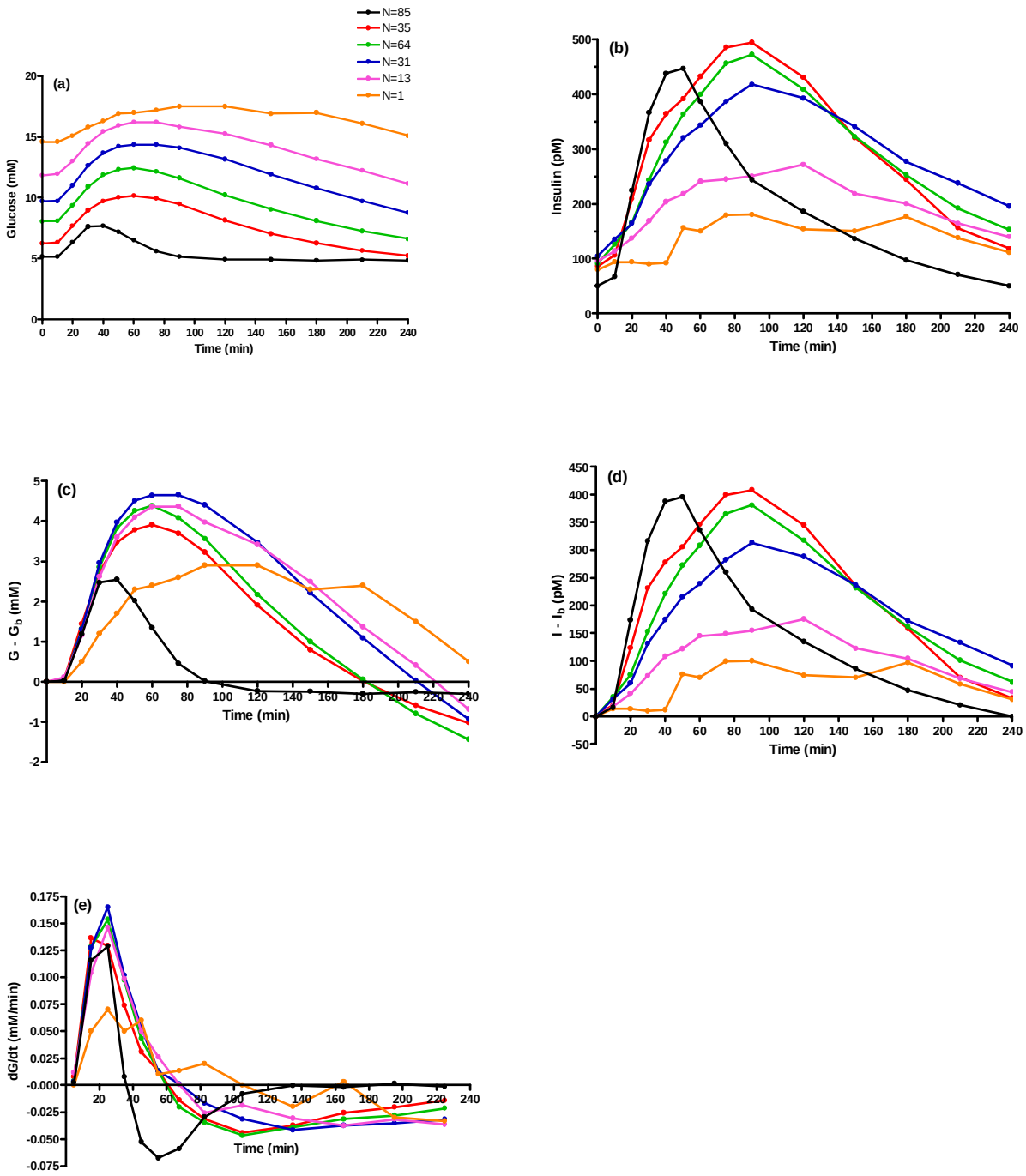

Fig. 5.4: (a) Plasma glucose and (b) plasma insulin for the subjects with type 2 diabetes at year 2 visit. The corresponding plasma profiles of (c) glucose and (d) insulin where the fasting values (t=0 min) have been subtracted. (e) The differentiated glucose profiles.

Year 5

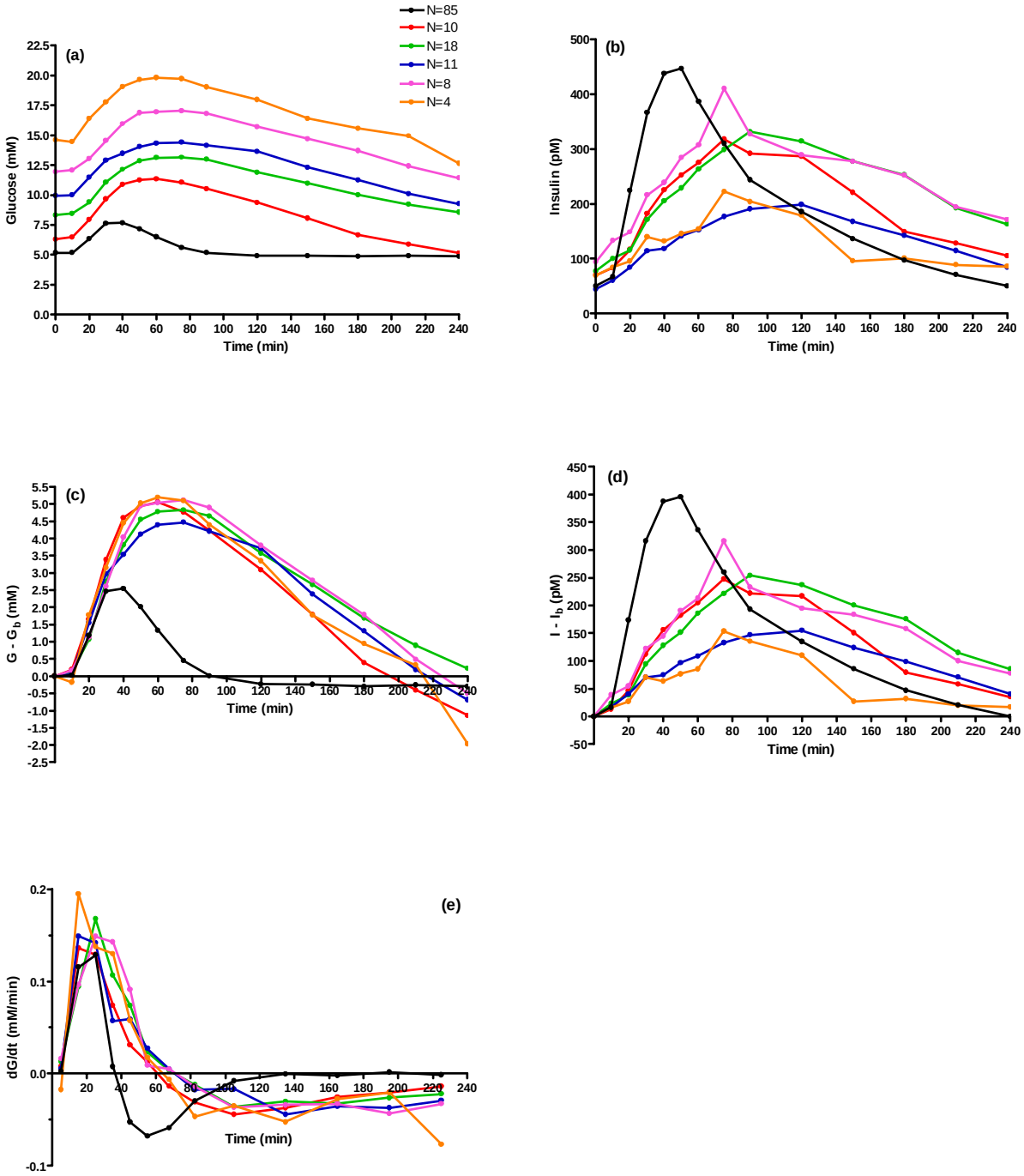

Fig. 5.5: (a) Plasma glucose and (b) plasma insulin for the subjects with type 2 diabetes at year 5 visit. The corresponding plasma profiles of (c) glucose and (d) insulin where the fasting values (t=0 min) have been subtracted. (e) The differentiated glucose profiles.

Year 10

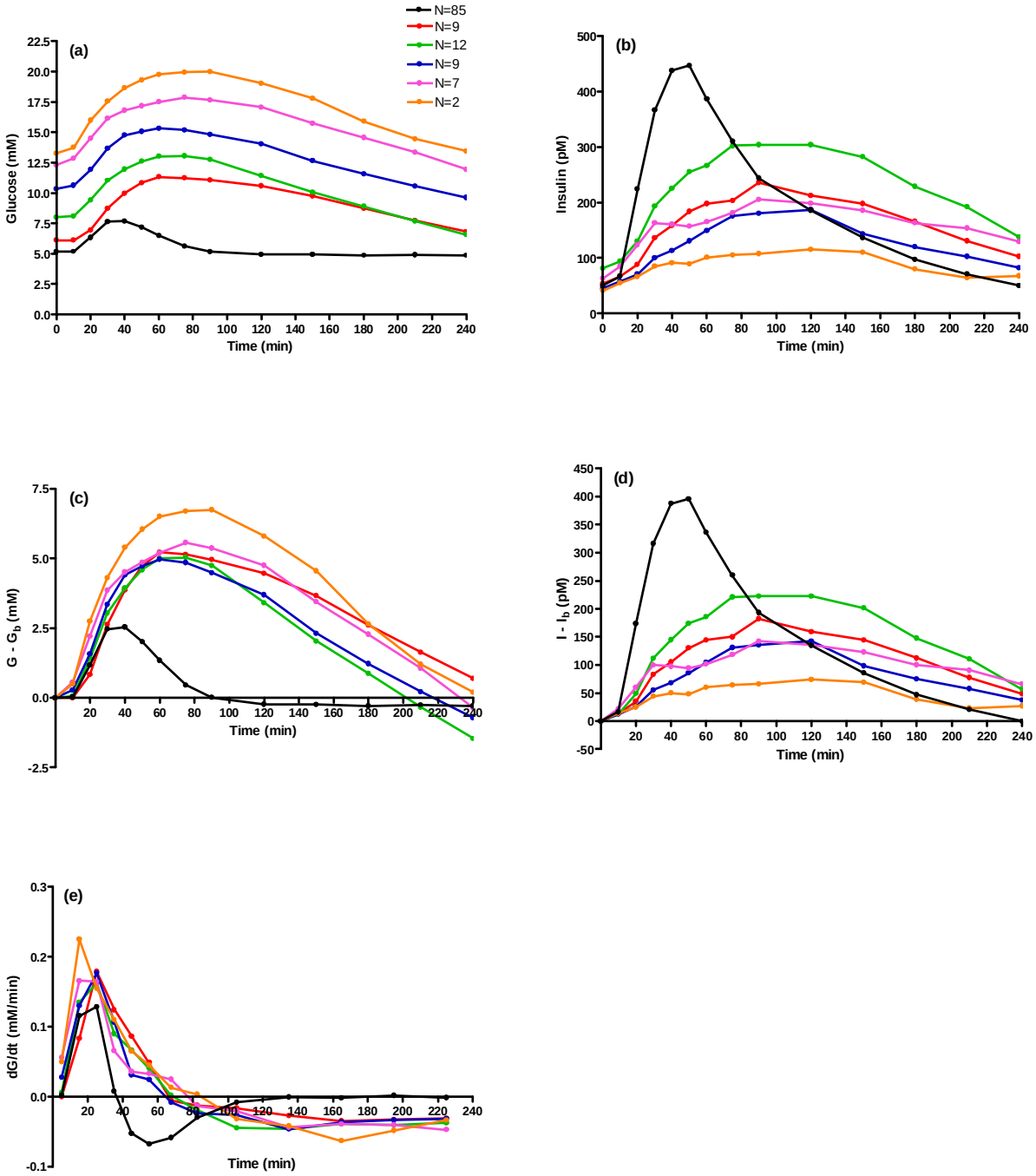

Fig. 5.6: (a) Plasma glucose and (b) plasma insulin for the subjects with type 2 diabetes at year 10 visit. The corresponding plasma profiles of (c) glucose and (d) insulin where the fasting values (t=0 min) have been subtracted. (e) The differentiated glucose profiles.

Fig. 5.7 shows the mean of the differentiated glucose profiles of the groupings for all the years and the corresponding insulin profiles, together with the healthy profiles. It is evident that the changes in glucose are similar for the subjects with type 2 diabetes, despite different insulin levels, and also despite different treatment throughout the years. The consistent difference between the healthy profile and the profile from the subjects with type 2 diabetes is also clear. Furthermore, the subjects with type 2 diabetes seem well-treated as the mean HbA1c goes from 8.7 at year 0 to 6.5, 6.8, and 7.0 at year 1, 5, and 10, respectively. Also notice the relatively large amount of subjects at each year from 356 at year 0, to 180, 144, 51, and 39 at year 1, 2, 5, and 10, respectively. Hence the conclusions are based on a large data material.

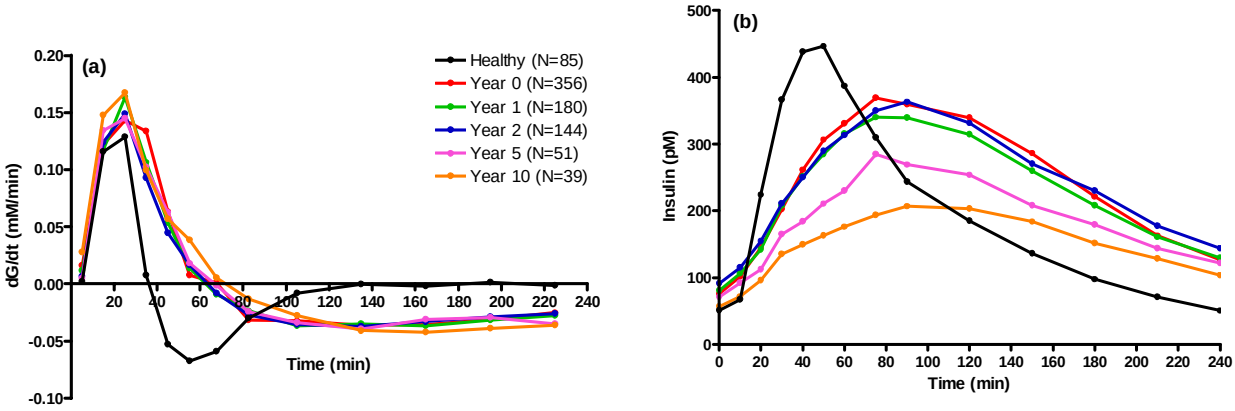

Fig. 5.7: (a) The time courses of the means of the differentiated glucose profiles for the subjects with type 2 diabetes at first visit (year 0), and follow up visits at year 1, 2, 5, and 10. (b) Corresponding time courses of mean plasma insulin profiles.

5.1.2 Same subjects followed through years

In the previous section the glucose and insulin profiles for the different years were analysed without taking into account if the same subjects were presented at all the years. Hence one could argue that the findings are not consistent, as both the number of subjects and the specific subject vary from year to year.

To address this issue, I inspected the database, and found that the same 44 subjects were followed at the year 0, 1, and 5. I disregarded the year 2 subjects in this analysis as it was expected to give similar results as with the year 1 subjects, due to the similar insulin profiles, cf. Fig. 5.7(b), and due to the relatively small time lapse between the visits. Unfortunately only very few subjects were left if I included the subjects at year 10. Hence these were dropped in this analysis.

To examine the insulin dependency of the glucose profiles for the remaining subjects, i.e. the 44 subjects followed at year 0, 1, and 5, respectively, the subjects were grouped according to the mean AUC values of the year 1 insulin profiles above fasting value. Hence if a subject had a value of AUC of insulin (above fasting value) for the year 1 insulin profile that was above the mean the AUC of year 1 insulin profiles (above fasting values), the subject was arranged in group 1. Correspondingly if the value of the AUC of the year 1 insulin profile (above fasting values) was below (or at) the value of the mean of the year 1 insulin AUC, the subject was arranged in group 2.

I choose to stratify according to the mean AUC value of the year 1 profile as year 1 is special in the sense that this is the first visit at which the subjects received treatments before the visit, also this was the smallest time lapse for progression of the disease. Hence it was expected that any effect of insulin on the glucose profiles was most prominent with this choice of stratification. Stratification according to mean insulin AUC of year 0 or 5 was however also performed, with similar results as the chosen stratification procedure (results not shown).

Fig. 5.8 shows the results of the 44 subjects arranged in two groups according to the mean AUC of insulin above fasting values at year 1 together with the healthy data. Again the overall conclusions are the same. The effect of insulin is primarily on the glucose peak time and value, whereas the glucose downstrokes declines linearly and almost in parallel. Some effect of insulin on the glucose profile are however visible at the highest insulin levels where it is most prominent for the subjects at year 1 in grp. 2, where also a considerable glucose undershoot develops at the end of the test. However the overall similarities between the groups of subjects with type 2 diabetes are clear from Fig. 5.8(c), where the differentiated glucose profiles are almost overlapping. Again the differences between the healthy and the subjects with type 2 diabetes are undeniable.

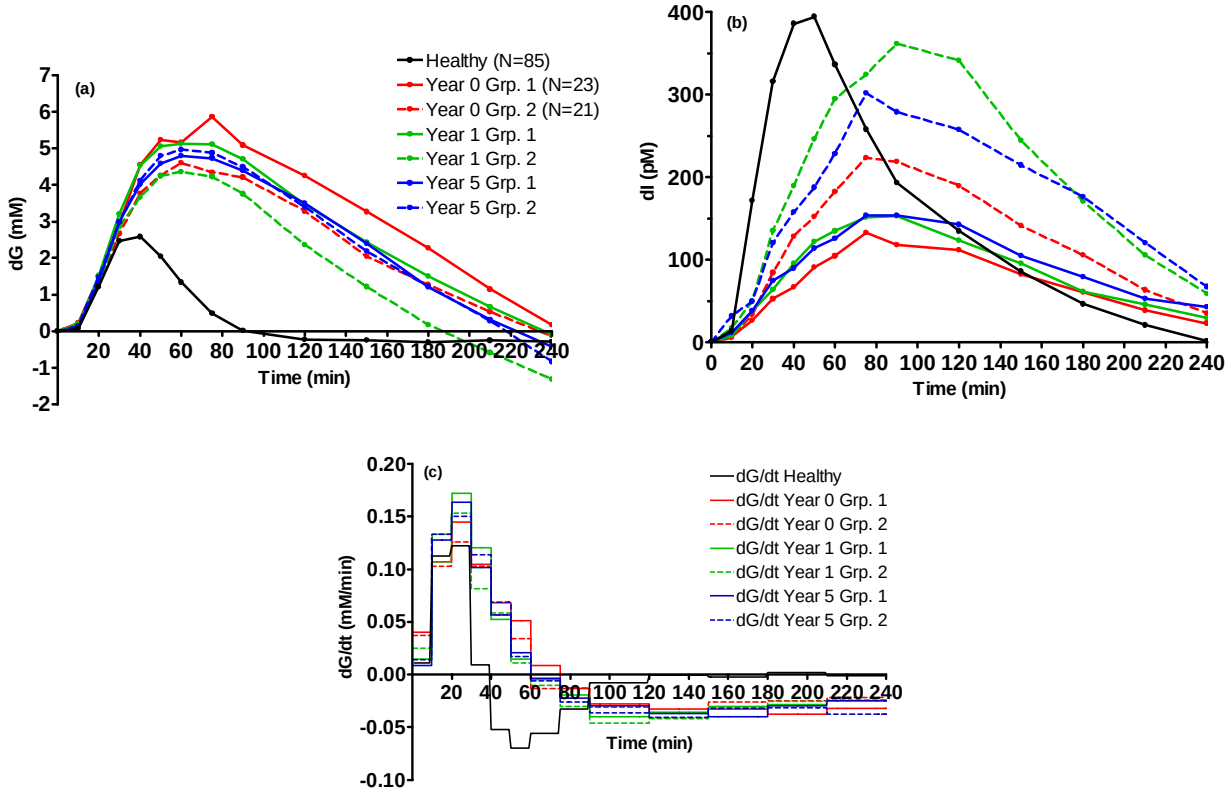

Fig 5.8: The subjects with type 2 diabetes are grouped according to the mean of the *Area Under the Curve*, AUC insulin time courses above fasting value. (a) Time course of mean plasma glucose concentration above fasting values. (b) Time course of mean plasma insulin concentration above fasting. (c) Time course of the mean of the differentiated individual plasma glucose concentration time courses.

5.1.3 Fundamental difference between healthy and subjects with type 2 diabetes

As pointed out several times now there is a clear difference between the glucose profiles of the healthy subjects and the subjects with diabetes as shown in Fig. 5.9. Here the differentiated mean plasma glucose responses are shown for all the subjects with type 2 diabetes and the healthy subjects. The figure shows the net glucose fluxes and the curves correspond to the difference between the glucose appearance, R_a and the glucose disappearance, R_d. The initial upstroke flux is similar for the subjects with type 2 diabetes and the healthy subjects , but it lasts longer for the subjects with type 2 diabetes. For the healthy the downstroke is brief and vanishes as the fasting value is reached. For the subjects with type 2 diabetes the downstroke lasts longer and continues even after the fasting has been reached.

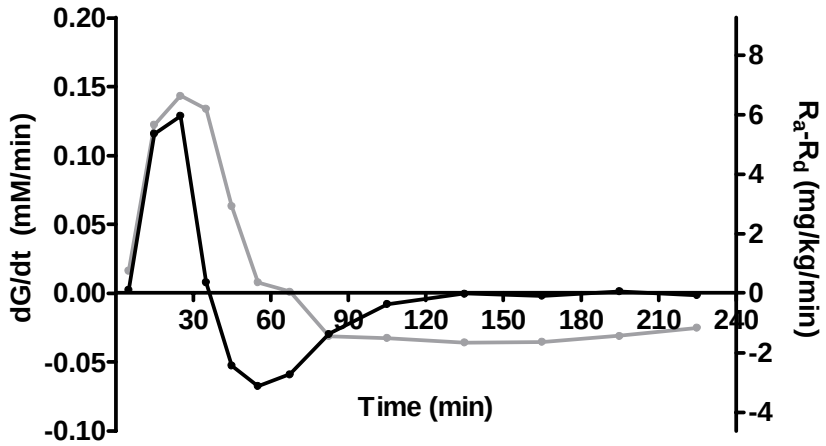

Fig. 5.9: The mean of the differentiated individual glucose profiles for the healthy (black line), and the subjects with type 2 diabetes (grey line). Left y-axis shows the difference between the appearance, R_a and disappearance, R_d of glucose.

The positive rate of change of glucose ($dG/dt > 0$) is commonly used as an indicator for the first phase insulin secretion, where in the oral case it is denoted the dynamic phase, cf. chapter 3. As evident from Fig. 5.9 the dynamic phase is longer for the subjects with type 2 diabetes, lasting approximately 60 min, whereas for the healthy subjects the dynamic phase is finished within approximately 40 min. Hence the assessment of the dynamic phase insulin secretion is based on different glucose stimulation pattern, which makes the interpretation of the dynamic phase index difficult.

Fig. 5.10 shows the increase of plasma glucose and plasma insulin above the fasting values for the healthy subjects. Glucose is normalised within two hours but insulin is still increased, implying that insulin is still released. The increased insulin release for decreasing glucose as compared with the insulin release for increasing glucose was described in Chapter 4 by the delayed component in the relation between insulin and glucose, cf. Eqs. (4.1), (4.3). For the C-peptide minimal model this was described by the static secretion component.

An even more interesting observation that can be extracted from the figure is that the increased insulin does not lead to hypoglycaemia.

Normally the increased insulin after a meal inhibits the hepatic glucose output and increases glucose uptake, hence it would be expected that the still elevated insulin when glucose has returned to FPG would lead to hypoglycaemia, as a result of an apparent net increased glucose uptake. However this

is seemingly not the case and the figure suggests that the effect of insulin, i.e. the net disappearance of glucose is controlled in such a way as to follow the rate of appearance of glucose.

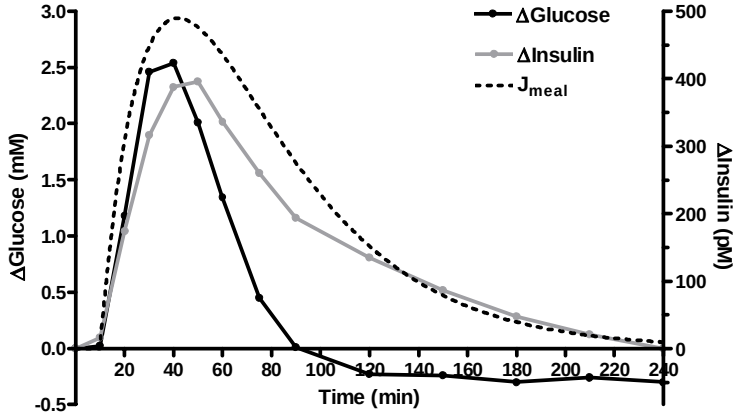

Fig. 5.10: The increase of mean plasma glucose concentration above fasting value after a meal for healthy subjects (black line, left y-axis), and the corresponding increase of mean plasma insulin above fasting value (grey line, right y-axis). The dashed black line illustrates the time course of the appearance rate of glucose from the meal. The effect of insulin seems to be controlled in such a way as to follow the rate of appearance of glucose.

The situation is quite different for the subjects with type 2 diabetes as shown in Fig. 5.11. After the peak glucose value has been reached, the glucose profile from the subjects with type 2 diabetes, in contrast with the healthy subjects, continue to decline slowly and in an almost linear fashion throughout the rest of the 4-hour test period.

The elevated insulin level seems to have minor impact on the glucose profile, however the elevated insulin at the end of the test period seems to provoke glucose undershoot.

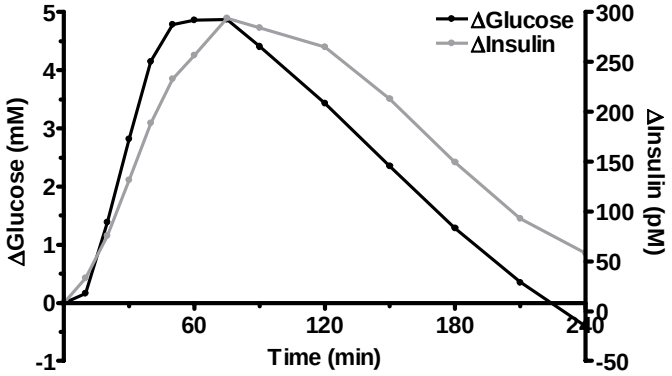

Fig. 5.11: The increase of mean plasma glucose concentration above fasting value after a meal for subjects with type 2 diabetes (black line, left y-axis), and the corresponding increase of mean plasma insulin above fasting value (grey line, right y-axis).

As mentioned earlier the post-prandial glucose profile is determined by the balance between the net glucose appearance, i.e. the sum of the rate of absorption of glucose from the meal and the net heapatic (and kidney) glucose output, and the net glucose uptake rate, primarily by muscle and adipose tissue. The meal-derived glucose, i.e. the rate of absorption has been found to be similar for healthy and in subjects with impaired fasting plasma glucose and/or impaired glucose tolerance (Bock *et al.* 2006). In subjects with type I diabetes, insulin given 20 min prior to a mixed meal yielded no significant difference in the meal-derived glucose rate of appearance, as compared with basal insulin administration (Pennant *et al.* 2008). Hence these studies indicate that meal-derived glucose rate of appearance is similar for healthy and subjects with diabetes. The debate is then on the balance between (and regulation of) the hepatic glucose output and the peripheral tissue uptake.

Traditionally the main regulating substance of the post-prandial glucose flux is considered to be insulin, or more precisely the insulin/glucagon ratio. More recently also the effect of glucose, i.e. glucose effectiveness, has been suggested to play a major role in the regulation of both hepatic glucose production as well as peripheral tissue glucose uptake (Nielsen 2008).

Interpreting the findings regarding the Owens meal response data in light of this would then imply that the glucose profiles from the subjects with type 2 diabetes are lowered more or less solely due to the glucose effectiveness, as insulin does not seem to have a major effect on the glucose profiles, i.e. they appear to be completely insulin resistant. The term glucose effectiveness does however prompt some issues.

First of all, glucose uptake by the tissue depends both on the glucose concentration as well as on the insulin concentration (Yki-Järvinen *et al.* 1987) as shown in Fig. 5.12. The glucose uptake at fixed insulin levels is saturable due to the transport by special glucose transporters, cf. Fig 5.12(a), and the insulin-mediated glucose uptake at fixed glucose levels can be described by a hill function, cf. Fig. 5.12(b). Hence from the figure it is clear that no constant measure for the glucose effectiveness can be defined as it depends on the prevailing glucose as well as the insulin level.

Secondly as shown in the next section the effect of glucose on the hepatic glucose output differ from the glucose effect on the peripheral tissue uptake.

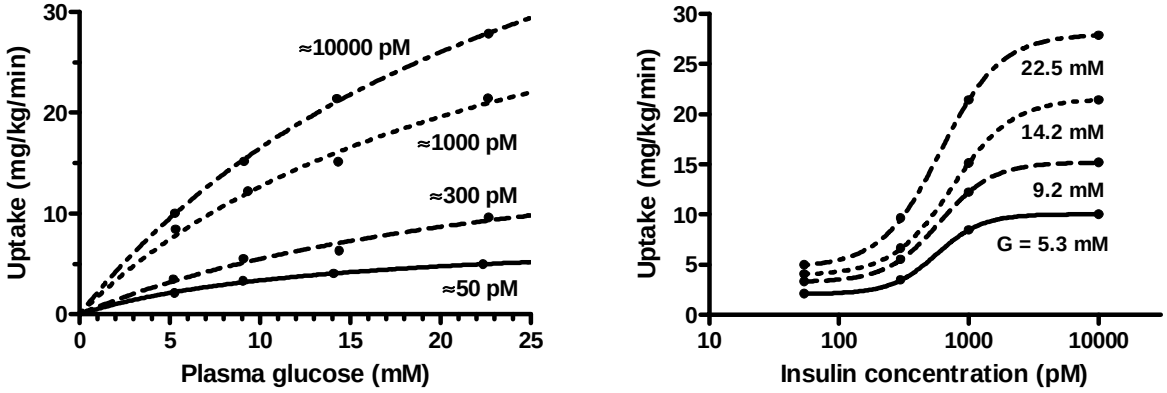

Fig 5.12: Whole body glucose uptake versus (a) plasma glucose at different insulin levels, and (b) insulin concentration at different plasma glucose levels. Adapted from Yki-Järvinen *et al.* (1987).

If the subjects are severely insulin resistant, the glucose effectiveness would be the dominating glucose lowering effect. One explanation to the similarities between the meal responses of the subjects with type 2 diabetes could then be that due to the intrinsic saturability of the glucose uptake, cf. Fig 5.12(a), the effect of glucose to increase its own uptake would be similar and almost constant for the subjects, and hence the glucose responses would be similar.

The glucose dependent glucose uptake can be described by a Michaëlis-Menten relation with a half-saturable constant K_M = 5 mM (Hallgreen *et al.* 2008). The glucose concentrations for the subjects with type 2 diabetes vary over a wide range, with FPG going from below 7 mM to above 15 mM. At 7 mM the glucose transport is 58% saturated, and at 15 mM glucose transport is 75% saturated. Hence unless the glucose transporters are severely damaged in the subjects it would be expected that the uptake of glucose is different in the subjects, and hence a clear difference would be visible in the glucose responses.

Glucose has to pass the capillary wall to enter the interstitial space, where it can be taken up by the cells. The passage across the capillary wall introduces some delay between changes in plasma concentration and the resulting uptake, hence in reality the relation between plasma glucose concentration and uptake is more flat than a Michäelis-Menten relation with K_M=5 mM would yield. However unless the passage across the capillary wall, which is generally assumed to be by mere diffusion (Zierler 1999), is severely damaged, it would still be expected that the glucose uptake differ between the subjects.

Neither the glucose rate of appearance nor the glucose uptake (or disappearance) rate has been determined in the subjects, hence it cannot be determined how the balance between these two

fluxes nor their regulation influences the meal responses. Some authors find normal meal regulation of hepatic glucose production but impaired glucose uptake in subjects with pre-diabetes and diabetes (Bock *et al.* 2006) as compared with control, while others find impaired after-meal regulation of hepatic glucose production to be most important for the glucose meal response (Gerich 1991).

Whatever flux may be most important, the curves of the differentiated after meal glucose profile show that the net effect of the fluxes are more or less similar for the subjects with type 2 diabetes at any degree of impaired fasting plasma glucose, at any insulin level, at any treatment, and at any diabetes progression state, cf. Fig. 5.7.

The balance between the effect of insulin and the effect of glucose on the meal responses cannot clearly be determined from the present data. The effect of glucose is much debated (Nielsen 2008). Investigators report unchanged (Alzaid *et al.* 1994; Nielsen 2008) or even increased (Henriksen *et al.* 1994) glucose effectiveness in subjects with pre-diabetes or diabetes. Most of the results are based on minimal model assessment of both the insulin and the glucose effect, hence these results are model-dependent, and the ability of the minimal model to correctly assess the effect of glucose as well as insulin is questionable, cf. chapter 3. The minimal model independent methods to estimate glucose effectiveness are often based on infusion of somatostatin to inhibit the insulin secretion such that insulin can be infused to match the healthy insulin profile. However, somatostatin elicits a multitude of actions (Lahlou *et al.* 2004) and treatment with a somatostatin analog has been shown to decrease glucose effectiveness (Kahn *et al.* 1990). Hence also these model-independent methods with somatostatin infusion seem to contain questionable steps, and the results should be handled cautiously.
Hence the question to what extend the glucose effectiveness play a role seems still to contain a somewhat blurred answer.

No matter what, the regulation of after-meal glucose in subjects with type 2 diabetes is clearly impaired as compared with the healthy regulation, cf. Fig. 5.9, and insulin seems just to follow the glucose and not controlling it, to any significant extend. However glucose undershoot do seem to develop at the end of the meal test period for some of the subjects with type 2 diabetes with the highest insulin levels, cf. Fig. 5.2.

Strikingly the healthy glucose disappearance seems to be regulated in such a way as to follow the appearance, cf. Fig. 5.10. This seems to be a totally new aspect in the regulation of meal

glucose responses, and it will be further discussed in chapter 7. Certainly in the subjects with type 2 diabetes this regulation seems to be highly impaired.

The subjects with type 2 diabetes at the different years are all well-treated. As the meal-responses are quite similar the main effect of treatment seems to be on the fasting plasma glucose, FPG. The next section will focus on the variability and regulation of FPG.

5.2 Fasting plasma glucose

Even though, as noted in the previous section, the meal-related glucose responses for the subjects with type 2 diabetes seem quite similar, the fasting plasma glucose values vary greatly and spread in the range from 5-21 mM, cf. Fig. 4.2. Hence this section will concentrate on the variability and regulation of the fasting plasma glucose, where the fasting plasma glucose is the concentration of glucose in the (arterial) plasma when the body is in the fasting state. The fasting state is the state where there is no intestinal absorption of glucose. Hence the fasting plasma glucose concentration is determined by the balance between the hepatic glucose output and the disappearance of glucose by uptake.

In the fasting state, the liver breakdowns the glycogen that has been stored during fed state via glycogenolysis and releases free glucose. Furthermore, the liver makes new glucose via precursors, with the main contributors being lactate, glycerol, and amino acids, primarily alanine, by the process of gluconeogenesis, GNG. In the fasting state the skeletal muscle tissue primarily oxidise fatty acids, FA, and glucose is spared or turned into lactate that goes to the liver for rebuild of glucose. The adipocytes breakdown fat, TG via lipolysis and releases FA and glycerol. The FA goes to the skeletal muscle for oxidation and the glycerol goes to the liver for rebuild of glucose by GNG.

Normally these processes work in concert to maintain a relatively constant fasting plasma glucose concentration where the insulin/glucagon ratio plays a prominent role by directing the different fluxes in the right direction by regulating the activities of the involved enzymes. In subjects with type 2 diabetes the high diversity in the fasting plasma glucose values may be caused by an imbalance between these processes.

5.2.1 Variability of FPG

Fig. 5.13(a) shows the scatter plot between HbA1c and FPG for the newly-diagnosed subjects with type 2 diabetes from the Owens database, cf. Chapter 3. From this plot, for a given HbA1c value a "mean" FPG value can be determined, cf. the red line in the figure.

Fig. 5.13(b) shows the distribution of the difference between the individual FPG values and the estimated "mean" value from Fig. 5.13(a) for a given value of HbA1c. The distribution is seen to resemble a normal distribution with a mean at 0 mM and a standard deviation of 2 mM. Hence as already noticed, there is a large spread in the FPG values. Similar distributions as the one shown in Fig. 5.13 is found for the subjects at year 1, 5, and 10 (results now shown), hence FPG have large variability for all the years.

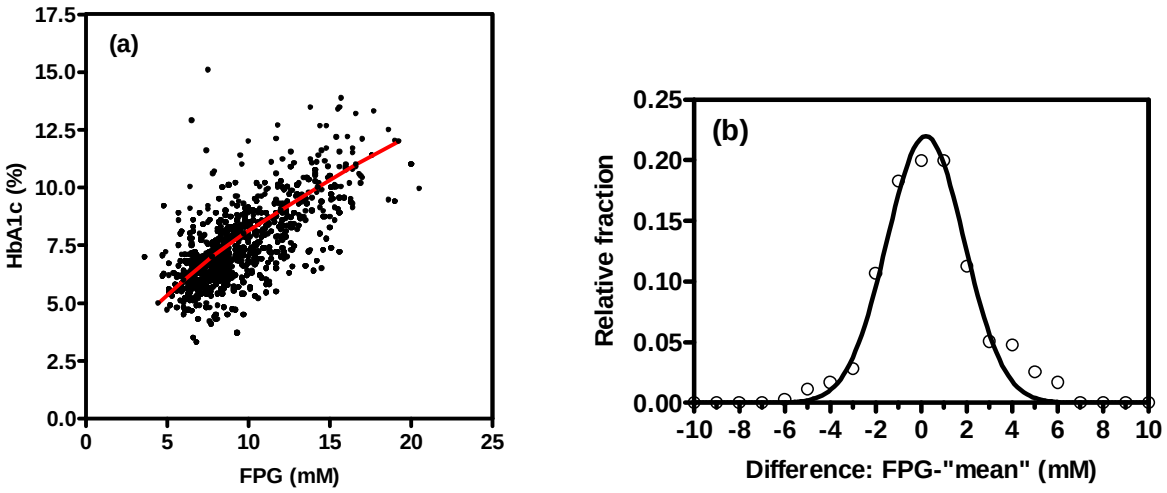

Fig. 5.13: (a) The scatter plot between HbA1c and fasting plasma glucose, FPG values for newly-diagnosed subjects with type 2 diabetes from the Owens database, cf. Chapter 3. From the plot a "mean" value of FPG can be determined for a given HbA1c, i.e. the red line (b) The distribution of the difference between individual FPG and the "mean" determined from (a). The distribution resemble a normal distribution, full drawn curve, with a standard deviation, SD = 2 mM.

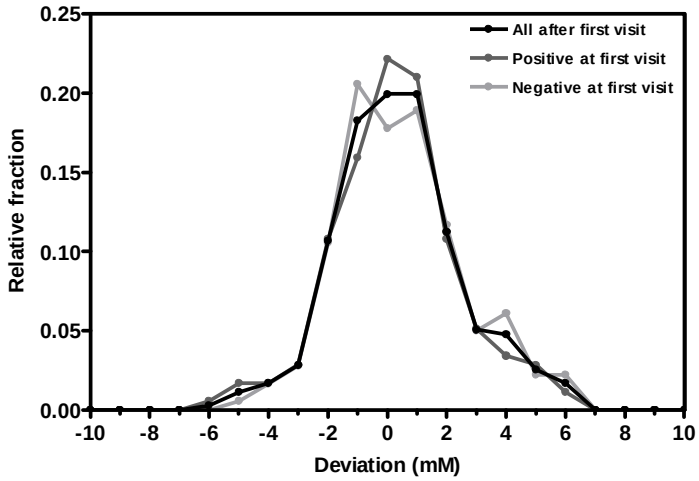

Fig. 5.14: For the subjects at the second visit (year 1), the distribution of the difference between the individual FPG value and the "mean" FPG value is split in two, according to if the subjects with type 2 diabetes had a positive difference (dark grey) or a negative difference (light grey) at the first visit (year 0) when they where newly-diagnosed. The two distributions are similar to the distribution found at first visit for all subjects (black and Fig. 5.13(b)). Hence the variation in FPG is completely random.

Fig. 5.14 shows the distributions of the differences between the individual FPG value and the "mean" as determined according to Fig. 5.13(a) for the subjects at year 1, where the subjects are grouped according to whether they had a positive or a negative value of the difference at the year 0. Both distributions, the positive as well as the negative are similar to the one found for all subjects at year 0. Hence the variations of the FPG over time are large and seem to be completely random.

Fig 5.15 shows the changes in fasting plasma insulin concentration, FPI from year 1 to year 5 against the changes in fasting plasma glucose concentration, FPG from year 1 to year 5 for the subjects with type 2 diabetes from the Owens database. The main tendency is that the large changes in FPG is not seen in the changes in FPI as it only changes moderately, both for increased as well as decreased FPG values.

Hence not only is the "relation" between FPG and FPI complex, cf. Fig. 4.2, but also the changes over time of FPG for both decreased as well as increased values seems unrelated and not caused by changes in FPI levels. In note we found the waist circumference to be an explaining variable for the variability in fasting plasma insulin, cf. Chapter 4.

Furthermore Radziuk and Pye (Radziuk and Pye 2006) found that the 24-h fasting plasma glucose concentration in subjects with type 2 diabetes elicited a particular diurnal rhythm driven by the hepatic glucose output via changes in gluconeogenesis. Fasting plasma glucose values rose from

a minimum value of around 6 mM to a peak value of around 8 mM. No similar pattern was found in the insulin profile that decreased slightly throughout the 24-h period. In contrast, the healthy fasting plasma glucose profile remained essentially constant throughout the period while decreasing slightly towards the end. Insulin levels decreased slightly throughout the period.

Thus the fasting plasma glucose for subjects with type 2 diabetes does not only elicit a large variation from year to year, but also on a daily-basis a large variation can be observed depending on the time of the day, while independent on the prevailing insulin level.

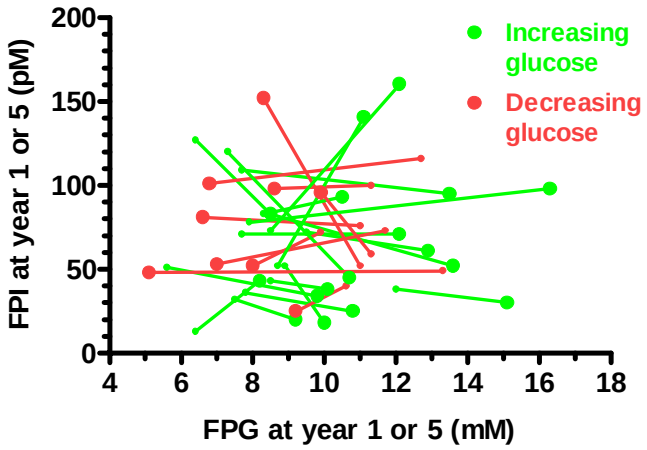

Fig. 5.15: Changes in fasting plasma insulin, FPI from year 1 to year 5 plotted against the corresponding changes in fasting plasma glucose, FPG for subjects with type 2 diabetes from the Owens database. The small dot indicates values at year 1, and the big dot indicates values at year 5. The main tendency for both decreasing (red) and increasing (green) glucose values from year 1 to year 5, is that large changes in the FPG occurs while FPI only changes moderately (almost constant). Hence changes in FPG seem independent of changes in FPI.

5.2.2 Relation between FPG and HGO

Investigators report of a positive correlation between FPG and HGO as shown in Fig. 5.16.

On the other hand in hyperglyceamic clamp studies with constant insulin, HGO has been found to be inhibited by the glucose level in subjects with diabetes to a similar degree as in healthy control subjects, cf. Fig. 5.17.

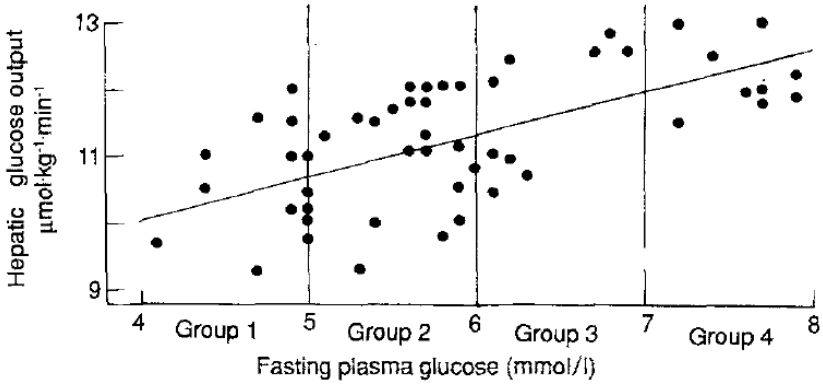

Fig. 5.16: Positive correlation between hepatic glucose output and fasting plasma glucose. Adapted from (Gerich 1991).

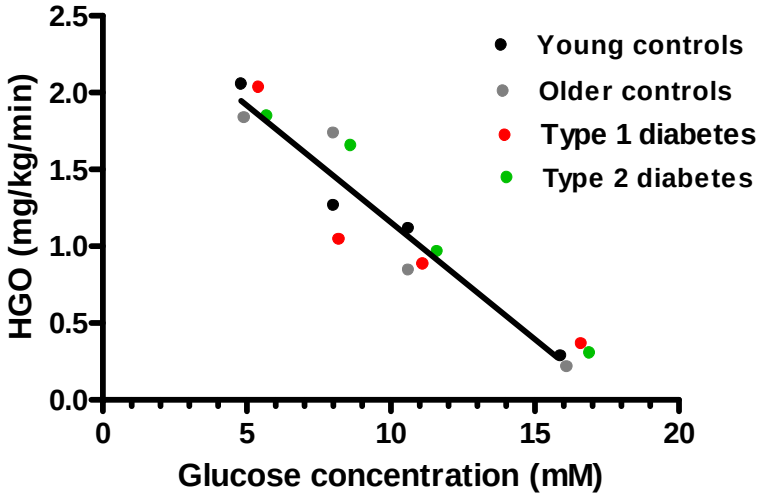

Fig. 5.17: Relation between hepatic glucose output, HGO and glucose clamp levels in a hyperglycaemic clamp study with constant insulin. HGO is seen to be inhibited similarly in healthy as well as in subjects with diabetes. Adapted from (Del Prato *et al.* 1997).

Thus contradicting results exists regarding the relation between FPG and HGO. The different results may arise from the fact that it is very difficult to estimate HGO, and the different methods applied have different accuracy (Basu *et al.* 2008).The circumstances under which the methods are applied will also give different results.

Furthermore as the fasting plasma glucose also depends on the disappearance rate of glucose by cellular uptake and in cases of high glucose values (> 10 mM) also by renal excretion the situation is more complex. Fig. 5.18 shows the major glucose fluxes during the fasting state.

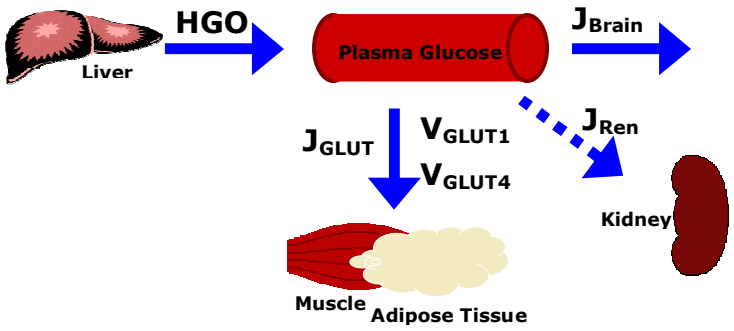

Fig. 5.18: Glucose fluxes in the fasting state. Fasting plasma glucose is determined by the balance between the hepatic glucose output, HGO and the cellular uptake by muscle and adipose tisseu, J_{GLUT}, the brain glucose uptake, J_{Brain}, and in cases of high glucose values (>10mM) also renal excretion, J_{Ren}

The equation governing the fluxes given in Fig. 5.19 can be written (Hallgreen *et al.* 2008)

$$V_G \frac{dG}{dt} = HGO - J_{upt} \tag{5.1}$$

where V_G is plasma glucose distribution volume, G is plasma glucose, and J_{upt} is the sum of cellular glucose uptake and renal excretion, given by

$$J_{upt} = J_{brain} + V_{GLUT} \frac{G}{K_M + G} + J_{Ren} \tag{5.2}$$

where J_{brain} = 80 mg/min is the normally constant brain uptake, V_{GLUT} is the sum of the maximal activities of the saturable glucose transporters GLUT1 and GLUT4, with K_M = 5 mM being the half-saturation value, and J_{Ren} is the renal excretion rate shown in Fig. 5.19.

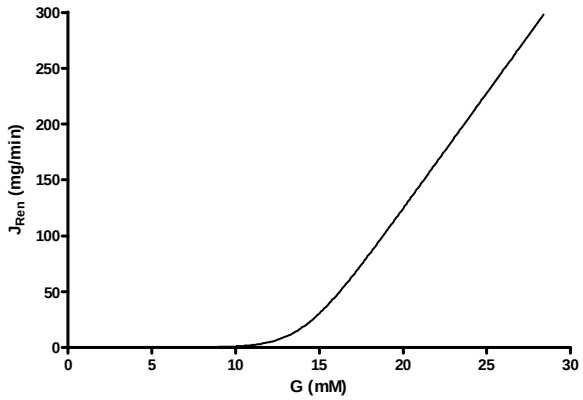

Fig. 5.19: Renal glucose extraction rate. Adapted from (Hallgreen *et al.* 2008).

From Eqs. (5.1) and (5.2) we have in the fasting state

$$HGO = J_{brain} + V_{GLUT}\frac{G}{K_M + G} + J_{Ren} \tag{5.3}$$

The fasting HGO (overnight fast) is in the order of 140 mg/min. Of this the brain takes 80 mg/min. The remainder, 60 mg/min, is the glucose dependent uptake. With K_{GLUT}=5 mM and a fasting glucose of 5 mM, the fasting value of $V_{GLUT} = V_{GLUT1} + V_{GLUT4}$ becomes 120 mg/min.

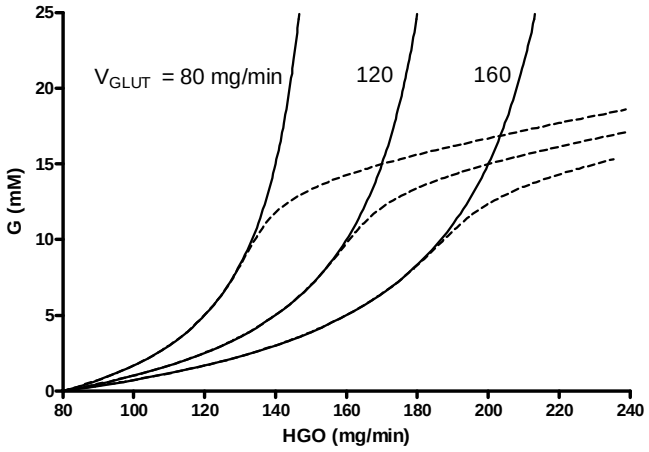

Fig. 5.20: Relation between plasma glucose concentration and hepatic glucose concentration in the fasting state as determined by Eq. (5.3) for different values of V_{GLUT} corresponding to different values of insulin. Even for moderate changes in HGO an increase is V_{GLUT} is necessary for keeping low levels of glucose. The renal extraction sets in for glucose concentration values above 10 mM (dashed line), and hence a much weaker dependency on HGO is seen for large glucose values.

The relation between G and HGO in the fasting state as determined by Eq. (5.3) is shown in Fig. 5.20 for different values of V_{GLUT}, corresponding to different fasting insulin concentrations. It is seen that even moderate increases in HGO requires an increase in V_{GLUT} to keep G low. The renal extraction work as a safety valve that keeps the glucose within reasonable limits, so above a G of 10-15 mM there is a much weaker dependency on HGO.

Hence the exact relation between fasting plasma glucose and hepatic glucose output depends on the glucose transport activities as well as on the renal extraction that both may vary considerably. As we shall see in the next chapter the overall control of fasting plasma glucose concentration gets even more complicated.

The glucose and insulin responses for a large number of subjects with type 2 diabetes and healthy subjects have been re-assessed in a new and simple way. The novelty of the method was based on the evaluation of the meal-related responses, i.e. the responses corrected by the fasting values, and the differentiated after-meal glucose profile. This representation of the response data revealed completely new facets of the glucose dynamics for both the healthy as well as the subjects with type 2 diabetes. The findings were:

- ***The mean meal-related glucose responses for newly-diagnosed untreated subjects with type 2 diabetes were strikingly independent of the prevailing insulin levels as well as on the fasting plasma glucose values, however insulin was shown to affect the glucose peak and peak-time value and glucose undershoot developed for large insulin levels at the end of the test period***
- ***Subjects with type 2 diabetes followed at years 1, 2, 5, and 10 after diagnoses and well-treated according to need showed similar results as with the newly-diagnosed subjects with type 2 diabetes with a slowly, almost linear, declining glucose response***
- ***The meal-related glucose responses for subjects with type 2 diabetes thus seem to be strikingly unaffected by the prevailing insulin level, the fasting plasma glucose, and the treatment and/or disease progression. Insulin levels in subjects with type 2 diabetes seem just to follow the glucose profile, but not controlling it to any significant extend***
- ***The similarities of the meal-responses for the subjects with type 2 diabetes were even more prominent when evaluated by the differentiated glucose profile that represents the meal-related glucose fluxes***
- ***Healthy glucose was quickly lowered within 90 min and stayed at fasting value throughout the rest of the 4-hour test period. This was fundamentally different from the subjects with type 2 diabetes with a slowly linear declining glucose throughout the test period.***
- ***Strikingly in the healthy subjects insulin was still released when glucose was at fasting value. This lead to the novel conclusion that the apparent glucose uptake for healthy subjects is regulated in such a way as to follow the glucose rate of appearance as the glucose stayed at the fasting value even when insulin continued to be elevated.***

Chapter 6

Glucose sensing and control

The common view of regarding the glucose-insulin control system as an isolated system to control plasma glucose concentration is shown to be much more complex. Firstly the glucose sensing mechanisms in the beta cell is shown to possess important intrinsic non-linear properties and the beta cell works in a complex network with other glucose sensors. Secondly, the handling of metabolites inside and between the different organs is shown to be critical for glucose control. Insulin and the nervous system are important components in the control system.

When the plasma glucose concentration increases, e.g. after a meal, the consecutive increased plasma insulin concentration lowers the glucose concentration primarily by inhibiting hepatic glucose output and stimulating glucose uptake in muscle and adipose tissue cells. In that respect, the glucose-insulin control system is often viewed as an isolated system to keep plasma glucose concentration within narrow limits, where the system is described by a closed-loop, or feedback loop, in terms of classic control theory, cf. Fig. 6.1. In this context, the controlled variable CO would be plasma glucose concentration, and the desired value CI, the fasting plasma glucose value. The controller signal CC would represents plasma insulin (or secretion), and CS the converted sensor signal to be processed by the controller. Hence one would regard the beta cell as representing the controller and sensing part, whereas the glucose uptake would be represented by the effector subsystem.

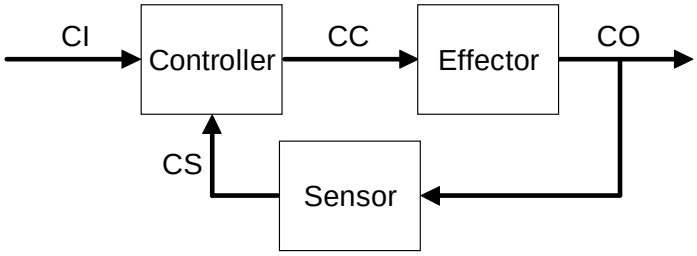

Fig. 6.1: Schematic structure of the three main parts of a classic control system; The controller, the effector and the sensor. CI is the desired value (or trace) of the controlled variable CO. CC is the signal from the controller to the effector, and CS is the signal from the sensor to the controller. Adapted from (Hallgreen *et al.* 2008).

The control system is classified according to how the controller handles the difference between the desired value, CI and the controlling variable CO, where CI and CO are characterised in same the modalities (Hallgreen *et al.* 2008). The most common application is to describe the beta cell as a Proportional-Integral-Differential, PID controller. The PID description of the sensing and controlling mechanisms in the beta cell has gained interests in the task of developing a closed-loop insulin delivery system to be used e.g. in subjects with type 1 diabetes or in subjects with developed type 2 diabetes for the automatic delivery of insulin based on PID control strategies (Panteleon *et al.* 2006).

A drawback of the PID control system is that it needs an error, i.e. difference between the actual CO and the desired CI value, to work. For the error to be small the gain, i.e. the ratio between the controller output and input, has to be large. However large system gain may lead to undesirable instabilities, oscillations etc. (Hallgreen *et al.* 2008).

A way to improve the control is by the use of feed-forward control, often denoted model predictive control, MPC. The idea behind the MPC strategy is to construct a control signal, CC_{FF} that reflects the expected time-course of CC that is needed to keep CO close to CI (Hallgreen *et al.* 2008).

The human biological system elicits many examples of both PID as well as MPC control strategies, where the MPC strategy often is conveyed by neural signals (Hallgreen *et al.* 2008; Peters *et al.* 2002). However, in contrast with classic control theory, biological systems have intrinsic non-linearities, that most often are crucial for the proper function. More over biological systems are interwoven, with many seemingly redundant signalling and controlling pathways, with the result that it is very difficult to intervene if something goes wrong. On the other hand the complexity and redundancy makes the biological system robust (Hallgreen *et al.* 2008; Peters *et al.* 2002).

With that in mind the chapter will focus on how glucose is sensed and handled in the human body, and to what extend classic control theory can be used to describe the complexity of the glucose-insulin control theory. Firstly, the glucose sensing will be described, and then secondly the glucose handling or uptake.

6.1 Time-dependent mechanisms in the beta cell glucose sensing

The beta cell is able to sense glucose and secrete insulin. Hence in a structural context the beta cell is viewed as presenting both the sensing and controlling subsystems as given in Fig. 6.1. The classic view of presenting the beta cell as a PID controller has its roots in the biphasic release pattern elicited by the beta cell, when stimulated by a square-wave glucose pulse (Steil *et al.* 2006).

In order to describe the different secretion phases elicited by the beta cell based on a more mechanistic basis, in contrast with classic control theory, we developed a new model to describe the time-dependent glucose-sensing mechanisms in the beta cell (Hallgreen *et al.* 2008; Korsgaard and Colding-Jorgensen 2006).

6.1.1 Glucokinase, GK: The key enzyme in the glucose sensing mechanisms in the beta cell

GK is essential in all glucose sensing cells and due to its co-localisation with the glucose transporter GLUT2 and its affinity for glucose in the physiological range it has laid the foundation of the glucose sensor concept (Korsgaard and Colding-Jorgensen 2006; Sweet and Matschinsky 1995). The transport across the cell membrane in the beta cell is done by GLUT2, with a K_M in the order 10-20 mM (Johnson *et al.* 1990; Thorens 1996), hence the intracellular glucose concentration mirrors the glucose in the physiological range. Furthermore, GK has a low affinity for glucose with half saturation at 8 mM (Meglasson and Matschinsky 1986), a value which is 50-100 times higher than other hexokinases, making GK maximal sensitive for the normal physiological range of glucose concentration.

These characteristics make GK the key regulatory step in the glucose sensing of the beta cell. Further evidence for the important role of GK in the glucose sensing mechanism has been found from studies showing that GK translocate from an inactive (bound) state to an active state upon glucose stimulation, with a relatively fast time constant in the order of 20-60 min (Miwa *et al.* 2004; Rizzo *et al.* 2002). The result is a varying (dynamic) amount of active GK in the cell. To give a clear presentation of the effects of the different mechanisms behind insulin release, the model is presented in steps. First the model without the GK translocation is presented.

6.1.2 The model without GK translocation

The structure of the model is shown in Fig. 6.2. Glucose is transported across the cell membrane by the glucose transporter GLUT2. Except its own phosphorylation, glucose does not appear to play a role inside the cell, hence it is quickly phosphorylated to glucose-6-phosphate, G6P by GK.
The signalling pathway from glucose enters the cell to final secretion of insulin is complex, but the main triggering pathway is well studied. In short, the increased ATP/ADP due to glucose metabolism closes ATP sensitive potassium-channels that results in membrane depolarisation which closes the voltage-dependent sodium channels. The resulting increase of intracellular sodium then triggers the release of insulin. It is assumed that a signal substance, S in combination with the increased ATP/ADP ratio trigger insulin release, R according to

$$R = \begin{cases} Q \cdot (S - S_0) + R_0, & \text{for } S > S_o \\ R_0, & \text{otherwise} \end{cases} \qquad (6.1)$$

where Q is a proportionality factor, R_0 is basal insulin release and S_0 the threshold value of S for glucose dependent insulin release.

Hence with this formulation of insulin release, the signal substance S determines the connection between glucose and insulin release.

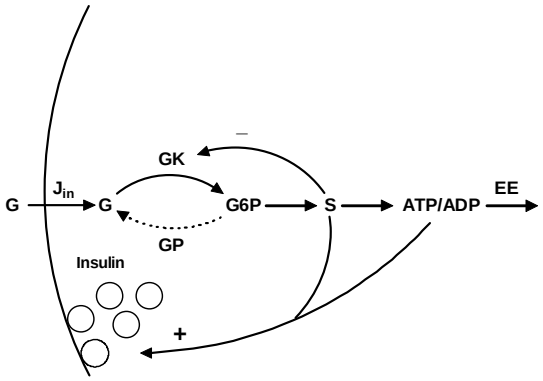

Fig. 6.2: Model structure. Glucose, G is transported across the cell membrane by GLUT2, hence the extracellular glucose concentration mirrors the intracellular glucose concentration. G is phosphorylated by glucokinase, GK to glucose-6-phosphate, G6P and fed into the glycolytic pathway. The glycolytic intermediate S is assumed to trigger insulin release in combination with the increased ATP/ADP ratio. The net flow of glucose J_{in} must match the energy expenditure, EE, assumed to be achieved by inhibition of GK by S.

6.1.3 Flux conservation

The beta cell has little or no glucose-6-phosphatase and lactate dehydrogenase (Giroix *et al.* 1987; Matschinsky 1996; Perales *et al.* 1991; Sekine *et al.* 1994), hence removal of excess G6P by conversion to glucose or lactate is not possible or in any case very limited. Furthermore the beta cell has little or no glycogen and fat storage (Newgard and Matschinsky 2001), hence removal of excess G6P by these routes is not possible either. The result is that all the inflowing glucose, J_{in} must be oxidised to match the energy expenditure, EE.

The glucose influx, J_{in} is given by the product of the amount of glucokinase, GK and the phoshorylation rate of a single GK enzyme, v

$$J_{in} = vGK \tag{6.2}$$

with the phosphorylation rate, v of the single GK enzyme described by the hill equation (Cornish-Bowden and Cárdenas 2004)

$$v = \frac{v_{max} G^h}{K_{hill}^h + G^h} = v_{max} f_{Hill}(G) \tag{6.3}$$

where v_{max} is the maximal phosphorylation rate, h = 1.7 is the hill coefficient, and K_{hill} = 8 mM is the concentration for half saturation (Magnuson and Matschinsky 2004).

Thus the inflow of glucose depends on the amount of GK and the glucose concentration, but as the energy expenditure, EE generally is independent of G, this call for a regulation. Here we assume that the inflow of glucose is inhibited by the substrate S, or some substrate proportional to S, but other assumptions can be made, yielding however similar result (Korsgaard and Colding-Jorgensen 2006). Assuming a first order inhibition of J_{in} by S, the equation describing the development of S is given by (Korsgaard and Colding-Jorgensen 2006)

$$K_I \frac{dS}{dt} = \frac{J_{in}}{1+S} - EE \tag{6.4}$$

where K_I is a constant determining the degree of inhibition of the inflow by S, and where S is written in units of K_I.

Eq. (6.4) implies that J_{in} must be larger than EE for S to be non-zero and positive in steady state. This means that if J_{in} is too small EE will go down. However in reality other nutrients as fatty acids and amino acids can also contribute to EE (Newgard and Matschinsky 2001). To account only for the contribution of glucose oxidation to EE, we modify Eq. (6.4)

$$K_I \frac{dS}{dt} = \frac{J_{in}}{1+S} - \frac{E_0 S}{a+S} \tag{6.5}$$

with a being a constant, and E_0 denoting the resting energy expenditure.
We assume that E_0 is constant even though this might not be true when insulin is released (Fridlyand *et al.* 2003; Kennedy *et al.* 2002).

From Eq. (6.5) we find that the steady state relation between S and G is given by

$$S = \frac{J_{in} - E_0 + \sqrt{(J_{in} - E_0)^2 + 4aJ_{in}E_0}}{2E_0} \tag{6.6}$$

with J_{in} determined by Eqs. (6.2) and (6.3).

Fig. 6.3 shows the steady state relation between the normalised S and glucose, G given by Eqs. (6.2), (6.3) and (6.6), for different values of the parameter k_S described by

$$k_S = \frac{v_{max} GK_T}{E_0} \tag{6.7}$$

with GK_T denoting the actual total amount of GK.

k_S is the ratio between the maximal glucose influx and the resting energy expenditure, where we assume that k_S is relatively small, i.e. k_S = 2 -10 (Korsgaard and Colding-Jorgensen 2006).

As evident from Fig. 6.3, decreasing the amount of GK or increasing E_0, as with lower k_S values, shift the steady state relation between S and G to the right, and hence lower the release of insulin.

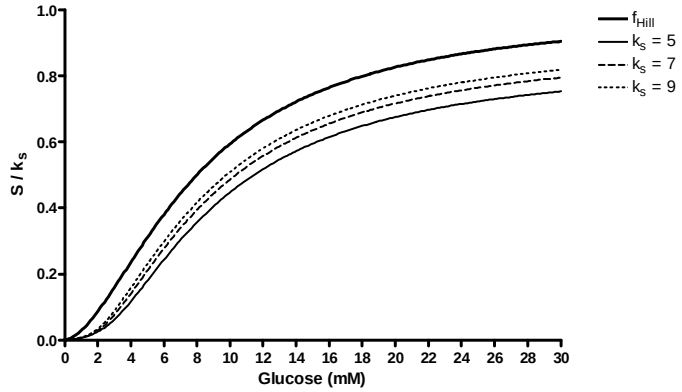

Fig. 6.3: Steady state relation between S and G described by Eq. (6.6) with a = 0.2 and varying k_S described by Eq. (6.7). Decreasing amount of GK shifts the curve to the right. The f_{Hill} curve described in Eq. (6.3) is plotted for comparison.

6.1.4 First phase

The first phase is modelled by assuming a simple first order delay on the inhibition by S of the glucose influx, i.e. Eq. (6.5) turns into

$$K_I \frac{dS}{dt} = \frac{J_{in}}{1+S^*} - \frac{E_0 S}{a+S} \tag{6.8}$$

with

$$\frac{dS^*}{dt} = \frac{1}{\tau}(S - S^*) \tag{6.9}$$

Hence S^* is delayed compared to S with the time constant τ.

Eq. (6.9) is applied based on the assumption that cellular diffusion takes some time. Hence, for fast changes in glucose concentration with the resulting fast changes in S, the inhibition effect will be delayed compared to S, due to the diffusion time.

Using Eqs. (6.2), (6.3), and (6.7), Eq. (6.8) can be written

$$\frac{dS}{dt} = \alpha\left(\frac{k_S f_{Hill}(G)}{1+S^*} - \frac{S}{a+S}\right) \tag{6.10}$$

with $\alpha = E_0/K_I$ being a rate constant.

Fig. 6.4 shows the effect of various values of α on the size of the first phase, when G is briskly increased from 5 mM to 15 mM at time t = 10 min. For decreasing values of α the first phase decreases accordingly. One of the earliest signs of type 2 diabetes is seemingly a decreased, or even absent first phase (Caumo and Luzi 2004). The model reproduces this reduced first phase with decreased α values. Increasing K_I values decreases α, and as K_I determines the inhibition effect of S on GK, with larger K_I values giving less inhibition, the decreased α value, and hence diminished first phase, could be part of a compensatory mechanism, whereby K_I is increased, hence less inhibition on GK, to counteract the lower amount of GK seen in type 2 diabetes (Matschinsky *et al.* 1993).

Fig. 6.5 shows the effect on the first phase for different rates of change of glucose concentration. The first phase is almost proportional with the rate of change of glucose dG/dt.

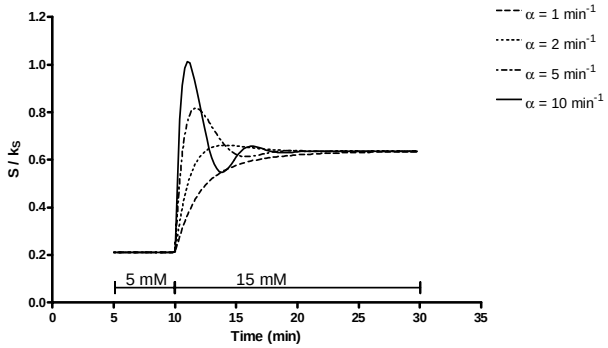

Fig. 6.4: Shape of the first phase as described by Eqs. (6.9) and (6.10) for various values of the rate constant α and with the parameters a=0.2 and τ = 1 min. Glucose is briskly increased from 5 mM to 15 mM at time t = 10 min. Decreasing α values decreases the first phase as a result of a compensatory mechanism for the lower amount of GK seen in type 2 diabetes.

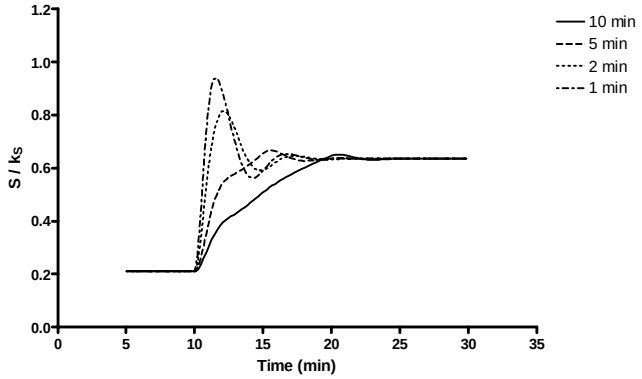

Fig. 6.5: Effect of different rates of changes of glucose, dG/dt on the shape of the first phase. A time t = 10 min, glucose is changed linearly from 5 mM to 15 mM within 1, 2, 5, and 10 min. For larger dG/dt a first phase develops almost proportional with dG/dt.

The proportionality of the first phase with the rate of change of glucose dG/dt can also be described mathematically. Assuming for simplicity that the glucose oxidation is a constant, G_{ox} (Hallgreen *et al.* 2008), Eq. (6.10) modifies to

$$\frac{dS}{dt} = \alpha\left(\frac{k_S f_{Hill}(G)}{1+S^*} - G_{ox}\right) \tag{6.11}$$

where G_{ox} is written in units of E_o.

According to Eq. (6.11) the steady state value for S* is given by

$$S^* = R_{ox} f_{Hill}(G) - 1 \tag{6.12}$$

with $R_{ox} = k_S/G_{ox}$ being the ratio between the maximal possible GK phosphorylation rate (in units of E_0) and the actual glucose oxidation rate (in units of E_0) (Hallgreen *et al.* 2008).

By differentiation with time in Eq. (6.12) we can eliminate S^* with Eq. (6.9), and hence we get

$$S = R_{ox}(f_{Hill}(G) + \tau f'_{Hill}(G)\frac{dG}{dt}) - 1 \qquad (6.13)$$

Eq. (6.13) shows that it seems reasonable to assume that S, and hence insulin release, responds in proportionality with the rate of change of glucose for fast changes in G as also suggested by Grodsky and Licko (Grodsky 1972; Licko 1973).

6.1.5 The model including translocation of GK

The model without the description of GK translocation has shown to be able to explain the insulin release pattern due to fast changes in glucose concentration, i.e. first phase, which occurs within 5-10 min, as a result of a delayed inhibition of GK, due to cellular diffusion. As described earlier, recent research has shown that GK translocate from an inactive state to an active state, upon glucose stimulation, with a time constant in the order of 20-60 min (Miwa *et al.* 2004; Rizzo *et al.* 2002). Hence the GK translocation is a somewhat slower regulation, than the regulation responsible for the first phase.

The structure of the model including the translocation of GK is shown in Fig. 6.6. As previously glucose is transported across the cell membrane by the glucose transporter GLUT2. Glucose is quickly phosphorylated to glucose-6-phosphate, G6P by GK. Now GK is assumed to be present in an inactive, GK_B and an active, GK_A state. Upon stimulation by glucose, GK is assumed to be translocated from GK_B to GK_A. The translocation is assumed to be regulated not by glucose, but by a substance S, assumed to be a glycolytic intermediate (G6P or other).

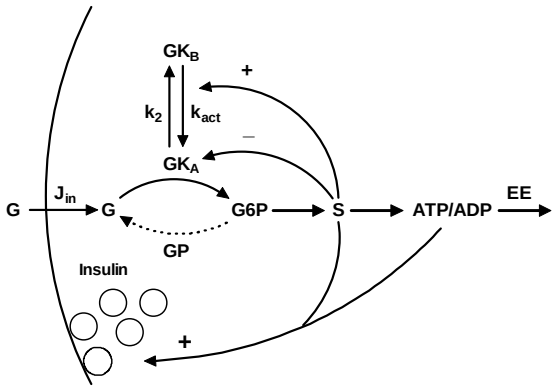

Fig. 6.6: Model structure with GK translocation. GK is assumed to translocate from an inactive state, GK_B to an active state, GK_A and the translocation is controlled by S. For further details see caption in Fig. 6.2.

For simplicity we have assumed that the translocation of GK can be described by a chemical reaction, with the rate constant k_2 and k_{act} as evident from Fig. 6.6. The total amount of GK, GK_T is now divided into the inactive amount, GK_B and the active amount GK_A, i.e.

$$GK_T = GK_A + GK_B \tag{6.14}$$

The activation (translocation) of GK by S is described by the rate constant k_{act}

$$k_{act} = k_1 + k_3 S \tag{6.15}$$

The equation describing the translocation is given by

$$\frac{dX_A}{dt} = k_{act}(1 - X_A) - k_2 X_A = k_{act} - (k_{act} + k_2)X_A \tag{6.16}$$

where X_A is the active fraction, i.e.

$$X_A = \frac{GK_A}{GK_T} \tag{6.17}$$

From Eq. (6.16) we find the steady state relation

$$X_A = \frac{k_{act}}{k_{act} + k_2} \tag{6.18}$$

Now the inflow of glucose, J_{in} depends on the active amount of GK, hence

$$J_{in} = v_{max} GK_T f_{Hill}(G) X_A \tag{6.19}$$

Fig. 6.7 shows the relation between S and G described by Eqs. (6.6), (6.18) and (6.19) at steady state translocation. The main effect of translocation is to introduce a glucose threshold value for S and hence insulin release, cf. Fig. 6.3.

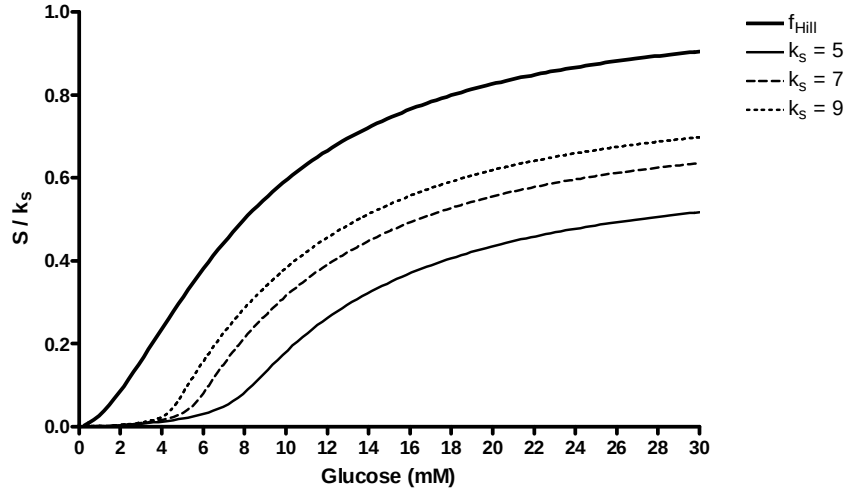

Fig. 6.7: Relation between the normalised S and G at steady state translocation, described by Eqs. (6.6), (6.18) and (6.19), for various values of k_S.The translocation property introduces a glucose threshold value for S and consequently insulin release.

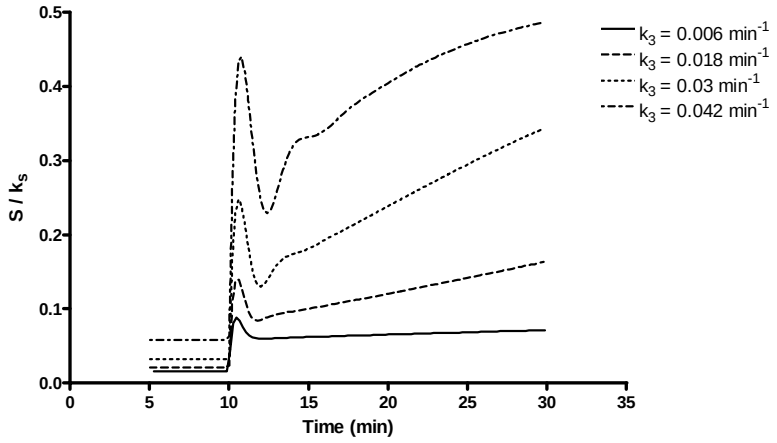

Fig. 6.8: At time t = 10 min, glucose is changed briskly from 5 mM to 15 mM and maintained at that elevated value. The variation with time of S is described by Eqs. (6.9), (6.16) and (6.20). The typical biphasic pattern is evident, with the first phase explained by delayed inhibition of GK, and the slowly rising second phase explained by the translocation (activation) of GK. For increasing k_3 the translocation, i.e. second phase, saturates. The parameters are $k_1 = 0.006\ \text{min}^{-1}$, $k_2 = 0.03\ \text{min}^{-1}$, $a = 0.2$, $\alpha = 10\ \text{min}^{-1}$, $\tau = 1$ min and $k_S = 7$.

With Eq. (6.19), Eq. (6.10) transforms into

$$\frac{dS}{dt} = \alpha\left(\frac{k_S X_A f_{Hill}(G)}{1+S^*} - \frac{S}{a+S}\right) \tag{6.20}$$

Fig 6.8 shows the variation with time of S when G is changed briskly at t = 10 min. A typical biphasic pattern is evident. The first phase is explained by the delayed inhibition of GK, and the slowly rising second phase is explained by the translocation, or activation, of GK by S. The second phase rises more or less linearly as also noted in (Elahi 1996). However the translocation, i.e. second phase, is saturable as seen for large values of k_3 which determines the effect of S on translocation.

6.1.6 Glucose memory

It has been shown several times that the beta cells display a memory effect towards glucose, i.e. the present insulin release depends on the pre-history of glucose stimulation. The mechanism by which this is achieved is unknown (Caumo and Luzi 2004; Grill *et al.* 1978; Nesher and Cerasi 2002). An explanation to the glucose memory could be increased GK_T, but such an increase appears to take days (Liang *et al.* 1992). An other option could be S itself, but many investigators point toward mechanisms depending on Ca^{2+} and/or insulin action via the beta cells insulin receptors (Aspinwall *et al.* 1999; Borge *et al.* 2002; Magnuson and Matschinsky 2004).

We assume that the insulin release is stimulated by its own release and described by the following equations

$$R = \begin{cases} Q \cdot (S - S_0) + R_0, & \text{for } S > S_o \\ R_0, & \text{otherwise} \end{cases} \tag{6.21}$$

$$\frac{dQ}{dt} = \beta(Q_\infty(R_\Delta) - Q) \tag{6.22}$$

$$Q_\infty(R_\Delta) = Q_0\left(1 + \frac{A \cdot R_\Delta}{K_R + R_\Delta}\right) \tag{6.23}$$

with $R_\Delta = R - R_0$, and where β, Q_0, A, K_R are constants.

$Q_\infty(R_\Delta)$ is the steady state amplification factor. For low insulin release, i.e. R_Δ small, $Q_\infty(R_\Delta)$ approaches the value Q_0, and for large insulin release $Q_\infty(R_\Delta)$ approaches the value $Q_0(1+A)$. Often

very large differences are seen (Grill *et al.* 1978; Nesher and Cerasi 2002), so in the simulations we have assumed A = 10.

Fig. 6.9 shows the steady state relation between insulin release, R and glucose for different values of k_S. The curves are sigmoidal, i.e. S-shaped, which is typical for autocatalytic processes. The total amount of GK is seen to control both the threshold value for insulin release, as well as the glucose sensitivity, i.e. the slope, with larger threshold values and lower glucose sensitivity for decreasing total amount of GK, i.e. decreasing k_S.

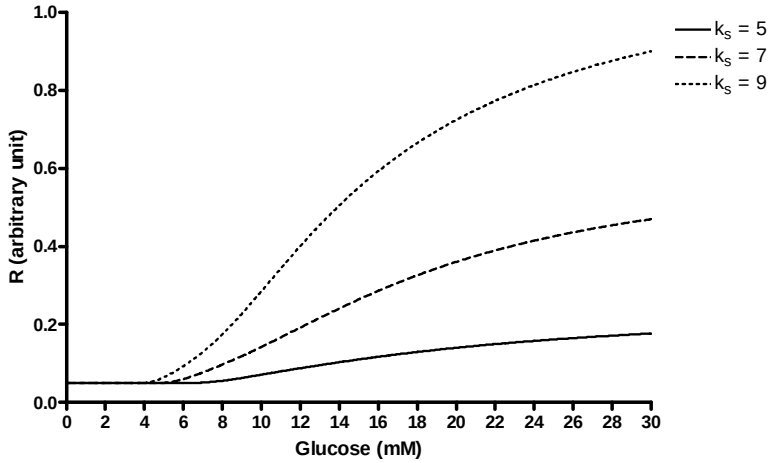

Fig. 6.9: Relation between insulin release, R and glucose at steady state for different values of k_S. Insulin release exerts an autocatalytic effect described by Eqs. (6.22) and (6.23). The parameters are $K_R = 1$, $Q_0 = 0.1$, and $\beta = 0.003$ min^{-1}.

The glucose memory effect is clearly visible when the beta cells undergo consecutive square wave glucose stimulation (Caumo and Luzi 2004; Grill *et al.* 1978; Nesher and Cerasi 2002). Fig 6.10 shows the insulin release pattern when two consecutive square waves, or pulses are applied. Both the first phase and the second phase are augmented at the second glucose pulse, in accordance with findings from other investigators (Caumo and Luzi 2004; Grill *et al.* 1978; Nesher and Cerasi 2002).

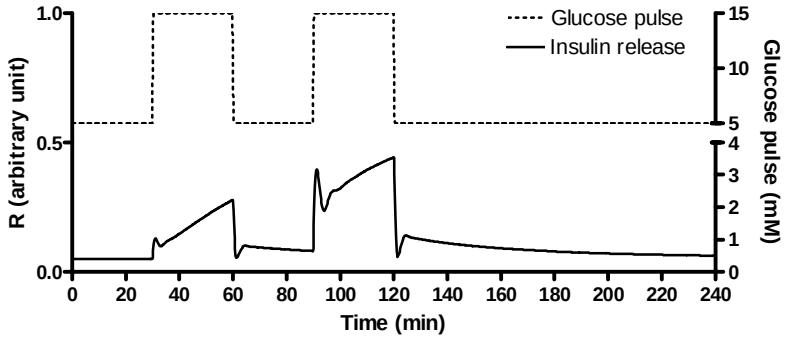

Fig. 6.10: The glucose memory effect elicited by two equal 30 min glucose pulses given 30 min apart. Both first and second phase are augmented at the second pulse. Other parameters are k_1 = 0.006 min^{-1}, k_2 = 0.03 min^{-1}, k_3 = 0.03 min^{-1}, k_S = 7, a = 0.2, Q_0 = 1, A = 10, K_R = 1, R_0 = 0.05, α = 10 min^{-1}, β = 0.003 min^{-1}, and τ = 1.43 min.

Summary

The model provides a novel mechanism-based explanation to the biphasic insulin release; The first phase is explained by a delayed inhibition of GK by the signal substance S. The delay is introduced due to the assumption that S has to diffuse through the intra-cellular environment before exerting its inhibitory effect on GK. The value of 1 min for the delay time constant τ needed to simulate a first phase in the order of 5 min, a time lapse that is generally found, is in agreement with findings demonstrating a delay on the order of 1 min from start of glucose increase to start of insulin release (Rorsman and Renstrøm 2003).The simulations showed that a decreased first phase, as observed in type 2 diabetes, is partly due to compensatory mechanisms in order to minimize the effect of diminished amount of total GK. Insulin in the readily releasable pool, RRP (Korsgaard and Colding-Jorgensen 2006) contribute to the first phase release, hence the diminished, or lack of, first phase insulin release in type 2 diabetes can be due to damaged signalling or defects in the exocytotic processes, or both. The model confirms the rate dependency of glucose changes of the first phase (cf. Fig. 6.5), giving the grounds for using dG/dt as an indicator for the first phase. However, as demonstrated by Eq. (6.13), the relation between dG/dt and first phase insulin release is more complex than merely being proportional.

The second phase is explained by the translocation of GK from an inactive to an active state upon stimulation by glucose. However it is not glucose, but some substance S downstream of the glycolysis that controls the translocation. This result in an autocatalytic process (positive feedback) giving a sigmoidal relation between glucose and S, hence insulin release, where the threshold value

and slope (glucose sensitivity) is determined by the amount of GK. Grodsky *et al.* describe the second phase insulin release as caused by mobilization, or provision, of insulin from a stabile pool to the labile, readily releasable, pool. In contrast, we have described the second phase as the result of the translocation property of GK.

The glucose memory effect adds yet another time-dependent effect upon the beta cell. We have described this as caused by another autocatalytic effect, whereby insulin release is augmented by its own release. The mechanisms responsible for the memory effect are not understood, and insulin has been found to both inhibit and enhance its own release (Korsgaard and Colding-Jorgensen 2006). However the model results with the assumption that the memory effect is caused by an autocatalytic process of insulin release resemble literature findings (Caumo and Luzi 2004; Grill *et al.* 1978; Nesher and Cerasi 2002), cf. Fig. 6.10.

During the exocytotic process, when the insulin granules are enclosed in the cell membrane, it is not clear what happens to the granule-bound GK. If GK is released to the cytoplasm and hence activated, it could contribute to the memory effect (Korsgaard and Colding-Jorgensen 2006).

As mentioned earlier, in terms of classic control theory the beta cell is often considered to work as a PID controller. With the GK translocation property, Eq. (6.13) modifies to

$$S = R_{ox} X_A \left(f_{Hill}(G) + \tau f'_{Hill}(G) \frac{dG}{dt} \right) - 1 \qquad (6.24)$$

The first term in the parenthesis of Eq. (6.24) correspond to the proportional, and the second term to the derivative control component. X_A, i.e. the translocation property, correspond to an integral control component. Hence it is seen from Eq. (6.24) that some parallels can be drawn between the characteristics of a classic PID controller and the actions of the beta cell. However the beta cell has intrinsic non-linear characteristics and work under saturable signals (Korsgaard and Colding-Jorgensen 2006). The result of these described time-dependent control mechanisms is that as long as glucose is elevated, insulin will continue to be released. The manner in which this is achieved can vary from person to person, and as long as glucose is normalised within a reasonable time frame, the control is characterised as being normal. This explains the wide range of values for the parameters describing beta cell function found even for healthy persons, cf. chapter 3.

6.2 Multiplicity of glucose sensors

The beta cells are not the only glucose sensitive cells in the body. It now appears that there are many glucose sensors, and that they are interwoven in a complex network (Herman and Kahn 2006; Matschinsky *et al.* 2006; Peters *et al.* 2002; Schuit *et al.* 2001; Thorens 2004a)designed to respond and cope with the different glucose loads a human body experience day after day, year after year. Glucose sensors are present in the intestine, the brain, the pancreas (alpha-cells, beta cells), the hepatic region, and perhaps other places (Herman and Kahn 2006; Matschinsky *et al.* 2006; Peters *et al.* 2002; Schuit *et al.* 2001; Thorens 2004a). The sensors each have their own regulatory function and respond to different glucose concentrations. As previously described, GK seems to be characteristic for many of the glucose sensors, and the sensing mechanisms resemble the sensing mechanisms found in the beta cells. Hence the beta cell model described in the previous section seems to apply as a general model of glucose sensing model in the body.

6.3 Glucose control

The glucose control or handling is depicted in Fig. 6.1 by the effector subsystem. Most common is to view the glucose uptake into the cell as the main effector to lower the plasma glucose concentration. In reality however, the picture is more complicated. When glucose enters the body, as for instance after an intake of a meal, it is taken up and/or shuffled between the different organs in the body, as shown in Fig 6.11.

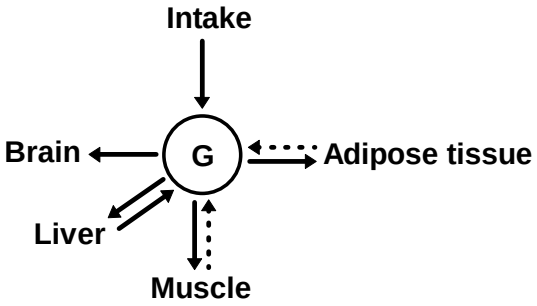

Fig 6.11: The most important organs in the body that use and/or reshuffle plasma glucose, G. Adapted from Hallgreen *et al.* 2008.

Once glucose is transported across the membrane, in either of the cells in the different organs, it is phosphorylated to glucose-6-phosphate, G6P, which cannot escape the cell; hence glucose is

trapped inside the cell as G6P. The liver and the kidney are the only major organs capable of releasing glucose again, by de-phosphorylation of G6P back to glucose. The other organs need to handle G6P by other means. Hence, the handling of G6P is of immense importance for the glucose control.

Fig 6.12 shows the most important pathways by which the cells in the organs can handle G6P. The handling of G6P is complex and different from one cell type to the other. The pathways are described in (Hallgreen *et al.* 2008). Shortly, G6P can be handled and removed by:

1. Oxidation: Present in all cells.
2. Glycogen storage: Primarily in muscle and liver cells.
3. Conversion into fat and stored: Normally in adipocytes
4. Conversion into lactate: Almost all cells.
5. Conversion into fatty acids: Primarily adipocytes and liver cells.
6. Conversion into glucose: Liver and kidney cells.

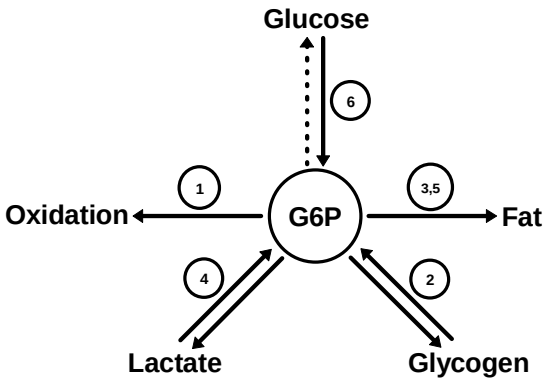

Fig. 6.12: The most important pathways by which glucose-6-phosphate, G6P can be handled by the cell types in the different organs. The dashed line indicates that only the liver (and kidney) cells are able to release free glucose from G6P. For details see text and (Hallgreen *et al.* 2008).

The different options outlined serve to redirect the metabolic fluxes between storage, release and oxidation. Options 4 and 5 are particularly important, as they seem to be the only ways the cells can adjust the net influx of glucose to their need (Hallgreen *et al.* 2008).

Fig 6.13 shows the main routes of glucose fluxes in the most important organs in the handling of glucose, i.e. liver, muscle, and adipocyte. After a meal, glucose is predominantly stored in the

muscle cells as glycogen, whereas fat is predominantly stored as triacylglycerols, TG in the adipose tissue cells (Hallgreen *et al.* 2008).

The details of the handling of glucose for each of the different cells have been described in (Hallgreen *et al.* 2008). In the following section, the control of glucose and its metabolites in the muscle cells will be discussed in details.

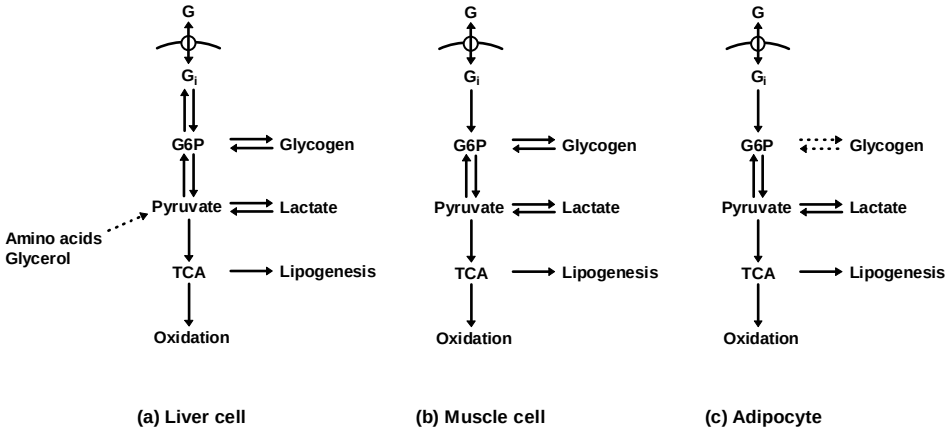

Fig. 6.13: The main routes of glucose fluxes in the most important cells for handling of glucose (a) Liver cell, (b) muscle cell, and (c) adipocyte. Adapted from (Hallgreen *et al.* 2008).

6.3.1 Glucose transport and phosphorylation in muscle tissue cells

The transport of glucose across the muscle cell membrane is as mentioned earlier via the transporters, GLUT1 and GLUT4. GLUT1 is denoted the insulin-independent glucose transporter. Its activity is fairly constant at the cell membrane, and fasting glucose uptake is predominantly via this transporter. GLUT4 is the insulin-dependent glucose transporter, where in the fasting state most of the transporters are sequestered in intracellular stores. Upon insulin stimulation, GLUT4 translocates to the membrane and hence increases glucose uptake.

Both transporters are saturable and can simplified be described by a Michäelis-Menten relation with the same half-saturation value K_M = 5 mM (Frayn 2003). Hence we have

$$J_{influx} = (V_{GLUT1} + V_{GLUT4}) \cdot \frac{G}{K_M + G} = V_{GLUT} \cdot \frac{G}{K_M + G} \qquad (6.25)$$

where J_{influx} is the glucose influx, V_{GLUT1} and V_{GLUT4} are the maximal transport capacity of GLUT1 and GLUT4, respectively, where V_{GLUT4} depends on insulin, and V_{GLUT} is the sum of V_{GLUT1} and V_{GLUT4}.

The glucose transporters are generally assumed to be symmetric (Klip and Marette 2001), hence intracellular glucose concentration, G_i can be transported out of the cell by the efflux, J_{efflux} described by

$$J_{efflux} = V_{GLUT} \cdot \frac{G_i}{K_M + G_i} \tag{6.26}$$

Hence the net uptake, J_{net} is given by the difference between the influx and efflux

$$J_{net} = J_{influx} - J_{efflux} = V_{GLUT} \cdot \left(\frac{G}{K_M + G} - \frac{G_i}{K_M + G_i} \right) \tag{6.27}$$

To be further processed by the muscle cell, the intracellular glucose, G_i needs to be activated, i.e. phosporylated to G6P. In the muscle cell this is achieved by hexokinase. The activity of hexokinase is regulated by both G_i and G6P via a mixed inhibition (Toews 1966), hence the flux through hexokinase, J_{hex} can be described by

$$J_{hex} = \frac{V_{hex} G_i}{(1 + \frac{G6P}{K_{G6P}})K_{hex} + (1 + \frac{G6P}{K^*_{G6P}})G_i} \tag{6.28}$$

where the constants K_{hex}=0.188 mM, K_{G6P}=0.068 mM, and K^*_{G6P}=0.022 mM are estimated from (Toews 1966).

As seen from Eq. (6.28) the flux through the hexokinase is dependent on the removal of G6P. Muscle cell lack glucose-6-phosphatase, hence once phosphorylated, glucose is trapped inside the cell as G6P. As a result the glucose uptake becomes critically dependent on the removal of G6P, as seen in the following.

To simplify, we assume that the removal rate or flux of G6P, J_{G6P} is proportional to the concentration of G6P according to

$$J_{G6P} = R_{G6P} \cdot G6P \tag{6.29}$$

with R_{G6P} being a constant determining the G6P removal capacity.

To investigate the effect of the balance between the maximal net uptake, the maximal phosphorylation, and the maximal removal on the net uptake, we evaluated the fluxes given by Eqs. (6.27)-(6.29) in the steady state, i.e.

$$J_{net} = J_{hex} = J_{G6P} \tag{6.30}$$

To simplify the system given by Eq. (6.30), we introduced the ratio, A describing the maximal glucose uptake in relation to the maximal phosphorylation rate, and the ratio, B describing the removal capacity in relation to the maximal phosphorylation rate, i.e.

$$A = \frac{V_{GLUT}}{V_{hex}} \qquad \text{and} \qquad B = \frac{R_{G6P}}{V_{hex}} \tag{6.31}$$

Fig 6.14(a) shows the increase of G_i as a consequence of increasing A values, for instance by increasing the insulin levels. Fig. 6.14(b) shows the relation between the normalised net uptake and the A parameter. Net uptake decreases for increasing values of A as a consequence of the increased G_i, cf. Eq. (6.27). The decreased uptake can be diminished by an increase in the B parameter, for instance by increasing the removal capacity of G6P.

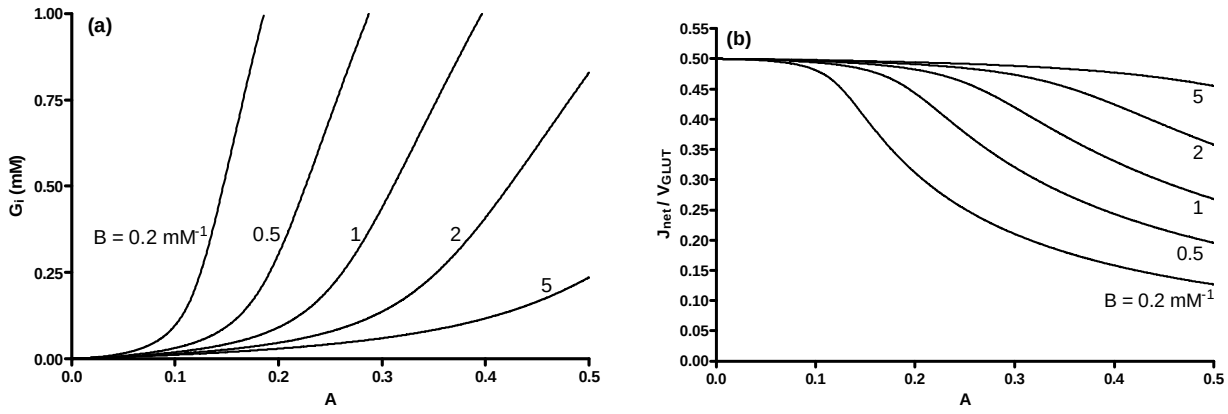

Fig. 6.14: (a) Relation between the intracellular glucose, G_i and the parameter A for different values of the parameter B (b) Relation between the normalised net glucose uptake J_{net} and the parameter A for different values of the parameter B assuming constant plasma glucose value, G = 5 mM. Relations are determined by the Eqs. (6.27)-(6.31). High G_i values are able to decrease net uptake as according to Eq. (6.27), depending on the capacity to remove G6P.

Fig. 6.15(a) shows that the concentration of G6P saturates for increasing values of A, with the result that the net uptake becomes independent of changes in A. Hence an isolated change in the glucose transporter activity, e.g. by increasing insulin levels to increase the amount of GLUT4 on the cell membrane will have no effect on the glucose uptake. G6P has to be removed, before glucose uptake can continue, as shown in Fig. 6.15(b). Thus the handling of G6P is a critical determining factor for the glucose uptake.

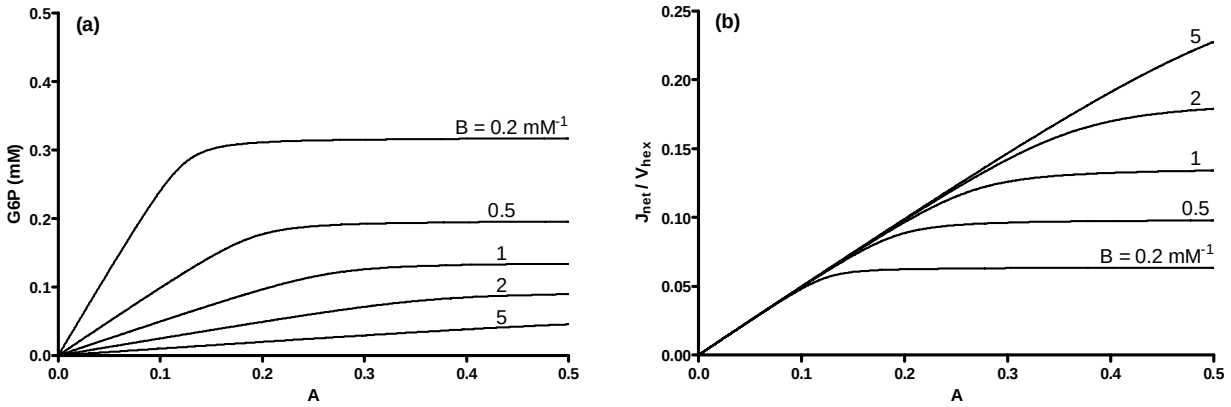

Fig. 6.15: (a) Relation between the glucose-6-phosphate, G6P and the parameter A for different values of the parameter B (b) Relation between the net glucose uptake J_{net} and the parameter A for different values of the parameter. Relations are determined by the Eqs. (6.27)-(6.31). High values of A, for instance as a consequence of high insulin levels, are able to saturate the concentration of G6P (a) As a consequence the net uptake becomes independent of the changes in A (b). The saturation can be diminished by increasing the removal capacity of G6P.

As shown in Fig. 6.13(b) the produced G6P can be removed by different processes. In the fed state the main G6P remover is glycogen synthesis as in the liver, and normally insulin stimulates the glycogen synthase strongly (Berg *et al.* 2006). In the fasting state, muscle cells only take up little glucose that mainly goes to oxidation. The energy need is met by oxidation of fatty acids, FA. The maximum glycogen storage in the whole-body has been estimated at some 1000 g for an untrained person (Acheson *et al.* 1988) with the storage predominantly being in muscle and liver cells. Hence the glycogen storage is limited and the storage rate declines exponentially (Hallgreen *et al.* 2008)

Hence a massive load of glucose can only be removed via the glycogen synthesis pathway for some time. Many authors report that during hyperinsulinaemic clamps, the glucose infusion rate and hence the glucose uptake does not decline substantially with time (Hallgreen *et al.* 2008) and plasma glucose does not appear to increase during glucose loads (Hallgreen *et al.* 2008). Hence the removal of G6P seems to continue for large glucose loads at least in healthy persons. In subjects with type 2 diabetes it may be possible that an insufficient removal of G6P and hence high intracellular glucose leads to decreased glucose uptake. As the resting muscle has low energy expenditure, the oxidation pathway does not contribute to the removal of G6P to any significantly extend. Two options are then left, cf. Fig. 6.13(b). G6P can be converted to lactate, and leave the cell, or G6P can be converted into fat.

Lactate formation seems to be the first choice. During high glucose uptake, lactate plasma concentration typically rises with a factor 2-3. As most cells can take up lactate for oxidation or storage as glycogen, this option seems to be a way surplus glucose can be reshuffled between the different organs. However in a whole-body perspective, this cannot continue when the glycogen stores are filled.

The only other option left then is the formation of fat via *de novo* lipogenesis, DNL, i.e. the formation of TG from glucose. It has been found that during overfeeding around 5 mg/kg/min of glucose could be converted to fat in the whole-body (Acheson *et al.* 1988). Hence a substantial amount of glucose can be converted into fat during overfeeding.

Normally DNL is considered to take place predominantly in the adipose tissue, and only to a minor extend in liver and muscle cells. However, DNL make take place in the muscle cells, at least temporarily, in cases of overfeeding (Hallgreen *et al.* 2008).

It is not known what happens with the produced FA in the muscle tissues; some may be oxidised, some, at least temporarily may be stored as fat and then later oxidised, and some may be transported to the adipose tissue for storage. Interestingly the produced FA in the muscle cell may inhibit GLUT4 activity leading to a kind of insulin resistance (Boden 2001; Dresner *et al.* 1999).

6.3.2 Integration of metabolism

The major organs participating in the control of plasma glucose concentration all have their particular metabolic profile for shuffling the glucose and metabolite fluxes between oxidation, storage, and release, cf. Fig 6.13.

In the fasting state glucose is normally kept at a relatively constant level, due to several things. Firstly in the liver glycogen is broken down via glycogenolysis to glucose and released into the blood. Secondly the adipocytes release glycerol and FA. Thirdly the muscle tissue mainly oxidises FA instead of glucose. Furthermore the glycerol released by the adipocytes goes to the liver for rebuild of glucose. All these processes are initiated by the decrease in the insulin levels. In the fed state, the muscle tissues shift the energy dependency to glucose and are the primary tissue for glucose uptake. Surplus of glucose may be exported as lactate, and rebuild as glucose in the liver, or reshuffled between oxidation, release or storage in other organs. In massive overfeeding glucose may temporarily be converted into FA in muscle cells and stored or oxidised, or transported to adipocytes for storage.

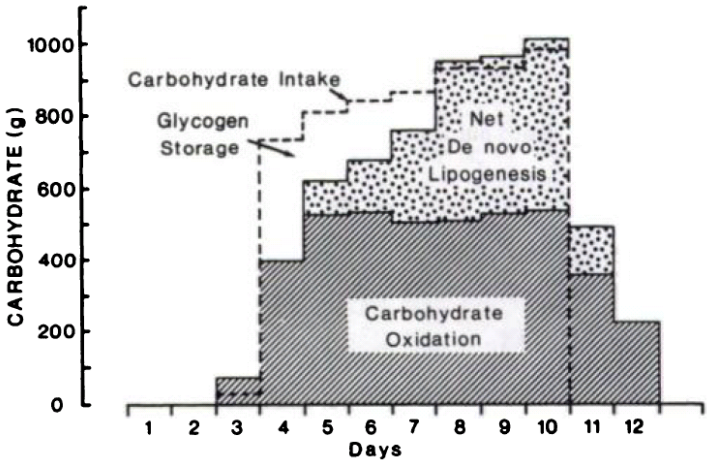

Fig. 6.16: The balance between glucose oxidation, glycogen storage, and *de novo* lipogenesis, DNL in healthy subjects undergoing massive glucose overfeeding. Adapted from (Acheson *et al.* 1988).

The contribution of glycogen storage, glucose oxidation, or DNL seems to be balanced in a graded manner as demonstrated in Fig. 6.16. In the muscle cells the lactate production that is needed to remove surplus glucose when the glycogen stores are filled, would lead to much higher plasma lactate concentration values than normally reported (Hallgreen *et al.* 2008), hence in these situations at least temporarily DNL must occur. The signal(s) for shifting between glycogen storage and DNL is not known, but it may be G6P that increases when the glycogen stores fills up.

Often subjects with type 2 diabetes have an increased fasting HGO that is primarily caused by increased GNG via increased lactate fluxes. The increased lactate fluxes must be a consequence of a decreased glucose oxidation, mainly due to increased levels of FA and hence an increased FA oxidation. Hence the glucose is not oxidised, but exported again as lactate that goes to the liver for rebuild of glucose via GNG, and the recycling continues. To lower fasting plasma glucose it would not be feasible to inhibit the GNG from lactate. This would just increase lactate levels in the liver and give lactoacidosis. Furthermore an increase in glucose uptake would just create more lactate. Instead the FA concentration should be lowered to increase glucose oxidation.

The idea is that the activity of the hormone sensitive lipase, HSL that stimulates lipolysis but normally is inhibited in a strongly insulin-dependent way, is increased, as a consequence of insulin resistance at the adipocytes. As a result more FA is released and oxidised and glucose oxidation is decreased.

However as a typical person with type 2 diabetes is obese, the lipolysis cannot go on forever. As previously mentioned a substantial amount of glucose can be converted into fat during

overfeeding, primarily in the adipocytes. The fat can then be stored or oxidised. In all cases the variable FPG in subjects with type 2 diabetes may be caused by a mismatch between fat and glucose oxidation.

In this chapter the glucose-insulin control system has been discussed and it has been assessed to what extend classic control theory can be used to describe the system. The first part of the chapter concerned a model of the glucose sensing in the beta cell based on the regulation of the enzyme glucokinase, GK. The model results showed that:

- ***GK is the key enzyme controlling glucose sensing activities in the beta cell***
- ***First phase insulin release can partly be explained by a delayed inhibition of GK, by signalling substance(s) downstream of the glycolytic pathway.***
- ***Diminished first phase release observed in subjects with type 2 diabetes can in part be explained by mechanisms in order to compensate for small amount of GK***
- ***Translocation of GK from an inactive to an active state is an autocatalytic process that controls the offset of insulin release and explain the second phase of insulin release***
- ***Damaged translocation of GK and/or diminished amount of GK may be responsible for the increased offset of insulin release and diminished slope observed in subjects with type 2 diabetes***
- ***Glucose memory in the beta cell may in part be explained by autocatalytic enhancement of insulin release***
- ***The beta cell has some characteristics of a classic PID controller. However the sensing mechanisms are highly non-linear and saturable that makes the classic PID controller description limited***
- ***The glucose sensing in the body is achieved by a complex interwoven network of different sensors in different parts of the body***

The second part of the chapter concerned the glucose handling and control. Each organ has its unique metabolic profile for handling glucose that makes the task of describing the handling of glucose much more complex than just describing the uptake of glucose into the cells.

More specifically it was shown that:

- ***The fate of G6P is critical for the handling and control of glucose***
- ***Particularly in the muscle cells, it was shown that insufficient removal of G6P resulted in glucose uptake that did not depend on the GLUT4 activity, i.e. increased insulin would not increase glucose uptake***
- ***During massive overfeeding when glycogen stores are saturated, glucose may be converted to fat in the muscle cell that may lead to insulin resistance at the muscle cell***
- ***Normally there is a tight balance between glucose oxidation, glycogen storage and de novo lipogenesis during overfeeding***

Hence the handling of glucose by the body is determined by a complex shuffling of glucose and metabolites between the need for oxidation, storage and release of glucose and conversions to and from other nutrients within and between the organs, where the traffic are regulated by insulin as well as the nervous system. In light of this, an effect of e.g. insulin on glucose uptake is hard to quantify, as the resulting effect depends on the dynamical balance between oxidation, storage and release.

Chapter 7

Discussion and conclusion

There is no doubt that an understanding of the way the beta cells work is a tremendous task, but likevise a very important one. The preceding chapters have described and discussed the different components that are needed to establish a test of beta cell functionality. From the different protocols designed to receive data and the mathematical models linking data with indices used to quantify beta cell functionality and insulin action in chapter 2, 3 and 4, to the mechanism-based description of the processes behind beta cell functionality and effects of insulin within the glucose-insulin control system in chapter 6. Chapter 5 provided a novel way to look at meal response data that pointed at strikingly new results for the responses of both the healthy and the subjects with type 2 diabetes.

7.1 Discussion

Mathematical modelling

Mathematical models with different levels of complexity are used intensively in order to gain a coherent picture of beta cell functionality (Bertuzzi *et al.* 2007; Giugliano *et al.* 2000; Korsgaard and Colding-Jorgensen 2006; Pedersen *et al.* 2010). The level of complexity of the model is generally a result of the question being asked. Minimal models, as implied by the name, are based on the concept that the dynamics of the biological system should be described by a minimum number of identifiable parameters. Hence these parameters should describe the main characteristics of the system. In contrast, maximal models are comprehensive descriptions which consolidate large amount of biological knowledge. Maximal models are generally not identifiable, and therefore not designed to quantify specific processes, but serve to simulate the behaviour of the system, and test new hypothesis.

The minimal model approach has its strengths in its simplicity and ability to give quantitative measures of specific processes. The simplicity can however also be a weakness of this approach. Biological systems are complex and most definitely not identifiable. To force the criteria of identifiability on the description of biological systems restricts the domain of validity of the model.

The strength of the maximal model approach is the implementation of biological knowledge. By this approach, as much knowledge as possible about the biology is intended to be taken into account, and thus a more correct description than that gained with the minimal model approach is to be expected. Yet again, the strength of this approach may become its weakness. To include more and more biological knowledge in a mathematical model is not only an immense laborious task, but more importantly the model becomes more and more difficult to validate. Furthermore the circumstances under which the model is going to be used should be kept in mind.

Assessment of beta cell functionality

No gold standard exists for the assessment or testing of the beta cell functionality. The deconvolution method proposed by Eaton-Polonsky (Eaton *et al.* 1980; Polonsky *et al.* 1986) has been termed the gold standard. However as previously discussed this method determines absolute insulin secretion, and not the ability to respond to stimuli, i.e. beta cell function. Furthermore it is cumbersome and may underestimate the actual secretion, as pointed out in chapter 2

By no doubt, the most reliable test to use for the assessment of beta cell functionality could be the MTT, and secondary the OGTT. These tolerance tests resemble daily life most appropriate, with the MTT as preference due to the influence of also proteins and fatty acids. Furthermore they are relatively convenient, however they require some blood samples, but this is not different from any other test. With that said I wrote “could be” in regards with reliability of these tests. This is due to the vital importance of the right mathematical model to be used. As previously described, even after decades of intense research regarding the biphasic nature of insulin secretion, there are still many missing pieces to the puzzle; we are not there yet, but we are approaching.

Hence for now, maybe the most reliable test to assess at least the first phase insulin secretion appears to be the IVGTT or the glucose clamp. However the first phase insulin secretion bot be evaluated in light of the insulin action, due to the adaptive nature of the beta cell function to the insulin sensitivity via the disposition index.

The disposition index

The disposition index was first introduced by (Bergman *et al.* 1981) as an index to quantify the ability of the beta cell to adapt to the prevailing insulin sensitivity. Numerous studies have since then confirmed this ability (Cobelli *et al.* 2007). Strikingly, even though the disposition index has been denoted “the hyperbolic law” (Stumvoll *et al.* 2005), the mechanism(s) responsible for this

adaptation has yet to be clearly established. (Stumvoll *et al.* 2003) provided evidence to show that glucose itself is the signal responsible for the compensating increased insulin release, as measured by AIR, in case of developed insulin resistance. Despite constant disposition index, the authors found changes in fasting plasma glucose and 2-hour postprandial glucose value. Hence even when the beta cell was able to compensate for changes in insulin sensitivity, glycemia was changed. The logic they put forward for this view was that when insulin resistance develops (for whatever reason), glucose increases with a resulting increase in insulin release. (Bergman 2005) induced insulin resistance and hyperinsulinemia in dogs by a high fat diet. He found no changes in glucose, GLP-1, cortisol or growth hormone pattern, but found a significant increase in FFA overnight, and hypothesized that this nocturnal increase of FFA was the signal responsible for the compensating increase in insulin release. In section 6.3.1 we argued that the produced FFA in muscle cells during overfeeding could induce insulin resistance. Hence FFA may also provide as a link for the adaptation of beta cell function to the insulin action.

Recently (Maiztegui *et al.* 2009) performed a study with rats, where insulin resistance where induced by a fructose rich diet. The investigators found normal fasting plasma glucose values, but impaired glucose tolerance and increased insulin release. The compensating increase in insulin release where explained to be due to the found increase in GK activity and protein levels. This reasoning is in line with the model we presented in section 6.1 regarding the beta cell functionality, where the translocation of GK from an inactive state to an active state was found to be an important mechanism in the glucose sensing mechanism of the beta cell. Thus recent evidence gives further supports for the importance of GK translocation in insulin release.

Another recent interesting study (Bouche *et al.* 2010) investigated the effect of insulin on its own secretion in healthy humans during clamps. The investigators found that pre-exposure to exogenous insulin (4-h) were able to enhance the glucose stimulated insulin release, as the clearance of insulin did not change. Hence presumably, the ability of insulin to enhance its own release could explain the compensating link between decreased insulin action and resulting increased insulin release. This study is also interesting as it highlights the importance of insulin signalling in the beta cell. In the model we proposed in section 6.1 we also took into account that insulin (or rather release) was able to enhance its own release. This mechanism was able to explain the glucose memory (or potentiation) phenomenon. However the study by (Anderwald *et al.* 2011) showed that insulin enhances its own secretion only in insulin sensitive subjects. In insulin-resistant and subjects with type 2 diabetes, insulin appeared to be suppress its own secretion.

Assessment of insulin sensitivity

The findings in chapter 6 that the fate of G6P is a critical regulator for the handling and uptake of glucose have important consequences. Firstly, as shown, an insufficiently removal of G6P can result in a kind of insulin resistance. Secondly in glucose clamp studies which are widely used for the assessment of the glucose-insulin control system and the action of new insulin types, the level of the GIR value is important. The clamp is typically performed after an overnight fast (Hallgreen *et al.* 2008).

With small to moderate insulin levels the GIR mainly goes to glucose oxidation and to replace decreased hepatic glucose production. Lipolysis is most sensitive to insulin with a half-maximal suppression value, EC50 of around 60 pM, with the inhibiting effect of insulin on the hepatic glucose production being secondary with an EC50 value around 150 pM. Thus at low insulin values and hence low GIR values, the clamp mainly evaluates the insulin action on the lipolysis and secondarily the action on the hepatic glucose production. A large insulin value may require a GIR of 10 mg/kg/min or more, a value that corresponds to massive overfeeding (Hallgreen *et al.* 2008). As was shown in Fig. 6.21, the glucose uptake during massive overfeeding is determined by a dynamic balance between oxidation, storage as glycogen and conversion into fat. Thus the clamp assesses the glucose removal and the specific action of insulin is determined by the relative contribution of the glucose removal pathways. Hence focus must also be directed to what goes on in the cell and not just the description of the uptake of glucose.

Despite these limitations, the hyperinsulinemic-euglycemic clamp still offers the best direct way of assessing insulin action (Muniyappa *et al.* 2008). However it is time-consuming, thus if precise and reliable value are not that important other surrogate indices may be used (Muniyappa *et al.* 2008). The minimal model of glucose kinetics could also be used, however as also shown in chapter 3, the model may once in a while produce spurious result (Muniyappa *et al.* 2008).

Glucose-sensing in the beta cell

In technical applications the beta cell has often been considered working as a PID. The oral C-peptide minimal model has been compared to the characteristics of a PID controller in connection with the use of a model for a closed-loop design (Steil *et al.* 2003). In contrast with a PID controller, the C-peptide minimal model only make use of the positive rate of change of the glucose concentration to characterise the dynamic beta cell secretion phase, and introduces a delay between glucose stimulation and resulting insulin secretion described by the static secretion component.

Despite equal performances during a glucose clamp (Steil *et al.* 2003), the C-peptide minimal model proved unstable in closed-loop conditions where the action of insulin was modelled through the glucose minimal model (Steil *et al.* 2003). It has been shown that both the dynamic as well as the delayed action of glucose on the secretion are necessary components to describe C-peptide data in healthy as well as impaired glucose tolerant subjects undergoing OGTT (Breda *et al.* 2002). Other studies have shown that in some subjects the secretion is more appropriately described by a proportional secretion component with no delay, although a delay was evident in most subjects (Steil *et al.* 2004). Interestingly in a recent study (Pedersen *et al.* 2010), the authors provided further evidence for the importance of the three main control components in the C-peptide oral minimal model, i.e. derivative control, proportional control, and delay. The authors showed that a previous publiced model (Pedersen *et al.* 2008), which incorporate present knowledge of intracellular events, could in a straight forward manner explain these technical control elements, thus providing a link between a minimal model and a maximal model capable of describing the biological events in the exocytosis.

In chapter 4 we found that the insulin concentration response after a MTT in healthy and in subjects with type 2 diabetes was most appropriately described by a combination of proportional and delayed effects of glucose. We omitted a rate of change of glucose (dynamic) component as the estimation of this component did not converge.

In chapter 6 we showed that the biphasic nature of the beta cell secretion can be explained by the regulation of the glucose sensor enzyme, glucokinase, and that the beta cell has characteristics of a PID controller, but with non-linear and saturable components. We stated the importance of the translocation of GK from an inactive to an active state for the glucose sensing. Such importance was again established in a recent study (Maiztegui *et al.* 2009). The recent advance in the knowledge of the intracellular events in the glucose sensing of the beta cell where discussed in section 2.2.3, where the importance of the metabolic amplifying pathway was discussed, especially in connection with glucose potentiation. We modelled the glucose potentiation (or memory) as a result of an autocatalytic effect of insulin secretion; however the signal substance S we introduced could as easily be a messenger in the proposed amplifying pathway. The non-sense to glucose is an important marker for type 2 diabetes. In our model this could be obtained by a reduced amount of total GK and/or an impaired translocation capability. Both dearangement have been observed in literature. Interestingly GK has been found to be bound to the insulin granules, cf. chapter 6. Upon insulin release it is not clear what happens to the now unbound GK. One possibility

is that it could partake in a potentiation effect. Furthermore it will be interesting in future studies to integrate the property of GK translocation with the amplifying pathway, and a description of the granules in the distinct pools.

Physiological mechanisms governing the meal response

The finding that the glucose meal responses for the subjects with type 2 diabetes were quite similar despite different levels of insulin, different levels of fasting plasma glucose values, different disease stages and different treatments is novel and remarkable. The analysis of the healthy glucose meal response led to the novel conclusion that for the healthy subjects, the apparent glucose rate of appearance seems to be controlled in such a way as to follow the glucose uptake. Furthermore the analysis showed a fundamental and consistent difference between the responses of healthy and the subjects with type 2 diabetes. These findings contradict the current knowledge of insulin as being the single most important player in the control of glucose and triggers several questions: If other mechanism(s) than the well-studied insulin-dependent mechanisms play a role during a meal, then what are these mechanisms and how are they conveyed? Can they explain the difference observed in the meal responses between the healthy and subjects with type 2 diabetes? How should this be taken into account when evaluation beta cell functionality?

A step towards answering the first of these questions may be taken by investigating the actions of a glucose sensor situated in the hepatoportal vein (Thorens 2004b). This hepatoportal glucose sensor, HPS is activated by a positive glucose gradient between the portal vein and the arterial blood, exactly the situation encountered during meal absorption. The activity of the sensor depends on GLP-1 and GLUT2 and probably also glucokinase. Furthermore, the action is inhibited by somatostatin. Thus the sensing mechanisms of the hepatoportal glucose sensor resemble that of the beta cell. The effect of the sensor is a nerve signal that goes to the central nervous system, CNS. The sensor has been shown to elicit a nerve-mediated increase of the first phase insulin secretion activities. Moreover HPS has been shown to trigger a nerve-mediated insulin-independent glucose uptake that act via GLUT4, similar to the action of exercise (Burcelin *et al.* 2003). In fact the system has been observed to be so strong as to induce hypoglycemia without increase in the insulin concentration (Burcelin *et al.* 2000).

The fact that the activity of HPS depends on GLP-1 may explain the reason for the production of GLP-1 in the intestine. It has been calculated that only 10-15% of the produced GLP-1 in the intestine reaches the systemic circulation (Holst 2007). As the half-life of GLP-1 in plasma

is < 2 min (Holst 2007; Holst *et al.* 2008) the amount reaching the pancreatic beta cell may be even less. Thus it may be speculated that the action of GLP-1 is primarily to trigger HPS that act via the nervous system, and thus the action of GLP-1 may primarily be nerve-mediated.

It has been found difficult to relate the index of dynamic phase secretion of insulin during meal tests with the corresponding first phase secretion indices found with either IVGTT or HGC studies (Steil *et al.* 2004) taken as the AUC of insulin during the first 10 min. This may primarily be explained by the cephalic phase insulin secretion acting during the first 10 min before any noticeable increase in the plasma glucose concentration (Ahrén and Holst 2001). However the activation of HPS via GLP-1 may also to some extent contribute to the difference between the oral index and the intravenous indices.

The activation of HPS when only a positive gradient between the portal vein and arterial blood is present means that HPS measures the glucose absorption rate (Hallgreen *et al.* 2008). The translocation of GLUT4 by the activation of HPS is interesting. It provides a mechanism by which glucose is lowered independently of the action of insulin. The principle of the action of HPS in the overall glucose control after a meal can be seen from the equation describing the glucose dynamics after a meal (Hallgreen *et al.* 2008)

$$V_G \frac{dG}{dt} = J_{abs} + HGO - J_{brain} - (V_{GLUT1} + V_{GLUT4}) \frac{G}{K_{GLUT} + G} \tag{7.1}$$

where V_G is the glucose distribution volume, G is plasma glucose concentration, J_{abs} is the glucose absorption rate, HGO is hepatic (and kidney) glucose output, J_{brain} is the brain glucose uptake, V_{GLUT1} and V_{GLUT4} is the maximal insulin-independent and maximal insulin dependent glucose uptake, respectively, and K_{GLUT} is the Michaëlis-Menten constant for the glucose transporters.

Assuming that the main role of the glucose control system is to maintain the glucose concentration at a constant level, we get from Eq. (7.1)

$$V_{GLUT4} = (J_{abs} + HGO - J_{brain}) \frac{K_{GLUT} + G}{G} - V_{GLUT1} = aJ_{abs} + b \tag{7.2}$$

where G is assumed constant and variations in HGO are neglected. a is a constant and b is the value of V_{GLUT4} before the meal (Hallgreen *et al.* 2008).

Eq. (7.2) show that under these assumptions the control system must, to ensure controlled levels of glucose, work in a way such that GLUT4 is translocated in proportion with the rate of absorption of glucose. However, the insulin system works with considerable delays from the increase of glucose to increase of glucose uptake (Hallgreen *et al.* 2008).

The HPS can in this context be regarded as a feed-forward control signal, where the anticipated glucose change is measured via the rate of glucose appearance, and a nerve-mediated signal is send out to accelerate the control of glucose.

Hence it seems that at least two glucose-controlling systems are active during a meal. The classic insulin-dependent pathway and the control system activated by the glucose absorption rate and with actions conveyed by HPS. In this view the classic insulin-dependent control system seems more directed to the control of the fasting state, whereas the control system working via HPS seems more directed to the control of meal-related fluxes. Interestingly a recent study (Faerch *et al.* 2009)evaluating the natural history of insulin sensitivity and insulin secretion in the progrssion from normal glucose tolerance to impaired fasting glucose and impaired glucose tolerance found evidence to show that isolated impaired fasting glucose and isolated impaired glucose tolerance appear from different underlying mechanisms, much in line with the above statement

With that hypothesis it seems plausible to suggest that the action of the HPS is responsible for the observation that in the healthy subjects, the glucose uptake is regulated in such a way as to follow the rate of glucose appearance.

The observation in the subjects with type 2 diabetes that the glucose meal-response seems independent of the prevailing insulin level put further evidence to the proposed hypothesis. The fundamental difference between the glucose meal-responses of the healthy subjects and the subjects type 2 diabetes could be explained by an impaired HPS control system within the subjects with diabetes. The differences observed in the glucose peak values and times of the glucose meal responses for the subjects with type 2 diabetes could then be explained by the different insulin levels acting via the insulin-dependent fasting control system.

7.2 Conclusion

This thesis has shown different findings that urge the need for a new way to think of a test of beta cell function, but also highlight the importance of even more modelling efforts. The most important results being those found for the glucose meal-responses of the healthy subjects and the subjects with type 2 diabetes that led to the hypothesis of a major role played by insulin-independent mechanisms in the control of after-meal glucose concentrations. This really challenges the current way and usefulness of testing beta cell function. The findings highlight the importance of a more holistic approach to the understanding of the functionality of the beta cell in healthy subjects and in

subjects with diabetes, and its role in the overall control of glucose, where neither of the elements described throughout this thesis can be left out.

A: Technical report

A population based mixed effect model of postprandial glucose-insulin responses in a cross-sectional group of newly-diagnosed subjects with type 2 diabetes mellitus

JELIC K[1], OVERGAARD RV[1], KORSGAARD TV[1], COLDING-JØRGENSEN M[1],

INGWERSEN SH[1], DAMSBO P[1], LUZIO SD[2], DUNSEATH G[2], OWENS DR[2]

[1]Novo Nordisk A/S, Bagsværd, Denmark. [2]Llandough Hospital, Penarth, United Kingdom.

Short title: Analysis of insulin in subjects with type 2 diabetes.

ABSTRACT

Purpose: To describe postprandial insulin profiles in subjects with type 2 diabetes (T2DM) using population-based mixed effects modelling, including covariate analysis.

Methods: 417 subjects with newly diagnosed T2DM and 85 non-diabetic control subjects underwent mixed meal tolerance tests. The postprandial glucose and insulin concentrations were used to characterize the glucose-insulin relationship and relate it to their demographic and baseline characteristics using a population mixed effects modelling approach.

Results: Several empirical models were tested. The resulting final model incorporated an instantaneous and a delayed stimulation by glucose on insulin. Effects of covariates on the model parameters were analysed. Only two covariates were retained in the model: Fasting plasma glucose was a covariate on the insulin response (both instantaneous and delayed effects) and waist circumference was a covariate on the insulin baseline. All other covariates failed to explain more than 10% of the remaining variation. The delayed effect of glucose on insulin response decreases faster than the rapid effect of glucose on insulin response in subjects with T2DM compared with controls. This difference in the two parameters is a novel finding from the population model analysis.

Conclusion: We have proposed a new model to assess postprandial insulin responses using a mixed effects modelling approach.

Keywords: Mathematical model, type 2 diabetes, MTT, population approach, NONMEM.

AUC: Area under the curve; FPG: Fasting plasma glucose; FPI: Fasting plasma insulin; HOMA: Homeostatic model assessment; MTT: Meal tolerance test; T2DM: Type 2 diabetes mellitus; WST: Waist circumference.

INTRODUCTION

The pathogenesis of type 2 diabetes mellitus (T2DM) is not yet fully understood. Both insulin resistance and inadequate insulin secretion are important determinants in the development of T2DM. The main culprit of hyperglycaemia in subjects with T2DM is the decline in the beta cells ability to secrete sufficient and timely insulin to match the peripheral insulin resistance.

The purpose of this study was to quantitatively describe the subject's ability to secrete insulin after a mixed meal and to relate postprandial insulin to demographics and baseline characteristics in a population of non-diabetic control subjects and subjects with newly diagnosed T2DM. For this purpose, we used a population-based mixed effects modelling approach. The use of mixed effects modelling has been shown to be very useful in pharmacokinetic and pharmacokinetic/pharmacodynamic studies, especially in regards to demonstrating the importance of covariates on model parameters. Here, the same approach is used with data on postprandial insulin concentrations in subjects with T2DM in order to identify covariates of importance for the postprandial insulin response. We analysed postprandial glucose and insulin responses from 502 subjects who had undergone mixed meal tolerance tests (MTT's). Demographics and baseline characteristics such as age, sex, BMI, waist circumference (WST), fasting plasma glucose (FPG), HbA1c, lipids, etc. were tested as covariates on the estimated model parameters.

RESEARCH DESIGN & METHODS

Subjects

The study was carried out at a single centre. Subjects without T2DM and subjects with newly diagnosed, treatment naïve T2DM according to WHO criteria (WHO 1999) participated in the

study. The study was approved by the Bro Taf Local Research Ethics Committee and undertaken after the patients had given written informed consent and was conducted in accordance with the Declaration of Helsinki. The demographic and baseline details are shown in table 1.

Experimental design

The MTT was commenced at 08.00h after a 10h overnight fast. An intravenous cannula was inserted into an antecubital fossa vein in the patient's forearm and a slow running saline infusion started to maintain patency of the vein. Fasting samples were taken at –30 min and at 0 min. Following the 0 min sample a standard 500kcal mixed meal (58% carbohydrate, 22% fat and 20% protein; 75g glucose) was given to the patient and consumed within 10 minutes. Post-meal samples were collected over the 4 hour test period from the commencement of the meal, every 10 min during the first hour, every 15 min during the next half hour and then half hourly for the remainder of the test.

Following blood sampling, the samples were separated as soon as possible. Blood was centrifuged (2000g, 5 min) in a refrigerated centrifuge at 4°C and the plasma aliquoted and frozen at –20°C immediately, remaining frozen until assay. All specimens were processed in a single laboratory at the Diabetes Research Unit at Llandough Hospital.

Analytical methods

Samples were taken into fluoride-oxalate for assay of plasma glucose (YSI 2300; YSI, Aldershot, Hants, U.K.) and lithium heparin for assay of insulin by a two-site sandwich immunoassay (MLT Research, Cardiff, UK). The assay was specific for human insulin with no cross-reactivity with intact proinsulin.

Data analysis

As a first step, we examined the data using a descriptive and statistical-based (non-compartmental) analysis of the glucose and insulin data (see "Patients and Data" in Results section). Thereafter we developed a model-based analysis of insulin concentrations using the mixed effects modelling approach in the NONMEM software (Version V).

For the non-compartmental analysis S-PLUS was used. Subject characteristics and baseline blood parameters were expressed as fasting values. For each subject, insulin plasma concentrations were also expressed as area under the curve (AUC) following the meal (0 to 240 min), calculated by the trapezoidal rule. The incremental AUC for both insulin and glucose was calculated by the difference between AUC and basal AUC (with basal AUC being the theoretical AUC due to fasting value over 240 min). HOMA indexes (%B and IR) were calculated based on the Homeostatic model assessment (HOMA model) (Levy *et al.* 1998; Matthews *et al.* 1985).

Fasting plasma glucose (FPG) and insulin concentrations (FPI) together with incremental insulin were correlated against demographic data (such as lipids, BMI, etc.). Furthermore, we divided the subjects into six groups of FPG (1 group for the controls, and 5 groups for the subjects with T2DM) and analysed for trends between their insulin response and their demographic characteristics. The FPG cut-off points/groups were: Group 0: Controls, all with FPG < 7 mM (85), Group 1: FPG < 7 mM (45), Group 2: FPG: [7-9[mM (118), Group 3: [9-11[mM (84), Group 4: [11-13[mM (68), Group 5: ≥13 mM (102). The number of subjects in each group is presented in brackets.

Additionally, we divided the six FPG groups into 3 groups (tertiles) of waist circumference (WST) to examine for effects of obesity. The WST tertiles were: <95 cm, [95-105[cm and >105 cm. For group 0 (controls): 66 subjects were in the first WST tertile, 10 subjects in the second and

4 subjects in the last tertile. Group 1 had 6, 21, and 18 subjects in tertiles 1, 2, and 3, respectively. Group 2 had 23, 44, and 45 subjects in tertiles 1, 2, and 3, respectively. Group 3 had 10, 32, and 39 subjects in tertiles 1, 2, and 3, respectively. Group 4 had 14, 28, and 24 subjects in tertiles 1, 2, and 3, respectively. Group 5 had 36, 32, and 26 subjects in tertiles 1, 2, and 3, respectively.

Model development in NONMEM

A number of different insulin models were tested on the data set, using the maximum likelihood approximation given by the first-order conditional estimation (FOCE) method in the NONMEM software (Version V) (Beal and Sheiner 1998). Structural models were evaluated using visual fit to data, objective function values, and residual variation, as further described in the discussion.

The model parameters were assumed to be log-normal distributed. Intersubject variability terms were initially included on all parameters, but the importance of this variability on parameters was evaluated during model selection. In order to allow for maximal model flexibility different error models with additive and/or proportional random residuals were also tested.

The structural model evaluation included both elements describing insulin disposition (1), and effects of glucose on insulin appearance (2), which were evaluated using goodness-of-fit plots, objective function values, and residual variation.

1. Insulin disposition was modelled by a first order disposition model with a fixed half life of insulin (6 min) or a direct model of insulin (i.e. where insulin disposition is included in the secretion model). .
2. For the dynamic model of the effects of glucose on insulin concentrations, the following structural components were evaluated: 1) glucose above baseline, 2) delayed glucose above baseline, and 3) the positive part of the rate of change in glucose. Combinations of these effects were also evaluated.

RESULTS

Patients and data

The population of subjects with T2DM had an approximately 50% increased average FPI compared to the non-diabetic control group, whereas FPG was around double and with a wider range (5-21 mM) compared to the control group (4-7 mM). The average time–concentration profiles of glucose and insulin are shown in figure 1 (A-B). There were considerable differences between the groups and large intersubject variations. Average maximal insulin response was reached more quickly in the control group (t_{max}=50 min) compared to the group with T2DM (t_{max}=75 min). The average maximal insulin concentration was higher in the control subjects than the diabetic subjects (446 vs 388 pM), but this did not reach statistical significance (P=0.098).

Due to the heterogeneity in FPG in the studied population, we divided the subjects into six groups of FPG. Figure 2 illustrates the glucose-insulin phase plot (average concentrations) for each FPG group. The groups 0-2 (i.e. FPG below 9 mM) demonstrated the steepest slopes of the glucose-insulin curves indicating higher beta cell glucose responsiveness than the other groups (figure 2).

In order to show if the average fasting and average postprandial insulin response varied with FPG and WST (Unpaired t-test, P<0.05; Welch correction if variances were significantly different) we divided the six FPG groups in tertiles of WST, cf. figure 3. In all six FPG groups average FPI was higher in subjects with WST > 105 cm compared to subjects with WST ≤ 105 cm (although groups with N<10 were not significantly different, cf. methods section). In subjects with FPG above 13 mM (Grp. 5) average FPI was borderline statistically insignificant (P=0.07) (cf. figure 3A). Average FPI was not significantly different between those subjects with WST < 95 cm and those with WST between 95 and 105 cm (except for the control group Grp. 0, P=0.01). Regarding the average postprandial insulin response (figure 3B), groups 0 and 2 showed increasing average

incremental insulin with increasing WST (although group 0 was not significant). For Grp. 2 and 3-5 (FPG ≥ 9 mM), WST did not correlate with the average insulin response after MTT. Grp. 1-2 had similar average incremental responses for WST ≥ 95 cm.

Structural model selection

Regarding insulin disposition, we found that the first order elimination model was associated with convergence problems and had a higher objective function value than a direct model of insulin (OBJ=-7668.605 vs OBJ= -7788.605.). The latter indicate insulin secretion to be very fast, potentially even faster than the rise in glucose, which could be related to cephalic insulin secretion. Hence, it was chosen to use a model where insulin disposition is integrated with the insulin appearance model so that insulin concentrations are modelled directly.

For the model of effects of glucose on insulin concentrations, we found that the delayed effect of glucose was superior a model of direct effects of glucose (OBJ = -5386.849 vs OBJ = 1161.395). A significant improvement to a model containing only delayed effects of glucose could be obtained, either by including direct effects of glucose, or by including also the rate of change in glucose. Although these models were visually similar, the direct effects of glucose provided the lowest objective function value (OBJ = -7788.605 vs OBJ = -6659.414), the lowest variance of the individual residuals (CV = 5.48% vs CV = 6.69%), and the parameter estimates appeared more robust to small changes in the model. Hence the combination of delayed and direct effects of glucose on insulin was chosen, and only modest improvements could be obtained by including all 3 model components (OBJ = -7862.538 vs OBJ = -7788.605). We speculate that the derivative component could be more important in healthy volunteers where the first phase secretion is more pronounced, and possibly also more important for the OGTT. In support of this, it should be noted

that Steil *et al.* (2004) also had problems relating the derivative component in the MTT to first phase secretion in the hyperglycemic clamp.

The structural model

The final selected structural model assumes the following parts and mechanisms:

1) Glucose above basal has a rapid ("immediate") stimulatory effect on insulin. This effect is represented by a linear function $X(t) = G(t) - G_B$. G(t) is the plasma glucose concentration in mM, G_B is the measured fasting plasma glucose concentration (FPG) in mM. If the plasma glucose concentration, G(t), is below the fasting value, G_B, the function X(t) is assumed to be zero.

2) The beta cell has a "glucose memory". The memory mechanism is represented by the function $Y(t) = \frac{1}{\tau} \cdot \int_{-\infty}^{t} X(s) \cdot e^{-\frac{1}{\tau}(t-s)} ds$, where s denotes all previous times until time t. The Y(t) function ensures that all previous glucose concentrations until time t are taken into account, and the exponentially decaying function in Y(t) ensures that glucose values closest to the present time t, contribute more to the insulin, than glucose values further back in time. The τ parameter determines how fast the delayed effect decays. A large value of τ will give a fast decay and thus a small contribution to insulin and vice versa - a small value of τ will result in a slow decay and thus a larger contribution to the insulin. τ is therefore a measure of the "glucose memory" in the beta cell.

3) A basal insulin concentration (the parameter I_0) estimated for each individual subject.

The model of insulin dynamics can therefore be described by the following three equations:

$$X(t) = \begin{cases} G(t) - G_B, & \text{for } G(t) > G_B \\ 0, & \text{otherwise} \end{cases} \qquad (1)$$

$$\frac{dY(t)}{dt} = \frac{1}{\tau} \cdot (X(t) - Y(t)) \quad (2)$$

$$I(t) = \alpha \cdot X(t) + \beta \cdot Y(t) + I_0 \quad (3)$$

Where I(t) is the plasma insulin concentration in pM. The parameter α (pM insulin/mM glucose) determines the magnitude of the immediate response of insulin to glucose concentrations above basal and the parameter β (pM insulin/mM glucose) determines the magnitude of the delayed glucose effects on insulin.

The differential equation describing the time dependency of the function Y(t) in Eq. (2) can be obtained by differentiation of the integral expression of Y(t) given in part 2).

Inter- and intra-subject variation

The structural model was fitted as a population model, i.e. including both inter- and intra-subject variation. Intersubject variation was included on parameters α, β and I_0. τ was included as a fixed effect, since intersubject variation did not improve the fit and the individual estimates of τ proved not to be robust to small changes in the model. Intersubject variation on parameters α, β and I_0, was implemented using a proportional model: $\theta \cdot \exp(\eta)$, where θ is the typical value of the parameter and η is a normal distributed random variable that varies between subjects. The individual parameters ($\theta \cdot \exp(\eta)$) give rise to a set of individual insulin predictions, whereas the typical parameters (θ) give rise to a set of population predictions. A full covariance matrix was used to incorporate the correlation between the individual parameters. Intrasubject variation was modelled by log-transforming the data – corresponding to the proportional model: $I(t)_{predicted} = I(t)_{observed} \cdot \exp(\varepsilon)$, where ε is normal distributed.

Covariate selection and analysis

Individual parameter estimates obtained from the initial model without covariates were used to explore the relationship between the chosen covariates (cf. table 1) and model parameters. Based on graphical tools and calculated correlation coefficients, continuous covariates (e.g., BMI or age) were included either by a linear: $\theta_{ind} = \theta_1+\theta_2\cdot(cov-cov_0)$, or a log-linear: $\theta_{ind} = \theta_1\cdot exp(\theta_2\cdot(cov-cov_0))$ model, where θ is the typical value of the parameter given a set of covariates, cov is the value of the covariate, cov_0 is the average value of the covariate in the entire population, θ_1 represents the typical value of the parameter when $cov = cov_0$ and θ_2 represents the effect of the covariate on the parameter. Categorical covariates (such as sex, smoking, and family disease history) were included in the model using indicator variables, as shown in the following equation: $\theta_{ind} = \theta_1+\theta_2\cdot ind$, where ind is an indicator variable with ind = 1 when the covariate is present, otherwise ind = 0.

Given the large number of individuals, many covariate effects were found to be statistically significant. The relationship between the parameters and each of the covariates (cf. table 1) were explored graphically and pair wise checked for correlation. To sort out covariates that, although significant, explained only a small part of the intersubject variation, a value of 10% for R^2 was used as a selection criterion. The correlations between covariates and parameter estimates are shown in table 2.

Lipids (LDL, HDL, triacylglycerol, and total cholesterol), smoking, age, family history, urea, and creatinine accounted for less than 5% of the variance in the parameters and were thus considered to be insignificant covariates on the model parameters (cf. Table 2). Only FPG, HbA1c, and type (healthy/patients) accounted for more than 10% of the variance on α and β. These covariates were incorporated into a full model. Covariates that were not significant or did not contribute to explain the variance were excluded by a backwards elimination procedure from the full model. However, when the effects of FPG were included also, HbA1c and type did not explain

more than 5% of the remaining variability. FPG was selected over HbA1c, because of a slightly higher correlation and a better objective function value. Similarly, WST and BMI were significant covariates that –when included alone - each accounted for more than 10% of the variability in I_0. WST proved to be a slightly superior explanatory factor, and BMI did not explain more than 5% of the variance in the final model with WST included.

Thus, in the final model only three covariates were left: FPG on α and β, and WST on I_0. The final model including covariates was able to capture the individually predicted insulin concentrations versus the experimentally measured insulin values (R=0.971) (figure 4A). The experimentally measured insulin values were correlated to the population predicted insulin concentrations with R=0.618 (figure 4B). In the model without covariates the correlations were R=0.971 and R=0.246, respectively, thus, inclusion of covariates improved the population predictions considerably. The correlation between the estimated insulin baseline (I_0) and the experimentally determined FPI concentration was R=0.953.

In the final model with covariates only FPG was left as a covariate on the two glucose-stimulated insulin responses α and β (figure 5A-B). The population averages of α and β were 24.4 and 35.1 pM insulin/mM glucose respectively. From the covariate parameter estimates we found that α decreased with 16% when plasma glucose increased with 1 mM, so that the expected α-value dropped from 56.5 to 47.3 pM insulin/mM glucose if FPG increased from 5 to 6 mM. Similarly, β decreased with 25% from 139 to 104 pM insulin/mM glucose. The population estimate for τ was 49 min. The population average of the estimated basal insulin (I_0) was 53.6 pM. WST was an indicator for the individual I_0 (figure 5C). If WST increased by 10 cm I_0 increased by 6.6%. The geometric mean parameter values of the non-diabetic control subjects and the subjects with type 2 diabetes are listed in table 3.

Comparison between model parameters and HOMA

The model parameters and HOMA indices were compared (details not shown). HOMA%B correlated with both α and β (Using an Emax model: R=0.770 and R=0.771, respectively). HOMA IR did not correlate with α or β. HOMA%B correlated hyperbolically with FPG (R=0.773 using a hyperbolic function). We found a strong hyperbolic correlation between basal insulin concentrations (both the estimated I_0 and the experimentally measured FPI) and HOMA IR (R=0.925 and R=0.947, respectively).

DISCUSSION

To the best of our knowledge, this is the first time that population-based covariate analysis has been used for assessment of MTT profiles in subjects with T2DM and controls. Our results show that despite large intersubject variation, insulin concentrations could be described by the current model structure – explaining most of the variation in insulin responses following MTT. We find that those subjects with the lowest FPG values have the steepest slopes – this is also evident from the descriptive analysis shown in figure 2. Ferrannini *et al.* have reported a similar relationship between insulin secretion rate and plasma glucose in subjects with normal glucose tolerance, IGT and T2DM (Ferrannini *et al.* 2005). However, a novel finding from the present analysis is that the delayed effect (estimated by the parameter β) of glucose on insulin response decreases faster than the rapid effect (estimated by the parameter α) of glucose on insulin response in subjects with T2DM. (Godsland *et al.* 2004) found loss of beta cell function, as assessed via an IVGTT, with increasing FPG in *non-diabetic* subjects - in their study the decline began at FPG concentrations of around 5-5.4 mM for first phase secretion and around 6 mM for late phase secretion. Our study results

corroborate this finding; however, we did not assess the beta cell function via an IVGTT but an MTT.

The delayed effect of glucose on insulin has similarities with results previously shown experimentally (Cerasi 1975b; Cerasi 1975a; Grill *et al.* 1978; Nesher and Cerasi 2002; Nesher and Cerasi 1987; Zawalich and Zawalich 1996)- where the secretory responsiveness of the beta cell can be markedly increased by prior short term exposure to a stimulatory glucose concentration. In our study the time needed to obtain a markedly insulin appearance is identified as the parameter τ which was estimated to almost 50 min. Thus, the beta cell will respond with an enhanced insulin secretion after about an hour of glucose stimulation.

The model results compare well with the phase plots relating postprandial plasma glucose to insulin concentrations (figure 2). Thus, the sum of the model parameters $\alpha+\beta$ represent the slope of the curve of the phase plot, whereas β represents the magnitude of the hysteresis: The larger the loop the higher the β, such that subjects with high FPG have small loops (e.g. low hysteresis).

Interestingly, the delayed effect (β) decreases more with increasing FPG (25% per mM Glucose) than the rapid effect (α) (16% per mM Glucose), indicating that the development of diabetes is associated with decreased “memory” response. This is in agreement with figure 2, in which the delay causing a hysteresis loop decreases for patients with higher FPG. It is interesting to find out whether effective anti-diabetic treatment will restore the memory response to normal concentrations, or whether it is a non-reversible event. In the future, this could be explored by examining the subjects after effective glycemic treatment.

From the data analysis it is seen that fasting insulin increased the greater the WST. For subjects with FPG above 9 mM incremental insulin responses did not differ between WST tertiles. Furthermore, the influence of WST on incremental insulin in subjects with FPG below 9 mM was not as clear (cf. figure 3B). This indicates that obesity does not influence postprandial insulin

responses equally in our population of subjects with T2DM but that this effect is correlated with the degree of fasting hyperglycemia. Thus, obesity affects the fasting and the postprandial insulin responses differently.

In the population based model WST was demonstrated to be a covariate on basal insulin (figure 5C). This is both in accordance with our statistical analysis (cf. figure 3A) and with findings from other groups (see for instance (Lemieux *et al.* 2000; Pouliot *et al.* 1994)). We did not find WST to be a covariate on α and β, which is also in agreement with the data analysis shown in figure 3B.

A number of methods have been established for assessing beta cell responsiveness based on either C-peptide or insulin kinetics. These include: A) the minimal model of insulin kinetics during IVGTT (Toffolo *et al.* 1980), B) the model of C-peptide secretion during IVGTT (Toffolo *et al.* 1995), C) the combined model of insulin and C-peptide secretion during IVGTT (Watanabe *et al.* 1989), D) the model of C-peptide kinetics during MTT (Hovorka *et al.* 1998), E) the Homeostasis Model Assessment (HOMA) (Levy *et al.* 1998; Matthews *et al.* 1985), F) the continuous infusion of glucose method (Hosker *et al.* 1985), G) the models advocating simultaneous treatment of insulin and glucose (De and Arino 2000), H) the model for insulin secretion during IVGTT and OGTT (Overgaard *et al.* 2006), and I) the models of C-peptide kinetics during OGTT and MTT (Breda *et al.* 2001; Mari *et al.* 2002b; Mari *et al.* 2002a; Steil *et al.* 2004). Of these models, D) and I) have been developed for estimation of beta cell responsiveness following *MTT*, but they differ from ours as they use C-peptide data. Our model differs from the other models, A)-F), as it incorporates both a rapid and a delayed effect of glucose on the insulin concentrations. The models G)-I) also distinguish between different glucose effects, for example by including the derivative of glucose.

Since C-peptide is co-secreted with insulin in equimolar amounts and since insulin (unlike C-peptide) is subject to a large and variable first pass hepatic extraction, insulin secretion and glucose responsiveness of the beta cell is most often assessed using C-peptide data. Use of C-peptide data has the advantage that it is a more direct measure of insulin secretion, as it is unaffected by a potentially variable hepatic extraction across the studied population. Typically C-peptide secretion is estimated via deconvolution (Ferrannini and Cobelli 1987b) under the assumption of a linear kinetic model of C-peptide with a set of typical parameters. However, it should be acknowledged that the obtained glucose responsiveness may be less than optimal, due to intersubject variability in the C-peptide kinetic model and parameters (Ferrannini and Cobelli 1987a; Ferrannini and Cobelli 1987b).

One advantage of analyzing insulin concentrations as described here is that the kinetics of insulin is fast (half-life around 5 min) (Luzi *et al.* 2007) compared to the slower C-peptide kinetics (half-life around 35 min), so that small changes in insulin secretion leads to more pronounced changes in insulin concentration than in C-peptide concentration. However, a consequence of analyzing insulin concentrations alone is that elimination and secretion cannot be separated, so we cannot determine to what extent our model predicts beta cell responsiveness and/or peripheral insulin elimination. Since our model results show good agreement with previously published results, we believe that the model characterizes beta cell glucose responsiveness. Both methods have their advantages, but the largest difference lies in the outcome: C-peptide models more precisely reflect the state of the beta cells, whereas insulin models more precisely describe the important factor for peripheral glucose disposition.

The presented model has some structural similarity with that of a simple one-compartment system of insulin kinetics. However, the time constant τ = 49 min is 5-10 times larger in magnitude

than the half life of insulin elimination (5-10 min). However, it should be noted that the parameter τ is not a measure of insulin elimination, but a measure of the "glucose memory" in the beta cell.

This study cannot elucidate the mechanisms behind this correlation between basal insulin and WST, but it may be speculated if this is somehow linked to non-esterified fatty acids (NEFA) metabolism. Increased NEFA (coming from visceral fat) may increase hepatic glucose production and insulin secretion ("the portal theory" (Bergman *et al.* 2006)).

The HOMA model allows for estimation of both beta cell responsiveness (HOMA%B) and insulin resistance (HOMA IR) from the fasted state. HOMA%B was correlated with both α and β, and HOMA IR was correlated with I_0 and to FPI. The correlation between FPI and HOMA IR has been found by several other groups, including Matthews *et al.* (1985).

Incretins, e.g. GLP-1 and GIP, are nutrient dependent gut hormones that enhance insulin secretion. We have not measured these, and thus we cannot discriminate between effects of meal nutrients and incretins on the insulin response and thus also on the estimated parameter value. Furthermore, it is possible that meal size, composition or timing could also affect the values of α and β. This is something that would need further investigation by analysis of data from such studies.

In summary, we have been able to describe postprandial insulin profiles in 417 subjects with T2DM and 85 controls using population-based mixed effects modelling. Only FPG was a significant covariate on the glucose-dependence of the insulin response. WST was the only covariate on baseline insulin. This confirms that the beta cell glucose responsiveness is increasingly impaired in T2DM and correlated with FPG. Furthermore, waist circumference influenced the fasting and postprandial insulin concentrations differently. This result is to our knowledge new, and should be investigated further. The model also shows the importance of time-dependent effects in the development of the disease, as the delayed insulin response is strongly impaired in T2DM and

decreases faster than the rapid insulin response. All the subjects in the patient group had T2DM, were newly diagnosed and treatment naïve. It will be of interest to extend the analysis of these subjects following treatment in order to identify any subgroups which may appear with regard to disease progression.

ACKNOWLEDGEMENTS

This work was in part supported by the European Commission through the BIOSIM project (contract number LSHB-CT-2004-005137), which is gratefully acknowledged. Dr. Per Falk, Dr. Thomas Andersson, and Dr. Lars Hansen, all at Novo Nordisk A/S, are also acknowledged for support.

Table 1. Subject demographics and baseline characteristics. Data are averages± SE.

	Non-diabetic subjects	*Type 2 diabetic subjects*	*P-value*
N	85	417	-
Age (years)	51.3 ± 1.1	54.5 ± 0.5	0.0053
Sex – m/f (n)	46/39	108/309	<0.0001
BMI (kg/m^2)	26.0 ± 0.5	30.7 ± 0.3	<0.0001
Waist circumference (cm)	85.0± 1.4 (N=80)	102.8 ± 0.6 (N=398)	<0.0001
Waist-to-hip ratio	0.84 ± 0.01 (N=79)	0.94 ± 0.00 (N=384)	<0.0001
HbA1c (%)	4.7 ± 0.1 (N=84)	8.2 ± 0.1	<0.0001
FPG (mM)	5.2 ± 0.1	10.7 ± 0.2	<0.0001
FPI (pM)	50 ± 3.	74 ± 3	0.0001
Family history - no/yes	45/17 (N=62)	178/233 (N=411)	0.0467
Smoking: no/yes/ex (n)	49/21/1 (N=71)	149/104/140 (N=393)	<0.0001
Total cholesterol (mM)	5.5 ± 0.1 (N=83)	5.6 ± 0.1	0.4406
Triacylglycerol (mM)	1.5 ± 0.1 (N=83)	2.8 ± 0.1	<0.0001
HDL (mM)	1.37 ± 0.04 (N=81)	1.09 ± 0.02 (N=411)	<0.0001
LDL (mM)	3.4 ± 0.1 (N=81)	3.3 ± 0.1 (N=390)	0.5356
SBP (mmHg)	119 ± 2 (N=81)	135 ± 1	<0.0001
DBP (mmHg)	77 ± 1 (N=81)	83 ± 1	0.0009
Urea (mM)	4.9 ± 0.1 (N=82)	5.3 ± 0.1 (N=416)	0.0152
Creatinine (μM)	89 ± 1 (N=82)	81 ± 1 (N=415)	<0.0001

Table 2. Correlations values (R^2-values in %) between model parameters (log-transformed α, β and I_0) and demographic parameters (covariates)

	α	β	I_0
Type (healthy/patients)	22.0	16.1	3.77
Age	0.60	0.001	0.31
Sex	0.81	0.88	0.0007
BMI	2.94	0.74	29.0
Waist circumference	0.16	0.09	27.2
Waist-to-hip ratio	1.00	1.50	7.04
HbA1c	45.0	54.5	2.40
FPG	50.4	58.9	4.02
Family history	1.25	1.46	0.25
Smoking	2.71	1.89	0.72
Total cholesterol	3.55	3.62	0.28
Triacylglycerol	1.44	2.13	2.83
HDL	1.54	2.25	3.84
LDL	1.65	1.86	0.83
SBP	0.17	0.73	1.38
DBP	0.37	0.03	0.76
Urea	1.36	0.15	0.30
Creatinine	4.03	5.95	0.10

Table 3. Geometric mean parameter values for the non-diabetic controls and subjects with type 2 diabetes mellitus (T2DM).

	Controls subjects	Subjects with T2DM
α (pM Insulin / mM Glucose)	73.6	19.9
β (pM Insulin / mM Glucose)	139.8	27.1
I_0 (pM)	42.9	63.3

Figure legends.

Figure 1: Average plasma glucose (A) and average plasma insulin (B) during meal tolerance test (75 g CHO, 500 kcal) in 417 subjects with T2DM (open circles) and in 85 control subjects (full circles). Error bars represents standard deviations.

Figure 2: Phase-plots between the average plasma glucose and average plasma insulin during meal tolerance test in subjects grouped by FPG. The following groups were applied: Grp. 0: Controls, all with FPG < 7 mM (85), Grp. 1: FPG < 7 mM (45), Grp. 2: FPG: [7-9[mM (118), Grp. 3: [9-11[mM (84), Grp. 4: [11-13[mM (68), Grp. 5: ≥13 mM (102). Number of subjects in each group is presented in brackets.

Figure 3: (A) Average fasting plasma insulin (FPI) and (B) average incremental insulin ($AUC_{0\text{-}240\ min}$) categorized by waist circumference (WST) and FPG for all subjects. WST is categorised by tertiles: <95 cm (open bars), 95-105 cm (black bars), >105 cm (hatched bars). The number of subjects in each group is listed in table 3.

Figure 4: (A) The actual (measured) insulin concentrations (DV) versus the individually predicted insulin concentrations (IPRED). (B) The actual (measured) insulin concentrations (DV) versus the population predicted insulin concentrations (PRED).

Figure 5: The correlation between the fasting glucose values and the individual parameter estimate for α – the rapid glucose stimulated insulin response (A) – and the estimate for β – the delayed glucose stimulated insulin response (B). The correlation between waist circumference and the individual parameter estimate for I_0 (C). Subjects with T2DM are shown as filled circles and non-diabetic control subjects are shown as open circles.

Figure 1.

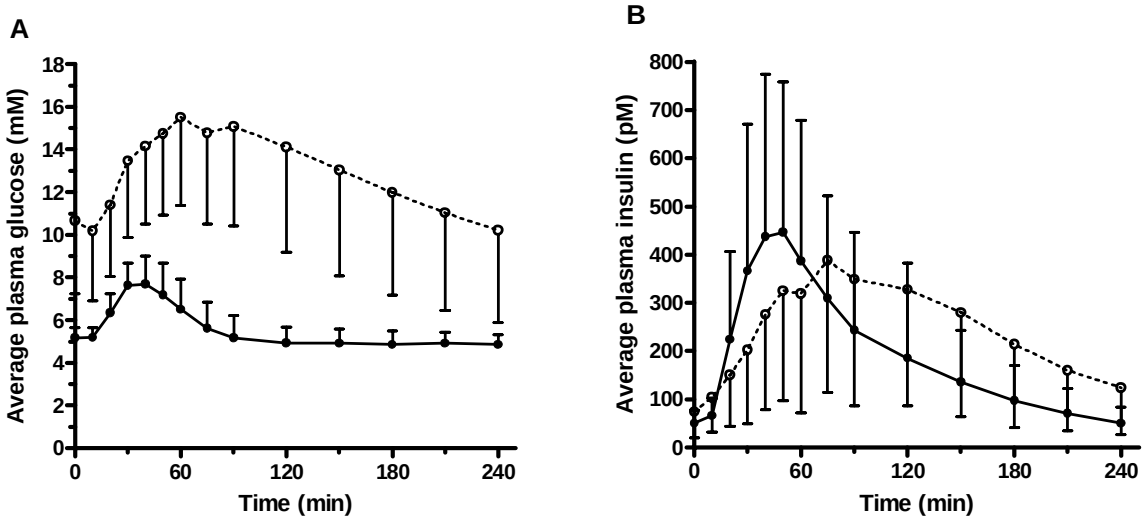
A
Average plasma glucose (mM)
0
2
4
6
8
10
12
14
16
18
0
60
120
180
240
Time (min)
B
Average plasma insulin (pM)
0
100
200
300
400
500
600
700
800
0
60
120
180
240
Time (min)

Figure 2.

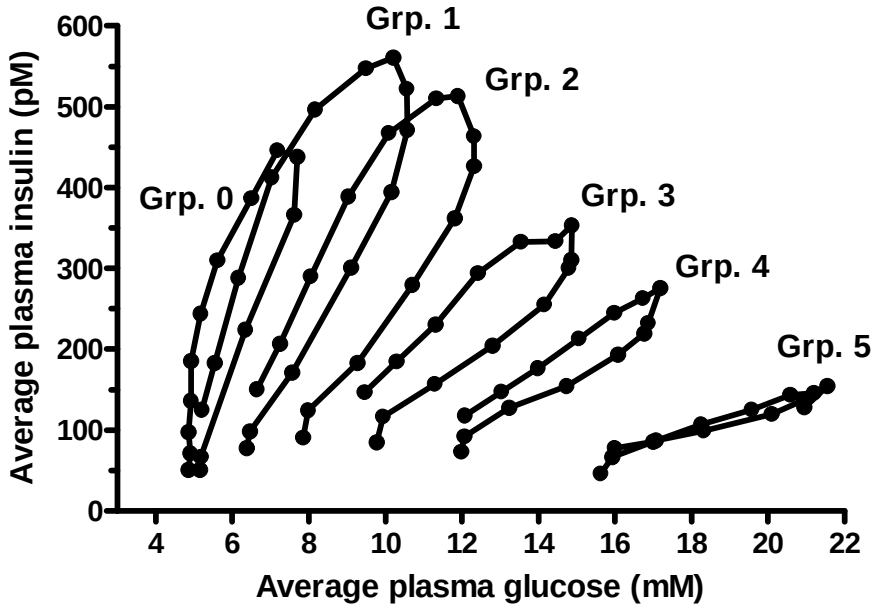
Grp. 1
Grp. 2
Grp. 0
Grp. 3
Grp. 4
Grp. 5
Average plasma insulin (pM)
600
500
400
300
200
100
0
4
6
8
10
12
14
16
18
20
22
Average plasma glucose (mM)

Figure 3.

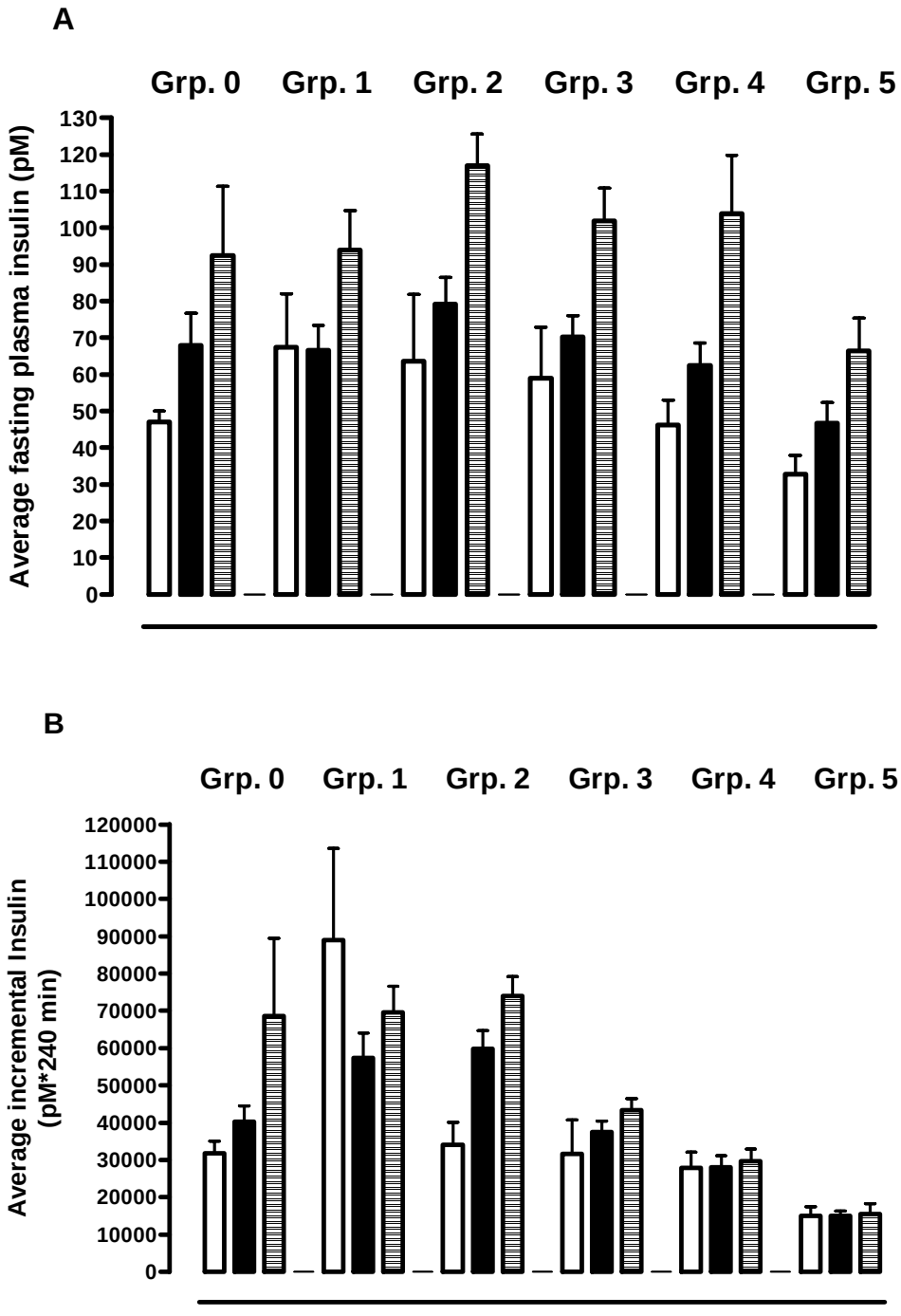
A
Grp. 0
Grp. 1
Grp. 2
Grp. 3
Grp. 4
Grp. 5
Average fasting plasma insulin (pM)
130
120
110
100
90
80
70
60
50
40
30
20
10
0
B
Grp. 0
Grp. 1
Grp. 2
Grp. 3
Grp. 4
Grp. 5
Average incremental Insulin (pM*240 min)
120000
110000
100000
90000
80000
70000
60000
50000
40000
30000
20000
10000
0

Figure 4.

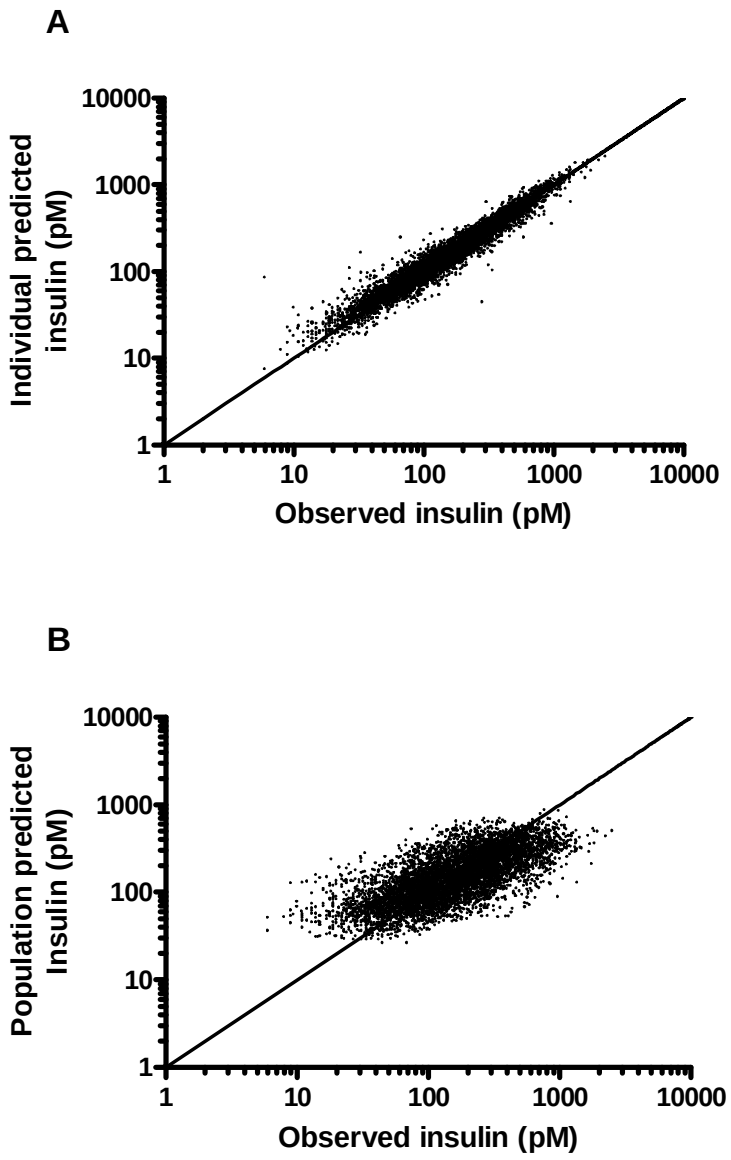
A
Individual predicted insulin (pM)
10000
1000
100
10
1
1
10
100
1000
10000
Observed insulin (pM)
B
Population predicted Insulin (pM)
10000
1000
100
10
1
1
10
100
1000
10000
Observed insulin (pM)

Figure 5.

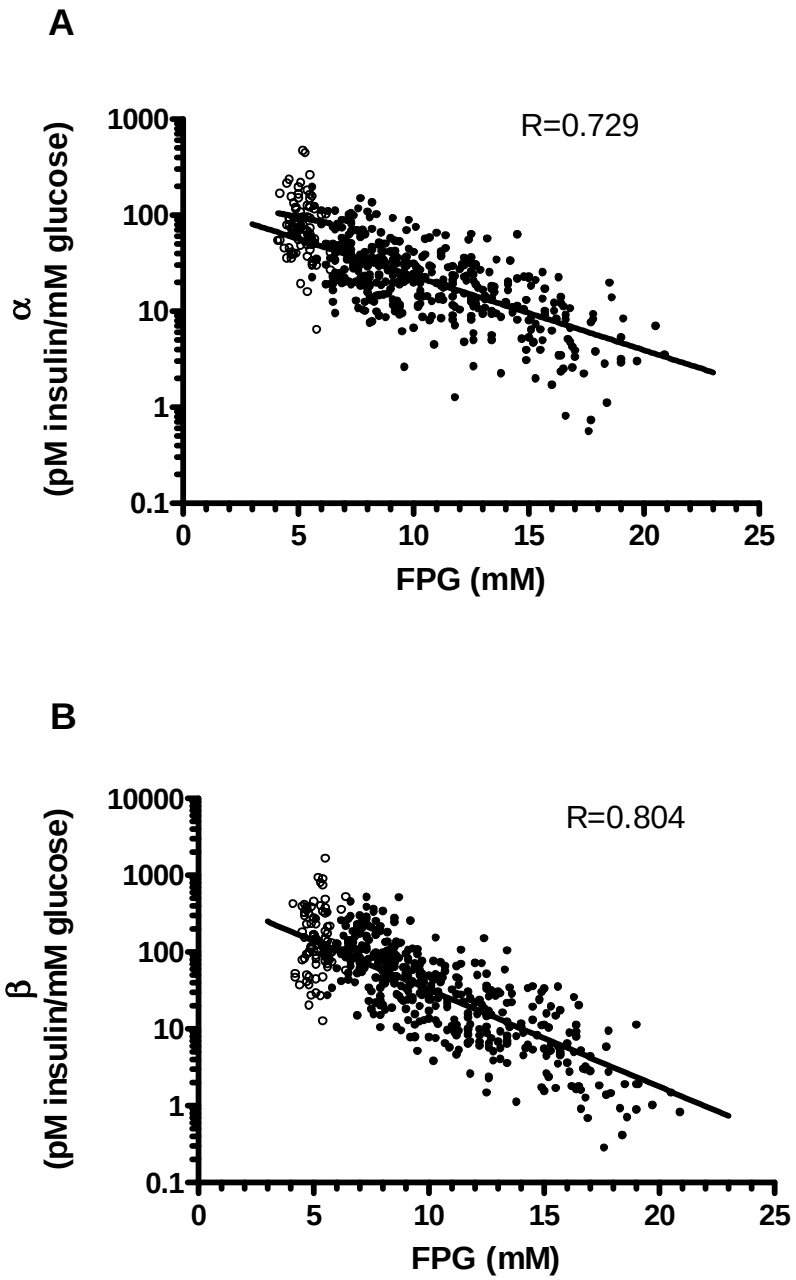
A
R=0.729
α
(pM insulin/mM glucose)
1000
100
10
1
0.1
0
5
10
15
20
25
FPG (mM)
B
R=0.804
β
(pM insulin/mM glucose)
10000
1000
100
10
1
0.1
0
5
10
15
20
25
FPG (mM)

C

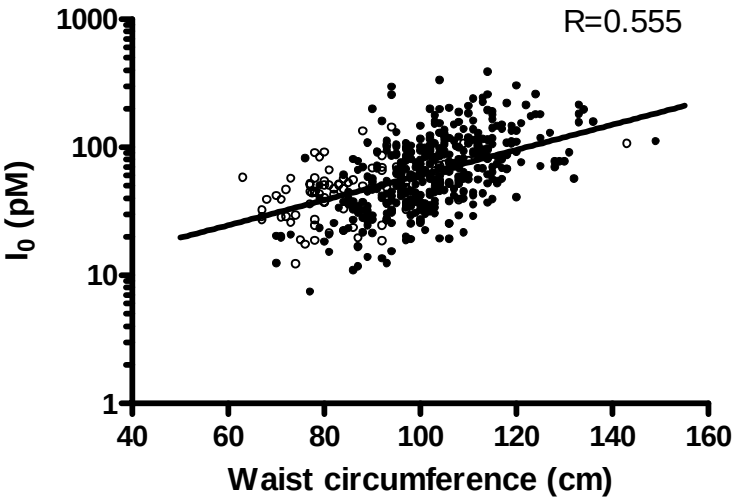
R=0.555
1000
100
10
1
I_0 (pM)
40
60
80
100
120
140
160
Waist circumference (cm)

Bibliography

Acheson, K. J., Schutz, Y., Bessard, T., Anantharaman, K., Flatt, J. P., and Jéquier, E. (1988). Glycogen storage capacity and de novo lipogenesis during massive carbohydrate overfeeding in man. *Am J Clin Nutr* **48**(2), 240-247.

Ahrén, B., and Holst, J. J. (2001). The cephalic insulin response to meal ingestion in humans is dependent on both cholinergic and noncholinergic mechanisms and is important for postprandial glycemia. *Diabetes* **50**(5), 1030-1038.

Ahren, B., and Pacini, G. (2004). Importance of quantifying insulin secretion in relation to insulin sensitivity to accurately assess beta cell function in clinical studies. *Eur J Endocrinol* **150**(2), 97-104.

Alberghina, l., and Westerhoff, H. V. Systems Biology: definitions and perspectives. 2005. Heidelberg, Springer-Verlag. Topics in current genetics.
Ref Type: Serial (Book,Monograph)

Altinok, A., Lévi, F., and Goldbeter, A. (2008). Optimizing temporal patterns of anticancer drug delivery by simulations of a cell cycle automanton. In *Biosimulation in drug development* (M.Bertau, E.Mosekilde, and H.V.Westerhoff, Eds.), pp. 403-423. WILEY-VCH Verlag GmbH & Co. KGaA, Weinheim.

Alzaid, A. A., Dinneen, S. F., Turk, D. J., Caumo, A., Cobelli, C., and Rizza, R. A. (1994). Assessment of insulin action and glucose effectiveness in diabetic and nondiabetic humans. *J Clin Invest* **94**(6), 2341-2348.

Anderwald, C., Tura, A., Grassi, A., Krebs, M., Szendroedi, J., Roden, M., Bischof, M. G., Luger, A., and Pacini, G. (2011). Insulin infusion during normoglycemia modulates insulin secretion according to whole-body insulin sensitivity. *Diabetes Care* **34**(2), 437-441.

Aspinwall, C. A., Lakey, J. R., and Kennedy, R. T. (1999). Insulin-stimulated insulin secretion in single pancreatic beta cells. *J Biol Chem* **274**(10), 6360-6365.

Basu, R., Breda, E., Oberg, A. L., Powell, C. C., la-Man, C., Basu, A., Vittone, J. L., Klee, G. G., Arora, P., Jensen, M. D., Toffolo, G., Cobelli, C., and Rizza, R. A. (2003). Mechanisms of the age-associated deterioration in glucose tolerance: contribution of alterations in insulin secretion, action, and clearance. *Diabetes* **52**(7), 1738-1748.

Basu, R., Chandramouli, V., Dicke, B., Landau, B. R., and Rizza, R. A. (2008). Plasma C5 glucose-to-2H2O ratio does not provide an accurate assessment of gluconeogenesis during hyperinsulinemic-euglycemic clamps in either nondiabetic or diabetic humans. *Diabetes* **57**(7), 1800-1804.

Beal, S. L., and Sheiner, L. B. (1998). NONMEM Users Guides: Parts I-VIII., Hanover, MD: GloboMax LLC.

Berg, J. M., Tymoczko, J. L., and Stryer, L. (2006). Biochemistry, W. H. Freeman and Company, USA, New York.

Bergman, R. N. (2005). Minimal model: Perspective from 2005. *Horm. Res.* **64**, 8-15.

Bergman, R. N., Ider, Y. Z., Bowden, C. R., and Cobelli, C. (1979). Quantitative estimation of insulin sensitivity. *Am J Physiol* **236**(6), E667-E677.

Bergman, R. N., Kim, S. P., Catalano, K. J., Hsu, I. R., Chiu, J. D., Kabir, M., Hucking, K., and Ader, M. (2006). Why visceral fat is bad: mechanisms of the metabolic syndrome. *Obesity (Silver. Spring)* **14 Suppl 1**, 16S-19S.

Bergman, R. N., Phillips, L. S., and Cobelli, C. (1981). Physiologic evaluation of factors controlling glucose tolerance in man: measurement of insulin sensitivity and beta-cell glucose sensitivity from the response to intravenous glucose. *J Clin Invest* **68**(6), 1456-1467.

Bertuzzi, A., Salinari, S., and Mingrone, G. (2007). Insulin granule trafficking in beta-cells: mathematical model of glucose-induced insulin secretion. *AM. J. PHYSIOL. ENDOCRINOL. METAB.* **293**(1), E396-E409.

Bock, G., Dalla, M. C., Campioni, M., Chittilapilly, E., Basu, R., Toffolo, G., Cobelli, C., and Rizza, R. (2006). Pathogenesis of pre-diabetes: mechanisms of fasting and postprandial hyperglycemia in people with impaired fasting glucose and/or impaired glucose tolerance. *Diabetes* **55**(12), 3536-3549.

Bock, G., Dalla, M. C., Campioni, M., Chittilapilly, E., Basu, R., Toffolo, G., Cobelli, C., and Rizza, R. (2007). Effects of nonglucose nutrients on insulin secretion and action in people with pre-diabetes. *Diabetes* **56**(4), 1113-1119.

Boden, G. (2001). Free fatty acids-the link between obesity and insulin resistance. *Endocr Pract* **7**(1), 44-51.

Borge, P. D., Moibi, J., Greene, S. R., Trucco, M., Young, R. A., Gao, Z., and Wolf, B. A. (2002). Insulin receptor signaling and sarco/endoplasmic reticulum calcium ATPase in beta-cells. *Diabetes* **51 Suppl 3**, S427-S433.

Bouche, C., Lopez, X., Fleischman, A., Cypess, A. M., O'Shea, S., Stefanovski, D., Bergman, R. N., Rogatsky, E., Stein, D. T., Kahn, C. R., Kulkarni, R. N., and Goldfine, A. B. (2010). Insulin enhances glucose-stimulated insulin secretion in healthy humans. *Proc. Natl. Acad. Sci. U. S. A.* **107**(10), 4770-4775.

Breda, E., Cavaghan, M. K., Toffolo, G., Polonsky, K. S., and Cobelli, C. (2001). Oral glucose tolerance test minimal model indexes of beta-cell function and insulin sensitivity. *Diabetes* **50**(1), 150-158.

Breda, E., Toffolo, G., Polonsky, K. S., and Cobelli, C. (2002). Insulin release in impaired glucose tolerance: oral minimal model predicts normal sensitivity to glucose but defective response times. *Diabetes* **51 Suppl 1**, S227-S233.

Bruggeman, F. J., Härdin, H. M., and van Schuppen, J. H. (2008). Silicon cell models: Construction, analysis, and reduction. In *Biosimulation in drug development* (M.Bertau, E.Mosekilde, and H.V.Westerhoff, Eds.), pp. 403-423. WILEY-VCH Verlag GmbH & Co. KGaA, Weinheim.

Burcelin, R., Crivelli, V., Perrin, C., Da-Costa, A., Mu, J., Kahn, B. B., Birnbaum, M. J., Kahn, C. R., Vollenweider, P., and Thorens, B. (2003). GLUT4, AMP kinase, but not the insulin receptor, are required for hepatoportal glucose sensor-stimulated muscle glucose utilization. *J Clin Invest* **111**(10), 1555-1562.

Burcelin, R., Dolci, W., and Thorens, B. (2000). Portal glucose infusion in the mouse induces hypoglycemia: evidence that the hepatoportal glucose sensor stimulates glucose utilization. *Diabetes* **49**(10), 1635-1642.

Byrne, M. M., Sturis, J., and Polonsky, K. S. (1995). Insulin secretion and clearance during low-dose graded glucose infusion. *Am J Physiol* **268**(1 Pt 1), E21-E27.

Campioni, M., Toffolo, G., Shuster, L. T., Service, F. J., Rizza, R. A., and Cobelli, C. (2007). Incretin effect potentiates β-cell responsivity to glucose as well as to its rate of change: OGTT and matched intravenous study. *AM. J. PHYSIOL. ENDOCRINOL. METAB.* **292**(1), E54-E60.

Caumo, A., Bergman, R. N., and Cobelli, C. (2000). Insulin sensitivity from meal tolerance tests in normal subjects: a minimal model index. *J Clin Endocrinol Metab* **85**(11), 4396-4402.

Caumo, A., Florea, I., and Luzi, L. (2007). Effect of a variable hepatic insulin clearance on the postprandial insulin profile: insights from a model simulation study. *Acta Diabetologica* **44**(1), 23-29.

Caumo, A., Vicini, P., and Cobelli, C. (1996). Is the minimal model too minimal? *Diabetologia* **39**(8), 997-1000.

Caumo, A., and Luzi, L. (2004). First-phase insulin secretion: does it exist in real life? Considerations on shape and function. *AJP - Endocrinology and Metabolism* **287**(3), E371-E385.

Cerasi, E. (1975a). Potentiation of insulin release by glucose in man. *Acta Endocrinol (Copenh)* **79**(3), 511-534.

Cerasi, E. (1975b). Potentiation of insulin release by glucose in man. I. Quantitative analysis of the enhancement of glucose-induced insulin secretion by pretreatment with glucose in normal subjects. *Acta Endocrinol (Copenh)* **79**(3), 483-501.

Cerasi, E., Fick, G., and Rudemo, M. (1974). A mathematical model for the glucose induced insulin release in man. *Eur J Clin Invest* **4**(4), 267-278.

Cobelli, C., Toffolo, G. M., la-Man, C., Campioni, M., Denti, P., Caumo, A., Butler, P., and Rizza, R. (2007). Assessment of beta-cell function in humans, simultaneously with insulin sensitivity and hepatic extraction, from intravenous and oral glucose tests. *AM. J. PHYSIOL. ENDOCRINOL. METAB.* **293**(1), E1-E15.

Cornish-Bowden, A., and Cárdenas, M. L. Glucokinase: A monomeric enzyme with positive cooperativity. Matschinsky, F. M. and Magnuson, M. A. (16), 125-134. 2004. Basel, S. Karger. Glucokinase and Glycemic Disease: From Basics to Novel Therapeutics.

Cretti, A., Lehtovirta, M., Bonora, E., Brunato, B., Zenti, M. G., Tosi, F., Caputo, M., Caruso, B., Groop, L. C., Muggeo, M., and Bonadonna, R. C. (2001). Assessment of beta-cell function during the oral glucose tolerance test by a minimal model of insulin secretion. *Eur J Clin Invest* **31**(5), 405-416.

Dalla Man, C., Campioni, M., Polonsky, K. S., Basu, R., Rizza, R. A., Toffolo, G., and Cobelli, C. (2005a). Two-hour seven-sample oral glucose tolerance test and meal protocol: Minimal model assessment of β-cell responsivity and insulin sensitivity in nondiabetic individuals. *Diabetes* **54**(11), 3265-3273.

Dalla Man, C., Caumo, A., Basu, R., Rizza, R., Toffolo, G., and Cobelli, C. (2004). Minimal model estimation of glucose absorption and insulin sensitivity from oral test: validation with a tracer method. *Am J Physiol Endocrinol Metab* **287**(4), E637-E643.

Dalla Man, C., Caumo, A., and Cobelli, C. (2002). The oral glucose minimal model: estimation of insulin sensitivity from a meal test. *IEEE Trans Biomed Eng* **49**(5), 419-429.

Dalla Man, C., Yarasheski, K. E., Caumo, A., Robertson, H., Toffolo, G., Polonsky, K. S., and Cobelli, C. (2005b). Insulin sensitivity by oral glucose minimal models: Validation against clamp. *AM. J. PHYSIOL. ENDOCRINOL. METAB.* **289**(6), E954-E959.

De, G. A., and Arino, O. (2000). Mathematical modelling of the intravenous glucose tolerance test. *J Math Biol* **40**(2), 136-168.

DeFronzo, R. A., Tobin, J. D., and Andres, R. (1979). Glucose clamp technique: a method for quantifying insulin secretion and resistance. *Am J Physiol* **237**(3), E214-E223.

Del Prato, S., Matsuda, M., Simonson, D. C., Groop, L. C., Sheehan, P., Leonetti, F., Bonadonna, R. C., and DeFronzo, R. A. (1997). Studies on the mass action effect of glucose in NIDDM and IDDM: evidence for glucose resistance. *Diabetologia* **40**(6), 687-697.

Del, G. S., Lupi, R., Marselli, L., Masini, M., Bugliani, M., Sbrana, S., Torri, S., Pollera, M., Boggi, U., Mosca, F., Del, P. S., and Marchetti, P. (2005). Functional and molecular defects of pancreatic islets in human type 2 diabetes. *Diabetes* **54**(3), 727-735.

Dresner, A., Laurent, D., Marcucci, M., Griffin, M. E., Dufour, S., Cline, G. W., Slezak, L. A., Andersen, D. K., Hundal, R. S., Rothman, D. L., Petersen, K. F., and Shulman, G. I. (1999). Effects of free fatty acids on glucose transport and IRS-1-associated phosphatidylinositol 3-kinase activity. *J Clin Invest* **103**(2), 253-259.

Eaton, R. P., Allen, R. C., Schade, D. S., Erickson, K. M., and Standefer, J. (1980). Prehepatic insulin production in man: kinetic analysis using peripheral connecting peptide behavior. *J Clin Endocrinol Metab* **51**(3), 520-528.

Elahi, D. (1996). In praise of the hyperglycemic clamp. A method for assessment of beta-cell sensitivity and insulin resistance. *Diabetes Care* **19**(3), 278-286.

Faerch, K., Vaag, A., Holst, J. J., Hansen, T., Jorgensen, T., and Borch-Johnsen, K. (2009). Natural History of Insulin Sensitivity and Insulin Secretion in the Progression From Normal Glucose Tolerance to Impaired Fasting Glycemia and Impaired Glucose Tolerance: The Inter99 Study. *Diabetes Care* **32**(3), 439-444.

Ferrannini, E., and Cobelli, C. (1987a). The kinetics of insulin in man. I. General aspects. *Diabetes Metab Rev.* **3**(2), 335-363.

Ferrannini, E., and Cobelli, C. (1987b). The kinetics of insulin in man. II. Role of the liver. *Diabetes Metab Rev.* **3**(2), 365-397.

Ferrannini, E., Gastaldelli, A., Miyazaki, Y., Matsuda, M., Mari, A., and DeFronzo, R. A. (2005). beta-Cell function in subjects spanning the range from normal glucose tolerance to overt diabetes: a new analysis. *J Clin Endocrinol Metab* **90**(1), 493-500.

Ferrannini, E., and Mari, A. (2004). Beta cell function and its relation to insulin action in humans: a critical appraisal. *Diabetologia* **47**(5), 943-956.

Ferrannini, E., Smith, J. D., Cobelli, C., Toffolo, G., Pilo, A., and DeFronzo, R. A. (1985). Effect of insulin on the distribution and disposition of glucose in man. *J Clin Invest* **76**(1), 357-364.

Frayn, K. N. (2003). Metabolic regulation - A human perspective, Blackwell Science Ltd..

Fridlyand, L. E., Tamarina, N., and Philipson, L. H. (2003). Modeling of Ca2+ flux in pancreatic beta-cells: role of the plasma membrane and intracellular stores. *Am J Physiol Endocrinol Metab* **285**(1), E138-E154.

Gerich, J. E. (1991). Is muscle the major site of insulin resistance in type 2 (non-insulin-dependent) diabetes mellitus? *Diabetologia* **34**(8), 607-610.

Giroix, M. H., Sener, A., and Malaisse, W. J. (1987). Hexose metabolism in pancreatic islets. Absence of glucose-6-phosphatase in rat islet cells. *Mol Cell Endocrinol* **49**(2-3), 219-225.

Giugliano, M., Bove, M., and Grattarola, M. (2000). Insulin release at the molecular level: metabolic-electrophysiological modeling of the pancreatic beta-cells. *IEEE Trans Biomed Eng* **47**(5), 611-623.

Godsland, I. F., Jeffs, J. A., and Johnston, D. G. (2004). Loss of beta cell function as fasting glucose increases in the non-diabetic range. *Diabetologia* **47**(7), 1157-1166.

Grill, V., Adamson, U., and Cerasi, E. (1978). Immediate and time-dependent effects of glucose on insulin release from rat pancreatic tissue. Evidence for different mechanisms of action. *J Clin Invest* **61**(4), 1034-1043.

Grodsky, G. M. (1972). A threshold distribution hypothesis for packet storage of insulin and its mathematical modeling. *J Clin Invest* **51**(8), 2047-2059.

Groop, L. C., Bonadonna, R. C., DelPrato, S., Ratheiser, K., Zyck, K., Ferrannini, E., and DeFronzo, R. A. (1989). Glucose and free fatty acid metabolism in non-insulin-dependent diabetes mellitus. Evidence for multiple sites of insulin resistance. *J Clin Invest* **84**(1), 205-213.

Hahn, R. G. (2005). Blood glucose increments as a measure of body physiology. *Critical Care* **9**, 155-157.

Hallgreen, C. E., Korsgaard, T. V., Hansen, R. N., and Colding-Jørgensen, M. (2008). The Glucose-Insulin Control System. In *Biosimulation in Drug Development* (M.Bertau, M.Mosekilde, and H.V.Westerhoff, Eds.), pp. 141-196. WILEY-VCH Verlag GmbH & Co. KGaA, Weinheim.

Hansen, R. N. Glucose Homeostasis - A biosimulation approach. 2004. PhD Thesis, Scientific Computing, Novo Nordisk A/S, Department of Physics, Technical University of Denmark.

Henquin, J. C. (2009). Regulation of insulin secretion: A matter of phase control and amplitude modulation. *Diabetologia* **52**(5), 739-751.

Henriksen, J. E., Alford, F., Handberg, A., Vaag, A., Ward, G. M., Kalfas, A., and Beck-Nielsen, H. (1994). Increased glucose effectiveness in normoglycemic but insulin-resistant relatives of patients with non-insulin-dependent diabetes mellitus. A novel compensatory mechanism. *J Clin Invest* **94**(3), 1196-1204.

Herman, M. A., and Kahn, B. B. (2006). Glucose transport and sensing in the maintenance of glucose homeostasis and metabolic harmony. *J Clin Invest* **116**(7), 1767-1775.

Hirota, K., Ishihara, H., Tsubo, T., and Matsuki, A. (1999). Estimation of the initial distribution volume of glucose by an incremental plasma glucose level at 3 min after i.v. glucose in humans. *Br J Clin Pharmacol* **47**(4), 361-364.

Holst, J. J. (2007). The physiology of glucagon-like peptide 1. *Physiol Rev.* **87**(4), 1409-1439.

Holst, J. J., Deacon, C. F., Vilsboll, T., Krarup, T., and Madsbad, S. (2008). Glucagon-like peptide-1, glucose homeostasis and diabetes. *Trends in Molecular Medicine* **14**(4), 161-168.

Hosker, J. P., Matthews, D. R., Rudenski, A. S., Burnett, M. A., Darling, P., Bown, E. G., and Turner, R. C. (1985). Continuous infusion of glucose with model assessment: measurement of insulin resistance and beta-cell function in man. *Diabetologia* **28**(7), 401-411.

Hovorka, R., Chassin, L., Luzio, S. D., Playle, R., and Owens, D. R. (1998). Pancreatic beta-cell responsiveness during meal tolerance test: model assessment in normal subjects and subjects with newly diagnosed noninsulin-dependent diabetes mellitus. *J Clin Endocrinol Metab* **83**(3), 744-750.

Hovorka, R., and Jones, R. H. (1994). How to measure insulin secretion. *Diabetes Metab Rev* **10**(2), 91-117.

Ishihara, H., and Giesecke, A. H. (2007). IDVG and extracellular fluid volume. In *Fluid volume monitoring with glucose dilution* pp. 39-48. Springer, Hong Kong.

Ishiyama, N., Ravier, M. A., and Henquin, J. C. (2006). Dual mechanism of the potentiation by glucose of insulin secretion induced by arginine and tolbutamide in mouse islets. *Am. J. Physiol. - Endocrinol. Metab.* **290**(3), E540-E549.

Johnson, J. H., Newgard, C. B., Milburn, J. L., Lodish, H. F., and Thorens, B. (1990). The high Km glucose transporter of islets of Langerhans is functionally similar to the low affinity transporter of liver and has an identical primary sequence. *J Biol Chem* **265**(12), 6548-6551.

Kahn, S. E., Klaff, L. J., Schwartz, M. W., Beard, J. C., Bergman, R. N., Taborsky, G. J., Jr., and Porte, D., Jr. (1990). Treatment with a somatostatin analog decreases pancreatic B-cell and whole body sensitivity to glucose. *J Clin Endocrinol Metab* **71**(4), 994-1002.

Kennedy, R. T., Kauri, L. M., Dahlgren, G. M., and Jung, S. K. (2002). Metabolic oscillations in beta-cells. *Diabetes* **51 Suppl 1**, S152-S161.

Kjems, L. L., Christiansen, E., V°lund, A., Bergman, R. N., and Madsbad, S. (2000). Validation of methods for measurement of insulin secretion in humans in vivo. *Diabetes* **49**(4), 580-588.

Klip, A., and Marette, A. Regulation of Glucose Transporters by Insulin and Exercise: Cellular Effects and Implications for Diabetes. Jefferson, L. S. and Cherrington, A. D. (II). 2001. USA, Oxford University Press. Handbook of physiology.

Korsgaard, T. V., and Colding-Jorgensen, M. (2006). Time-dependent mechanisms in beta-cell glucose sensing. *Journal of Biological Physics* **32**(3-4), 289-306.

Korsgaard, T. V., and Jönsson, R. Mathematical modelling of beta cell functionality in health and type II diabetes - a biosimulation approach. 2005. Master Thesis, Preclinical Development, Novo Nordisk A/S, Department of Physics, Technical University of Denmark.

Lahlou, H., Guillermet, J., Hortala, M., Vernejoul, F., Pyronnet, S., Bousquet, C., and Susini, C. (2004). Molecular signaling of somatostatin receptors. *Ann N Y. Acad. Sci* **1014**, 121-131.

Lemieux, I., Pascot, A., Couillard, C., Lamarche, B., Tchernof, A., Almeras, N., Bergeron, J., Gaudet, D., Tremblay, G., Prud'homme, D., Nadeau, A., and Despres, J. P. (2000). Hypertriglyceridemic waist: A marker of the atherogenic metabolic triad (hyperinsulinemia; hyperapolipoprotein B; small, dense LDL) in men? *Circulation* **102**(2), 179-184.

Levy, J. C., Matthews, D. R., and Hermans, M. P. (1998). Correct homeostasis model assessment (HOMA) evaluation uses the computer program. *Diabetes Care* **21**(12), 2191-2192.

Liang, Y., Najafi, H., Smith, R. M., Zimmerman, E. C., Magnuson, M. A., Tal, M., and Matschinsky, F. M. (1992). Concordant glucose induction of glucokinase, glucose usage, and glucose-stimulated insulin release in pancreatic islets maintained in organ culture. *Diabetes* **41**(7), 792-806.

Licko, V. (1973). Threshold secretory mechanism: a model of derivative element in biological control. *Bull Math Biol* **35**(1), 51-58.

Luzi, L., Zerbini, G., and Caumo, A. (2007). C-peptide: a redundant relative of insulin? *Diabetologia* **50**(3), 500-502.

Magnuson, M. A., and Matschinsky, F. M. Glucokinase as a glucose sensor: Past, present and future. Matschinsky, F. M. and Magnuson, M. A. (16), 1-17. 2004. Basel, S. Karger.

Maiztegui, B., Morelli, M. I., Raschia, M. A., Del, Z. H., and Gagliardino, J. J. (2009). Islet adaptive changes to fructose-induced insulin resistance: β-cell mass, glucokinase, glucose metabolism, and insulin secretion. *J. Endocrinol.* **200**(2), 139-149.

Mari, A. (2006). Methods of assessment of insulin sensitivity and β-cell function. *Immunol. Endocr. Metab. Agents Med. Chem.* **6**(1), 91-104.

Mari, A., Schmitz, O., Gastaldelli, A., Oestergaard, T., Nyholm, B., and Ferrannini, E. (2002a). Meal and oral glucose tests for assessment of beta -cell function: modeling analysis in normal subjects. *Am J Physiol Endocrinol Metab* **283**(6), E1159-E1166.

Mari, A., Tura, A., Gastaldelli, A., and Ferrannini, E. (2002b). Assessing insulin secretion by modeling in multiple-meal tests: role of potentiation. *Diabetes* **51 Suppl 1**, S221-S226.

Matschinsky, F., Liang, Y., Kesavan, P., Wang, L., Froguel, P., Velho, G., Cohen, D., Permutt, M. A., Tanizawa, Y., Jetton, T. L., and et.al. (1993). Glucokinase as pancreatic beta cell glucose sensor and diabetes gene. *J Clin Invest* **92**(5), 2092-2098.

Matschinsky, F. M. (1996). Banting Lecture 1995. A lesson in metabolic regulation inspired by the glucokinase glucose sensor paradigm. *Diabetes* **45**(2), 223-241.

Matschinsky, F. M., Magnuson, M. A., Zelent, D., Jetton, T. L., Doliba, N., Han, Y., Taub, R., and Grimsby, J. (2006). The network of glucokinase-expressing cells in glucose homeostasis and the potential of glucokinase activators for diabetes therapy. *Diabetes* **55**(1), 1-12.

Matthews, D. R., Hosker, J. P., Rudenski, A. S., Naylor, B. A., Treacher, D. F., and Turner, R. C. (1985). Homeostasis model assessment: insulin resistance and beta-cell function from fasting plasma glucose and insulin concentrations in man. *Diabetologia* **28**(7), 412-419.

Meglasson, M. D., and Matschinsky, F. M. (1986). Pancreatic islet glucose metabolism and regulation of insulin secretion. *Diabetes Metab Rev* **2**(3-4), 163-214.

Meier, J. J., Veldhuis, J. D., and Butler, P. C. (2005). Pulsatile insulin secretion dictates systemic insulin delivery by regulating hepatic insulin extraction in humans. *Diabetes* **54**(6), 1649-1656.

Miwa, I., Toyoda, Y., and Yoshie, S. Glukokinase in ß-Cell Insulin-Secretory Granules. Matschinsky, F. M. and Magnuson, M. A. (16), 350-359. 2004. Basel, S. Karger. Glucokinase and Glycemic Disease: From Basics to Novel Therapeutics.

Mourad, N. I., Nenquin, M., and Henquin, J.-C. (2010). Metabolic amplifying pathway increases both phases of insulin secretion independently of beta-cell actin microfilaments. *Am. J. Physiol. Cell Physiol.* **299**(2).

Muniyappa, R., Lee, S., Chen, H., and Quon, M. J. (2008). Current approaches for assessing insulin sensitivity and resistance in vivo: advantages, limitations, and appropriate usage. *Am J Physiol Endocrinol Metab* **294**(1), E15-E26.

Nesher, R., and Cerasi, E. (2002). Modeling phasic insulin release: immediate and time-dependent effects of glucose. *Diabetes* **51 Suppl 1**, S53-S59.

Nesher, R., and Cerasi, E. (1987). Biphasic insulin release as the expression of combined inhibitory and potentiating effects of glucose. *Endocrinology* **121**(3), 1017-1024.

Newgard, C. B., and Matschinsky, F. M. Substrte control of insulin release. Jefferson, L. S. and Cherrington, A. D. (II). 2001. USA, Oxford University Press.

Nielsen, M. F. (2008). Contribution of defects in glucose production and uptake to carbohydrate intolerance in insulin-resistant subjects. *Dan Med Bull* **55**(2), 89-102.

Noble, D. (2008). Heart simulation, arrythmia, and the actions of drugs. In *Biosimulation in drug development* (M.Bertau, E.Mosekilde, and H.V.Westerhoff, Eds.), pp. 259-272. WILEY-VCH Verlag GmbH & Co. KGaA, Weinheim.

Nucci, G., and Cobelli, C. (2000). Models of subcutaneous insulin kinetics. A critical review. *Computer methods and programs in biomedicine* **62**(3), 249-257.

Overgaard, R. V., Jelic, K., Karlsson, M., Henriksen, J. E., and Madsen, H. (2006). Mathematical beta cell model for insulin secretion following IVGTT and OGTT. *Ann Biomed Eng* **34**(8), 1343-1354.

Panteleon, A. E., Loutseiko, M., Steil, G. M., and Rebrin, K. (2006). Evaluation of the effect of gain on the meal response of an automated closed-loop insulin delivery system. *Diabetes* **55**(7), 1995-2000.

Pedersen, M. G., Corradin, A., Toffolo, G. M., and Cobelli, C. (2008). A subcellular model of glucose-stimulated pancreatic insulin secretion. *Philos Transact A Math Phys Eng Sci* **366**(1880), 3525-3543.

Pedersen, M. G., Toffolo, G. M., and Cobelli, C. (2010). Cellular modeling: Insight into oral minimal models of insulin secretion. *AM. J. PHYSIOL. ENDOCRINOL. METAB.* **298**(3).

Pennant, M. E., Bluck, L. J. C., Marcovecchio, M. L., Salgin, B., Hovorka, R., and Dunger, D. B. (2008). Insulin administration and rate of glucose appearance in people with type 1 diabetes. *Diabetes Care* **31**(11), 2183-2187.

Perales, M. A., Sener, A., and Malaisse, W. J. (1991). Hexose metabolism in pancreatic islets: the glucose-6-phosphatase riddle. *Mol Cell Biochem* **101**(1), 67-71.

Peters, A., Schweiger, U., Fr³hwald-Schultes, B., Born, J., and Fehm, H. L. (2002). The neuroendocrine control of glucose allocation. *Exp Clin Endocrinol Diabetes* **110**(5), 199-211.

Polonsky, K. S., Licinio-Paixao, J., Given, B. D., Pugh, W., Rue, P., Galloway, J., Karrison, T., and Frank, B. (1986). Use of biosynthetic human C-peptide in the measurement of insulin secretion rates in normal volunteers and type I diabetic patients. *J Clin Invest* **77**(1), 98-105.

Pouliot, M. C., Despres, J. P., Lemieux, S., Moorjani, S., Bouchard, C., Tremblay, A., Nadeau, A., and Lupien, P. J. (1994). Waist circumference and abdominal sagittal diameter: best simple anthropometric indexes of abdominal visceral adipose tissue accumulation and related cardiovascular risk in men and women. *Am J Cardiol.* **73**(7), 460-468.

Quon, M. J., Cochran, C., Taylor, S. I., and Eastman, R. C. (1994). Non-insulin-mediated glucose disappearance in subjects with IDDM. Discordance between experimental results and minimal model analysis. *Diabetes* **43**(7), 890-896.

Radziuk, J., and Pye, S. (2006). Diurnal rhythm in endogenous glucose production is a major contributor to fasting hyperglycaemia in type 2 diabetes. Suprachiasmatic deficit or limit cycle behaviour? *Diabetologia* **49**(7), 1619-1628.

Rizzo, M. A., Magnuson, M. A., Drain, P. F., and Piston, D. W. (2002). A functional link between glucokinase binding to insulin granules and conformational alterations in response to glucose and insulin. *J Biol Chem* **277**(37), 34168-34175.

Rorsman, P., and Renstrøm, E. (2003). Insulin granule dynamics in pancreatic beta cells. *Diabetologia* **46**(8), 1029-1045.

Saad, M. F., Anderson, R. L., Laws, A., Watanabe, R. M., Kades, W. W., Chen, Y. D., Sands, R. E., Pei, D., Savage, P. J., and Bergman, R. N. (1994). A comparison between the minimal model and the glucose clamp in the assessment of insulin sensitivity across the spectrum of glucose tolerance. Insulin Resistance Atherosclerosis Study. *Diabetes* **43**(9), 1114-1121.

Schuit, F. C., Huypens, P., Heimberg, H., and Pipeleers, D. G. (2001). Glucose sensing in pancreatic beta-cells: a model for the study of other glucose-regulated cells in gut, pancreas, and hypothalamus. *Diabetes* **50**(1), 1-11.

Sekine, N., Cirulli, V., Regazzi, R., Brown, L. J., Gine, E., Tamarit-Rodriguez, J., Girotti, M., Marie, S., MacDonald, M. J., Wollheim, C. B., and et.al. (1994). Low lactate dehydrogenase and high mitochondrial glycerol phosphate dehydrogenase in pancreatic beta-cells. Potential role in nutrient sensing. *J Biol Chem* **269**(7), 4895-4902.

Steil, G., Rebrin, K., and Mastrototaro, J. J. (2006). Metabolic modelling and the closed-loop insulin delivery problem. *DIABETES RES. CLIN. PRACT.* **74**(SUPPL. 2), S183-S186.

Steil, G. M., Hwu, C. M., Janowski, R., Hariri, F., Jinagouda, S., Darwin, C., Tadros, S., Rebrin, K., and Saad, M. F. (2004). Evaluation of insulin sensitivity and beta-cell function indexes obtained from minimal model analysis of a meal tolerance test. *Diabetes* **53**(5), 1201-1207.

Steil, G. M., Rebrin, K., Janowski, R., Darwin, C., and Saad, M. F. (2003). Modeling beta-cell insulin secretion--implications for closed-loop glucose homeostasis. *Diabetes Technol. Ther* **5**(6), 953-964.

Stumvoll, M., Tataranni, P. A., and Bogardus, C. (2005). The hyperbolic law - A 25-year perspective. *Diabetologia* **48**(2), 207-209.

Stumvoll, M., Tataranni, P. A., Stefan, N., Vozarova, B., and Bogardus, C. (2003). Glucose allostasis. *Diabetes* **52**(4), 903-909.

Sweet, I. R., and Matschinsky, F. M. (1995). Mathematical model of beta-cell glucose metabolism and insulin release. I. Glucokinase as glucosensor hypothesis. *Am J Physiol* **268**(4 Pt 1), E775-E788.

Thorens, B. (1996). Glucose transporters in the regulation of intestinal, renal, and liver glucose fluxes. *Am J P-Gast* **33**(4), G541-G553.

Thorens, B. (2004a). Mechanisms of glucose sensing and multiplicity of glucose sensors. *Ann Endocrinol (Paris)* **65**(1), 9-12.

Thorens, B. (2004b). The hepatoportal glucose sensor. In *Glucokinase and Glycemic Disease, from Basics to Novel Therapeutics* (F.M.Matschinsky and M.A.Magnuson, Eds.), pp. 327-338. Karger, Basel.

Toews, C. J. (1966). Kinetic studies with skeletal-muscle hexokinase. *BIOCHEM. J.* **100**(3), 739-744.

Toffolo, G., Bergman, R. N., Finegood, D. T., Bowden, C. R., and Cobelli, C. (1980). Quantitative estimation of beta cell sensitivity to glucose in the intact organism: a minimal model of insulin kinetics in the dog. *Diabetes* **29**(12), 979-990.

Toffolo, G., Breda, E., Cavaghan, M. K., Ehrmann, D. A., Polonsky, K. S., and Cobelli, C. (2001). Quantitative indexes of beta-cell function during graded up&down glucose infusion from C-peptide minimal models. *Am J Physiol Endocrinol Metab* **280**(1), E2-10.

Toffolo, G., Campioni, M., Basu, R., Rizza, R. A., and Cobelli, C. (2006). A minimal model of insulin secretion and kinetics to assess hepatic insulin extraction. *Am. J. Physiol. -Endocrinol. Metab.* **290**(1), E169-E176.

Toffolo, G., Cefalu, W. T., and Cobelli, C. (1999). Beta-cell function during insulin-modified intravenous glucose tolerance test successfully assessed by the C-peptide minimal model. *METAB. CLIN. EXP.* **48**(9), 1162-1166.

Toffolo, G., De, G. F., and Cobelli, C. (1995). Estimation of beta-cell sensitivity from intravenous glucose tolerance test C-peptide data. Knowledge of the kinetics avoids errors in modeling the secretion. *Diabetes* **44**(7), 845-854.

Turner, R. C., Holman, R. R., Matthews, D., and et, a. (1979). Insulin deficiency and insulin resistance interaction in diabetes: estimation of their relative contribution by feedback analysis from basal plasma insulin and glucose concentrations. *METAB. CLIN. EXP.* **28**(11), 1086-1096.

Van-Cauter, E., Mestrez, F., Sturis, J., and Polonsky, K. S. (1992). Estimation of insulin secretion rates from C-peptide levels. Comparison of individual and standard kinetic parameters for C-peptide clearance. *Diabetes* **41**(3), 368-377.

Wallace, T. M., Levy, J. C., and Matthews, D. R. (2004). Use and abuse of HOMA modeling. *Diabetes Care* **27**(6), 1487-1495.

Watanabe, R. M., Volund, A., Roy, S., and Bergman, R. N. (1989). Prehepatic beta-cell secretion during the intravenous glucose tolerance test in humans: application of a combined model of insulin and C-peptide kinetics. *J Clin Endocrinol Metab* **69**(4), 790-797.

WHO. World Health Organization. Definition, diagnosis and classification of diabetes mellitus and its complications. Report of a WHO Consultation. Part 1: diagnosis and classification of diabetes mellitus. Department of Noncommunicable Disease Surveillance.WHO/NCD/NCS/99.2. 1999. Genova.

Yki-Järvinen, H., Young, A. A., Lamkin, C., and Foley, J. E. (1987). Kinetics of glucose disposal in whole body and across the forearm in man. *J Clin Invest* **79**(6), 1713-1719.

Zawalich, W. S., and Zawalich, K. C. (1996). Species differences in the induction of time-dependent potentiation of insulin secretion. *Endocrinology* **137**(5), 1664-1669.

Zierler, K. (1999). Whole body glucose metabolism. *Am. J. Physiol. -Endocrinol. Metab.* **39**(3), E409-E426.